Satellite control with saturating inputs.

Josep Boada

DISSERTATION

Presented
to obtain the degree of

Doctor in Philosophy from Université de Toulouse

Ecole Doctorale de Systèmes

by

Josep Boada Bauxell

Satellite control with saturating inputs

Presented in December 10^{th} *2010 to the following dissertation committee:*

Prof. Caroline Berard	President
Prof. Matthew C. Turner	Reviewer
Dr. Hélène Piet-Lahanier	Reviewer
Prof. Jamal Daafouz	Member
Prof. Brigitte d'Andréa-Novel	Member
Dr. Catherine Charbonnel	Member
Dr. Sophie Tarbouriech	Advisor
Dr. Christophe Prieur	Advisor
Dr. Christelle Pittet	Invited
Dr. Andrés Marcos	Invited

Supported by CNES and Thales Alenia Space.
Prepared at the LAAS-CNRS
7, Avenue Colonel Roche − 31077 Toulouse Cedex 4, France.

Acknowledgements

I would like to express my sincere gratitude to those who helped me to complete this endeavor:

A mes directeurs de thèse, Dr. Sophie Tarbouriech et Dr. Christophe Prieur, pour son support et sa patience aux moments difficiles de cette thèse. Merci pour m'aider dans les moments de doute et pour être toujours à l'écoute. J'espère Christophe que tu aies profité des tapas à Barcelone. Sophie, merci pour ton dernier mot au jury de thèse, je vais essayer de garder toujours mon côté séducteur.

A mes responsables industriels, Dr. Christelle Pittet et Dr. Catherine Charbonnel, qui ont été toujours très attentifs aux évolutions de la thèse et qui ont agit comme deux vrais directeurs de thèse et pas comme de *superviseurs*. Je veux remercier Christelle par son exigence. Parfois c'était dur mais le remarques les plus dures sont celles qui te font avancer le plus. A Catherine juste lui dire que chaque fois qu'on a travaillé ensemble cela a été un vrai plaisir.

Thank you to all the PhD committee for the time invested in the reading and correction of my dissertation. A special thanks to Prof. Caroline Berard as she was the person who told me, four years ago, about the PhD position.

Merci aux collegues du groupe MAC qui m'ont appris qu'au délà de l'intérêt scientifique, les gens sont aussi importantes pour te sentir bien dans ton poste de travail. Grand merci à mes *amis* de bureau: Dr. Vincent Andrieu (mon premier voisin), Dr. Christophe Louembet (même s'il nous a abandonné) mon frère par vélo et le future Dr. Jean-François Trégouët (alias JF) mon deuxième de cordée. Je voudrais aussi rappeler les beaux souvenirs au groupe MAC comme les blagues d'Isabelle, la finesse sur la neige de Denis ou le peignoir de Mirko mais la liste serait trop longue.

Un record a la meva àvia Pietat Novich que m'estarà mirant des del cel, tot renyant l'avi. Aquesta tesi és una realitat en gran part gràcies a ella, a les seves torrades amb xocolata, als seus flams, a la seva fe cega amb mi. També recordar al meu cosí Joel que abans de morir em digué: *ets un crac, arribaràs lluny.* A la meva família, que encara que no entenguin del tot de què va la tesis sempre m'han recolzat.

No tinc paraules per descriure l'importància de la persona que m'ha acompanyat al llarg d'aquest viatge, na Mariana. El seu amor ha set vital per trobar forçes en aquells moments on tot semblava perdut. El capitol quatre és seu, sense ella encara hi seria. Gràcies per donar sentit als meus actes.

Agradecer especialmente a Alex su papel en esta tesis. Más allá de ser mi hermano toulousino, siempre ha estado allí para aclararme las dudas y motivarme para seguir.

Finalement, je voudrais remercier à tous mes amis qui m'ont suivi au long de la thèse: Renaud, Xavi, Javi, Gabi, Brice, Urko, Arnau, Valentin et une longue liste qui restera

toujours avec moi. Merci à tous.

Résumé

La théorie de la commande a évolué de façon significative dans le domaine de l'automatique non-linéaire. Cependant, les méthodes utilisées actuellement dans l'industrie aérospatiale sont le plus souvent basées sur des techniques de commande linéaire. Les spécifications, toujours plus exigeantes en termes de fiabilité et performance, imposent l'utilisation de techniques de plus en plus complexes. Ainsi, l'industrie cherche des solutions dans les nouvelles techniques de la théorie de la commande non-linéaire. En particulier, la limitation des actionneurs représente un phénomène non-linéaire commun dans la plupart des systèmes physiques. Des actionneurs saturés peuvent engendrer la dégradation de la performance, l'apparition de cycles limites ou d'états d'équilibre non désirés et même l'instabilité du système bouclé. Le but de la thèse est d'adapter et de développer les techniques de synthèse anti-windup à la commande de haute précision des axes angulaires et linéaires de satellites. Dans le domaine spatial, cet objectif se retrouve dans les missions de commande en accélération et aussi du vol en formation. Ces missions utilisent des propulseurs de haute précision où leur capacité maximale est très basse. Ces systèmes propulsifs présentent une modélisation particulière. Des fonctions de répartition adaptées à la synthèse anti-windup ont été étudiées. De plus, en tenant compte de l'état de l'art de la synthèse anti-windup, il y a un vrai besoin d'utiliser des techniques de symétrisation pour la fonction saturation. Le but principal de ce travail consiste à utiliser les techniques développées sur une application aérospatiale. A titre d'exemple, une stratégie complète est proposée afin de contrôler l'attitude et la position relative d'une mission de vol en formation.

Abstract

Automatic control theory has significantly evolved in the field of the non-linear control. However, the methods used in the aerospace industry lie usually on linear techniques applied to linearized models. The increasing requirements in terms of operational reliability and performance ask for the development of new control techniques more complex in order to meet the new demands. Therefore the industry is moving to the modern control theory looking for new non-linear approaches. In particular, actuators saturation represents a non-linear phenomenon common in almost all physical applications. This can then lead to performance degradation, limit cycle appearance, non-desired equilibrium conditions and even system instability. The objective of this thesis is to adapt and develop the anti-windup compensator design to the control with high precision for the angular and the linear axes of a satellite. In the aerospace application field, this situation meets with the drag-free or the formation flying missions. These missions use high precision thrusters as actuators whose capacity appears to be critically low. Moreover thrusters have a particular modelling. Allocation functions adapted to the anti-windup design are then explored. In addition considering the current state of the art of the anti-windup design, there is a strong necessity of using symmetrizing techniques for the saturation. The main objective of this work consists in applying the developed tools on an aerospace study case. As an example, a complete methodology is proposed to control a formation flying mission controlling both attitude and relative position.

Contents

List of Figures

List of Tables

Notation

AF	Allocation Function
f	Allocation function
AW	Anti-Windup
$\phi_{(\underline{u},\bar{u})}(\cdot)$	Asymmetric dead-zone function
$sat_{(\underline{u},\bar{u})}(\cdot)$	Asymmetric saturation function
BMI	Bilinear Matrix Inequality
F_{ci}	Controlled force computed for Satellite i
C_{ci}	Controlled torque computed for Satellite i
$Co\{\cdot\}$	Convex hull
$\partial\mathcal{S}$	Denotes the boundary of the set $\mathcal{S}$
$diag(x)$	Diagonal matrix obtained from vector x
DLAW	Direct Linear Anti-Windup
$\|x\|$, $\|x\|$	Euclidian norm of vector x, absolute value of real number x
EMRAW	Extended Model Recovery Anti-Windup
F_i	Force applied to Satellite i
M	Influence matrix
M_i	Influence matrix of satellite i
IMC	Internal Model Control
LDI	Linear Differential Inclusion
LFT	Linear Fractional Transformation
LMI	Linear Matrix Inequality
m	Mass of the satellite
$x_{max}(0)$	Maximal admissible intial condition for x
MCC	Minimal Control Capacity
MRAW	Model Recovery Anti-Windup
Multi-sat AF	Multi-saturation based AF
MIMO	Multiple Input Multiple Output
$0_{m\times n}$	Null matrix of $m \times m$ dimension
$Ker(A)$	Null space of matrix A
M^*	Pseudo-inverse matrix of M

$Re(x)$	Real part of x
$\theta_{x_{ij}}, \theta_{y_{ij}}, \theta_{z_{ij}}$	Relative attitude between Satellite i and j in $x/y/z$-axis
$\dot{\theta}_i$	Satellite i angular velocity
$\mathcal{F}_{sati}$	Satellite i associated frame
$\theta_{x_i}, \theta_{y_i}, \theta_{z_i}$	Satellite i attitude in $x/y/z$-axis
J_G	Satellite inertia
$\Delta y, \Delta z$	Satellite relative position in y/z-axis
$\Delta \dot{z}$	Satellite relative velocity
$\underline{u}$	Saturation lower bound
$\bar{u}$	Saturation upper bound
$\Re^{m \times n}$	Set of Matrices of $m \times m$ dimension
$\Re^+$	Set of positive real numbers
$\Re$	Set of real numbers
T^k	Set of thrusts generating k^{th} component of the control output
$\Re^m$	Set of vectors of m dimension
$sign(\cdot)$	Sign function
SIMO	Single Input Multiple Output
SISO	Single Input Single Output
$*$	Symbol $*$ stands for symetric blocks
u_0	Symmetric bound
$\phi_{(u_0)}(\cdot)$	Symmetric dead-zone function
$He(A)$	Symmetric matrix $A' + A$
$sat_{(u_0)}(\cdot)$	Symmetric saturation function
C_i	Torque applied to Satellite i
A'	Tranpose of matrix A
D_{awT}	*Trivial* anti-windp
VKF	Variable Kernel Function
$A > 0$	A is a positive-definite matrix
$A_{(i)}$	i^{th} row of matrix A
$A_{(:,i)}$	i^{th} column of matrix A
$x_{(i)}$	i^{th} component of x
$T_{i(j)}$	j^{th} component of Satellite i Thrust
I_m	m^{th}-order identity matrix
$x \succeq 0$	$x_{(i)} \geq 0 \ \forall i$

Introduction

Background and thesis framework

Automatic control theory has significantly evolved in the field of the non-linear control. Analysis and synthesis methods have appeared providing constructive tools to solve the control problems [TGGE07, KGE02, KA01, Val10]. Conversely, the methods used in the aerospace industry usually rely on linear techniques applied to linearized models. The increasing requirements in terms of operational reliability and performance ask for the development of new and more complex control techniques in order to meet the new demands [PCU+05, PDTP08, KTP08]. Therefore industry is moving to modern control theory looking for new non-linear approaches which are still unexplored when applied in the real control applications. Such approaches improve the control solutions as some non-linear behaviors of the considered system (omitted in the traditional linear approach) are introduced in the synthesis process. Moreover, the implementation of the non-linear analysis tools may be translated into a reduction of the validation time as the gap between the synthesis model considered and the real flight certification model would be reduced. These improvements would be also translated into a reduction of the cost and the resources addressed to flight control law validation. Therefore there exists a real necessity of adapting the new non-linear control tools to real industrial problems.

In particular, the control limitation due to the constraints of the actuators' maximum capacity represents a non-linear phenomenon common in almost all physical applications. Traditionally, a classical solution, at least in industry, consists in imposing important margins in order to prevent the actuators from reaching their maximum capacity, that is, to avoid saturation [CNE05]. In that manner, one tries to ensure the linearity of the system. However this *a posteriori* validation be insufficient because, non-nominal disturbances, transitions between operational modes, and the presence of system failures can force the actuators to reach their limits. Actuator saturation can then lead to performance degradation, limit cycle appearance, non-desired equilibrium conditions and even system instability [AR89, HL01, KGE02, Ste89].

The non-linear techniques dealing with saturation can be classified in two main research lines. The first one seeks to introduce the non-linear saturation in the synthesis

process of the controller [PTH07, GT91, GH85, HL01, SS99]. The second one introduces an extra layer to the existing linear controller, accounting for the non-linearities. This strategy, also called anti-windup design, allows the designer to keep the existing linear controller (already validated) and only to introduce a compensator which is only active when the non-linearity arises [KCMN94, CLW02, WL03, GdSJT05]. In that manner, the control design process is not completely changed as it would be with the first approach. Therefore, the development of constructive methods for the anti-windup design dealing with the saturation non-linearity is completely justified. See for example, the recent survey [GTTZ09, TT09] and the numerous references therein. In a context where the applicability of the modern technique is sought, the second approach is kept.

The objective of this thesis is to adapt and develop anti-windup compensator design to high precision control of the linear and angular displacements of a satellite. In the aerospace application field, this situation meets with the drag-free or the formation flying missions. These missions use thrusters as actuators with a high precision and fine-quantification. However their maximal propulsion capacity appears to be critically low. These actuators have also to ensure the transition coming from less precise flying modes to other more accurate modes, the robustness to the environmental disturbances and in certain cases, the survival of the satellite. In these modes the actuators may reach their maximum capacity introducing the non-linear effects of saturation. Consequently, the introduction of the anti-windup becomes an interesting technique to ensure the mission requirements and its reliability.

Space missions involving thrusters as actuators are modelled in a particular way. The control variables of the physical systems and the action provided by thrusters are not the same. An allocation function is included in the modelling of the actuators to distribute the control among the actuators [Dur93, NW99, BHSB96]. In the classical linear approach this function can be omitted, however, when the saturation of the actuators arises, its behavior has to be considered in the control design [BHSB96]. Allocation functions adapted to the anti-windup design have to be explored. Moreover the presence of thrusters introduces a peculiar formulation of the saturation function. The saturation presents asymmetric bounds with the minimum equal to zero. Considering the current state of the art of the anti-windup design, there is a strong necessity of using symmetrizing techniques for the saturation.

The symmetrizing procedure and the allocation function defined are put along with the anti-windup design to be applied in a spacecraft mission configuration. The control of both attitude and position in a formation flying becomes an interesting benchmark to test the functionality of developed techniques. The multi-objective behavior of the formation flying mission introduces couplings between the linear and the angular dynamics which can activate the saturation. Additionally, the transition from a low precision mode to high precision one may lead to the saturation of the actuators. For these situations where linear control theory is insufficient, the introduction of the anti-windup compensator represents a potential way of improvement.

Thesis outline

This manuscript is organized in five chapters. The first three chapters are dedicated to the theoretical concepts and the main results of the thesis. On the other hand, the last two chapters are completely focused on the application of the previous results to different satellite configurations.

Chapter 1 presents the basic tools for the analysis of the stability of the systems presenting a saturation non-linearity. Concepts like Lyapunov stability, non-linear sector condition or dead-zone function are recalled. These tools represent the bases of the results presented in Chapter 3.

The main issue of the manuscript is anti-windup compensator design. However, first, in Chapter 2 the problem of the saturation symmetrization is analyzed. The chapter presents the context where this problem is solved. Symmetrizing techniques are given along with some practical examples [BPT+09]. With these symmetrizing tools the problem considered can be written in a general context where the anti-windup techniques apply.

Chapter 3 is dedicated to anti-windup compensator design. A general overview of the problem is given analyzing the state of the art of the anti-windup technique. More precisely, a complete description of the two main approaches in anti-windup design is provided. Constructive techniques for each approach are given. In addition a third new approach is proposed as an alternative to the previous ones [BPT+10b]. Finally, The validity of the anti-windup results with asymmetric saturations is studied. An illustration of these approaches allows the reader to have an overview of the advantages and drawbacks of each one.

The last two chapters are dedicated to the presentation of the applications where the anti-windup techniques are tested. First, Chapter 4 presents three formation flying scenarios. The modelling of these study cases is introduced. Finally, simulations illustrate the advantages of the anti-windup compensator [BPT+10a]. Second, Chapter 5 deals with the drag-free control problem. A model of a drag-free configuration is tested with an anti-windup compensator in the loop. Simulations show the benefits of the anti-windup compensation.

A general conclusion and some perpectives recall the main results presented. An appendix ends this manuscript.

Educational example

Aim of the example

Let us first present an educational example. This example will illustrate the theory presented in the first three chapters of the thesis. It is called educational because it consists in a very basic example whose aim is only to provide a fixed framework throughout the reading. The choice has been sought to avoid the numerical problems that may introduce poor conditioning or a high order of the system. We pretend to make easier the comprehension of the different results presented in this thesis. Moreover this example should make the text more consistent as all results will be related through it, being a useful tool for the reader to set relationships between results.

The example can be slightly modified in some cases to show clearly the improvement of the concerned result. In these cases, a justification will be provided as well as a detailed description of the modifications.

Finally remark that the example has a physical meaning and therefore, some comments on the results will be also used in the second part of this manuscript.

Model description

The example is based on the control of the attitude of a satellite along one axis. The values are obtained from Microscope satellite model [PPT+05]. Figure 1 shows the example block representation. The plant $\mathcal{P}$ is modelled by a double integrator scaled by the inertia

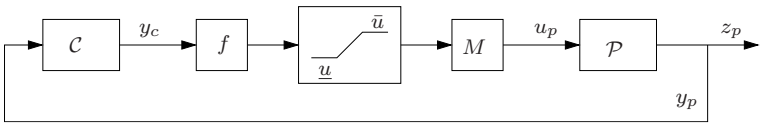

Figure 1: Control Loop

matrix:

$$\mathcal{P}: \begin{cases} \dot{x}_p = A_p x_p + B_p u_p = \begin{bmatrix} 0 & 1 \\ 0 & 0 \end{bmatrix} \begin{bmatrix} \theta \\ \dot{\theta} \end{bmatrix} + \begin{bmatrix} 0 \\ J^{-1} \end{bmatrix} u_p \\ y_p = C_p x_p = [1 \quad 0] x_p = \theta \\ z_p = C_z x_p = [1 \quad 0] x_p = \theta \end{cases} \tag{1}$$

where $x_p = [\theta \quad \dot{\theta}]'$ is the state vector composed by the attitude of the satellite and its time-derivative; $u_p \in \Re$ is the control input which in this case is a control torque as the angular axis is controlled; $y_p = \theta$ is the measured output and $z_p = \theta$ is the performance output which, in this particular case, is equal to y_p. J stands for the inertia of the satellite and is equal to $J = 37.5\text{kgm}^2$.

The stability of the linear closed-loop system (i.e. when $u_c = y_p$) is provided by a controller $\mathcal{C}$. The controller is a fourth order controller whose coefficients have been taken from the controller used in the Microscope mission [PPT+05]. The state space representation of this controller reads:

$$\mathcal{C} : \begin{cases} \dot{x}_c = A_c x_c + B_c y_p \\ y_c = C_c x_c + D_c y_p \end{cases} \tag{2}$$

with

$$A_c = \begin{bmatrix} -8 \cdot 10^{-4} & 0.13 & -0.49 & 0.7 \\ -7.2 \cdot 10^{-5} & -8 \cdot 10^{-4} & -8.6 \cdot 10^{-2} & 0.12 \\ 0 & 0 & -5.87 & 8.37 \\ 0 & 0 & 0 & -5.87 \end{bmatrix} \tag{3}$$

$$B_c = \begin{bmatrix} 0.17 \\ 0.029 \\ 1.98 \\ -4.87 \end{bmatrix} \tag{4}$$

$$C_c = [-12.93 \quad 0 \quad -37.97 \quad 24.19] \tag{5}$$

$$D_c = -12.54 \tag{6}$$

The controller is computed assuming the unconstrained interconnection $u_p = y_c$. However, the system uses thrusters as actuators. Actuator function is modelled by the following equation:

$$u_p = M sat_{(\underline{u},\bar{u})}(f(y_c)) \tag{7}$$

where $sat_{(\underline{u},\bar{u})}(\cdot)$ is a saturation function with $\underline{u} = 0$ and $\bar{u} = 150\mu N$. Such a non-linearity will be detailed in Chapter 1.

Only a two thrusters configuration is considered, the first one provides the positive command and the second one the negative one. Hence, $M = [1 \quad -1]$ is the influence matrix which sets the relationship between the thrust provided and the control input u_p performed. More explanations on the influence matrix are given in Chapter 2.

Finally f is an allocation function. It *allocates* the control y_c between the different thrusters available. f is designed to verify $u_p = Mf(y_c) = y_c$, allowing the designer to neglect the actuators. Nevertheless, this relation is no longer true because of the presence of the saturation function. The actuator is then modelled by equation (7). More details on the allocation are given in Chapter 2.

The closed-loop system formulation CL for the example reads:

$$CL: \begin{cases} \dot{x}_p = A_p x_p + B_p M sat_{(\underline{u},\bar{u})}(f(y_c)) \\ \quad = \begin{bmatrix} 0 & 1 \\ 0 & 0 \end{bmatrix} \begin{bmatrix} \theta \\ \dot{\theta} \end{bmatrix} + \begin{bmatrix} 0 & 0 \\ J^{-1} & -J^{-1} \end{bmatrix} sat_{(0,\bar{u})}(f(y_c)) \\ \dot{x}_c = A_c x_c + B_c C_p x_p \\ y_c = C_c x_c + D_c C_p x_p \\ z_p = C_z x_p = [1 \quad 0] x_p = \theta \end{cases} \tag{8}$$

The allocation function f is left undefined. There are many possible formulations of f available. This issue is treated in Chapter 2 where further explanations are given. Indeed, the example (8) will allow us to test the different choices of f proposed in Chapter 2.

In order to illustrate the effect of the saturation non-linearity, system (8) is simulated. First, to avoid the problem of the allocation function, the actuator (7) is modelled by a symmetric saturation between $\bar{u} = 150\mu N$ and $\underline{u} = -150\mu N$. Then the actual system tested in the following simulation reads:

$$\begin{cases} \dot{x}_p = A_p x_p + B_p sat_{(\underline{u},\bar{u})}(y_c) \\ \quad = \begin{bmatrix} 0 & 1 \\ 0 & 0 \end{bmatrix} \begin{bmatrix} \theta \\ \dot{\theta} \end{bmatrix} + \begin{bmatrix} 0 \\ J^{-1} \end{bmatrix} sat_{(-1.5\cdot 10^{-4}, 1.5\cdot 10^{-4})}(y_c) \\ \dot{x}_c = A_c x_c + B_c C_p x_p \\ y_c = C_c x_c + D_c C_p x_p \\ z_p = C_z x_p = [1 \quad 0] x_p = \theta \end{cases} \tag{9}$$

with A_c, B_c, C_c and D_c defined in (3)-(6).

The simulation considers the initial condition $x_p(0) = [-7 \cdot 10^{-4} \quad 0]'$. Figure 2 shows the response z_p in both the linear and the non-linear (saturated) cases.

Figure 3 presents the plant input u_p of system (9). In Figures 2 and 3 one observes easily that the presence of the saturation induces undesirable oscillations on the system. Assuming no saturation, the linear system reaches the origin in less than 50 seconds. However, as soon as the non-linearity of the actuator arises, the system starts to oscillate, still converging, but being closer to instability.

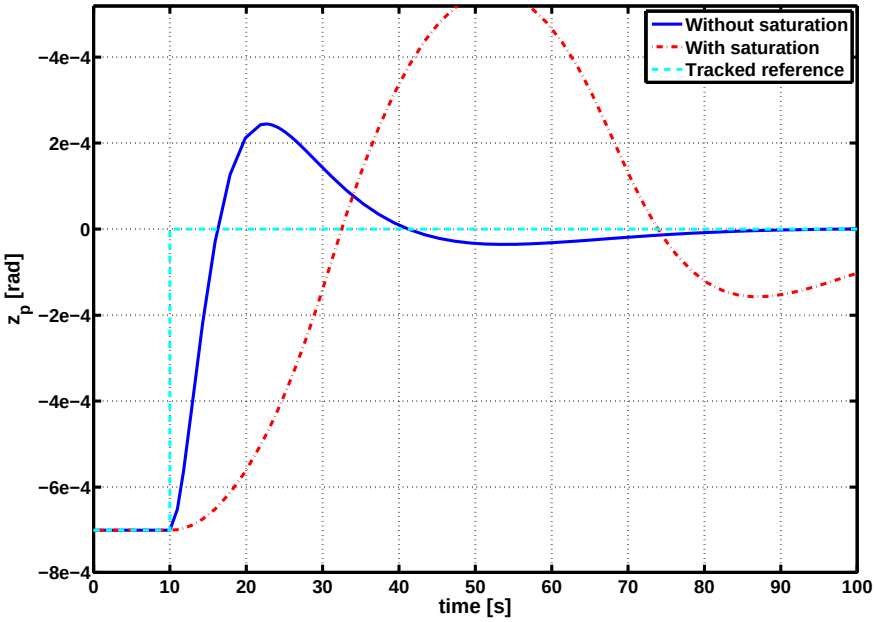

Figure 2: Effect of the saturation non-linearity on system (9).

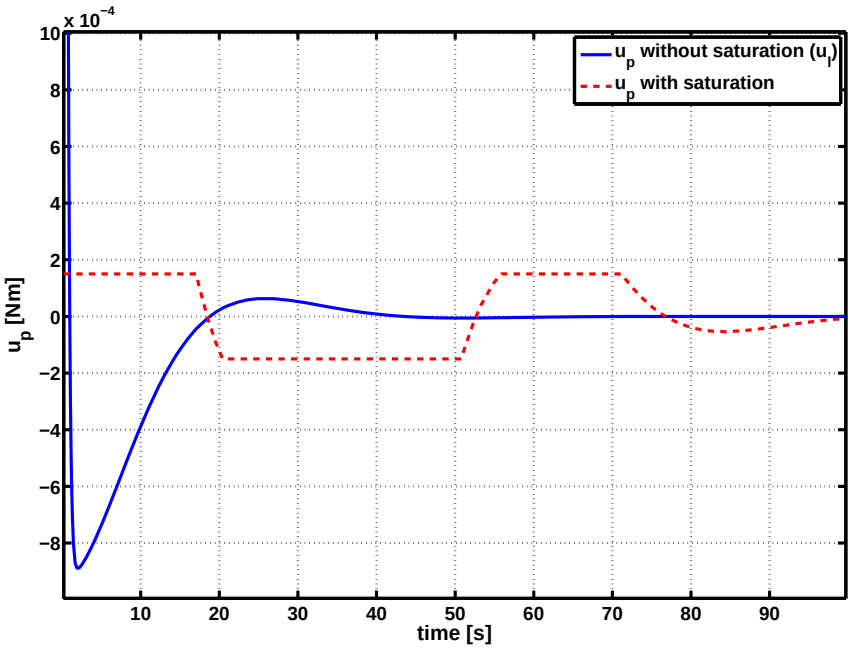

Figure 3: Effect of the saturation non-linearity on u_p of system (9).

Chapter 1

On the stability of saturated systems

Outline of the chapter

1.1 Introduction

Stability theory plays a central role in dynamical control systems theory. There are several ways to define the stability of a system in the literature. This section seeks to present the approaches most commonly used. Some basic concepts are then reviewed.

Initially, autonomous systems are introduced and a general definition of stability for these kinds of dynamic systems is exposed. Afterwards, given this general definition, a point on the particularity of the linear systems is done. Once this kind of systems is treated, the Lyapunov stability theory is detailed as well as the second Lyapunov method and the notions of local and global stability. From that point, the LaSalle *invariance principle* is presented as well as the concept of the region of attraction of the origin.

A specific class of dynamic systems pays the attention of this work: the systems under input constraints. This kind of systems presents a non-linearity that has to be modelled before any stability theory may be investigated. Therefore, some results dealing with non-linear constraints such as saturation or the dead-zone function are provided.

The Lyapunov theory is used to study the stability of the non-linear systems under input constraints. The saturation function modelling does not provide quadratic conditions. Some mathematical work is done to obtain quadratic conditions that can be solve with existing optimization algorithms.

Finally, the conditions to estimate the stability domain are presented. Moreover, several possibilities to optimize the stability domain are introduced. The stability analysis techniques are applied to the educational example.

Several definitions and results are presented in this chapter. No proofs are given as they are classical results and could be easily found in the literature. See, for example, works from Khalil [Kha92], Slotine and Li [SL91] and Vidyasagar [Vid92].

1.2 Stability of dynamic systems

1.2.1 Autonomous systems

Consider the function f locally Lipschitz in the set $\mathcal{X} \subseteq \Re^n$:

$$f : \begin{cases} \mathcal{X} \longrightarrow \Re^n \\ x \longmapsto f(x) \end{cases} \tag{1.2.1}$$

The autonomous system is characterized by

$$\dot{x}(t) = f(x(t)) \tag{1.2.2}$$

Then suppose $x_e \in \mathcal{X}$ is an equilibrium point of (1.2.2), in other words, $f(x_e) = 0$. The characterization and the study of the stability of the autonomous system (1.2.1) is related to the analysis of the stability of x_e.

In order to simplify the problem, all the definitions and results are stated considering $x_e = 0$ as equilibrium point. There is no loss of generality because any equilibrium point can be brought back to the origin via a change of variables.

Remark 1.1. *Through the change of variables $\bar{x} = x - x_e$, the resulting system $\dot{\bar{x}} = f(\bar{x})$ has its equilibrium point at $\bar{x}_e = 0$.*

1.2.2 Lyapunov stability

For a system like (1.2.2), Lyapunov stability which was introduced at the end of 19^{th} century [Lya92], can be formulated as follows.

Definition 1.1. *[Kha92] The equilibrium point $x_e = 0$ of system (1.2.2) is*

1. **stable** *if for all $\epsilon > 0$, there is a scalar $\eta > 0$ such that:*

$$\|x(0)\| \leq \eta \Rightarrow \|x(t, x(0))\| \leq \epsilon, \forall t \geq 0 \tag{1.2.3}$$

   where $x(t, x(0))$ is the solution of (1.2.1) with initial condition $x(0)$.

2. **attractive** *if there exists η such as*

$$\lim_{t \to \infty} x(t, x(0)) = 0, \forall \, \|x(0)\| \leq \eta \tag{1.2.4}$$

3. **asymptotically stable** *if stable and attractive.*

4. **unstable** *if it is not stable.*

This notion of stability is directly related to the notion of a neighborhood of the origin. The neighborhood $\mathcal{W}(x, \epsilon)$ of a point x is a set characterized by the parameter ϵ containing x inside its interior. Then from Definition 1.1, to prove the stability of the origin, for any value ϵ defining a neighborhood $\mathcal{W}(0, \epsilon)$, we have to find a neighborhood defined by the value of η, $\mathcal{W}(0, \eta)$, such that every trajectory starting from $\mathcal{W}(0, \eta)$ will remain confined in $\mathcal{W}(0, \epsilon)$. In addition, if inside $\mathcal{W}(0, \epsilon)$ the trajectory goes towards the origin $x = 0$, the system is called asymptotically stable. On the other hand, a system is unstable means

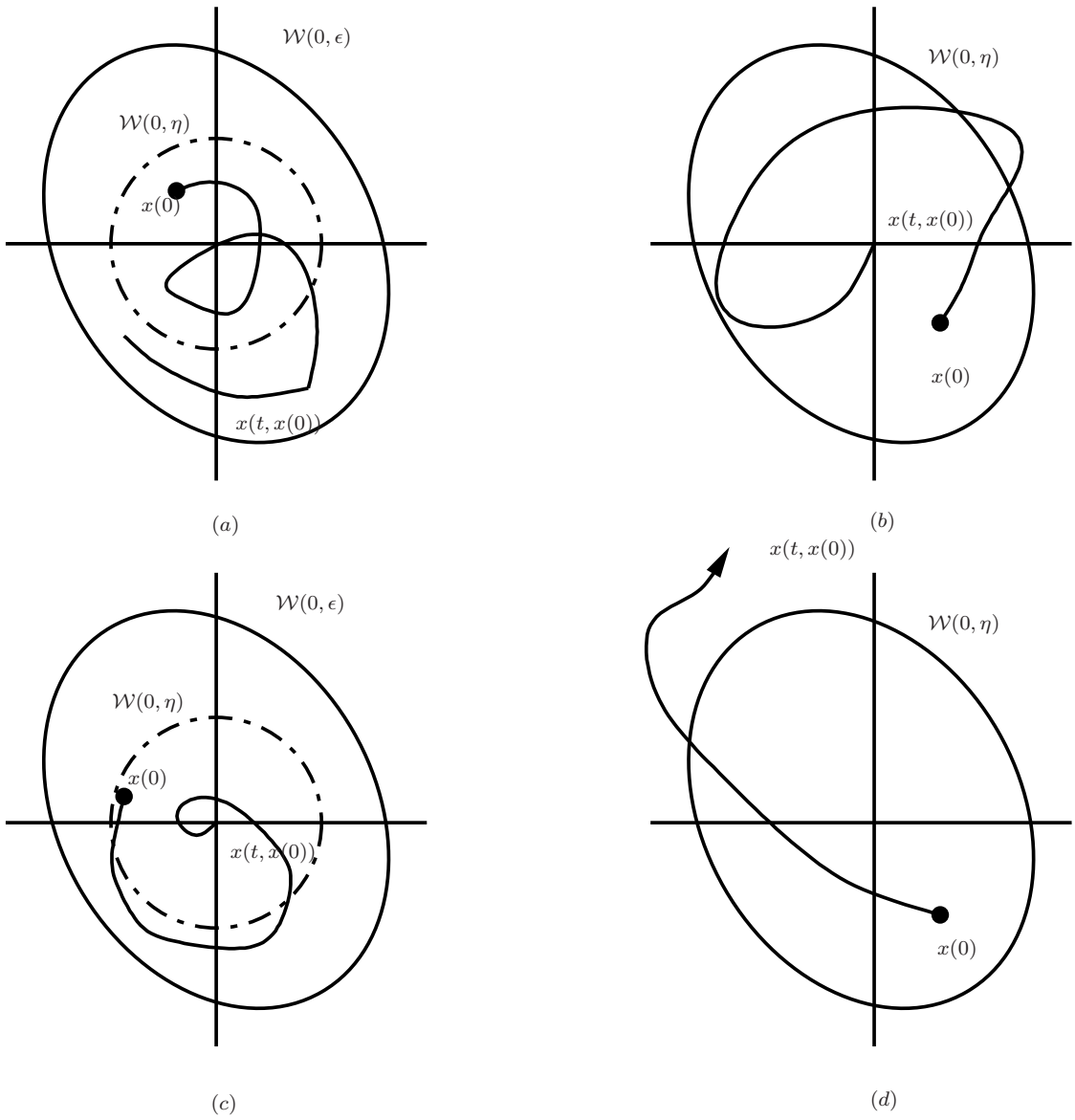

Figure 1.1: (a) Stable; (b) Attractive; (c) Asymptotically stable; (d) Unstable

that there is, at least, a trajectory with $x(0) \in \mathcal{W}(0,\eta) \subset \mathcal{W}(0,\epsilon)$ which does not remain in $\mathcal{W}(0,\epsilon)$ for $\epsilon > 0$ and for any $\eta > 0$ (See Figure 1.1 for illustration).

Given the previous definition and its explanation, we may define the concept of the domain of attraction of the origin as follows.

Definition 1.2. *The domain of attraction of the origin is the set $\mathcal{D}$ constituted by all the initial conditions, $x(0)$, from which any trajectory $x(t)$ of the system (1.2.2) converges to the origin.*

Remark 1.2. *Given a system (1.2.2), the domain of attraction of the origin can be either a strict subset of $\Re^n$ (local case) or the whole state space $\Re^n$ (global case).*

Definition 1.3. *The equilibrium of the origin is defined as*

1. **locally** *asymptotically stable, if the domain of attraction is strictly included in* $\Re^n$, $\mathcal{D} \subset \Re^n$.
2. **globally** *asymptotically stable, if the domain of attraction is* $\Re^n$, $\mathcal{D} = \Re^n$.

Theoretically, given Definition 1.1, to conclude stability of system (1.2.2), we need to know all the trajectories of the system which is, in general, really difficult, even impossible. Therefore, another formulation of the Lyapunov stability, using the notion of Lyapunov function, might be formulated. That is called the Lyapunov's second method.

1.2.2.a Lyapunov's Second Method

This so-called Lyapunov's second method seeks to characterize the stability of the equilibrium point without knowing explicitly the behavior of the trajectories near to this point. This method is based on the use of the Lyapunov functions. So let us first, define what we name a Lyapunov function.

Definition 1.4. *A candidate Lyapunov function is a function* $V : \mathcal{X} \subseteq \Re^n \to \Re^+$ *such that* V *is continuous as well as its partial derivatives, and,* V *is positive definite (i.e* $V > 0$ *for all* $x \neq 0$ *and* $V(0) = 0$*).*

The following theorem gives sufficient conditions for the stability of system (1.2.2).

Theorem 1.1. *Let* $\mathcal{X} \subset \Re^n$ *be an open set containing the origin and let* $V : \mathcal{X} \to \Re^+$ *be a candidate Lyapunov function.*

1. *If* $\dot{V}(x) \leq 0$ *for all* $x \in \mathcal{X}$*, then the origin is* **locally stable**.
2. *If* $\dot{V}(x) < 0$ *for all* $x \in \mathcal{X}$, $x \neq 0$ *, then the origin is* **locally asymptotically stable**.

where $\dot{V}$ *is the time-derivative of* V *along the system* (1.2.2) *defined as* $\dot{V} = \frac{\partial V}{\partial x}\ f(x)$.

A function V, as in Definition 1.4 is known as a *positive definite* function. A weaker condition could be $V(x) \geq 0$ for $x \neq 0$, which is said to be *positive semidefinite*. A function V is said to be *negative definite* or *negative semidefinite* when the function $-V$ is positive definite or positive semidefinite, respectively. Using this terminology the previous theorem may be reformulated as: *if there is a differentiable and positive definite function* V *such*

that its time-derivative $\dot{V}$ is negative semidefinite, then the origin is stable. Moreover if $\dot{V}$ is negative definite then the origin is asymptotically stable.

Considering $\mathcal{X} = \Re^n$, we can formulate, using Theorem 1.1, the sufficient conditions to assure global stability.

Theorem 1.2. *$x = 0$ is a globally stable equilibrium point for the system (1.2.2) if and only if there is a continuously differentiable function, $V : \Re^n \to \Re^+$ which verifies*

1. *$V(x) > 0$, $\forall x \neq 0$ and $V(0) = 0$,*
2. *$\dot{V}(x) < 0$ for all $x \in \Re^n$, $x \neq 0$*
3. *$\|x\| \to \infty \Rightarrow V(x) \to \infty$.*

Remark 1.3. *Theorem 1.2 gives sufficient conditions for the stability. If we are not able to find a Lyapunov function verifying Lyapunov's theorem, no conclusion may be extracted from that. Notice that the choice of the candidate Lyapunov function constitutes a hard task. There is no general procedure to find it and normally the experience or the physical behavior of the dynamic system may guide us into this choice.*

Typically, a common candidate Lyapunov function, widely used, has the following form: $V(x) = x'Px$, where P is a symmetric positive definite matrix. Such a function V is a quadratic function.

This kind of Lyapunov function is particularly interesting for linear or nonlinear systems with a linear part [Kha92, Vid92, Isi89]. Indeed, linear systems have a special interest as in practice a large number of systems can be studied through their linear representation. The characterization of the stability of the origin for the linear systems is presented in the next subsection.

1.2.3 Stability for autonomous linear systems

Consider a linear time-invariant system described by

$$\dot{x}(t) = Ax(t) \tag{1.2.5}$$

Then it has a unique equilibrium point at $x = 0$ if $det(A) \neq 0$, or equivalently, A is nonsingular. However, if the A matrix is singular there is a non trivial null space, and then the system (1.2.5) has a subspace of equilibrium points. From that point we only focus on the study of the stability of the origin $x = 0$.

A common result in linear systems theory is that the stability analysis of $x = 0$ may be achieved through the examination of the eigenvalues of A. The following theorem characterizes the stability properties of the origin [Che84, Lev95].

Theorem 1.3. *For the system (1.2.5), the equilibrium point is*

1. **asymptotically stable** *if* $Re(\lambda_i(A)) < 0, \forall i = 1, ..., n$. *In that case* A *is said to be Hurwitz.*
2. **critically stable** *if* $Re(\lambda_i(A)) \leq 0$, $\forall i = 1, ..., n$ *and for every eigenvalue* $Re(\lambda_j) = 0$, *its algebraic multiplicity* m_j *is associated to* m_j *eigenvectors.*
3. **critically unstable** *if* $Re(\lambda_i(A)) \leq 0$, $\forall i = 1, ..., n$ *and at least one eigenvalue* $Re(\lambda_j) = 0$, *with algebraic multiplicity* m_j, *is associated to less than* m_j *eigenvectors.*
4. **unstable** *if there is an eigenvalue of* A *which verifies* $Re(\lambda_i(A)) > 0$.

Remark 1.4. *For a given eigenvalue,* $\lambda_i(A)$, *its algebraic multiplicity is related to its multiplicity as a root from the characteristic polynomial of* A. *On the other hand, its geometric multiplicity is the number of eigenvectors of* A, *linearly independent, associated to* $\lambda_i(A)$ *[Che84]. Therefore, system (1.2.5) is critically stable if the Jordan decomposition of* A, *associated to the eigenvalues* $Re(\lambda_i(A)) = 0$, *is block-diagonal.*

1.2.4 Positive invariance and contractivity

There are two concepts that would be interesting to introduce as they are strongly related to the Lyapunov stability approach presented in Section 1.2.2: positive invariance and contractivity.

First, let us consider an autonomous system as it has been formulated in the system (1.2.2). Given $x_0 = x(0) \in \Re^n$ an initial condition for (1.2.2), then a trajectory for the system starting from x_0 is denoted $x(t, x_0)$.

Definition 1.5. *The set* $\mathcal{D} \subset \Re^n$ *is positively invariant with respect to the system (1.2.2) if* $\forall x_0 \in \mathcal{D}$ *we have* $x(t, x_0) \in \mathcal{D}, \forall t \geq 0$.

Definition 1.6. *The set* $\mathcal{D} \subset \Re^n$ *is contractive with respect to the system (1.2.2) if* $x(t) \in \alpha(t)\mathcal{D}$, *where* $\alpha(t) \leq 1$ *(and if* $0 \leq \alpha(\tilde{t}) < \alpha(t)$, *with* $\tilde{t} > t$, *such that* $x(\tilde{t}) \in \alpha(\tilde{t})\mathcal{D}$*), for a suitable function* $\alpha : [0, \infty) \to [0, \infty)$.

From Definition 1.5, we call a set $\mathcal{D}$ as positively invariant with respect to the system (1.2.2) if any trajectory starting in $\mathcal{D}$ remains in $\mathcal{D}$. On the other hand, a set $\mathcal{D}$ is contractive if any trajectory starting in $\mathcal{D}$ evolves to a smaller subset contained in $\mathcal{D}$. It is easy to see that a contractive set with respect to the system (1.2.2) is also positively invariant. The converse may be false. This is illustrated on Figure 1.2.

These concepts may be related to the definition of Lyapunov stability as in Definition 1.4. However, first we have to introduce the concept of Lyapunov surface.

Definition 1.7. *Given V a candidate Lyapunov function and c a positive scalar. The surface defined in the state space as*

$$\partial\Omega_c = \{x \in \Re^n; V(x) = c\}$$

with

$$\Omega_c = \{x \in \Re^n; V(x) \leq c\}$$

is called a Lyapunov surface.

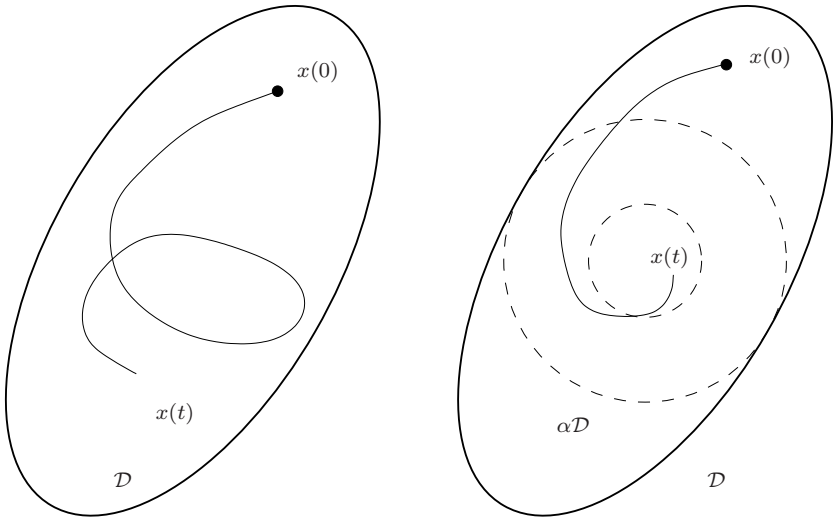

Figure 1.2: (a) Positive Invariance; (b) Contractivity

Then, if $\dot{V}(x) \leq 0$ for $x \in \mathcal{D}$ such as $V(x) = c$, the origin is a stable equilibrium point for the system (1.2.2), as the first condition of Theorem 1.1 is verified. At the same time, the set $\Omega_c = \{x \in \Re^n; V(x) \leq c\}$ bounded by the Lyapunov surface, $\partial\Omega_c = \{x \in \Re^n; V(x) = c\}$ is a positively invariant set, as any trajectory starting in Ω_c remains in it. Moreover, if $x = 0$ is stable then there exists a positive invariant set containing it. In addition, if $\dot{V}(x) < 0$ for all $x \neq 0$, by the second condition of Theorem 1.1, we can affirm that the origin is an asymptotically stable equilibrium point for the system (1.2.2). Moreover, the set Ω_c is a contractive set as all the trajectories go *asymptotically* towards a smaller set containing $x = 0$.

1.2.4.a LaSalle Invariance Principle

Theorem 1.1 provides a useful method to ensure the stability of dynamic systems. However, if the chosen Lyapunov function only verifies $\dot{V}(x) \leq 0$, then no conclusion about asymptotic stability can be obtained. Although there are other points different from the origin where $\dot{V}(x) = 0$, if we can assure that any trajectory may not stay at these points, except from $x = 0$, then the trajectories must converge to zero. That is what is

called LaSalle's Theorem or the LaSalle Invariance Principle. This result is stronger than Theorems 1.1 and 1.2.

Theorem 1.4. *Let*

1. $\mathcal{M}$ *be a positively invariant set with respect to the system (1.2.2).*
2. $V : \mathcal{M} \to \Re$ *be a function such that* $\dot{V}(x) \leq 0, \ \forall x \in \mathcal{M}$.
3. $E = \{x \in \mathcal{M}; \dot{V}(x) = 0\}$.
4. L *be the largest invariant set contained in* E.

Then, every trajectory starting in $\mathcal{M}$ *converges to* L.

If we want to prove the asymptotic stability, we need $x(t) \to 0$ as $t \to \infty$. In other words, from Theorem 1.4, we need to prove that the largest invariant set in E is reduced to the origin. In that case, we can formulate two corollaries allowing us to conclude on the asymptotic stability of the origin.

Corollary 1.1. *Let*

1. $x = 0$ *be an equilibrium point of the system (1.2.2).*
2. $V : \mathcal{M} \to \Re$ *be a Lyapunov function candidate such that* $\dot{V}(x) \leq 0, \ \forall x \in \mathcal{M}$.
3. $E = \{x \in \mathcal{M}; \dot{V}(x) = 0\}$ *and suppose that no trajectory can stay in* E*, other than the origin.*

Then, $x = 0$ *is asymptotically stable.*

Corollary 1.2. *Let*

1. $x = 0$ *be an equilibrium point of the system (1.2.2).*
2. $V : \Re^n \to \Re$ *be a Lyapunov function candidate such that* $\|V(x)\| \to \infty$ *as* $x \to \infty$ *and* $\dot{V}(x) \leq 0, \ \forall x \in \Re^n$.
3. $E = \{x \in \Re^n; \dot{V}(x) = 0\}$ *and suppose that no trajectory can stay in* E*, other than the origin.*

Then, $x = 0$ *is globally asymptotically stable.*

1.3 Modelling of dynamic systems under input constraints

In this section, the tools to describe a non-linear system under input constraints are presented. The model of the saturation function is carried out. Also, because of its practical interest, the dead-zone function is introduced.

1.3.1 Saturation and dead-zone functions

Let $u \in \Re^m$ be the control vector of a dynamical system, we define the saturation function as follows:

$$\Psi_{(\underline{u},\bar{u})} : \begin{cases} \Re^m & \rightarrow & \Re^m \\ u & \rightarrow & \Psi_{(\underline{u},\bar{u})}(u) = sat_{(\underline{u},\bar{u})}(u) \end{cases} \tag{1.3.1}$$

where $\underline{u}_{(i)} < 0$ and $\bar{u}_{(i)} > 0$, $\forall i = 1, ..., m$, are the lower and the upper limits of the saturation. Generally only the Lipschitz-memoryless-decentralized saturation function is considered for each i=1,...,m.

$$sat_{(\underline{u},\bar{u})}(u(t))_{(i)} = sat_{(\underline{u},\bar{u})}(u_{(i)}(t)) = \begin{cases} \bar{u}_{(i)} & \text{if} \quad u_{(i)}(t) > \bar{u}_{(i)} \\ u_{(i)}(t) & \text{if} \quad \underline{u}_{(i)} \leq u_{(i)}(t) \leq \bar{u}_{(i)} \\ \underline{u}_{(i)} & \text{if} \quad u_{(i)}(t) < \underline{u}_{(i)} \end{cases} \tag{1.3.2}$$

Commonly, in order to simplify the mathematical development, the saturation is taken as symmetric. That is equivalent to $\bar{u} = -\underline{u}$. When both upper and lower bounds are equal in absolute value the notation is simplified by replacing them by $u_0 = |\bar{u}| = |\underline{u}|$. Figure 1.3a shows the general aspect of a symmetric saturation function. Symmetric saturations are then denoted: $sat_{(u_0)}(u)$.

The saturation function is an intuitive formulation to describe the physicial limitation of the actuators. However from a theoretical point of view the called dead-zone appears to be a more interesting tool. The dead-zone function presented in Figure 1.3b is an alternative non-linear function to represent the control constraint. The advantage of the dead-zone formulation is that it can be seen as a disturbance which is null in the linear domain. On the other hand, when the actuator saturates, the dead-zone is active modifying the linear dynamics. Its formulation is given in the following equation:

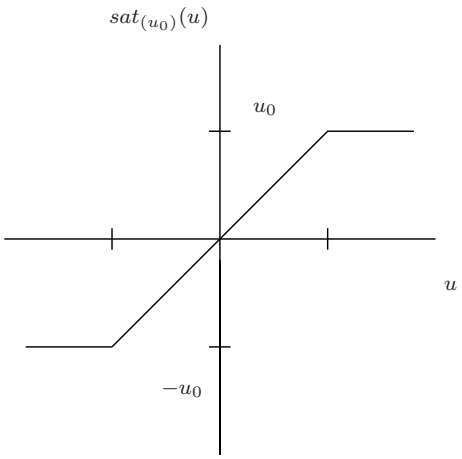

(a)

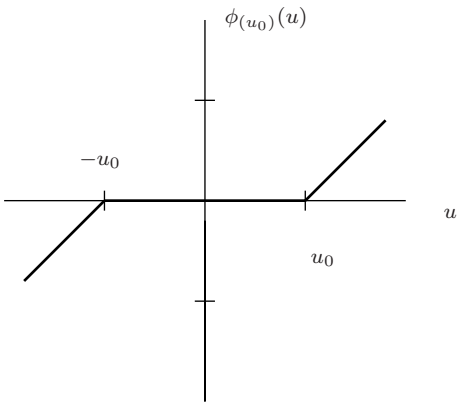

(b)

Figure 1.3: Saturation and Dead-zone non-linear functions.

$$\begin{aligned} \phi_{(\underline{u},\bar{u})}(u) &= u - sat_{(\underline{u},\bar{u})}(u) \\ \phi_{(\underline{u},\bar{u})}(u_{(i)}) &= \begin{cases} u - \bar{u}_{(i)} & \text{if} \quad u_{(i)} > \bar{u}_{(i)} \\ 0 & \text{if} \quad \underline{u}_{(i)} \leq u_{(i)} \leq \bar{u}_{(i)} \\ u - \underline{u}_{(i)} & \text{if} \quad u_{(i)} < \underline{u}_{(i)} \end{cases} \end{aligned} \tag{1.3.3}$$

Similarly, a symmetric version of the dead-zone (1.3.3) is considered:

$$\begin{aligned} \phi_{(u_0)}(u) &= u - sat_{(u_0)}(u) \\ \phi_{(u_0)}(u_{(i)}) &= \begin{cases} u - u_{0(i)} & \text{if} \quad u_{(i)} > u_{0(i)} \\ 0 & \text{if} \quad -u_{0(i)} \leq u_{(i)} \leq u_{0(i)} \\ u + u_{0(i)} & \text{if} \quad u_{(i)} < -u_{0(i)} \end{cases} \end{aligned} \tag{1.3.4}$$

Both saturation and dead-zone non-linearities are depicted in Figure 1.3.

1.3.2 Closed-loop system with static state feedback

Consider a linear time-invariant system defined by

$$\dot{x}(t) = Ax(t) + Bu(t) \tag{1.3.5}$$

where $A \in \Re^{n\times n}$ and $B \in \Re^{n\times m}$.

Consider now that the input $u(t)$ is saturated by a saturation function like (1.3.2). And suppose that the system presented in (1.3.5) is in closed-loop with a static saturated state feedback. Then, the feedback loop can be defined through the following expression

$$u(t) = sat_{(u_0)}(Kx(t)),\ K \in \Re^{m\times n} \tag{1.3.6}$$

The final expression for the closed-loop system with the previous feedback (1.3.6) and the system (1.3.5) is written as follows:

$$\dot{x}(t) = Ax(t) + Bsat_{(u_0)}(Kx(t)) \tag{1.3.7}$$

It is easy to see, by the definition of the saturation function (1.3.2), that the set

$$S_l(u_0) = \{x \in \Re^n; -u_{0(i)} \leq K_{(i)}x \leq u_{0(i)},\ \forall i = 1, ..., m\} \tag{1.3.8}$$

is the region of linearity for the system (1.3.7). Therefore, in this domain, the non-linear system (1.3.7) behaves like

$$\dot{x}(t) = (A + BK)x(t). \tag{1.3.9}$$

Remark 1.5. *For all $x \in S_l(u_0)$ the saturated system (1.3.7) follows the time-invariant system (1.3.9). However, even if an initial condition $x(0) \in S_l(u_0)$, we cannot conclude that the resulting trajectory $x(t)$ stays in $S_l(u_0)$, $\forall t > 0$, even if the closed-loop system (1.3.7) is asymptotically stable ($Re(\lambda_i(A + BK)) < 0$). This is the reason why the non-linearity introduced by the saturation has to be taken into account in order to analyze the behavior of system (1.3.7). To ensure linear behavior for all trajectories we should find the largest invariant set included in $S_l(u_0)$. Then, any trajectory $x(t, x(0))$ starting in this invariant set would be described by the dynamics of system (1.3.9) [Kha92].*

Finally the system (1.3.7) may be rewritten replacing the saturated function by a dead-zone function (1.3.4) as follows:

$$\dot{x}(t) = (A + BK)x(t) - B\phi_{(u_0)}(Kx(t)) \tag{1.3.10}$$
$$\dot{x}(t) = \tilde{A}x(t) + \tilde{B}\phi_{(u_0)}(Kx(t)) \tag{1.3.11}$$

with obvious definitions of $\tilde{A}$ and $\tilde{B}$.

Remark 1.6. *Writing the system as in (1.3.10)-(1.3.11) gives the possibility to represent the system through a LFT (Linear Fractional Transformation) where the dead-zone is an uncertainty of the linear system [RBTP07].*

Considering system (1.3.11) the negativity condition of the time-derivative of a quadratic Lyapunov function $V(x) = x^{'}Px$, $P = P^{'} > 0$, reads:

$$\dot{V}(x) = \dot{x}^{'}Px + x^{'}P\dot{x} = x^{'}(\tilde{A}^{'}P + P\tilde{A})x + x^{'}P\tilde{B}\phi_{(u_0)}(Kx) + \phi_{(u_0)}(Kx)^{'}\tilde{B}^{'}Px < 0 \tag{1.3.12}$$

then, since the term $x^{'}P\tilde{B}\phi_{(u_0)}(Kx)$ is a real, $x^{'}P\tilde{B}\phi_{(u_0)}(Kx) = \phi_{(u_0)}(Kx)^{'}\tilde{B}^{'}Px$ and hence relation (1.3.12) reads:

$$\dot{V}(x) = \dot{x}^{'}Px + x^{'}P\dot{x} = x^{'}(\tilde{A}^{'}P + P\tilde{A})x + 2x^{'}P\tilde{B}\phi_{(u_0)}(Kx) < 0 \tag{1.3.13}$$

When the variables P and K are unknown, the inequality (1.3.13) is non-linear and it is difficult to directly compute the domain of the state space where it is verified. This domain is generally called the domain of stability. The strategy to compute this domain consists in proposing a characterization (conservative) of the saturation (dead-zone) function which provides a sufficient convex condition for the relation $\dot{V}(x) < 0$.

First, the modelling by non-linear sector condition is presented. Afterwards, the saturation regions approach and the polytopic approach are developed. Only a brief formulation is exposed.

1.3.3 Non-linear sector condition

Memoryless function like saturation can be modelled by a sector non-linearity. An approach has been developed in [GdSJT05, TPGdSJ06] to include the saturation in a non-linear sector. Consider a dead-zone function $\phi_{(u_0)}(\cdot)$, as it has been defined in (1.3.4) and a closed-loop system (1.3.11). Finally, consider the following polyhedral set:

$$\mathcal{S}(u_0) = \left\{(u, \omega) \in \Re^m \times \Re^m; \left|u_{(i)} + \omega_{(i)}\right| \leq u_{0_{(i)}}, i = 1, ..., m\right\} \tag{1.3.14}$$

With all these elements the following Lemma may be stated.

Lemma 1.1. *[TPGdSJ06] Consider the function $\phi_{(u_0)}(u)$ defined in (1.3.4). If u and ω belong $\in \mathcal{S}(u_0)$ then the relation*

$$\phi_{(u_0)}(u)'T[\phi_{(u_0)}(u) + \omega] \leq 0 \tag{1.3.15}$$

is verified for any matrix $T \in \Re^{m\times m}$ diagonal and positive definite.

This lemma is proven in [TPGdSJ06] for a general case of nested saturations whereas the simple case of one saturation is studied in [GdSJT05]. Condition (1.3.15) is called a modified sector condition since it can be considered as an extension of the classical one described in [Kha92]:

$$\phi_{(u_0)}(u)'T[\phi_{(u_0)}(u) - \Lambda u] \leq 0 \tag{1.3.16}$$

where Λ stands for a diagonal matrix fixed *a priori* verifying $0 < \Lambda < I_m$. Replacing $\omega = -\Lambda u$ in relation (1.3.15), one gets (1.3.16). The classical sector condition (1.3.16) is a particular case of the modified sector condition (1.3.15) hence the classical sector condition is more conservative than the modified one [TT09, TGGE07]. Moreover, the classical condition (1.3.16) is only valid locally for values of u in the interval $[-L, L]$, as depicted in Figure 1.4.

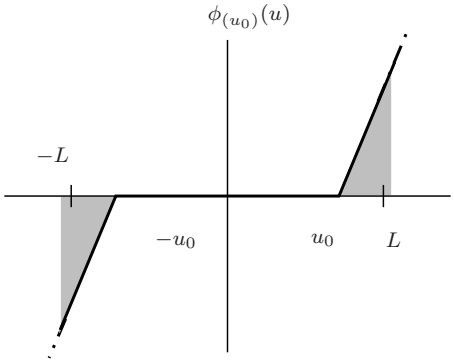

(a) Modified sector condition (1.3.15)

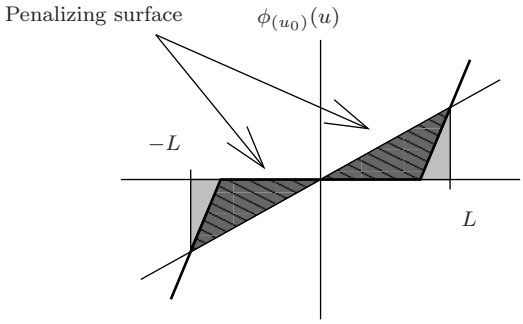

(b) Classical sector condition (1.3.16)

Figure 1.4: Graphic interpretation of sector conditions.

A graphical interpretation of the previous result is proposed in the Figure 1.4 for the case of a single input $m = 1$. The grey zone represents the different possible values

of $\phi_{(u_0)}(\cdot)$ verifying the modified sector condition (see Figure 1.4a). It is important to point out that the dead-zone function is not the only function belonging to this sector. Therefore, one deduces that some conservatism is induced by this modelling. Nevertheless, this conservatism is null in the linear domain (interval $[-u_0, u_0]$) for the modified sector condition (1.3.15). On the other hand, the classical sector condition (see Figure 1.4b) adds more conservatism than the modified one. This additional conservatism is remarkable in the linear domain as there are values satisfying the sector condition while in the modified case (1.3.15) any extra value is included. Graphically, one can see the extra conservatism introduced by (1.3.16) with respect to (1.3.15) as there exists a penalizing surface (darker zone) which contains extra values verifying the sector condition.

Other ways to represent the saturation can be considered. Some of them are now briefly presented.

1.3.4 Saturation regions approach

The exact representation of the saturation function may be carried out by dividing the state space in 3^m different regions [JR98, GdSJT99, GdSJ97].

First of all, define a vector $\xi \in \Re^m$ where each element $\xi_{(i)} = \{-1, 0-1\}, i = 1, ..., m$. Each element is related to a component of the control vector u. Then, the value 1, 0 or -1, for $\xi_{(i)}$ means that the associated control component is saturated to the upper limit, non-saturated or saturated to the lower limit, respectively. All this might be stated as:

1. If $u_{(i)} = u_{0(i)}$, then $\xi_{(i)} = 1$.
2. If $u_{(i)} = K_{(i)}x$, then $\xi_{(i)} = 0$.
3. If $u_{(i)} = -u_{0(i)}$, then $\xi_{(i)} = -1$.

Thus, each vector ξ represents a possible combination between saturated or non-saturated inputs. It is easy to realize that we need 3^m vectors ξ in order to fully describe the behavior of the constrained input system. For each one of these vectors ξ, x belongs to a *saturation region*. Each region, related to a vector $\xi_{(i)}, i = 1, ..., 3^m$, can be defined by the polyhedral set:

$$\mathcal{S}(R_i, d_i) = \{x \in \Re^n; R_i x \preceq d_i\} \tag{1.3.17}$$

where $d_i \in \Re^{l_i}$ is a vector composed by the saturation limits $\pm u_0$ and $R_i \in \Re^{l_i \times n}$ a matrix composed by the rows of $\pm K$.

Remark 1.7. *Such a representation is mainly used for stability analysis purpose, and, in general, in the case of systems with few inputs. As it is remarked in [GdSJ97, GdSJTR05], as the dimension of the input vector increases, the algorithm tends to become numerically untractable. For example, in the case of a two inputs constrained system the number of regions to consider is already large:* $m = 2 \rightarrow 3^m = 9$ *regions.*

1.3.5 Polytopic approach

In this section we present the polytopic representation proposed by [HLC02] and based on the use of linear differential inclusion (LDI). Other previous developments regarding polytopic representation for saturated systems can be found in [BT96, HT99, GdSJT06].

Let us first give the definition of a LDI [BEGFB01].

Definition 1.8. *A linear differential inclusion (LDI) is given by:*

$$\dot{x} \in \Omega_x;\ x(0) = x_0$$

where Ω_x *is a subset of* $\Re^n$.

By this way the following result applying to the saturated system (1.3.7) can be stated.

Define the polyhedral set $S_p(H, u_0)$:

$$S_p(H, u_0) = \left\{x \in \Re^n; -u_{0(i)} \leq H_{(i)}x \leq u_{0(i)}, i = 1, ..., m\right\} \tag{1.3.18}$$

Lemma 1.2. *[HLC02] If* $x \in S_p(H, u_0)$ *then the saturated term satisfies:*

$$sat_{(u_0)}(Kx) \in Co\left\{(G_jK + (I_m - G_j)H)x, j = 1, ..., 2^m\right\} \tag{1.3.19}$$

where $G_j, j = 1, ..., 2^m$, *are diagonal matrices whose diagonal elements take the value 1 or 0 and Co stands for the closed convex hull.*

Then, it follows for $x \in S_p(H, u_0)$:

$$\dot{x} \in Co\left\{A + B(G_jK + (I_m - G_j)H)x, j = 1, ..., 2^m\right\} \tag{1.3.20}$$

Relation (1.3.20) means that for $x \in S(H, u_0)$ the saturated system (1.3.7) can be represented by a polytopic model:

$$\dot{x} = \sum_{j=1}^{2^m} \lambda_j (A + B(G_jK + (I_m - G_j)H)x \tag{1.3.21}$$

with $\sum_{j=1}^{2^m} \lambda_j = 1, \lambda_j \geq 0$.

For more details about this kind of model, the reader can consult [HL01]. Some extensions to the case of non-linear differential inclusions (NLDI) have been proposed by Alamo and his co-workers [ACL05]. Moreover, note that the dead-zone $\phi_{(u_0)}(Kx)$ could be also approximated through LDI [CTQ08].

Remark 1.8. *One of the main drawbacks of the polytopic approach is a potential larger numerical complexity, in comparison with the modified sector condition modelling mainly to the tests to provide on 2^m parties. In [TPGdSJ06] a comparison between both approaches is done and the LMI complexity for each case is discussed.*

1.4 Analysis of a dynamic systems under input constraints

The polytopic modelling presented in Section 1.3.5 provides matrix inequalities for assessing the stability of system (1.3.11). These results are interesting for the stability analysis of saturated systems or even the synthesis of controllers considering the saturation [HL01, KGE02, PTH07]. However this is not the case when another approach to handle the saturation is considered [HLC02, CLW02, HTZ05]. This is the anti-windup synthesis problem which is briefly introduced in Section 1.4.2 and fully detailed in Chapter 3. Nevertheless, let us remark that the use of the polytopic approach asks for the resolution of a non-convex problem when the anti-windup resolution is sought, even if only the static case is considered [CLW02].

The main objective of this manuscript is to provide constructive methods for the anti-windup design and their evaluation for control of satellites. The modelling by sector condition presents convex conditions for the static anti-windup synthesis and under certain conditions, for the dynamic anti-windup synthesis. Therefore, in this manuscript the sector condition modelling is kept instead of using the polytopic or the saturation regions approaches.

In this section a theorem for stability analysis is presented. These conditions are presented in terms of Linear Matrix Inequalities (LMI) providing an estimation of the stability domain. Moreover, optimization techniques are introduced to maximize the computed estimation. Finally, a brief introduction to the windup problem and its related solution, the anti-windup compensator, are given.

1.4.1 Stability domain estimation

Let us define a saturated system like (1.3.11):

$$\left\{\begin{array}{lcl} \dot{x} & = & Ax + B\phi_{(u_0)}(y) \\ y & = & Cx \in \Re^m \\ x(0) & = & x_0 \in \Re^n \end{array}\right. \tag{1.4.1}$$

Then, the purpose of the analysis is to find the larger domain of the state space where the stability of the constrained system (1.4.1) is verified.

Remark 1.9. *The feedthrough between $\phi_{(u_0)}$ and y is null, as nested saturations are avoided. This choice is motivated by the following reasons: several definitions and results are presented in this chapter. No proof is given as they are classical results and could be easily found in the literature. See, for example, works from Khalil [Kha92], Slotine and Li [SL91] and Vidyasagar [Vid92].*

- *Nested saturations arise when limitations such as rate saturation are considered. In some case this phenomenon may be avoided with the modelling proposed in [BTF06].*
- *Extra theoretical considerations have to be taken into account to treat nested saturations, increasing the level of conservatism which is undesirable for synthesis purpose. Some solutions can be however considered in this case: see, for example [TPGdSJ06, BL02].*

The following theorem allows the characterization of a stability domain for system (1.4.1) [GdSJT05, BTF06].

Theorem 1.5. (Stability domain analysis) *If there exist a symmetric positive-definite matrix $W \in \Re^{n\times n}$, a diagonal positive-definite matrix $S \in \Re^{m\times m}$ and a matrix $Y \in \Re^{m\times n}$ such as the following LMI conditions are verified:*

$$\left[\begin{array}{cc} WA' + AW & BS + Y' \\ * & -2S \end{array}\right] < 0 \tag{1.4.2}$$

$$\left[\begin{array}{cc} W & WC'_{(i)} - Y'_{(i)} \\ * & u^2_{0(i)} \end{array}\right] \geq 0, \quad \forall i = 1, ..., m \tag{1.4.3}$$

then the ellipsoid:

$$\mathcal{E}(P) = \{x \in \Re^n; x'Px \leq 1\} \tag{1.4.4}$$

with $P = W^{-1}$, is a domain of asymptotic stability for the system (1.4.1).

Proof of Theorem 1.5: Consider a quadratic Lyapunov function $V(x) = x'Px$ with $P = P' > 0$. Let us get back the expression of the time-derivative of the Lyapunov function in (1.3.13).

$$\dot{V}(x) = \dot{x}^{'} Px + x^{'} P\dot{x} = x^{'}(A^{'}P + PA)x + 2x^{'} PB\phi_{(u_0)}(Cx) \tag{1.4.5}$$

The sector condition (1.3.15) domain of validity is defined by the following set:

$$\mathcal{S}(u_0) = \left\{ x \in \Re^n ; \left| (C_{(i)} - G_{(i)})x \right| \leq u_{0_{(i)}}, i = 1, ..., m \right\} \tag{1.4.6}$$

One to guarantee that the sector condition is satisfied in the whole ellipsoid $\mathcal{E}(P)$ (1.4.4). This is assured by imposing $\mathcal{E}(P) \subseteq S(u_0)$. Then the following relationship has to hold:

$$x^{'}(C_{(i)} - G_{(i)})^{'} \frac{1}{u_{0(i)}^2}(C_{(i)} - G_{(i)})x \leq x^{'} Px \leq 1, i = 1, ..., m \tag{1.4.7}$$

to satisfy (1.4.7) it suffices to verify:

$$P - (C_{(i)} - G_{(i)})^{'} \frac{1}{u_{0(i)}^2}(C_{(i)} - G_{(i)}) \geq 0, i = 1, ..., m \tag{1.4.8}$$

Hence, by Schur's complement one obtains the following matrix inequality:

$$\begin{bmatrix} P & C_{(i)}^{'} - G_{(i)}^{'} \\ * & u_{0(i)}^2 \end{bmatrix} \geq 0, \ i = 1, ..., m \tag{1.4.9}$$

Finally by pre- and post-multiplying (1.4.9) by $diag(P^{-1}, I)$, one obtains relation (1.4.3) with $W = P^{-1}$ and $Y = GW$.

Therefore, the satisfaction of relation (1.4.3) guarantees that $\mathcal{E}(P) \subseteq S(u_0)$. Then sector condition (1.3.15) is verified in the ellipsoid (1.4.4) defined by the quadratic Lyapunov function.

Applying the sector condition (1.3.15) in Lemma 1.1 with $\omega = -Gx$ and using the $\mathcal{S}$-procedure [AG64] the inequality (1.4.5) becomes:

$$\begin{aligned} \dot{V}(x) \leq \dot{x}^{'} Px + x^{'} P\dot{x} &= x^{'}(A^{'}P + PA)x + 2x^{'} PB\phi_{(u_0)}(Cx) \\ &- 2\phi_{(u_0)}(Cx)'T[\phi_{(u_0)}(Cx) - Gx] \end{aligned} \tag{1.4.10}$$

for any $x \in \mathcal{E}(P)$.

With $S = T^{-1}$ and $W = P^{-1}$, the right-hand term of relation (1.4.10) can be expressed in a matrix formulation:

$$\mathcal{L} = \begin{bmatrix} x^{'}W^{-1} & \phi_{(u_0)}^{'} S^{-1} \end{bmatrix} \begin{bmatrix} WA^{'} + AW & BS + WG^{'} \\ * & -2S \end{bmatrix} \begin{bmatrix} W^{-1}x \\ S^{-1}\phi_{(u_0)} \end{bmatrix}$$

Finally by using the change of variables $GW = Y$ one recovers condition (1.4.2). Therefore, the satisfaction of relation (1.4.2) ensures that $\mathcal{L} < 0$ or equivalently $\dot{V}(x) \leq \mathcal{L} < 0$, that is, the negativity of the time-derivative of Lyapunov function for any x in the ellipsoid $\mathcal{E}(P)$ (1.4.4).

In conclusion, $\mathcal{E}(P)$ is a region of asymptotic stability for system (1.4.1).

End of Proof.

Theorem 1.5 provides conditions to find a possible domain of stability. However the problem can be transformed into an optimization problem. A possible manner is to maximize the volume of the stability domain $\mathcal{E}(P)$. Indeed, the volume of an ellipsoid defined by relation (1.4.4) is proportional to the determinant of the matrix $W = P^{-1}$. Hence, to maximize the volume of $\mathcal{E}(P)$ is equivalent to maximize the trace of W, which can be written as a convex problem [VBW98, TGGE07]. Then the problem is stated as

$$min\ \rho \text{ s.t. } (1.4.2), (1.4.3) \text{ and:}$$

$$\begin{bmatrix} W & I_n \\ * & \rho I_n \end{bmatrix} \geq 0 \tag{1.4.11}$$

It is also possible to maximize the domain of stability $\mathcal{E}(P)$ in a given direction v of the state space. This is translated to the minimization of the objective β. This optimization is stated as

$$min\ \beta \text{ s.t. } (1.4.2), (1.4.3) \text{ and:}$$

$$\begin{bmatrix} W & v \\ * & \beta \end{bmatrix} \geq 0 \tag{1.4.12}$$

Some other solutions are proposed by [HL01].

1.4.1.a Educational example

Let us recover the education example to illustrate the computation of the stability domain estimation. The system considered is described by (9). With some tedious algebra,

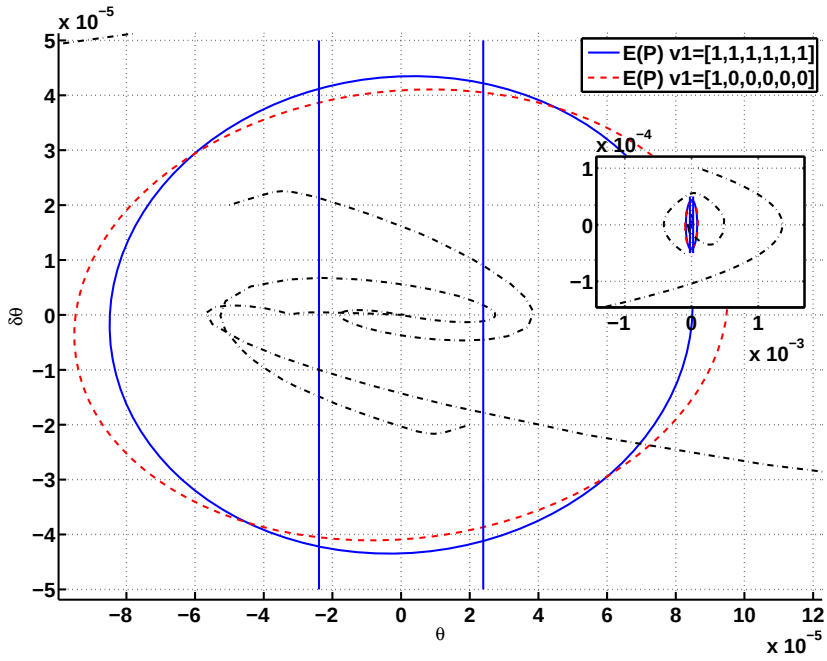

Figure 1.5: Stability domain estimation of system (9).

one obtains the closed-loop matrices and set the relationship with the general system considered in (1.4.1). The closed-loop matrices then read:

$$A = \begin{bmatrix} A_p + B_p D_c C_p & B_p C_c \\ B_c C_p & A_c \end{bmatrix}; B = [B_p' \;\; 0]'; C = [D_c C_p \;\; C_c]. \tag{1.4.13}$$

with the state $x = [x_p' \;\; x_c']'$ and the output $y = y_c$.

Given matrices (1.4.13) one may apply directly Theorem 1.5. Two problems are solved. First the size of the stability domain is maximized through the trace of P, thus optimization problem (1.4.11) applies. Then the optimization of the stability domain in a given direction v is performed, thus (1.4.12) applies. The solutions to these problems are compared in Figure 1.5. In this example $v = [1 \;\; 0 \;\; 0 \;\; 0 \;\; 0 \;\; 0]'$, that is, the domain is maximized in the $x_{(1)}$, direction which corresponds in the education example case to $x_{p(1)} = \theta$.

Figure 1.5 shows the stability domain estimation in the $(\theta, \dot{\theta})$ plane. Normally the stability domain is a $\Re^6$ space. However, the controller state x_c can be considered to be initialized at the origin [CNE05]. Then, the section $x = [x_p' \;\; 0]'$ is representative of the actual stability domain. In the figure one can see the interest to maximize towards a given direction instead of seeking the whole domain as we may obtain a better estimation of the initial admissible state. Moreover because of the fact that x_c is normally initialized at the origin it seems more judicious to steer the optimization towards the sensible state directions. In addition several trajectories of the system have been plotted showing that the domain computed is a conservative estimation as some initial conditions outside the

domain still converge. Parallel lines limit the linear domain, that is the set defined in (1.3.8).

1.4.2 The windup phenomenon

The windup is a phenomenon which becomes manifest by an important overshoot in the control and output signals and an excessive reaction time due to the saturation of the actuators. The windup phenomenon was first documented in the middle of the 20^{th} century [Loz56]. It usually appears in systems which include actuators subject to saturations and present a feedback loop through a controller including integrators, like for example a PID [FR67, AR89]. When the saturation is active, the continuous error is integrated, distorting the control commands. Neglecting these limitations can be a source of undesirable or even catastrophic behaviors for the closed-loop system as a strong degradation of performance in even the loss of stability [BHSB96]. An approach to deal with this phenomenon is the *anti-windup compensation* [TT09, GTTZ09].

The basic idea is to introduce control modifications, in the previously designed linear controller, in order, for example, to enlarge the region of stability of the closed-loop system or to recover as much as possible the performance of the unsaturated (linear) system. The anti-windup compensator, therefore, is an extra layer which is added to the linear controller in order to consider the non-linear behavior.

Figure 1.6 presents the general principle of the anti-windup technique. There is a separation between the "unconstrained" controller and anti-windup compensator showing this idea of extra layer. The anti-windup receives as an input the difference between the saturated and unsaturated control signal, to generate two output signals, one (v_y) which modifies the controller output and another (v_x) which modifies the controller dynamics.

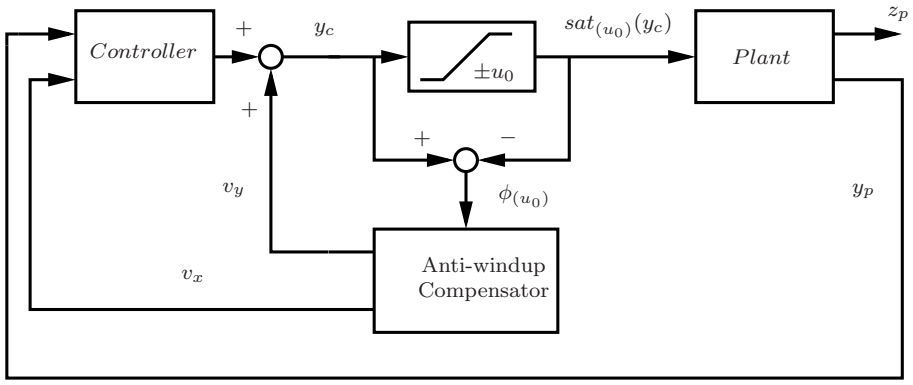

Figure 1.6: General anti-windup structure

Remark 1.10. *The signal v_x may influence the controller either by modifying directly the controller state equation (i.e. v_x has the same dimension of the state vector) or by being*

added to the plant output y_p (i.e. v_x and y_p have the same dimension), without changing substantially the stability and optimality conditions.

Chapter 3 will be dedicated to different approaches in the literature and constructive techniques for designing suitable anti-windup compensator.

1.5 Conclusion

The main elements on the stability of saturated system have been provided in this chapter.

First, a review of the main concepts on the stability of dynamic systems has been presented. Stability, attraction and asymptotic stability concepts have been fully described in the framework of Lyapunov stability. In particular, Lyapunov's second method has been shown as an interesting practical method to study the stability of dynamic systems.

The modelling of a particular case of dynamic system has been tackled: namely systems presenting a non-linearity input constraint. Two models for this particular non-linearity have been provided: the saturation function and the dead-zone function. These functions have to be characterized to apply Lyapunov's second method. Three characterizations have been presented: the sector condition approach, the saturation regions approach and the polytopic approach.

Finally, some analysis tools for the dynamic systems under input constraints have been given. The application of Lyapunov second method along with the sector condition characterization of the saturation function have provided constructive conditions for the estimation of the domain of stability. These conditions have been given into the form of Linear Matrix Inequalities conditions. They have been briefly applied in the case of the educational example.

Chapter 2

Symmetrizing saturations

Outline of the chapter

2.1 Introduction

Saturations are present in most modern industrial applications. The synthesis of non-linear control laws considering saturation is an important issue in the literature. The saturations can be a source of undesirable or even catastrophic behaviors for the closed-loop

system (as loss of stability of the system [BHSB96]). Research has focused on stability domain estimation [SS99, VBW98], control design under actuator constraints [HL01, KGE02] and even on so-called anti-windup compensator design [Tee99, BRTZ00, TGGE07]. For example, amplitude and/or rate limitations of the actuator have been implicated in various aircraft crashes and the meltdown of the Chernobyl nuclear power station [Ste89].

Spacecraft control is also subject to saturation problems. Future space missions present more demanding requirements in terms of control precision. Even though new actuators can satisfy the demands on high precision, the maximal propulsion capacity appears to be critically low, which could lead to saturation of the actuator.

Traditionally, on-board satellite control has been focused on attitude control. It seeks to ensure the right orientation of the satellite in order to satisfy the needs of the mission. This kind of control system is performed with an architecture based on the use of reaction wheels as primary torque actuator [CNE05]. The principle is to counteract external disturbance torques by a closed-loop strategy with the previous mentioned actuators and attitude sensors. Future missions requirement includes acceleration or relative position control which requires actuators that can provide an effort in the linear axis. Therefore propulsive systems apply.

Moreover, systems using a propulsive system usually present an *allocation problem* [Dur93]. Dynamical systems like satellites are modelled by the classic equations of rigid body dynamics which are expressed in terms of angular and linear accelerations as a function of an effort vector composed by forces and torques. However, as the action is performed through a propulsive system, which provides unidirectional impulses, a function is needed to determine how to generate a specified generalized effort (forces and torques) from a redundant set of actuators. Allocation functions are normally highly non-linear and, thus, it is difficult to set mathematical conditions to ensure stability and performance level. Some works have instead considered optimal MIMO controllers which stabilize the closed-loop system as well as perform the control allocation. In this work only the first approach is considered. A general introduction to the allocation function and possible approximations for it are proposed in this chapter.

Saturations associated to thrusters appear to be asymmetric. Indeed this kind of actuators only provides a positive thrust. Generally, in the literature, in either stability domain estimation or anti-windup compensator design for systems under actuator constraints, only the symmetric saturation has been considered. Some few works have symmetrized the saturations by a conservative approach such as [Lan03]. In this chapter two symmetrizing techniques are proposed to enable further analysis and anti-windup loop synthesis methods.

This chapter is organized as follows. First, in Section 2.2 the structure of the system considered is introduced. Then, the allocation problem is provided in Section 2.3. Afterwards, some allocations functions are proposed in Section 2.4. Finally symmetrizing techniques are proposed in Section 2.5.

2.2 System structure description

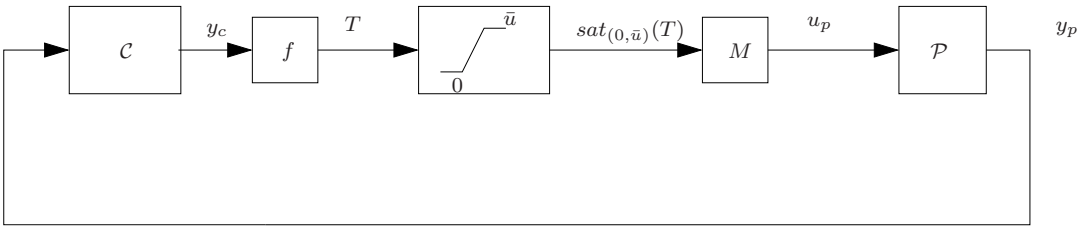

Figure 2.1: Closed-loop system under study.

Let us consider the block-diagram in Figure 2.1 describing the control diagram of a system presenting an allocation function and thrusters as actuators. The plant is described by the following equations:

$$\mathcal{P} : \begin{cases} \dot{x}_p &= A_p x_p + B_p u_p \\ y_p &= C_p x_p \end{cases} \tag{2.2.1}$$

with $x_p \in \Re^{n_p}$ the state of the plant, $y_p \in \Re^q$ the output of the plant and $u_p \in \Re^{m_c}$ the control input. Matrices A_p, B_p and C_p are real constant matrices of appropriate dimensions. Pairs (A_p,B_p) and (C_p,A_p) are assumed to be controllable and observable, respectively.

A controller, computed by whatever way, is given and it ensures the asymptotic stability and some performance level for the unconstrained (i.e. linear) closed-loop system. A state space representation of the controller $\mathcal{C}$ is given by the following formulation:

$$\mathcal{C} : \begin{cases} \dot{x}_c &= A_c x_c + B_c y_p \\ y_c &= C_c x_c + D_c y_p \end{cases} \tag{2.2.2}$$

where $x_c \in \Re^{n_c}$ is the state of the controller and $y_c \in \Re^{m_c}$ is the control output. A_c, B_c, C_c, D_c, are real constant matrices of appropriate dimensions.

The relationship between the control output y_c and the control input u_p is performed by a propulsive system. Thrusters do not perform directly the signal of the control output y_c. The relationship between y_c and the thrust vector $T \in \Re^m$ is set by an allocation function f. On the other hand, the thrust T is linked with the control input u_p through the influence matrix $M \in \Re^{m_c \times m}$. These elements are described later in Section 2.3. Finally, thrusters present power limitations which are modelled by a saturation function. Moreover thrusters only provide a positive thrust as they only can thrust towards one direction. Thrusters are modelled by a decentralized non-symmetric saturation between 0 and $\bar{u}$:

$$sat_{(0,\bar{u})}(T_{(i)}) = \begin{cases} \bar{u}_{(i)} & \text{if} \quad T_{(i)} > \bar{u}_{(i)} \\ T_{(i)} & \text{if} \quad 0 \leq T_{(i)} \leq \bar{u}_{(i)} \\ 0 & \text{if} \quad T_{(i)} < 0 \end{cases} \quad , i = 1, ..., m. \tag{2.2.3}$$

2.3 Introduction to allocation functions

An allocation function (AF) is an algorithm needed for optimal distribution of control outputs to the different actuators. The generalized control force (forces and torques) y_c is generated by a controller, assuring the stability of the linear closed-loop system. Regardless the control loop, the AF algorithm is responsible for calculating an optimal solution of actuator (thrusters) set-points that at all times satisfy the presumed attainable generalized force signal. A characteristic feature of control allocation problems is that there are more control signals than the number of controlled forces and moments, such that the system is over-actuated.

In general, finding an AF is a dynamic non-linear optimization problem since there are sector limitations such as actuator maximum capacity. This problem can be solved using non-linear optimization techniques [NW99], e.g., quadratic programming. The aerospace community has addressed constrained AF methods since a long time. The two most frequently reported strategies are Durham's tailor-made generalized inverse [Dur93, Dur94b, Dur94a] and actuator daisy chaining [BHSB96]. The sets of admissible controls is usually an n-dimensional rectangle. The set of attainable thrusts is convex [Dur94b, Dur94a].

Most existing AF approaches rely on a linear model that describes the relationship between the actuators signals and the generalized forces. This allows least-squares solutions to be found in an explicit form. Thus the AF can be implemented using simple matrix computations such as generalized inverses [Sor97]. The actuators thrust denoted by the vector $T \in \Re^m$ is related to the control input u_p by the influence matrix $M \in \Re^{m_c \times m}$. The matrix M contains the information concerning the geometric distribution and orientations of the thrusters. In the linear domain, the influence of the thrusters on u_p is defined by the following expression:

$$u_p = MT, \quad \text{where} \quad T = \begin{bmatrix} T'_{(1)} & T'_{(2)} & \cdots & T'_{(m)} \end{bmatrix}' \tag{2.3.1}$$

Given the influence matrix and considering the positivity constraint of the T vector, let us define the AF as:

Definition 2.1. *A function $f : \Re^{m_c} \to \Re^m$ is an allocation function (AF) if:*

- $T = f(y_c) \succeq 0$, $\forall y_c \in \Re^{m_c}$,
- $u_p = Mf(y_c) = y_c$ *and,* $f(0) = 0$.

Choosing the optimization criterium of minimizing the thrust provided, proportionally to $\sum_{i=1}^{m} (T_{(i)})^2$, then we get an analytic solution to the AF which is the pseudo-inverse

matrix of the influence matrix:

$$T = \underbrace{M^{'}(MM^{'})^{-1}}_{M^{*}} y_c \tag{2.3.2}$$

However this solution does not ensure sector constraints of positivity. Thrusters are devices which only provide a positive action as they are unidirectional. Several algorithms exist in order to modify the least-squares algorithm solution to verify the positivity of the thrusts. An example is the algorithm based on the Householder decomposition of the influence matrix (used in CNES Microscope mission [PPT+05]). Allocation function algorithms have to deal with real-time implementation when they are designed for on-board use. Finite convergence of the algorithm is not assured yet. Therefore, to satisfy the real-time implementation constraint two options arise: 1) the algorithm has usually to be truncated at a suitable iteration [BD95, PPT+05] or 2) it has to use explicit solutions [Fos02, Sor97, SJ09, JFT05]. However these options are either conservative in terms of utilizing only a limited fraction of the attainable control input u_p set[1] or not optimal in terms of power consumption [Fos02, Sor97, JFT05]. Figure 2.2 shows the attainable control set (left) given the attainable thrust set (right). At the same time, the minimal control capacity (MCC) could be defined as the minimum norm of the control y_c which reaches the actuator capacity bounds. On the other hand, AF mathematical expression is usually too complex to be formulated and highly non-linear [BD95, PPT+05]. That complicates the analysis of other non-linearities such as the saturation.

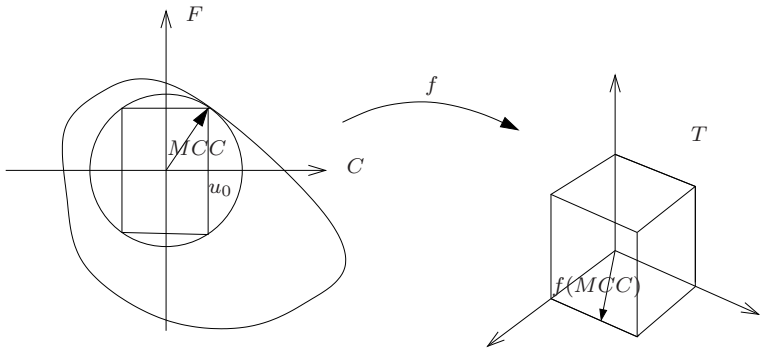

Figure 2.2: Attainable control set vs attainable thrust set.

Considering the saturation function (2.2.3) and the AF Definition 2.1, the general expression connecting y_c and u_p is given by:

$$u_p = Msat_{(0,\bar{u})}(T) = Msat_{(0,\bar{u})}(f(y_c)) \tag{2.3.3}$$

[1]The attainable control input set is the set of control inputs that can be generated by the thrusters while fulfilling the constraints.

then, the closed-loop system can be written:

$$\begin{cases} \dot{x}_p &= A_p x_p + B_p u_p \\ y_p &= C_p x_p \\ \dot{x}_c &= A_c x_c + B_c y_p \\ y_c &= C_c x_c + D_c y_p \\ u_p &= M sat_{(0,\bar{u})}(f(y_c)) \end{cases} \tag{2.3.4}$$

In order to analyze its stability and performance, an expression for AF is needed. Some AF are proposed hereafter in order to provide an explicit expression which may be exploited easily in other analysis. The simplicity is sought rather than the optimality or the achievement of the sector constraints. This choice will be also justified.

2.4 Choosing an allocation function

As explained before, the allocation function used on real applications is a highly non-linear function. Thus, it is difficult to set a mathematical expression for $f(y_c)$. The presence of a non-linear function makes the treatment of the saturation harder. In the linear case, the term $Mf(y_c)$ is reduced to y_c. Hence, the non-linear behavior is hidden. However, as the saturation of the actuator applies, the simplification is not possible anymore. We seek to find a simplified model for $f(y_c)$ while keeping its main properties and without modifying plant behavior.

Roughly speaking, the considered allocation function is based on switching structure, ensuring the positivity of the computed thrust guaranteing the validity of the equality $u_p = y_c$. Even though this family of allocation functions is not optimal, it represents an interesting benchmark for study.

2.4.1 The easiest allocation function: the pseudo-inverse matrix

A possible strategy for the allocation function f is to use the pseudo-inverse matrix of the influence matrix M. We can denote such a pseudo-inverse matrix as M^*. Even if it does not verify the positivity constraints and thus, providing a not-optimal solution, this approach provides a simple relation which is not iterative. Therefore, there are no convergence problems, differently to some other existing AF. As the pseudo-inverse based model does not provide positive thrust, there is no guarantee of stability. In fact, the plant may become unstable when saturations are active.

Usually, the AF has the function of setting a thrust vector providing the right control vector y_c and checking the actuators limitations [Dur93, Dur94b]. However this specification demands for a complex AF. Proposing the pseudo-inverse matrix as AF, the

properties are relaxed but the stability domain decreased. We know that the system may be unstable as soon as the actuator saturates, but its simplicity suggests an interesting option. The idea is to handle the actuator limitation from the control and not from the AF. Control modifications will be introduced expecting to recover (even increase) the stability domain and the performance (even improve) provided by a better but more complex AF.

The first proposal for the allocation function is:

$$T = f(y_c) = M^* y_c \tag{2.4.1}$$

Finally, the actuation is described by the following expression:

$$u_p = Msat_{(0,\bar{u})}\left(T\right) = Msat_{(0,\bar{u})}\left(f(y_c)\right) = Msat_{(0,\bar{u})}\left(M^* y_c\right) \tag{2.4.2}$$

2.4.2 The multi-saturation based allocation function

An alternative allocation function is proposed in [BPT+10a]. We seek to obtain a closer mathematical expression to the non-linear f. The idea is to treat each effort $y_{c(i)}$ individually, computing the right set of positive thrusts T^i needed to perform it, and finally add them all. Each column of $M^*_{(:,i)}$ times $y_{c(i)}$ provides the set of thrusts which performs a control input $u_{p(i)}$ equal to the control output $y_{c(i)}$.

However, when $M^*_{(:,i)}$ is multiplying an effort $y_{c(i)}$, the resultant set of thrusts is not necessary positive. The proposed approach introduces an additional saturation after each individual T^i computation. Extra saturations ensure a set of thrusts for each effort where all components are positive. All positive thrusts are summed providing a final thrust T where all components are positive.

$$\begin{aligned} T = f(y_c) =& sat_{1(0,\bar{u})}(M^*_{(:,1)} y_{c(1)}) + sat_{2(0,\bar{u})}(M^*_{(:,2)} y_{c(2)}) + \cdots \\ &+ sat_{m_c(0,\bar{u})}(M^*_{(:,m_c)} y_{c(m_c)}) \end{aligned} \tag{2.4.3}$$

Finally, the saturation issued from the physical limitations of the actuator applies to the computed thrust. Additional saturations (with subscript) are emphasized with respect to those belonging to the AF and the saturation representing thrusters limitations (no subscript). The equations modelling the allocation function and the whole actuator are:

$$u_p = Msat_{(0,\bar{u})}(T) = Msat_{(0,\bar{u})}\left(\sum_{i=1}^{m_c} sat_{i(0,\bar{u})}(M^*_{(:,i)} y_{c(i)})\right) \tag{2.4.4}$$

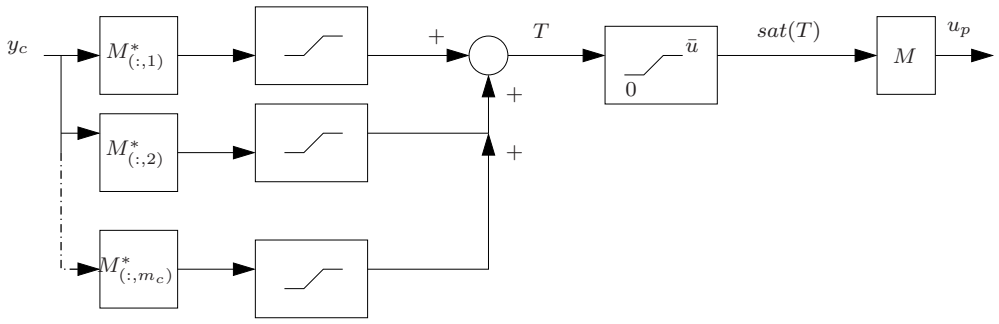

Figure 2.3: $f(y_c)$ and the actuator model

Figure 2.3 shows a block diagram of the actuator. Equation (2.4.3) represents an alternative f to the previous one presented in (2.4.1). However, one can realize that equations (2.4.2) and (2.4.4) are the same when $m_c = 1$. When y_c is a single variable, the chain of saturations is reduced to a unique saturation. Hence, (2.4.3) represents a real alternative way when $m_c > 1$, that is, a coupling appears as the same actuator is used for different efforts. This second choice represents a non-linear AF (but still mathematically treatable) which introduces a different behavior to the actuator when coupling is present. However, it can be noted that extra conservatism is added.

To illustrate the difference, let us consider a simple propulsive system composed by four thrusters, the influence matrix M and its pseudo-inverse could be represented by:

$$M = \begin{bmatrix} 1 & -1 & -1 & 1 \\ 1 & 1 & -1 & -1 \end{bmatrix} \quad M^* = \frac{1}{4}\begin{bmatrix} 1 & 1 \\ -1 & 1 \\ -1 & -1 \\ 1 & -1 \end{bmatrix}$$

Then let us assume a control output $y_c \in \Re^2$ where both components of the vector are larger than the saturation bound $\bar{u}$ and let us also suppose that[2] $y_{c(1)} >> y_{c(2)} >> u_{max}$, such as, $y_{c(1)} - y_{c(2)} > 4u_{max}$. Using (2.4.2) the resulting control u_p is:

$$\begin{aligned} u_p &= M sat_{(0,\bar{u})}\left(M^* y_c\right) \\ &= M sat_{(0,\bar{u})}\left(\frac{1}{4}\begin{bmatrix} y_{c(1)} + y_{c(2)} \\ -y_{c(1)} + y_{c(2)} \\ -y_{c(1)} - y_{c(2)} \\ y_{c(1)} - y_{c(2)} \end{bmatrix}\right) = M\begin{bmatrix} u_{max} \\ 0 \\ 0 \\ u_{max} \end{bmatrix} = \begin{bmatrix} 2u_{max} \\ 0 \end{bmatrix} \end{aligned} \tag{2.4.5}$$

[2] $\bar{u} \in \Re^4$ with $\bar{u}_{(j)} = \bar{u}_{(i)} = u_{max}$ for $i, j = 1, ..., 4$ with $i \neq j$.

Similarly, considering (2.4.4) one obtains:

$$\begin{aligned} u_p &= M sat_{(0,\bar{u})}\left(sat_{1(0,\bar{u})}(M^*_{(:,1)}y_{c(1)}) + sat_{2(0,\bar{u})}(M^*_{(:,2)}y_{c(2)})\right) \\ &= M sat_{(0,\bar{u})}\left(sat_{1(0,\bar{u})}\left(\frac{1}{4}\begin{bmatrix} y_{c(1)} \\ -y_{c(1)} \\ -y_{c(1)} \\ y_{c(1)} \end{bmatrix}\right) + sat_{2(0,\bar{u})}\left(\frac{1}{4}\begin{bmatrix} y_{c(2)} \\ y_{c(2)} \\ -y_{c(2)} \\ -y_{c(2)} \end{bmatrix}\right)\right) \\ &= M sat_{(0,\bar{u})}\left(\begin{bmatrix} u_{max}+u_{max} \\ u_{max} \\ 0 \\ u_{max} \end{bmatrix}\right) = M\begin{bmatrix} u_{max} \\ u_{max} \\ 0 \\ u_{max} \end{bmatrix} = \begin{bmatrix} u_{max} \\ u_{max} \end{bmatrix} \end{aligned} \tag{2.4.6}$$

which is different to (2.4.5).

It is important to emphasize that the pseudo-inverse based AF (2.4.1) yields the control which saturates the most ($y_{c(1)}$ in that case) as all the thrusting capacity ($2\bar{u}$) is used for the first component of u_p. On the other hand, the multi-saturation based AF (2.4.3) splits the capacity in both components of the control u_p. This different behavior has consequences for the stability of the saturated system. Because of this kind of distributing the thrusting capacity, the system is stable for the multi-saturation based AF as shown in Figure 2.4 (for a given initial condition).

2.4.2.a Educational example

Figure 2.4 represents the time-evolution of the first regulated output $z_{p(1)}$ of a modified version of the educational example.The education example system (8) is composed of a SISO-controller and a SISO-plant. We have increased the education example in order to obtain a system which can illustrate the difference between AF (2.4.1) and (2.4.3). The simulated state matrices read:

$$\tilde{\mathcal{P}} = diag(\mathcal{P},\mathcal{P}) \tag{2.4.7}$$

$$\tilde{\mathcal{C}} = diag(\mathcal{C},\mathcal{C}) \tag{2.4.8}$$

$$M = \begin{bmatrix} -1 & 1 & -1 & 1 \\ 1 & -1 & -1 & 1 \end{bmatrix} \tag{2.4.9}$$

where $\mathcal{P}$ stands for the plant (1) and $\mathcal{C}$ stands for the controller (2). The structure of the educational example has not been modified and thus the block diagram in Figure 1 still applies. With this increase of the system dimension there are two control outputs that have to be allocated to four thrusters. Thus AFs (2.4.1) and (2.4.3) have different behaviors.

Figure 2.4 depicts the response of the first output of the increased system (2.4.7)-(2.4.9). The plant initial condition has been set to $\tilde{x}_p(0) = 10^{-3}\cdot[10 \quad 0 \quad 1.1 \quad 0]'$. With this initial condition the system saturates and there is an input direction which related

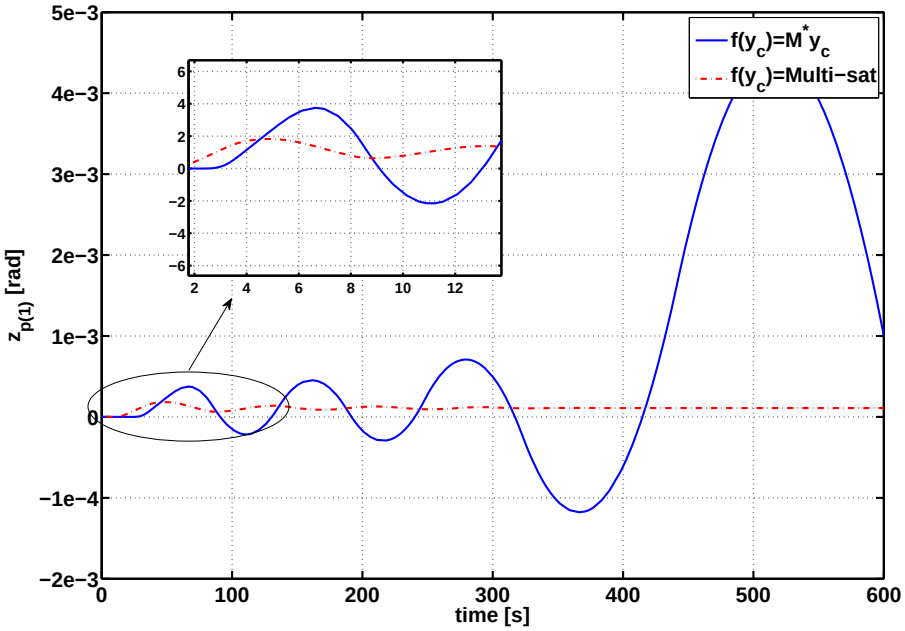

Figure 2.4: Comparison the output $z_{p(1)}$ with different allocation functions f

control output saturates more (it is further than the admissible limit) than the other input direction.

Figure 2.4 shows how the system becomes unstable when the AF is based on the pseudo-inverse of the influence matrix (solid line). On the contrary, the system is stable with the multi-saturation based allocation function (dash-doted line). Roughly speaking, one could say that the AF (2.4.1) forgets about some dynamics of the plant, and it diverges too much to recover them and, therefore, the whole system diverges. On the other hand, the AF (2.4.3) acts on all plant dynamics, stabilizing the system even in presence of a gap between y_c and $\bar{u}$. Hence, even if the complexity of the AF is increased, this new modelling provides a mathematical formulation for AF where the relaxations done are less important. Then, as the constrained system is stable, this AF should provide a bigger domain of stability and performances when the control modifications (to handle the saturation) will be introduced.

Henceforth, we will denote as pseudo-inverse matrix the allocation function described in (2.4.1) and as multi-sat the one in (2.4.3). The goal is to compare further results with a simpler but inefficient allocation function (pseudo-inverse matrix) with a good approximation of the non-linear f which is more complex and conservative but stable (multi-sat). In Chapter 4, we show the benefits of the anti-windup compensator in each case and we evaluate the necessity of complex AFs when the anti-windup compensator is in the loop.

2.5 Saturation symmetrization

2.5.1 First option: a conservative approach

Saturations have been an important research issue in the last century. In several works dealing with actuator limitation [HL01, PTH07, TGGE07], saturations are supposed to be symmetric, that is, the upper and lower bounds are equal in absoulte value. This assumption has been done to use quadratic lyapunov functions. Generally, this hypothesis is realistic as the actuators generally provide bi-directional efforts. From flight control problems [RBTP07] to marine vessel control [SS99], this hypothesis applies. However symmetric hypothesis is not always possible.

Saturating actuators may present different behavior in the upper-saturating zone and in the lower-saturating one. This situation arises when absolute values of the upper and lower bounds are different. In this case, saturation function is called asymmetric and it is defined by (1.3.2). In order to apply existing techniques on the saturated system analysis and control design, the saturation has to be symmetrized. This is defined as process where the saturation bounds are modified in order to obtain both upper and lower bound equal in absolute value. A first manner to symmetrize the saturation consist in keeping the smaller of both bound in absolute value [Lan03]. This approach can be stated in the following lemma:

Lemma 2.1. *Consider an asymmetric saturation* $sat_{(\underline{u},\bar{u})}(\cdot)$ *where* $\underline{u} < \bar{u}$*, the saturation can be symmetrized to* $sat_{(-u_0,u_0)}(\cdot)$ *with* u_0

$$u_0 = min(|\underline{u}|, |\bar{u}|) \tag{2.5.1}$$

where $\bar{u}$ *(resp.* $\underline{u}$*) is the upper (resp. the lower) bound of the asymmetric saturation.*

Lemma 2.1 introduces conservatism as some actuator capacity is being neglected. However, it is a manner to obtain a symmetric saturation allowing other analysis like the stability domain using simple methods.

Although it is a common technique, this option is unfeasible for the actuators considered throughout this manuscript.

Remark 2.1. *Systems using thrusters are actuators presenting saturation constraints where the minimum bound is zero. Thus, when procedure* (2.5.1) *is applied, the* symmetric *bound is* $u_0 = 0$ *which is useless. Therefore a different symmetrization technique has to be applied.*

2.5.2 Kernel symmetrization

It is well-known that the introduction of any constant vector into the saturation input can allow to modify the bounds of the saturation

Property 2.1. *Consider u and $N\zeta$ belonging to $\Re^m$, $N\zeta$ being a constant vector. The following equality holds:*

$$sat_{(0,\bar{u})}(u + N\zeta) = sat_{(-N\zeta,\bar{u}-N\zeta)}(u) + N\zeta \tag{2.5.2}$$

provided that

$$0 < N\zeta_{(i)} < \bar{u}_{(i)}, \quad i = 1, ..., m. \tag{2.5.3}$$

Hereafter, we use Property 2.1 in order to modify the bounds of the saturation block and the allocation function when the saturation occurs. Consider the scheme depicted in Figure 2.5.

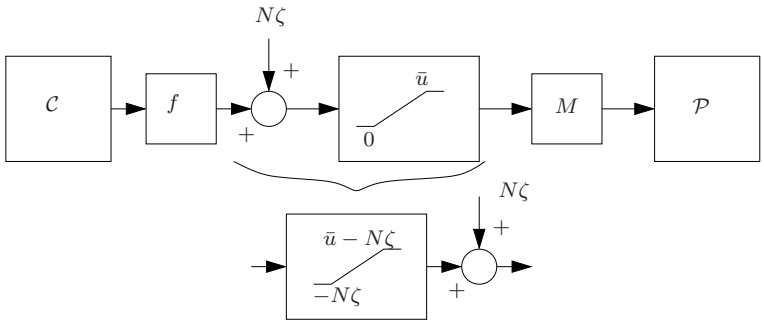

Figure 2.5: Saturation bounds modification

Nevertheless, some restrictions have to be imposed in order to verify the coherence of the new bounds of the saturation and keep the linear closed-loop dynamics unchanged. Adding $N\zeta$ to $f(y_c)$ the saturation bounds are modified, but, at the same time, u_p changes as well:

Lemma 2.2. *Suppose $N\zeta \in Ker(M)$, that is $MN\zeta = 0$. Then:*

1. *during the linear behavior (without saturation), u_p is unchanged since $u_p = MT = M(f(y_c) + N\zeta) = Mf(y_c) = y_c$ where $f(\cdot)$ satisfies Definition 2.1;*
2. *during the non-linear behavior (with saturation), u_p is slightly modified as $u_p = Msat_{(0,\bar{u})}(f(y_c) + N\zeta) = Msat_{(-N\zeta,\bar{u}-N\zeta)}(f(y_c))$.*

Lemma 2.2 implies that the introduction of the vector $N\zeta$ modifies the plant input u_p in the non-linear domain. Initially, this vector has been presented as a way to modify the saturation bounds. However it can be seen as a modification of the allocation function: $\tilde{f} = f(y_c) + N\zeta$. Actually, this modification changes the values of $\tilde{f}$ and centers its mean value between the bounds $(0, \bar{u})$ (instead of being centered around the lower bound (0) for f). However, one keeps the aim of $N\zeta$ vector to be a modification of the saturation bounds as it is consistent with the whole Section 2.5.

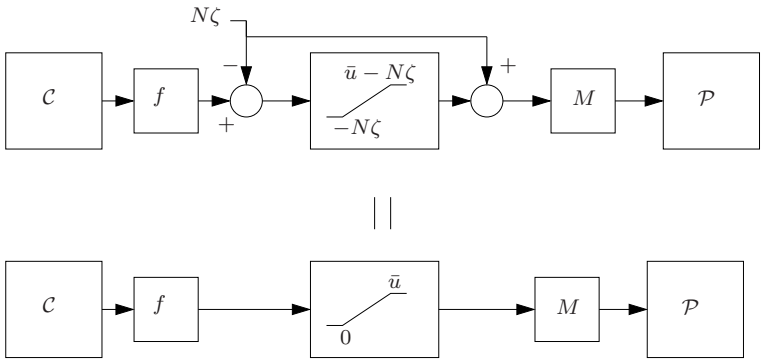

Figure 2.6: Equivalent saturations

Figure 2.6 shows two structures which are the same. Mathematically the relationship reads:

$$\begin{aligned} u_p &= M(sat_{(-N\zeta,\bar{u}-N\zeta)}(f(y_c) - N\zeta) + N\zeta) \\ &= M(sat_{(0,\bar{u})}(f(y_c)) + N\zeta - N\zeta) = Msat_{(0,\bar{u})}(f(y_c)) \end{aligned} \tag{2.5.4}$$

However this technique does not modify the behavior of $f(y_c)$ which appears to be critical when a pseudo-inverse AF is used. In general any allocation function which does not ensure the positivity of its output presents systematic saturation problems and consequently system performance degradation. Therefore, Property 2.1 is kept as symmetrizing technique as it provides an interesting $f(y_c)$ behavior.

To sum up, for any $N\zeta$ vector seeking to obtain a symmetric saturation, the previous Property 2.1 and Lemma 2.2 have to be verified. Thus, a symmetrizing vector candidate is defined as follows:

Definition 2.2. *If there exists a vector $N\zeta$ satisfying $0 < N\zeta_{(i)} < \bar{u}_{(i)}$, $i = 1, ..., m$, and $MN\zeta = 0$ (i.e. $N\zeta$ belongs to $Ker(M)$), then $N\zeta$ is called a symmetrizing vector candidate.*

With saturation bounds modified, the problem (as pointed out in Remark 2.1) about the presence of a null bound in the thrusters saturation is overcome. Then, one may apply Lemma 2.1 as first approach of saturation symmetrization.

The consevatism introduced by Lemma 2.1 may be avoided by forcing both terms in (2.5.1) to be equal. This is possible with a certain $N\zeta$ denoted symmetrizing vector:

Definition 2.3. *A symmetrizing vector candidate $N\zeta$ is a symmetrizing vector $N\zeta_{sym}$ when absolute value of both upper and lower bound are matched:*

$$|-N\zeta_{sym(i)}| = |\bar{u}_{(i)} - N\zeta_{sym(i)}|, \quad i = 1, ..., m. \tag{2.5.5}$$

Thus $N\zeta_{sym}$ reads:

$$N\zeta_{sym} = \frac{\bar{u}_{(i)}}{2}, i = 1, ..., m. \tag{2.5.6}$$

When such a vector exists then saturation may be symmetrized avoiding any conservatism:

Lemma 2.3. *[BPT+09] If there exists a symmetrizing vector candidate, then given a asymmetric saturation $sat_{(0,\bar{u})}(\cdot)$, the saturation can be symmetrized to $sat_{(-u_0,u_0)}(\cdot) = sat_{(u_0)}(\cdot)$ where u_0 is*

$$u_0 = \frac{\bar{u}}{2} \tag{2.5.7}$$

with a symmetrizing vector verifying Definition 2.3.

Remark 2.2. *Definition 2.2 imposes $MN\zeta_{sym} = 0$. Later in Section 2.5.5 conditions to satisfy the kernel belonging are provided. Physically, the condition can be stated as there exists a feasible thrust for all thrusters that produces a null control effort u_p.*

Finally, applying Lemmas 2.2 and 2.3 in (2.3.4) the closed-loop system may be rewritten as follows:

$$\begin{cases} \dot{x}_p = A_p x_p + B_p M sat_{(u_0)}(f(y_c)) \\ \dot{x}_c = A_c x_c + B_c C_p x_p \\ y_c = C_c x_c + D_c C_p x_p \end{cases} \tag{2.5.8}$$

with $u_{0(i)} = \frac{\bar{u}_{(i)}}{2}$ verifying Definition 2.3.

Remark 2.3. *As both lower and upper bounds are equal in absolute value (i.e. $|u_0|$), only one bound is shown in the saturation term in (2.5.8).*

2.5.3 Variable kernel function

When the saturation function (2.5.2) is transformed into a symmetric one, an additional term $N\zeta_{sym}$, verifying Definition 2.3, is added to f. In the absence of disturbance, the equilibrium point is $x_{eq} = 0$ and the performed control output is zero ($y_{c_{eq}} = 0$). However the thrust provided is non zero:

$$T_{eq} = f(y_{c_{eq}}) + N\zeta_{sym} = \underbrace{f(0)}_{0} + \frac{\bar{u}}{2} = \frac{\bar{u}}{2} \tag{2.5.9}$$

Even if there is no need for any thrust, because of the symmetrizing vector, thrusters are spending fuel at the equilibrium and, thus, the lifetime of the mission is clearly reduced. Therefore, there is a necessity to cancel the actual thrust at the equilibrium point ($u_{c_{eq}} = y_{c_{eq}} = T_{eq} = 0$) in order to avoid unnecessary fuel consumption.

The next step would be to propose a $N\zeta_{var}$ vector evolving with y_c such that it symmetrizes the saturation function when the control are high enough to saturate a thruster, and brings the consumption to zero at the equilibrium point.

Definition 2.4. *[BPT+09] A vector function $N\zeta_{var}(y_c) : \Re^{m_c} \to \Re^m$ is a Variable Kernel Function (VKF) if:*

1. $N\zeta_{var(i)} = \frac{\bar{u}(i)}{2} = N\zeta_{sym(i)}$ *if*

$$\left(f_{(i)}(y_c) + N\zeta_{var(i)}\right) < 0 \text{ or } \left(f_{(i)}(y_c) + N\zeta_{var(i)}\right) > \bar{u}_{(i)}$$

   In other words, the variable kernel function is equal to the symmetrizing one when the system saturates, that is $|f_{(i)}(y_c)| > \frac{\bar{u}_{(i)}}{2}$.

2. *In the commutation surface, $|f_{(i)}(y_c)| = \frac{\bar{u}_{(i)}}{2}$, $N\zeta_{var(i)}$ is continuous with $N\zeta_{sym(i)}$, that is $N\zeta_{var(i)} = N\zeta_{sym(i)} = \frac{\bar{u}_{(i)}}{2}$.*

3. *In the linear zone, $|f_{(i)}(y_c)| < \frac{\bar{u}_{(i)}}{2}$, $N\zeta_{var(i)}$ is such that*

$$0 \leq f_{(i)}(y_c) + N\zeta_{var(i)} \leq \bar{u}_{(i)}$$

4. *$N\zeta_{var(i)} \in Ker(M)$, that is, $MN\zeta_{var} = 0$.*

Remark 2.4. *In the saturated domain, the aim of adding a vector $N\zeta$ is to symmetrize the saturation. Hence, the VKF has to be equal to the symmetrizing vector $N\zeta_{sym}$ when saturation is active. On the other hand, in the linear domain, the VKF is not fixed. Any function is possible as long as it belongs to $Ker(M)$ and the system remains in the linear domain.*

For example, one could define an VKF such that it is null when the system attains its equilibrium state (i.e. $N\zeta_{var_{eq}} = 0$). Then replacing the symmetrizing vector by the VKF in (2.5.9) the provided thrust at the equilibrium is $T_{eq} = 0$ avoiding extra fuel consumption.

2.5.4 Saturation symmetrization for a multi-sat AF

The multi-sat AF introduces m_c extra saturations which have to be symmetrized for stability domain analysis or anti-windup computation purposes. The technique proposed in Section 2.5.2 sets a framework to do this. However, a slight modification has to be considered because of these extra saturations. Defining m_c different vectors for the m_c extra saturations ($N\zeta_i \in \Re^m$) and for the actual actuator saturation ($\widetilde{N\zeta} \in \Re^m$), using Property 2.1 saturations bounds can be modified:

$$T = sat_{(0,\bar{u})}\left(\sum_{i=1}^{m_c} sat_{i(0,\bar{u})}(M^*_{(:,i)}y_{c(i)} + N\zeta_i) + \widetilde{N\zeta}\right) = sat_{(-\eta,\bar{u}-\eta)}\left(\sum_{i=1}^{m_c} sat_{i(-N\zeta_i,\bar{u}-N\zeta_i)}(M^*_{(:,i)}y_{c(i)})\right) + \eta \quad (2.5.10)$$

where $\eta = \widetilde{N\zeta} + \sum_{i=1}^{m_c} N\zeta_i$ and $N\zeta_i$ are given vectors in $\Re^m$ for $i = 1, \ldots, m_c$. Writing $\widetilde{N\zeta} = N\zeta - \sum_{i=1}^{m_c} N\zeta_i$, we get $\eta = N\zeta$. Thus η is simplified from a sum of vectors to a unique independent constant vector $N\zeta$. Then the plant input u_p reads:

$$u_p = Msat_{(-N\zeta,\bar{u}-N\zeta)}\left(\sum_{i=1}^{m_c} sat_{i(-N\zeta_i,\bar{u}-N\zeta_i)}(M^*_{(:,i)}y_{c(i)})\right) + MN\zeta \quad (2.5.11)$$

Only the symmetrizing vector $N\zeta$, related to the physical saturation, appears in the system control input expression. Thus $N\zeta$ has to verify Definition 2.2 to disappear from (2.5.11), and we get:

$$u_p = Msat_{(-N\zeta,\bar{u}-N\zeta)}\left(\sum_{i=1}^{m_c} sat_{i(-N\zeta_i,\bar{u}-N\zeta_i)}(M^*_{(:,i)}y_{c(i)})\right) \quad (2.5.12)$$

Conversely, $N\zeta_i$ is only forced to follow the assumptions (2.5.3) presented in Property 2.1.

Saturations can be symmetrized without conservatism as exposed previously in Lemma 2.3. Choosing $N\zeta$ and $N\zeta_i$ to be the symmetrizing vector like in Definition 2.3, that is $N\zeta_{sym} = \frac{\bar{u}}{2}$ and $N\zeta_i = \frac{\bar{u}}{2}$, all saturations are symmetrized without conservatism.

Finally, we can quickly adapt the variable kernel function strategy by only replacing $N\zeta$ by $N\zeta_{var}$. On the other hand, $N\zeta_i$ vectors do not appear on the thrust T expression, hence they do not add extra consumption at the equilibrium. Therefore they can remain as constant vectors.

2.5.5 Symmetrizing kernel examples

In both Sections 2.5.2 and 2.5.3, symmetrizing techniques have been exposed. However some details are missing for a full comprehension. In the kernel symmetrization case, Definition 2.2 provides the conditions that a symmetrizing vector candidate has to verify. Furthermore, from Definition 2.3, a symmetrizing vector is $N\zeta_{sym} = \frac{\bar{u}}{2}$. The variable kernel function (VKF) case, only Definition 2.4 has been provided. In this section we provide two examples of VKF to illustrate how this function can be designed.

The symmetrizing vector $N\zeta_{sym} = \frac{\bar{u}}{2}$ has to verify conditions introduced by Definition 2.2. It is easy to see that $\frac{\bar{u}}{2} \in Ker(M)$ (i.e. $M\frac{\bar{u}}{2} = 0$) is the hard point to check.

First, let us consider all thrusters to be the same. Then $\bar{u}$ is a constant vector whose components are equal, that is, $\bar{u}_{(1)} = \bar{u}_{(i)} = \bar{u}_{(m)}$. This hypothesis seems to be coherent with the propulsive system design, as we expect to choose all the thrusters to be the same. Thus, the symmetrizing vector is rewritten as follows:

$$N\zeta_{sym} = \frac{\bar{u}_{(*)}}{2}[1 \cdots 1]'.$$

where $\bar{u}_{(*)} = \bar{u}_{(1)} = \cdots = \bar{u}_{(m)}$ is the maximum bound of the thrusters. Then $MN\zeta_{sym}$ writes:

$$MN\zeta_{sym} = M\frac{\bar{u}_{(*)}}{2}\begin{bmatrix} 1 \\ \vdots \\ 1 \end{bmatrix} = \frac{\bar{u}_{(*)}}{2}\begin{bmatrix} \sum_{i=1}^{m} M_{(1,i)} \\ \vdots \\ \sum_{i=1}^{m} M_{(j,i)} \\ \vdots \\ \sum_{i=1}^{m} M_{(m_c,i)} \end{bmatrix}$$
$$\text{for } i = 1, ..., m \text{ and } j = 1, ..., m_c. \tag{2.5.13}$$

Hence, the following Lemma can be stated:

Lemma 2.4. *$N\zeta_{sym} = \frac{\bar{u}}{2}$ is a symmetrizing vector candidate if $\sum_{i=1}^{m} M_{(j,i)} = 0$ and $\bar{u}_{(i)} = \bar{u}_{(k)}$ for $j = 1, ..., m_c$, $i = 1, ..., m$, $k = 1, ..., m$ and $i \neq k$.*

This result can be interpreted physically as the situation where the plant input u_p, generated by a set of thrusters producing the same thrust, is zero. That situation happens when a symmetric propulsive system is designed. Even if it represents a constraint into the propulsive systems design, it should not be significant as a symmetric configuration is usually pretended. Only in case of thruster failure, the condition would not be verified. However, this situation is not studied and left as future prospects. Finally, let us remark that it is a particular case of the physical interpretation given in Remark 2.2.

A second main point to analyze is the existence of a VKF.

Proposition 2.1. *Let us consider M and $\bar{u}$ verifying Lemma 2.4 and the following function:*

$$N\zeta_{var} = min\left(max_{(i)}(|f(y_c)|), N\zeta_{sym(i)}\right)\begin{bmatrix}1\\ \vdots\\ 1\end{bmatrix} \tag{2.5.14}$$

Then (2.5.14) is an VKF as introduced in Definition 2.4.

Proof of Proposition 2.1: First and second points of Definition 2.4 are easily proven using (2.5.14) and:

$$N\zeta_{var} = N\zeta_{sym} \text{ when } |f_{(i)}(y_c)| \geq \frac{\bar{u}_{(i)}}{2} \text{ for all } i = 1, ..., m.$$

Then, in the third condition we suppose

$$|f_{(i)}(y_c)| < \frac{\bar{u}_{(i)}}{2} \text{ for all } i = 1, ..., m.$$

Consequently,

$$N\zeta_{var} = max_{(i)}(|f(y_c)|)\,[1 \cdots 1]'$$

In the worst case:

$$(f_{(i)}(y_c) + N\zeta_{var(i)}) = 2max_{(i)}(|f(y_c)|) < \bar{u}_{(i)}, \text{ if } f_{(i)}(y_c) > 0$$

$$(f_{(i)}(y_c) + N\zeta_{var(i)}) = 0, \text{ if } f_{(i)}(y_c) < 0$$

Therefore, the third condition is verified.

Finally condition $MN\zeta_{var} = 0$ has to be verified. It follows from Lemma 2.4, $N\zeta_{sym} \in Ker(M)$. Hence, $N\zeta_{var}$ belongs to the $Ker(M)$ in the saturated domain as $N\zeta_{var} = N\zeta_{sym}$. In the linear domain, $N\zeta_{var(i)} = max_{(i)}(|f(y_c)|)\,[1 \cdots 1]'$. By analogy with $N\zeta_{sym} = \frac{\bar{u}_{(*)}}{2}[1 \cdots 1]'$ and recovering the same procedure in (2.5.13), one can easily realize that $N\zeta_{var} \in Ker(M)$ in the linear domain, with M verifying Lemma 2.4.

Therefore, (2.5.14) is a VKF.

End of Proof.

Remark 2.5. *VKF (2.5.14) brings the performed thrust back to zero at the equilibrium (i.e. $y_{c_{eq}} = 0$), avoiding extra-fuel consumption.*

The existence of another VKF can be explored. Let us, first, consider the following function:

$$N\zeta_{var(i)} = min(|f_{(i)}(y_c)|, N\zeta_{sym(i)}), i = 1, ..., m. \tag{2.5.15}$$

being the whole $N\zeta_{var}$ constructed component by component, that is

$$N\zeta_{var} = \begin{bmatrix} min(|f_{(1)}(y_c)|, N\zeta_{sym(1)}) \\ \vdots \\ min(|f_{(i)}(y_c)|, N\zeta_{sym(i)}) \\ \vdots \\ min(|f_{(m)}(y_c)|, N\zeta_{sym(m)}) \end{bmatrix}, i = 1, ..., m. \tag{2.5.16}$$

Let us then suppose the following influence matrix:

$$M = \begin{bmatrix} 1 & -1 & 1 & -1 \\ -1 & -1 & 1 & 1 \end{bmatrix} \tag{2.5.17}$$

For a peudo-inverse AF, that is, $f(y_c) = M^* y_c$, $N\zeta_{var} = |M^* y_c|$ reads:

$$|M^* y_c| = \frac{1}{4} \begin{bmatrix} |y_{c(1)} - y_{c(2)}| \\ |-y_{c(1)} - y_{c(2)}| \\ |y_{c(1)} + y_{c(2)}| \\ |-y_{c(1)} + y_{c(2)}| \end{bmatrix} = \frac{1}{4} \begin{bmatrix} |y_{c(1)} - y_{c(2)}| \\ |y_{c(1)} + y_{c(2)}| \\ |y_{c(1)} + y_{c(2)}| \\ |y_{c(1)} - y_{c(2)}| \end{bmatrix} \tag{2.5.18}$$

Finally, the plant input u_p reads:

$$u_p = M|M^* y_c| = \frac{1}{4} \begin{bmatrix} 1 & -1 & 1 & -1 \\ -1 & -1 & 1 & 1 \end{bmatrix} \begin{bmatrix} |y_{c(1)} - y_{c(2)}| \\ |y_{c(1)} + y_{c(2)}| \\ |y_{c(1)} + y_{c(2)}| \\ |y_{c(1)} - y_{c(2)}| \end{bmatrix} = 0 \tag{2.5.19}$$

showing that $N\zeta_{var}$ (2.5.15) belongs to the $Ker(M)$.

Consider then the definition of VKF (Definition 2.4), first and second points of the definition are easily verified by $N\zeta_{var}$ (2.5.15) as $N\zeta_{var(i)} = N\zeta_{sym(i)}$ when $|f_{(i)}(y_c)| > \frac{\bar{u}}{2}$.

Then, in the third condition we suppose

$$|f_{(i)}(y_c)| < \frac{\bar{u}}{2} \text{ for all } i = 1, ..., m$$

Consequently, $N\zeta_{var(i)} = |f_{(i)}(y_c)|$. Then,

$$(f_{(i)}(y_c) + N\zeta_{var(i)}) = 2|f_{(i)}(y_c)| < \bar{u}_{(i)} \text{ if } f_{(i)}(y_c) > 0$$

or

$$(f_{(i)}(y_c) + N\zeta_{var(i)}) = 0 \text{ if } f_{(i)}(y_c) < 0$$

Therefore, the third condition is verified.

Property 2.2. *Summing up previous considerations, one realizes that, for the particular case of the influence matrix* (2.5.17)*, the function* (2.5.15) *is a VKF.*

Remark 2.6. *The first three conditions in Definition 2.4 are satisfied by function* (2.5.15)*. Unfortunately we have not found yet sufficient conditions for the matrix M (like in Lemma 2.4)to ensure that the function* (2.5.15) *belongs to $Ker(M)$.*

However, as it has been shown, there exists a configuration for the influence matrix M where Definition 2.4 is satisfied. The particular structure of M that allows the function (2.5.15) to belong to $Ker(M)$ usually appears in practical applications. Therefore, even if function (2.5.15) cannot be proven to be a VKF, it is interesting to consider it for further simulations where (2.5.15) verifies VKF definition.

In the linear zone ($|f_{(i)}(y_c)| < \frac{\bar{u}}{2}$), when $f_{(i)}(y_c) < 0$, the provided thrust is $T_i = f_{(i)}(y_c) + max(|f_{(i)}(y_c)|) \geq 0$ for the VKF (2.5.14) case. On the other hand, for (2.5.15) case the thrust becomes $T_i = f_{(i)}(y_c) + |f_{(i)}(y_c)| = 0$. Therefore, when the control output provides a negative value, the function (2.5.15) adjusts the thrust to zero, avoiding extra-consumption. That is why we say that VKF (2.5.15) has a better behavior in terms of fuel consumption.

Remark 2.7. *One can be interested in using function* (2.5.15) *as it has a better behavior in terms of consumption than the one in* (2.5.14)*.*

2.5.5.a Educational example

In order to illustrate the benefits of the symmetrization, the educational example (8) is simulated. The pseudo-inverse AF is used, that is $f(y_c) = M^* y_c$. Then the system (8) reads:

$$CL(s): \begin{cases} \dot{x}_p = A_p x_p + B_p M sat_{(-N\zeta, \bar{u}-N\zeta)}(M^* y_c) \\ \dot{x}_c = A_c x_c + B_c C_p x_p \\ y_c = C_c x_c + D_c C_p x_p \\ z_p = C_z x_p = \theta \end{cases} \tag{2.5.20}$$

Notice that the system (2.5.20) saturation has already its bounds modified due to the use of the symmetrizing techniques. Two options are considered: $N\zeta = N\zeta_{sym}$ (2.5.6) and $N\zeta = N\zeta_{var}$ (2.5.14).

Figure 2.7 shows the response of the educational example (2.5.20) for an initial condition $x_p = [-7 \cdot 10^{-4} \;\; 0]'$ and $x_c = 0_{1\times 4}$. Three curves are plotted: the first response (solid line) is the system without saturation symmetrized ($N\zeta = 0$), the second and the third (dash-dotted line and line with dots respectively) present the output z_p behavior when the symmetrizing techniques are applied. The dash-dotted line uses a $N\zeta_{sym}$ vector like in (2.5.6) and the line with dots a $N\zeta_{var}$ vector like in (2.5.14). The Figure 2.7 shows how the system has a faster response as some of the negative solutions of the pseudo-inverse AF

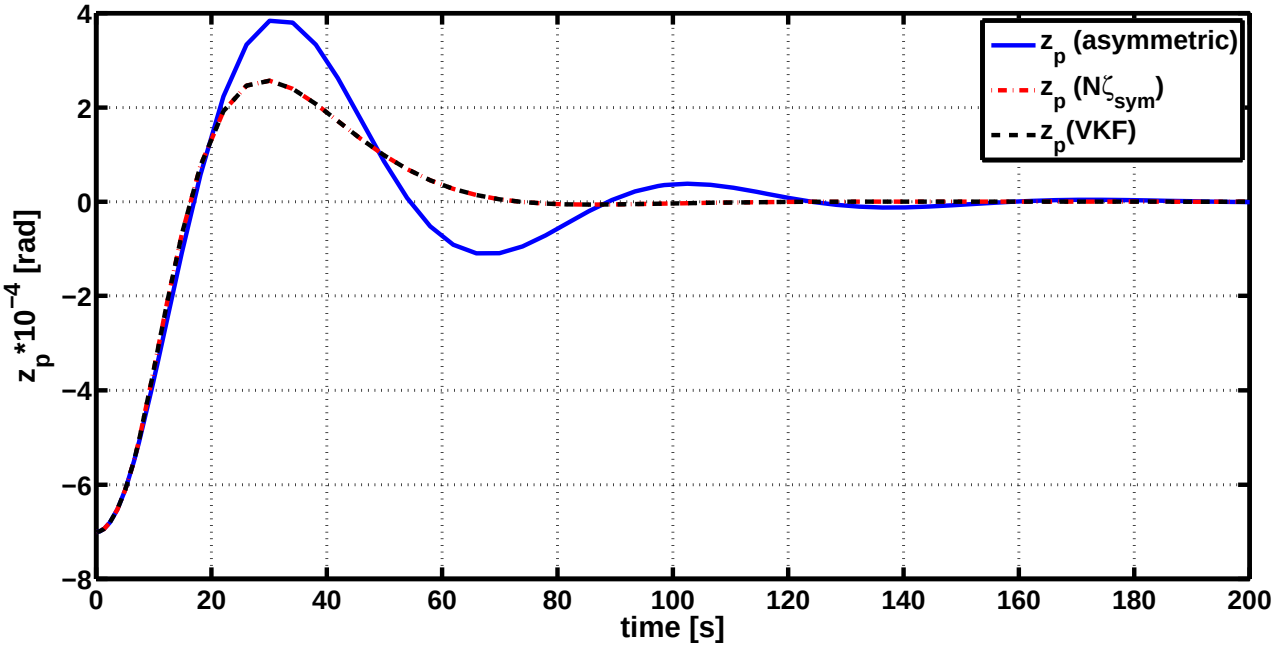

Figure 2.7: Attitude response with different symmetrizing vectors

fit in the saturation limits. Moreover both responses applying a symmetrizing technique are equal.

The thrust applied by the first thruster is shown in Figure 2.8. The comparison is more interesting because it illustrates the advantage of using a VKF. One may see how the dash-dotted line related with $N\zeta_{sym}$ vector converges towards a fixed value equal to $\frac{\bar{u}}{2}$ as it was announced in Section 2.5.3. Thus it becomes interesting to apply the variable kernel function approach to fix the thrust to zero as soon as the system attains the equilibrium.

Remark 2.8. *It would be interesting to compare the two proposed VKF* (2.5.14) *and* (2.5.15) *but for the educational example used is not possible. The simplicity of the influence matrix* ($M = [1 \quad -1]$) *makes both VKF to be equivalent (for* $M = [1 \quad -1]$ (2.5.15) *is VKF).*

Thus let us consider the extended version of the educational example previously presented in Section 2.4.2. The plant, the controller and the influence matrix are described by relations (2.4.7), (2.4.8) and (2.4.9) respectively. The pseudo-inverse AF and three symmetrizing vectors are applied, $N\zeta_{sym}$ like in (2.5.6) and $N\zeta_{var}$ like in (2.5.14) and (2.5.15).

Remark 2.9. *M matrix* (2.4.9) *formulation is such as* (2.5.15) *is an VKF as proven in Property 2.2.*

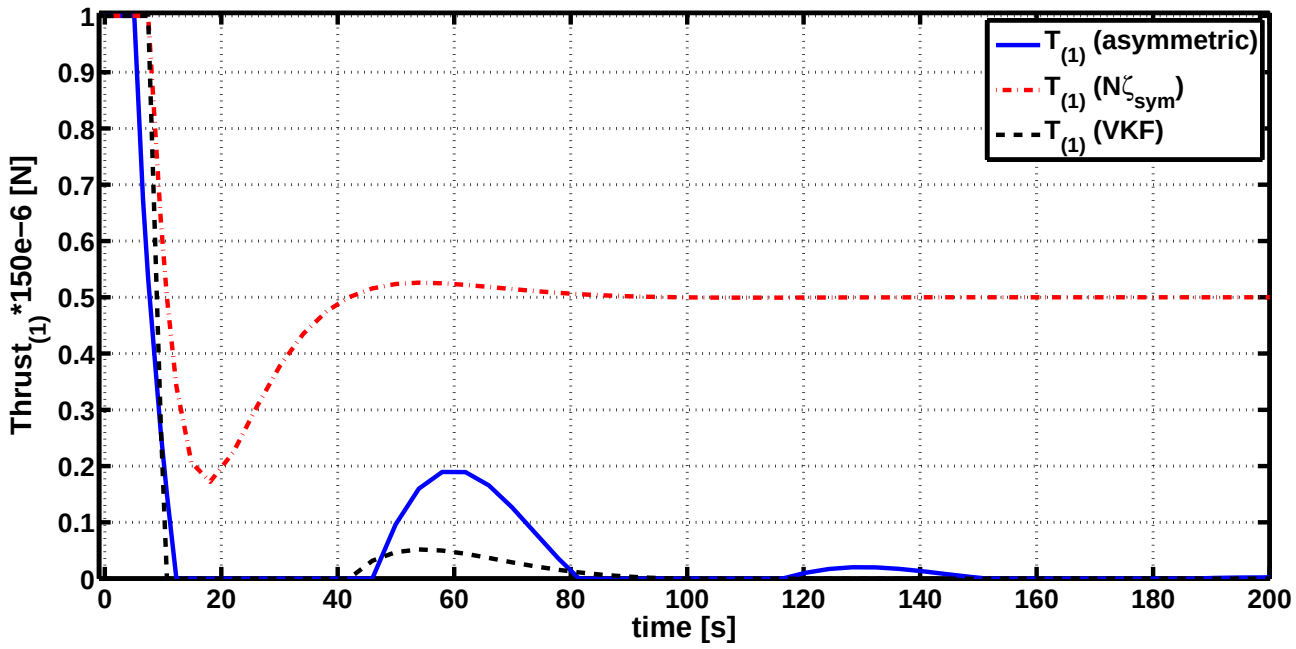

Figure 2.8: Thruster$_{(1)}$ response with different symmetrizing vectors

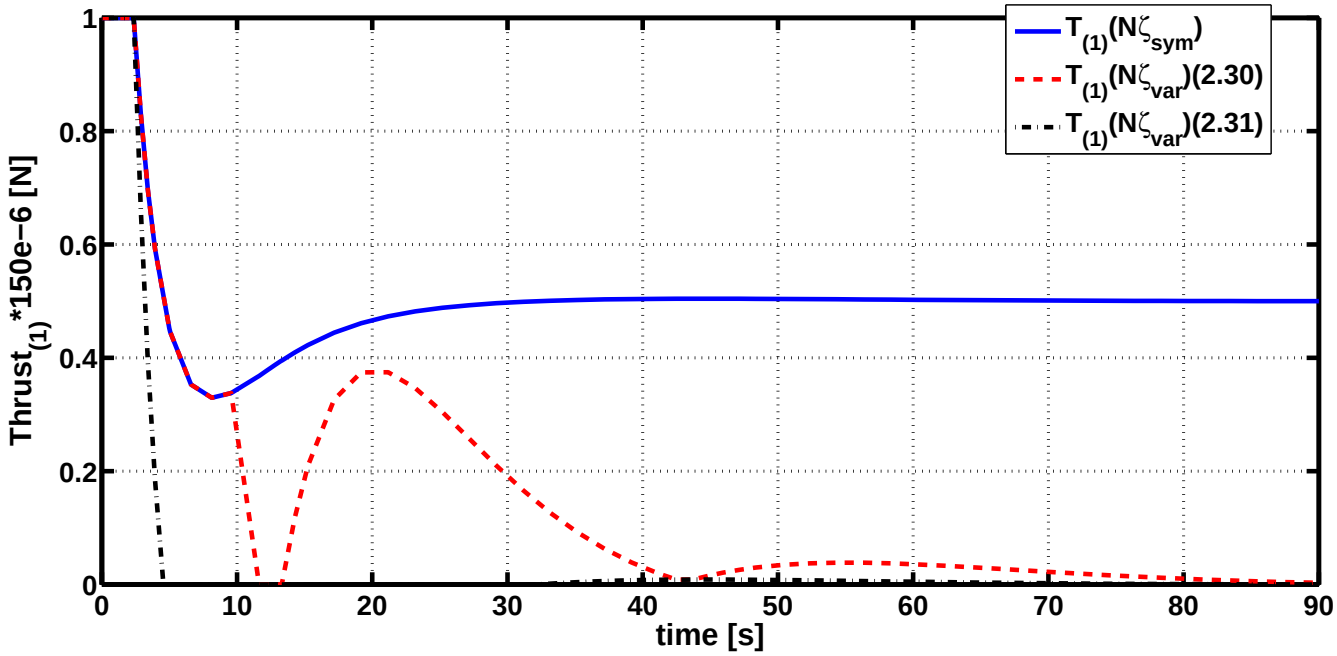

Figure 2.9: Thruster$_{(1)}$ response with different VKF

Figure 2.9 shows the first thruster response of the extended version of the educational example. Different symmetrizing strategies have been applied: the symmetrizing vector $N\zeta_{sym}$(2.5.6) (solid line), the VKF (2.5.14) (dashed line) and the VKF (2.5.15) (dot-dashed line). The initial condition for the simulation has been set to $x_p(0) = [-5 \;\; 0 \;\; -1 \;\; 0]'10^{-4}$. The important thing here is to realize the difference between the thrust provided by VKF in (2.5.15) with respect to VKF in (2.5.14). Because VKF in (2.5.15) handles the thrust of each thruster individually it is able to bring back the thrust to zero faster than in the VKF (2.5.14) case.

Assuming the consumption to be proportional to the integral of all the thrust responses one can compare the performance in terms of consumption between both VKF. Integrating the response of the four thrusters for each VKF one obtains:

$$VKF(2.5.14)\ Consumption: \quad \sum_{i=1}^{n} \int_0^t T(n)dt = 5.2 \cdot 10^{-2} \tag{2.5.21}$$

$$VKF(2.5.15)\ Consumption: \quad \sum_{i=1}^{n} \int_0^t T(n)dt = 3.3 \cdot 10^{-2} \tag{2.5.22}$$

Therefore, the integral shows that the actual consumption is lower when VKF presented in relation (2.5.15) is applied. To complete the analysis just remark that the thrusters are the 6 initial seconds active with VKF (2.5.14) while they are 30 seconds active with VKF (2.5.15)

2.5.6 Minimal control capacity: equivalent saturations

Actuator limitations define a convex set of attainable thrusts. As presented previously, this set is associated to an attainable control. The relationship through both sets is characterized by the AF. Instead of setting the saturation bounds in terms of thrusters limitation, one could look at the associated bound in the control output (i.e. y_c). Nevertheless, the norm of y_c allowed, before thrusters saturate, depends on its direction. A conservative choice is to use the minimal control capacity (MCC) as equivalent saturation in the control output domain. Figure 2.2 recalls these concepts. The MCC vector can be projected in the different components of y_c as it is shown in Figure 2.2. The projection defines saturation bounds u_0 which ensure that $||y_c||$ will never exceed the MCC. Hereafter, $sat_{(u_0)}$, where u_0 is obtained from the projection of the MCC vector to the axes control output domain, will be denoted as $sat_{(mcc)}$. This approach is critically conservative as one is neglecting a part of the control domain. However, in some cases, this approach could provide interesting preliminary results, as we can obtain a first (conservative) estimation of the stability domain.

The main advantage of this approach is that the allocation function is not considered in the closed-loop system. The saturation applies to the control output, then the input to the AF verifies the actuator limitations and, thus, the term Mf is reduced to the identity matrix. Thus $u_p = y_c$ holds and with Definition 2.1:

$$u_p = Msat_{(0,\bar{u})}(f(sat_{(mcc)}(y_c))) = Mf(sat_{(mcc)}(y_c)) = sat_{(mcc)}(y_c) \tag{2.5.23}$$

Consequently, the problems introduced by the AF non-linearity are avoided, allowing the AF design to be decoupled from the anti-windup compensator design, for example. Considering (2.5.23) the closed-loop system expression becomes:

$$\begin{cases} \dot{x}_p = A_p x_p + B_p sat_{(mcc)}(y_c) \\ \dot{x}_c = A_c x_c + B_c C_p x_p \\ y_c = C_c x_c + D_c C_p x_p \end{cases} \tag{2.5.24}$$

Finally let us remark that finding the MCC could not be an easy task. The minimization problem on iterative AF is not trivial. Then, Monte-Carlo tests may allow us to evaluate a representative sample of y_c directions. The minimum norm obtained is the MCC candidate.

Remark 2.10. *In order to find the exact MCC one should test all the directions of y_c and kept the minimum norm $||y_c||$ which saturates the thrusters. The MCC would be the minimun between the retained values of of $||y_c||$. However, it is impossible to test all the infinite directions of the control output. Therefore the resulting MCC from the Monte-Carlo test is only an estimation.*

2.6 Conclusion

In this chapter the problem of asymmetric saturation has been addressed. Particularly, the case where the system presents an allocation function in the control loop has been considered. Moreover, the attention of the chapter has been focused on the actuators providing only a limited positive action.

Generally, the allocation function presents non-linear formulations which are complicate to treat mathematically for stability purposes. In order to include them in further stability considerations two allocation functions have been introduced. Initially, the pseudo-inverse matrix has been proposed as allocation function as it is the solution of the minimum squares problem. Then, a more complex non-linear allocation function has been proposed. This last allocation function is based on a chain of saturations and thus, it remains treatable mathematically.

Afterwards, the problem of the saturation symmetrization has been tackled. Several possibilities have been proposed.

A first proposal is based on a conservative approach which takes the minimum of the two saturation bounds. However this technique has been shown useless for the applications considered.

A second approach, based on the introduction of a symmetrizing vector has been presented. A lemma giving conditions of validity of the symmetrizing vector has been

provided. However this particular approach has been detected to be undesirable for spacecraft application as it forces the actuators to be active even at the equilibrium. To solve this issue a variable kernel function strategy has been proposed. Particular examples of symmetrizing vector and variable kernel functions have been provided. These examples have been compared in the educational example framework.

Finally, another conservative symmetrizing approach has been given. It is based on the minimal control capacity. This limits the control output in order to avoid the allocation to saturate the actuator.

Chapter 3

Anti-windup compensators design

Outline of the chapter

3.1 Introduction

Saturations are present in all modern industrial problems and one of the most important challenges in non-linear control consists in computing a controller law that handles saturations. Several works treat this subject in the literature and various techniques have been developed in that direction.

Roughly speaking, two approaches in the literature [TT09] treat the saturation problem. The first one will be referred to as the *one stage* approach. The goal is to design a controller which takes into account the demands in terms of performance as well as the effect of the saturation. This controller, which may be non-linear, attempts to ensure the nominal specifications imposed, while also handling the input constraints. This approach has been studied in several works in the literature. Initially some researchers have presented different ways to compute the maximal set of initial states such that the saturation is avoided and the resulting closed-loop system follows a linear behavior [GT91, DS91]. However, the system is not necessary instable when the saturation is active. Therefore, the stability domain estimation obtained with this approach is critically conservative. Then, for this kind of approach, a further step is done. It consists in the computation of a control law which maximizes the stability domain allowing the saturation of the actuator [GH85, HL01, KGE02, PTH07, TGGE07, SSY94, Tee95]. Whereas this approach is satisfactory in principle, and has a significant portion of the literature devoted to it, it has often been criticized because of its conservatism, lack of intuition (in terms of tuning rules) and lack of applicability to some practical problems.

On the other hand, a second alternative approach is to separate the design of the controller in two phases. Therefore the approach will be referred to as the *two stages* approach. The first part of the computation is devoted to nominal performance. Actually, the controller is determined considering a linear unconstrained plant. The second part is devoted to handle the input constraint. One of the main *two stages* approach is also known as *anti-windup compensation*. A controller, designed using standard linear design tools, is given, then, a so-called *anti-windup* compensator is added. The presence of this compensator seeks to cope with the saturation constraints and to prevent its bad

effects as much as possible. One classical basic idea of the anti-windup design is to introduce control modifications in presence of saturation. It is only when saturation is encountered that the anti-windup compensator becomes active and acts to modify the closed-loop behavior. The goal is to find an anti-windup compensator which ensures the stability for a state space region as large as possible, while degrading as less as possible the performance of the closed-loop. It seems obvious that a certain trade-off will have to be done in the compensator design between performance and size of the stability domain. Such an approach is really attractive as the anti-windup loop may work with a priori given control laws. Indeed, it represents an interesting technique for the controller designers who can use familiar and intuitive techniques for them and then, simply add an extra layer which will consider the non-linear behavior. Originally, results on anti-windup design consist of ad-hoc methods intended to work with PID controllers [FR67, AR89], which are commonly used in industrial applications. The anti-windup approach has been proposed in several applications from different fields like aeronautic applications [QTG06, RBTP07], aerospace applications [PDTP08, BPT+09], mechanical applications [TZM06] or even in nuclear fusion control [SWHK05].

The anti-windup approach pretends to reduce the effect of the saturation. There are several strategies defining the compensator which where first presented in a unified framework in[KCMN94]. In these work two architectures in anti-windup have been distinguished [GTTZ09]. The first one is called direct linear anti-windup (DLAW) and a second one called model recovery anti-windup (MRAW). Some other strategies are proposed in the literature. An interesting approach is the so-called *coprime factor* anti-windup presented by [WP00]. However in this work we have decided to follow the distinction proposed by [GTTZ09].

The basic idea of the DLAW is to introduce a direct feedback from the saturation to the controller through the anti-windup compensator. In the last decade, the anti-windup problem dealing with exponentially unstable systems has been tackled. An important paper in this direction is [KM97, MP96], which addresses the static anti-windup problem. [GdSJT05], [CLW02] represent the first applications of LMIs to the synthesis of the static anti-windup problem assuring local asymptotic stability. Furthermore, [WL03] suggests a formulation allowing the computation of a dynamic anti-windup compensator. Recently, [BRT07, GHP+03] present LMI conditions to compute the anti-windup compensator dealing with the $\mathcal{L}_2$ performance. See [BT09] for a practical approach and also [WP98, BRT07, TGdSJB06] in global stability context.

MRAW follows a different paradigm on the anti-windup matrices definition. It is based on selecting the anti-windup compensator as a dynamic filter, incorporating a model of the plant. The aim of this filter is to try to recover the closed-loop response of the system when no saturation occurs. This approach stands on the companion papers [TK97a, TK97b] where the MRAW is called $\mathcal{L}_2$ anti-windup problem. Illustrations of this architecture can be found in [ZT02] for exponentially stable plants, in [TZM06] for marginally stable plants and in [Tee99] for exponentially unstable ones.

These architectures are different ways to present a solution to the same problem: the anti-windup computation. Each one has its advantages and drawbacks. In this work, a new architecture called Extended Model Recovery Anti-Windup (EMRAW) is proposed. The EMRAW is the main result of the chapter. This third possible anti-windup strategy consists in mixing both MRAW and DLAW approaches. EMRAW uses the filtering technique of the MRAW while a DLAW complements the control structure. This extension offers interesting results as one may improve the MRAW approach with the DLAW.

Both DLAW and MRAW and they combination, the EMRAW, propose a solution to the anti-windup computation. As introduced before there are other approaches on the anti-windup design. However, all can be related. For example the *coprime factor* anti-windup can be easily related to the MRAW in particular cases. See for example [WP00, HTP04, VMJ06, TP04] in this particular approach. In [WP00] the *coprime factor* anti-windup is also linked to IMC approach proposed in [CM90]. Therefore, even if there are several proposals for the anti-windup computation all may be described in a unified structure. Consequently, along this manuscript all presented approaches will be described by the generic anti-windup structure presented in Figure 1.6.

This chapter is organized as follows. First in Section 3.2 a general introduction of the anti-windup problem is provided, setting the separation between the DLAW and the MRAW approaches. The EMRAW interest is briefly introduced. Section 3.3 presents the main results on the DLAW approach, from the static anti-windup synthesis to the fixed order dynamic anti-windup. The MRAW strategy is then described in Section 3.4 with a short parenthesis on the particular case of a double integrator plant. In Section 3.5 the EMRAW architecture is presented and some algorithms solving the bilinear problem are presented. Afterwards, the application of these techniques with asymmetric saturation is tackled in Section 3.6. Finally, each approach main characteristics are illustrate with the educational example.

3.2 The anti-windup problem

The windup is a phenomenon which becomes apparent by an important overshoot in the output signal and an excessive reaction time. The windup phenomenon usually appears in systems which include actuators subject to saturation and present a feedback loop through a controller including integrators, for example a PID. When saturation is active, the error is still integrated even if the control applied to the system has been altered. Then integral state value tends to large levels, inducing undesired effects such as oscillations or even instability [FR67, AR89]. Even if the word windup comes from PID controllers, the word has been kept for modern problems when a non-linearity, like saturation, arises [FR67].

From a practical point of view that can be found in industrial environments the windup phenomenon is measured as the difference between the performance sought for the *un-*

constrained system (i.e. linear) and the actual non-linear one. The anti-windup problem has been always stated as the minimization of the deviation of the systems response with saturation in relation to the behavior without saturation. The designed response for the unconstrained system is considered as the ideal one and denoted as *unconstrained response*. Therefore, the anti-windup purpose could be summarized as follows:

1. If the controller output does not exceed the saturation levels, then the system response with anti-windup compensator coincides with the unconstrained response.
2. If the controller output does exceed the saturation levels, then the anti-windup compensator objective is to minimize the error between the non-linear and the linear responses.

Modern anti-windup design can be classified into families where other constructive techniques may fall. Let us first introduce the system considered in the following sections. The unconstrained LTI plant is described by the following state space description:

$$\mathcal{P}\begin{cases} \dot{x}_p &= A_p x_p + B_p u_p + B_d u_d \\ y_p &= C_p x_p + D_p u_p + D_d u_d \\ z_p &= C_z x_p + D_{zu} u_p \end{cases} \tag{3.2.1}$$

with $x_p \in \Re^{n_p}$ the state of the system, $y_p \in \Re^q$ the output of the system, $u_p \in \Re^{m_c}$ the control input and $u_d \in \Re^m$ the disturbance input vector. $z_p \in \Re^p$ is the regulated output vector. Matrices A_p, B_p, B_d, C_p, D_p, D_d, C_z and D_{zu} are real constant matrices of appropriate dimensions. Pairs (A_p,B_p) and (C_p,A_p) are assumed to be controllable and observable, respectively.

Considering the plant (3.2.1), a given controller ensures that the unconstrained (i.e. linear) closed-loop system is asymptotically stable and its performance is adjusted. Introducing the compensation inputs the controller state space representation can be written as follows:

$$\mathcal{C}\begin{cases} \dot{x}_c &= A_c x_c + B_c u_c + v_x \\ y_c &= C_c x_c + D_c u_c + v_y \end{cases} \tag{3.2.2}$$

where $x_c \in \Re^{n_c}$ is the state of the controller, $y_c \in \Re^m$ and $u_c \in \Re^q$ are the controller output and the controller input vector. v_x, v_y are extra inputs used for anti-windup purposes. In absence of saturation the interconnection (3.2.1)-(3.2.2) is set with the following relationships:

$$u_p = y_c,\ u_c = y_p,\ v_x = 0,\ v_y = 0 \tag{3.2.3}$$

Remark 3.1. *The closed-loop system* (3.2.1)-(3.2.3) *is supposed to be well posed [Sta09], that is, the matrix* $\Delta = (I - D_c D_p)$ *is invertible. Moreover, the unconstrained closed-loop system is assumed to be globally exponentially stable, that is, the closed-loop state matrix is Hurwitz which expression reads:*

$$\begin{bmatrix} A_p + B_p\Delta^{-1}D_c C_p & B_p\Delta^{-1}C_c \\ B_c + B_c D_p \Delta^{-1} D_c C_p & A_c + B_c D_p \Delta^{-1} C_c \end{bmatrix} \tag{3.2.4}$$

Remark 3.2. *Hereafter direct transmission are set to zero ($D_p = 0$, $D_d = 0$) to simplify the mathematical development. this allows the main ideas of the work to be conveyed while avoiding technical issues such as uniqueness and existence of solutions.*

Then the magnitude limitations on the input vector u_p are considered[1]:

$$|u_{p(i)}| \leq u_{0(i)},\ i = 1, ..., m_c \tag{3.2.5}$$

Due to the control limitation the interconnection between the plant and the controller is a saturated signal. Thus, u_p and y_c are related to the saturation function, that is, $u_p = sat_{(u_0)}(y_c)$.

$$u_p = sat_{(u_0)}(y_c), \quad u_c = y_p \tag{3.2.6}$$

Let us recall the definition for the decentralized symmetric saturation:

$$sat_{(u_0)}(y_{c(i)}) = sign(y_{c(i)})min(|y_{c(i)}|, u_{0(i)}),\ i = 1, ..., m \tag{3.2.7}$$

where u_0 is the level of saturation. The plant output saturation can also be considered. That is expressed as follows:

$$u_c = sat_{(u_0)}(y_p) \tag{3.2.8}$$

Relation (3.2.8) stands for the sensor saturation [TT06], however it is not tackled in this manuscript.

Given all these considerations, it is now possible to introduce the different anti-windup architectures.

3.3 Direct linear anti-windup

Let us consider the plant (3.2.1) and its associated controller (3.2.2) with the relationships (3.2.6):

$$\left\{\begin{array}{rcl} \dot{x}_p &=& A_p x_p + B_p sat_{(u_0)}(y_c) + B_d u_d \\ y_p &=& C_p x_p \\ z_p &=& C_z x_p + D_{zu} sat_{(u_0)}(y_c) \\ \dot{x}_c &=& A_c x_c + B_c y_p + v_x \\ y_c &=& C_c x_c + D_c y_p + v_y \end{array}\right. \tag{3.3.1}$$

[1]Saturations bounds are symmetric in this chapter. In Section 2.5 symmetrizing techniques were presented. Then we assume that these techniques have been applied previously and therefore the system saturations can be supposed symmetric.

All the results developed in the Direct Linear Anti-Windup (DLAW) context are based upon the use of the dead-zone non-linearities and associated modified sector conditions. Indeed, any system, where saturation is present, may be rewritten with dead-zone non-linearity. Let us recall that the dead-zone function is defined by: $\phi_{(u_0)}(y_c) = y_c - sat_{(u_0)}(y_c)$. System (3.3.1) with the dead-zone function as non-linear operator reads:

$$\begin{cases} \dot{x}_p &= A_p x_p + B_p y_c - B_p \phi_{(u_0)}(y_c) + B_d u_d \\ y_p &= C_p x_p \\ z_p &= C_z x_p + D_{zu} y_c - D_{zu} \phi_{(u_0)}(y_c) \\ \dot{x}_c &= A_c x_c + B_c y_p + v_x \\ y_c &= C_c x_c + D_c y_p + v_y \end{cases} \tag{3.3.2}$$

Signals v_x and v_y are the outputs of the anti-windup compensator. In the DLAW context, the anti-windup compensator is defined as follows:

$$\mathcal{AW} \begin{cases} \dot{x}_{aw} &= A_{aw} x_{aw} + B_{aw} \phi_{(u_0)}(y_c) \\ v_x &= [I_{n_c} \;\; 0] \left(C_{aw} x_{aw} + D_{aw} \phi_{(u_0)}(y_c) \right) \\ v_y &= [0 \;\; I_m] \left(C_{aw} x_{aw} + D_{aw} \phi_{(u_0)}(y_c) \right) \end{cases} \tag{3.3.3}$$

where $x_{aw} \in \Re^{n_{aw}}$ is the anti-windup state, $n_{aw} \geq 0$, $\phi_{(u_0)}(y_c)$, the dead-zone output is the anti-windup input, $v = [v_x' \;\; v_y']' \in \Re^{n_c+m}$ is the anti-windup output and A_{aw}, B_{aw}, C_{aw}, D_{aw} are matrices of appropriate dimensions. Figure 3.1 presents the block diagram describing the DLAW structure.

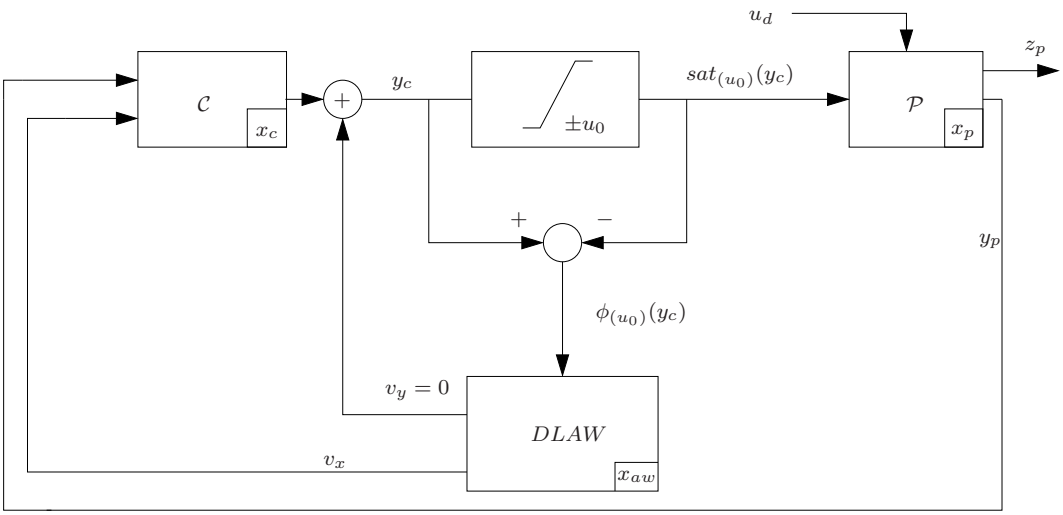

Figure 3.1: Direct Linear Anti-Windup Structure.

Remark 3.3. *The presence of the v_y introduces an implicit loop in the closed-loop system. By considering a simplified anti-windup compensator where the output is only injected in the controller dynamics x_c, the implicit loop can be avoided. Another way consist in filtering the signal v_y and therefore to inject $\bar{v}_y = F(s)v_y$. Thus, a lower-pass filter $F(s)$ can, for example, be used to avoid algebraic-loop-derived effects [BT09].*

Henceforth, only the anti-windup output v_x is kept and $v_y = 0$.

3.3.1 Introducing robustness and performance criterion

3.3.1.a Disturbance tolerance

In order to consider its disturbance influence in the anti-windup design, it is interesting to introduce it as a new state variable of the closed-loop system. The disturbance can be modelled by a step-like function which slowly decreases with time. This behavior may be described more generally by a linear system with a small-damping-decreasing exponential behavior [BTF06]. The space state representation of the disturbance is defined by:

$$\left\{ \begin{array}{rcl} \dot{x}_d & = & A_d x_d \\ u_d & = & C_d x_d \end{array} \right. \tag{3.3.4}$$

where $x_d \in \Re^{n_d}$ and A_d is Hurwitz. A_d and C_d are matrices of appropriate dimensions. For a slowly decreasing step function, matrices become $A_d = -\tau I_{n_d}$, $\tau > 0$, $C_d = I_{n_d}$ and the maximum disturbance amplitude $u_{d0} = x_d(0)$. With this modelling, the initial condition of the disturbance state system defines the amplitude of the step.

Remark 3.4. *The choice of a step-like disturbance allows the computation of the maximal admissible disturbance amplitude. Even if other modellings are possible all are reduced to a space state representation. Therefore, further considerations are valid for other kinds of disturbance models.*

Then we define the following set:

$$\mathcal{W}_\epsilon(\delta) = \left\{ x_d : \Re^{n_d}, x_d(t) = u_{d0} e^{-\tau t};\ \forall t \geq 0, \|u_{d0}\|^2 \leq \delta \right\} \tag{3.3.5}$$

Therefore, for example, the tolerance of the disturbance could be optimized by maximizing the stability domain in the disturbance state direction.

3.3.1.b Performance criterion

Let us define, the linear closed-loop system as follows:

$$\left\{ \begin{array}{rcl} \dot{x}_l & = & A_l x_l \\ z_l & = & C_l x_l \end{array} \right. \tag{3.3.6}$$

where $x_l \in \Re^{n_l}$ with $n_l = n_p + n_c$, $A_l = \left[\begin{array}{cc} A_p + B_p D_c C_p & B_p C_c \\ B_c C_p & A_c \end{array} \right]$ and $C_l = C_z$.

Following the anti-windup compensator objective of minimizing the error between the non-linear and the linear responses, [BTF06] proposes to introduce a performance criterion by comparing the non-linear response z_p to the linear one z_l. The goal is then to minimize the difference between the system output, z_p, and the unconstrained one, z_l. Therefore,

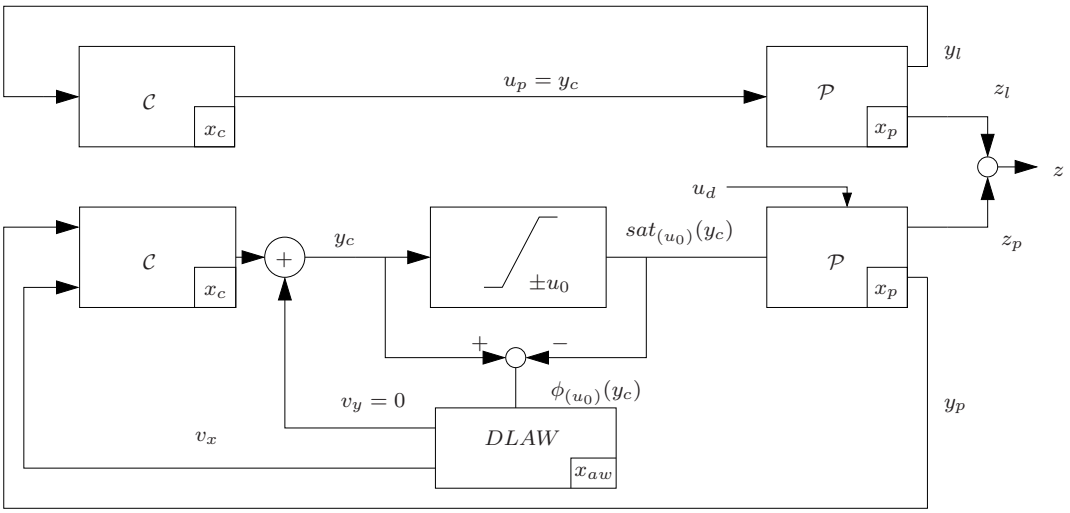

Figure 3.2: Performance optimization strategy.

the linear dynamics are set in parallel to the non-linear one. This strategy is presented in Figure 3.2 We define $z = z_p - z_l$, and we minimize the $\mathcal{L}_2$ norm of z.

Let us consider the saturated system (3.3.2), the disturbance dynamics (3.3.4) and the linear dynamics (3.3.6). Then, extending the state vector $\xi = [x_p^{'}\ x_c^{'}\ x_d^{'}\ x_l^{'}]^{'} \in \Re^{n_M}$, with $n_M = n_p + n_c + n_d + n_l$ the closed-loop system reads:

$$\begin{cases} \dot{\xi} = \mathbb{A}\xi + \mathbb{B}_\phi \phi_{(u_0)}(\nu) + \mathbb{B}_v v_x \\ \nu = \mathbb{K}\xi \\ z = \mathbb{C}\xi + \mathbb{D}_\phi \phi_{(u_0)}(\nu) \\ v_x = C_{aw} x_{aw} + D_{aw} \phi_{(u_0)}(\nu) \end{cases} \tag{3.3.7}$$

where $\mathbb{A} = \begin{bmatrix} A_p + B_p D_c C_p & B_p C_c & B_d C_d & 0 \\ B_c C_p & A_c & 0 & 0 \\ 0 & 0 & A_d & 0 \\ 0 & 0 & 0 & A_l \end{bmatrix}$, $\mathbb{B}_\phi = [-B_p^{'}\ \ 0\ \ 0\ \ 0]^{'}$, $\mathbb{B}_v = [0\ \ I_{n_c}\ \ 0\ \ 0]^{'}$, $\mathbb{K} = [D_c C_p\ \ C_c\ \ 0\ \ 0]$, $\mathbb{C} = [C_z + D_{zu} D_c C_p\ \ D_{zu} C_c\ \ 0\ \ -C_l]$ and $\mathbb{D}_\phi = -D_{zu}$.

The strategy chosen to arise a certain performance criterion doubles the plant and the controller states. This is clearly unefficient as the dymension of the considered closed-loop can become significant. Some numerical problems may be derived from this approach. Alternative mismatch system strategies can be found in [WP98, VMJ06]. However the strategy proposed by [BTF06] and kept in this thesis provides a more intuitive manner to tune the anti-windup computation.

Finally, the anti-windup state is included in the closed-loop state vector $\zeta = [\xi^{'}\ \ x_{aw}]^{'} \in \Re^n$, with $n = n_M + n_{aw}$. Consequently, the final expression for the closed-loop system

(3.3.7) with (3.3.3) is expressed as follows:

$$\begin{cases} \dot{\zeta} = \mathcal{A}\zeta + \mathcal{B}_\phi \phi_{(u_0)}(\nu) \\ \nu = \mathcal{K}\zeta \\ z = \mathcal{C}\zeta + \mathcal{D}_\phi \phi_{(u_0)}(\nu) \end{cases} \tag{3.3.8}$$

where $\mathcal{A} = \begin{bmatrix} \mathbb{A} & \mathbb{B}_v C_{aw} \\ 0 & A_{aw} \end{bmatrix}$, $\mathcal{B}_\phi = \begin{bmatrix} \mathbb{B}_\phi + \mathbb{B}_v D_{aw} \\ B_{aw} \end{bmatrix}$, $\mathcal{K} = [\mathbb{K} \;\; 0]$, $\mathcal{C} = [\mathbb{C} \;\; 0]$ and $\mathcal{D}_\phi = \mathbb{D}_\phi$.

3.3.2 Problem formulation

Once the final system is defined the problem to solve is defined as follows:

Problem 3.1. *Find an anti-windup compensator and a stability domain Ω such that*

- *the system (3.3.8) is stabilized by the anti-windup compensator;*
- *the domain Ω is maximized in the direction of the disturbance x_d (that is u_d);*
- *the selected output z_p of the plant remains as close as possible to the linear reference z_l (associated with the linear behavior), i.e. the upper-bound γ, such that $\|z\|_2^2 = \int_0^\infty z(t)'z(t)dt \leq \gamma$, is minimized.*

The objectives, when designing the anti-windup compensator, can be summed up:

1. The closed-loop stability of the non-linear system has to be ensured.
2. Robustness in front of disturbances is needed. In order to assure it, the stability domain has to be large enough to contain the disturbance initial condition $x_d(t = 0)$. Even if an actuator saturates, the system will be able to return to the origin once the disturbance is over.
3. The selected output of the system z_p has to be degraded as less as possible. The anti-windup compensator has to keep saturated behavior close to the unconstrained one.

3.3.3 Static anti-windup synthesis

Initially we seek to solve the particular case of the static anti-windup. In this situation one chooses $n_{aw} = 0$ and anti-windup matrices are null except D_{aw} ($A_{aw} = B_{aw} = C_{aw} = 0$). Even if it is a simpler case, because of the interesting results that are computed

[QTG06, BPT+09, BTF06] and the convexity of the optimization problem, it is important to treat it separately.

Defining $n = n_p + n_c + n_d + n_l + n_{aw}$ ($n_{aw} = 0$, that is $n = n_M$) and a static anti-windup output v_x:

$$v_x = D_{aw}\phi_{(u_0)}(\nu) \tag{3.3.9}$$

then the relations (3.3.7) and (3.3.8) are the same. Finally, a theorem with respect to the system (3.3.8) can be stated:

Theorem 3.1. (Static anti-windup synthesis). *Given $v \in \Re^n$, k_γ and k_ρ positive values, if there exist positive scalars γ and ρ, a symmetric positive-definite matrix $W \in \Re^{n\times n}$, a matrix $Y \in \Re^{m\times n}$, a matrix $Z \in \Re^{n_c\times m}$ and a diagonal positive-definite matrix $S \in \Re^{m\times m}$ satisfying min $k_\gamma\gamma + k_\rho\rho$ s.t.*

$$\begin{bmatrix} W\mathbb{A}' + \mathbb{A}W & \mathbb{B}_\phi S + \mathbb{B}_v Z + Y' & W\mathbb{C}' \\ * & -2S & S\mathbb{D}_\phi' \\ * & * & -\gamma I_p \end{bmatrix} < 0 \tag{3.3.10}$$

$$\begin{bmatrix} W & W\mathbb{K}_{(i)}' - Y_{(i)}' \\ \star & u_{0(i)}^2 \end{bmatrix} \geq 0, \quad \forall i = 1, ..., m \tag{3.3.11}$$

$$\begin{bmatrix} W & v \\ * & \rho \end{bmatrix} \geq 0 \tag{3.3.12}$$

then the static DLAW $D_{aw} = ZS^{-1}$ stabilizes the system (3.3.8) for any initial condition in the ellipsoid

$$\mathcal{E}(P) = \left\{\xi \in \Re^n; \xi' P \xi \leq 1\right\}$$

with $P = W^{-1}$, which is maximized in the v direction with the weight k_ρ, and the performance $1/\gamma$ is maximized with the weight k_γ.

Proof of Theorem 3.1: For the proof, refer to Appendix A.3.1. **End of Proof.**

Remark 3.5. *Relation (3.3.12) allows the maximization of the stability domain towards v by adding the optimization criterion min ρ. Indeed, if we set $v = [0_{n_p}\ \ 0_{n_c}\ \ x_d'(0)\ \ 0_{n_l}\ \ 0_{n_{aw}}]'$ the domain of stability is maximized in the disturbance state direction (i.e. the disturbance amplitude $u_d(0)$). The parameter ρ in Theorem 3.1 is related with admissible amplitude δ defining the set (3.3.5) by the following relation:*

$$\delta = 1/\sqrt{(\rho)} \tag{3.3.13}$$

Remark 3.6. *An extension of Theorem 3.1 for the static DLAW computation adapted to the multi AF (2.4.3) is introduced in Appendix A.3.2. Given closed-loop in (4.5.2) one may apply the extensions of Appendix A.3.2.*

3.3.4 Full order dynamic anti-windup synthesis

The results presented in this paragraph are derived from those in [BRT07, Roo97]. Proposition 3.1 below provides conditions for the computation of the dynamic anti-windup compensator presented in (3.3.3). Generally conditions appear as BMI (Bilinear Matrix Inequality). Nevertheless, conditions such that the problem becomes linear are recalled. Moreover, Proposition 3.1 introduces constraints to the anti-windup dynamics forcing A_{aw} eigenvalues to be larger than a certain threshold.

Defining $n = n_p + n_c + n_d + n_l + n_{aw}$ and $He(A) = A + A'$, the following proposition with respect to the system (3.3.8) can be stated:

Proposition 3.1. (Full order anti-windup synthesis) *Given $v \in \Re^n$, k_γ, k_ρ and λ positive values, if there exist positive scalars γ and ρ, matrices $A_{aw} \in \Re^{n_{aw}\times n_{aw}}$, $B_{aw} \in \Re^{n_{aw}\times m}$, $C_{aw} \in \Re^{n_c\times n_{aw}}$ and $D_{aw} \in \Re^{n_c\times m}$, a symmetric positive-definite matrix $W \in \Re^{n\times n}$, a matrix $Z \in \Re^{m\times n}$ and a diagonal positive-definite matrix $S \in \Re^{m\times m}$ satisfying min $k_\gamma\gamma + k_\rho\rho$ s.t.*

$$\begin{bmatrix} He\left[\begin{bmatrix} \mathbb{A} & B_vC_{aw} \\ 0 & A_{aw} \end{bmatrix} W + \lambda \begin{bmatrix} 0 & 0 \\ 0 & I_{n_{aw}} \end{bmatrix} W\right] & * & * \\ S\begin{bmatrix} \mathbb{B}_\phi + \mathbb{B}_v D_{aw} \\ B_{aw} \end{bmatrix} + Z & -2S & * \\ \mathcal{C}W & \mathcal{D}_\phi S & -\gamma I_p \end{bmatrix} < 0 \tag{3.3.14}$$

$$\begin{bmatrix} W & W\mathcal{K}'_{(i)} - Z'_{(i)} \\ \star & u^2_{0(i)} \end{bmatrix} \geq 0, \quad \forall i = 1, ..., m \tag{3.3.15}$$

$$\begin{bmatrix} W & v \\ * & \rho \end{bmatrix} \geq 0 \tag{3.3.16}$$

then the system (3.3.8) is asymptotically stable for any initial condition in the ellipsoid

$$\mathcal{E}(P) = \left\{\zeta \in \Re^n; \zeta' P\zeta \leq 1\right\} \tag{3.3.17}$$

with $P = W^{-1}$, which is maximized in the v direction, with the weight k_ρ, and the performance $1/\gamma$ is maximized with the weight k_γ. Moreover the output z is finite energy satisfying:

$$\int_0^\infty z'z dt \leq \gamma \tag{3.3.18}$$

Proof of Proposition 3.1: This proof is omitted as it follows the same mathematical development than the proof of Theorem 3.1. **End of Proof.**

Remark 3.7. *Like in Theorem 3.1 if one sets $v = [0_{n_p}\ \ 0_{n_c}\ \ x'_d(0)\ \ 0_{n_l}\ \ 0_{n_{aw}}]'$, the stability domain is maximized in the disturbance state direction (i.e. the disturbance amplitude $u_d(0)$).*

The introduction of λ imposes a lower bound for the A_{aw} eigenvalues in absolute value [Roo97]. This is interesting in the case where only the stability is under consideration, and consequently $k_\gamma = 0$. In that situation the optimization process tends to provide an anti-windup compensator as slow as possible. That could bring the anti-windup dynamics to levels which may be critically low if parameter λ was not there. Moreover, we set the threshold λ to avoid small values in A_{aw}. Therefore, λ improves the resulting conditioning number of the matrices.

The anti-windup Problem 3.1 is solved by the optimization of the decision variables W and the anti-windup matrices (A_{aw}, B_{aw}, C_{aw} and D_{aw}) simultaneously. Consequently, the inequality (3.3.14) losses its convexity and becomes a BMI. However, in the case of full order anti-windup, that is, $n_{aw} = n_M = n_p + n_c + n_d + n_l$, inequalities (3.3.14)-(3.3.16) present a particular structure which can be used to obtain a convex formulation. The resulting formulation is presented in the following proposition.

Proposition 3.2. (Full order anti-windup synthesis 2) *[RB08] Given $v \in \Re^n$, k_γ, k_ρ, λ positive values and $\Gamma = diag(N_v, I_m, I_{n_c})$ where N_v is the matrix which its columns form the basis of the $Ker(\mathbb{B}_v')$. There exists a full order anti-windup compensator such as conditions in Proposition 3.1 are satisfied if and only if there exist positive scalars γ and ρ, symmetric positive-definite matrices $X, Y \in \Re^{n_M \times n_M}$, matrices $U, V \in \Re^{m \times n_M}$, and a diagonal positive-definite matrix $S \in \Re^{m \times m}$ satisfying min $k_\gamma \gamma + k_\rho \rho$ s.t.*

$$\Gamma' \begin{bmatrix} \mathbb{A}'Y + Y\mathbb{A} & \mathbb{B}_\phi S + V' & Y\mathbb{C}' \\ * & -2S & S\mathbb{D}_\phi' \\ * & * & -\gamma I_p \end{bmatrix} \Gamma < 0 \tag{3.3.19}$$

$$\begin{bmatrix} \mathbb{A}X + X\mathbb{A}' - 2\lambda X & 2\lambda Y & X\mathbb{C}' \\ * & -2\lambda Y & 0 \\ * & * & -\gamma I_p \end{bmatrix} < 0 \tag{3.3.20}$$

$$\begin{bmatrix} X & X & U_{(i)}' \\ * & Y & Y\mathbb{C}_{\phi(i)}' - V_{(i)}' \\ * & * & u_{0(i)}^2 \end{bmatrix} \geq 0, \quad \forall i = 1, ..., m \tag{3.3.21}$$

$$\begin{bmatrix} X & X & v \\ * & Y & v \\ * & * & \rho \end{bmatrix} \geq 0 \tag{3.3.22}$$

Proof of Proposition 3.2: For the proof, refer to Appendix A.3.3. **End of Proof.**

Remark 3.8. *Reconstruction of the matrix W is done by applying the following relation:*

$$W = \begin{bmatrix} Y & I_{n_M}' \\ N & 0 \end{bmatrix} \begin{bmatrix} I_{n_M} & X^{-1} \\ 0 & M \end{bmatrix}^{-1} \tag{3.3.23}$$

Then conditions in Proposition 3.1 are not BMI but LMI and can be solved with existing LMI solvers [BcPS07].

3.3.5 Fixed order dynamic anti-windup synthesis

The resulting anti-windup compensator from Proposition 3.2 is an n_M order system. In some applications this order can be too large to be implemented in a real on-board calculator. Thus, the goal now is to find a low order anti-windup compensator. The following proposition presents a technique which allows the computation of a fixed order anti-windup compensator.

Proposition 3.3. *The matrix inequality* (3.3.14) *becomes convex if matrices* A_{aw} *and* C_{aw} *of the anti-windup compensator are fixed.*

Proof of Proposition 3.3: For the proof, refer to Appendix A.3.4. **End of Proof.**

This results allows the introduction of the following algorithm [BRT07]:

Algorithm 3.1. (Fixed order anti-windup synthesis)

1. *Choose matrices* A_{aw} *and* C_{aw} *of the controller to compute.*

2. *Solve min* $k_\gamma\gamma + k_\rho\rho$ *under LMI constraints* (3.3.14)-(3.3.16) *w.r.t. the decision variables* W, S, Y, $\tilde{B}_{aw}$ *and* $\tilde{D}_{aw}$.

3. *Compute matrices* B_{aw} *and* D_{aw} *inverting the variables change from Proposition 3.3.*

The main difficulty of this algorithm is the choice of matrices A_{aw} and C_{aw} in Step 1. In [BRT07] a practical method for the construction of the matrices is proposed. This method is based on the choice of the representative poles of the full order anti-windup compensator. Hence among the poles of the full anti-windup dynamics (i.e., A_{aw}), we can choose a suitable amount of poles: for example we can eliminate the fast and the slow dynamics. However, the way to select such a set of poles requires the knowledge of the system as well as the experience of the designer. Systematic methods to do this selection can be found in [BT09, KTP08]. Once the eigenvalues chosen, the resulting matrices A_{aw} and C_{aw} may be constructed and Algorithm 3.1 applies.

3.4 Model recovery anti-windup

As already introduced the Model Recovery Anti-Windup (MRAW) is based on a different paradigm. It consists in selecting the anti-windup compensator as a dynamical filter,

incorporating a model of the plant [GTTZ09]. The aim of this filter is to recover the unconstrained closed-loop dynamics. The plant control is limited by the saturation nonlinearity, thus, recovering the missing control and filtering it throughout the anti-windup compensator we can recover the missing dynamics of the plant. This recovered dynamics allows the system to keep tracking what the closed-loop response would be in the absence of saturation. The equations describing filter dynamics are stated by:

$$\begin{cases} \dot{x}_{aw} = A_p x_{aw} + B_p \left(v_1 - \phi_{u_0}(y_c + v_1)\right) \\ y_{aw} = C_p x_{aw} + D_p \left(v_1 - \phi_{u_0}(y_c + v_1)\right) \\ v_1 = g(x_{aw}) \end{cases} \tag{3.4.1}$$

where $x_{aw} \in \Re^{n_p}$ is the anti-windup compensator state, $y_{aw} \in \Re^q$ and $v_1 \in \Re^m$ its outputs.

The anti-windup compensator structure is represented in Figure 3.3.

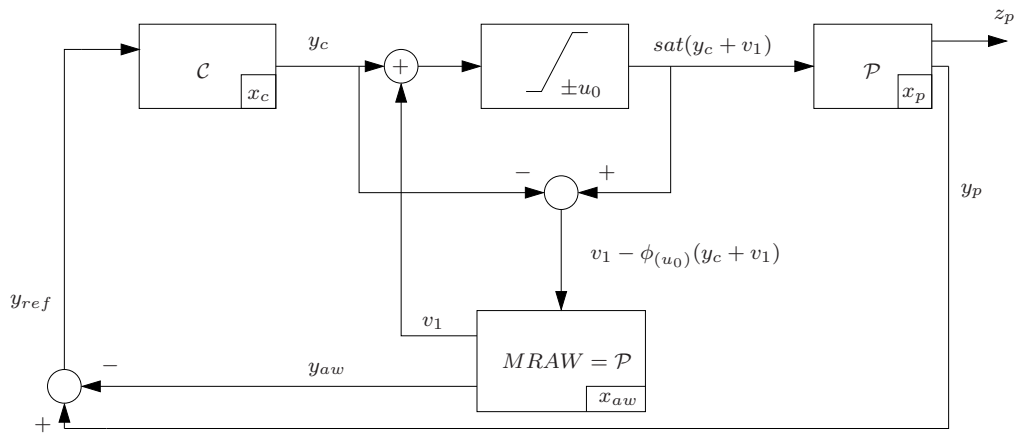

Figure 3.3: MRAW control block diagram

The plant and controller equations are related to the anti-windup compensator (3.4.1) through v_1 and y_{aw} as follows:

$$\mathcal{P}: \quad \begin{cases} \dot{x}_p = A_p x_p + B_p sat_{(u_0)}(y_c + v_1) \\ y_p = C_p x_p + D_p sat_{(u_0)}(y_c + v_1) \end{cases} \tag{3.4.2}$$

$$\mathcal{C}: \quad \begin{cases} \dot{x}_c = A_c x_c + B_c(y_p - y_{aw}) \\ y_c = C_c x_c + D_c(y_p - y_{aw}) \end{cases} \tag{3.4.3}$$

Remark 3.9. *From Remark 3.2, we have* $D_p = 0$.

Notice that the controller (3.2.2) can be recontruced from (3.4.2) and (3.4.3) by considering $u_c = y_p$ and inputs v_x and v_y as follows:

$$\begin{aligned} v_x &= -B_c y_{aw} \\ v_y &= -D_c y_{aw} + v_1 \end{aligned} \tag{3.4.4}$$

The block diagram of Figure 3.4 presents the MRAW approach in the general anti-windup context described by Figure 1.6.

Under the assumption of perfect knowledge of the plant the linear state can be recovered $x_l = x_p - x_{aw}$. The aim of the anti-windup is to drive the actual system towards the linear closed-loop behavior. If the anti-windup dynamics (3.4.1) are stable, x_{aw} converges to zero and the plant and the controller state $[x_p^{'} \;\; x_c^{'}]^{'}$ converges to the linear dynamics x_l. From Figure 3.3, the relationship $y_{ref} = y_p - y_{aw}$ holds. Hence, if the anti-windup is stable, $y_{aw} \to 0$ and the system output y_p converges to a fictitious reference y_{ref}. In the MRAW approach, y_{ref} is the linear system output y_l. The anti-windup dynamics are stabilized with a function $v_1 = g(x_{aw})$ suitably designed [TK97a, ZT02]. Therefore the goal is to find v_1 stabilizing the anti-windup loop.

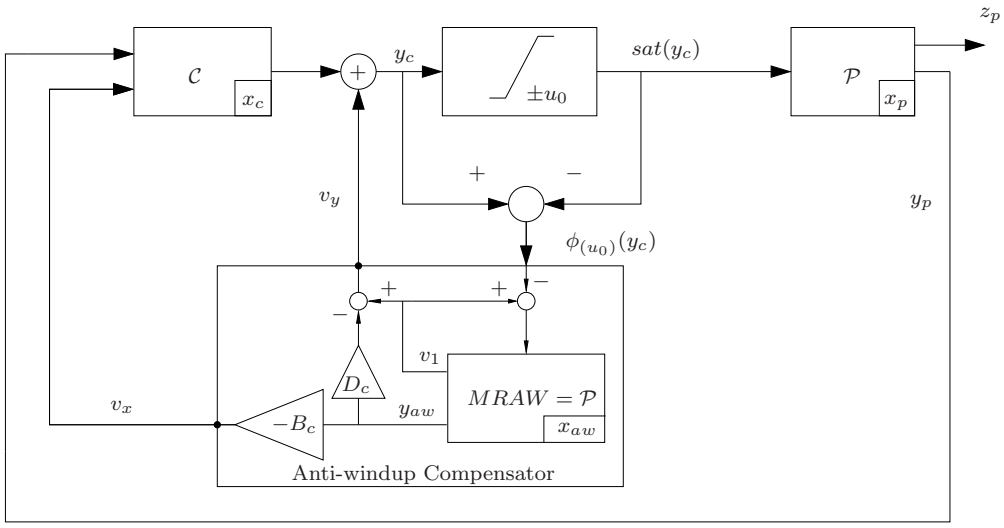

Figure 3.4: MRAW in a general anti-windup structure

MRAW architecture presents possible different solutions depending on how the signal v_1 is designed. Within this framework, the simplest v_1 that one can think of is the one that only focus on stabilizing the linear dynamics of the anti-windup loop (3.4.1). The anti-windup linear dynamics reads:

$$\begin{aligned} \dot{x}_{aw} &= A_p x_{aw} + B_p v_1 \\ y_{aw} &= C_p x_{aw} + D_p v_1 \\ v_1 &= g(x_{aw}) \end{aligned} \tag{3.4.5}$$

Therefore, a first possible solution to the MRAW problem is to select v_1 as a linear state feedback from x_{aw} designed completely disregarding the saturation effects. These solutions are associated to local stability properties but, for exponentially stable plants, the global stability is possible [GOTZ07].

Another type of solutions that one can propose within the MRAW compensation is to select v_1 as a non-linear function of the anti-windup compensator state x_{aw}. This type

of solution is certainly the most difficult to design and to implement but it is the most advanced scheme within this framework. Reference [GTZ07] gives constructive conditions to find such a stabilizing law v_1.

Several algorithms in function of the nature of the plant are presented in the literature. The works [MZ89, TK97a, ZT02] present different strategies to compute stabilizing feedback v_1 when the plant is exponentially stable (i.e. A_p Hurwitz). With exponentially stable plants, the simplest possible compensation scheme is given by the so-called IMC (Internal Model Control)-based anti-windup [CM90, MZ89]. In the context of MRAW, the IMC scheme simply amounts to selecting $v_1 = 0$. This strategy corresponds to blindly use the controller as if no saturation was in place and delivering to the plant the same signal as the controller would have produced without saturation.

In the case of marginally stable plants (plants without poles with positive real part) [TK97a, ZWT07] suggest algorithms to compute global asymptotically stable v_1. These methods are especially useful for practical situations with integrating plants which belong to the class addressed here. Finally, in the unstable plant case, first tackled by [Tee99], the region of attraction is bounded, and only local stability is guaranteed by the stabilizing feedback v_1. In [GTZ07] constructive conditions are proposed for this kind of plants.

In the particular case where the plant is modelled by a saturated double integrator[2] a non-linear v_1 introduced by [FGZ10] can be applied.

$$v_1 = g(x_{aw}) = -\frac{k}{b_0}\left(x_{aw}(1) + x_{aw}(2) max\left\{\frac{|x_{aw}(2)|\, b_0}{2u_0}, \frac{2\xi}{\sqrt{k}}\right\}\right) \tag{3.4.7}$$

where ξ and k are tuning parameters. The stabilizing feedback (3.4.7) is based on a bang-bang law. Indeed [FGZ10] shows that (3.4.7) is actually a bang-bang law when x_{aw} is far from the origin and it switches to a static feedback law as it gets closer. Moreover in [FGZ10] is proven that (3.4.7) ensure global asymptotic stability to the saturated double integrator.

Remark 3.10. *If the system is modelled by a saturated double integrator and one applies (3.4.7), then the anti-windup loop is global asymptotically stable. Hence, from implications given in [TK97a], the whole closed-loop is also global asymptotically stable.*

Note that the MRAW architecture is independent of the controller dynamics. By this fact, any stabilizing controller can be used within the MRAW structure and closed-loop stability will be guaranteed. However, extra assumptions on the controller dynamics are highly desirable because they are necessary for robustness [TK97a, ZT02].

[2]The double integrator plant is defined by the following state matrices:

$$A_p = \begin{bmatrix} 0 & 1 \\ 0 & 0 \end{bmatrix}; B_p = \begin{bmatrix} 0 \\ b_0 \end{bmatrix} \tag{3.4.6}$$

.

Perhaps the most important drawback of the MRAW is the same than the plant, which is often large. On the other hand, the fixed DLAW approach presents the possibility to compute a low-order anti-windup. This is not possible in the MRAW context. Recently, a reduced order MRAW approach has been implemented in the discrete context in [PZCG07].

3.5 Extended model recovery anti-windup

This section presents an extension of the MRAW approach by combining it with a static DLAW to compute a dynamic anti-windup compensator dealing with exponential unstable plants. This combination is called Extended Model Recovery Anti-Windup (EMRAW). The EMRAW follows the same paradigm of the MRAW. Therefore, the anti-windup compensator is constructed with the plant model state matrices. However the EMRAW extends the MRAW approach with the introduction of a static gain. This gain can be presented as a static DLAW itself. Figure 3.5 shows the EMRAW structure.

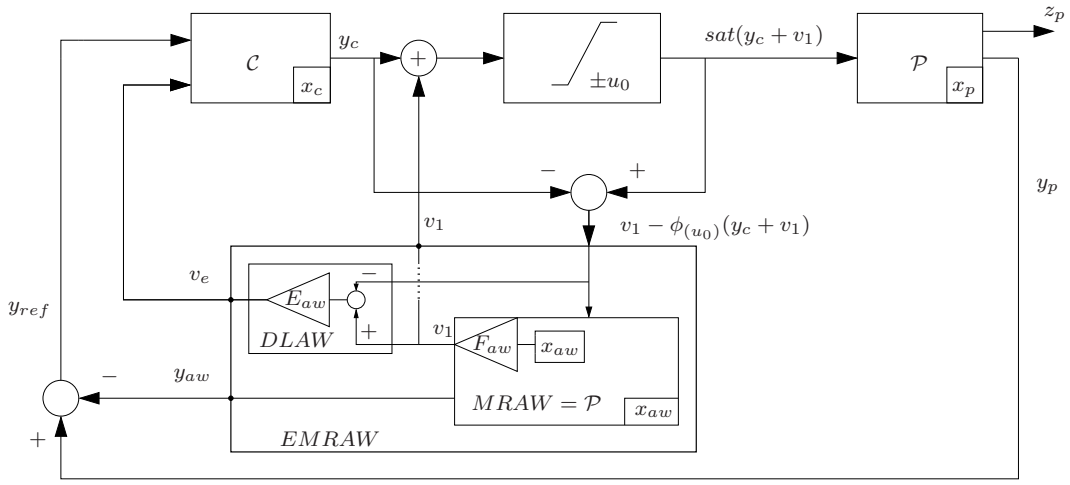

Figure 3.5: Extended MRAW block diagram.

Recovering the plant (3.4.2), the controller (3.4.3) and the MRAW (3.4.1) and extending them with a static DLAW, the EMRAW strategy is described by the following equations:

$$\mathcal{P} \; : \; \begin{cases} \dot{x}_p = A_p x_p + B_p sat_{(u_0)}(y_c + v_1) \\ y_p = C_p x_p \end{cases} \tag{3.5.1}$$

$$\mathcal{C} \; : \; \begin{cases} \dot{x}_c = A_c x_c + B_c(y_p - y_{aw}) + v_e \\ y_c = C_c x_c + D_c(y_p - y_{aw}) \end{cases} \tag{3.5.2}$$

$$\mathcal{AW} \; : \; \begin{cases} \dot{x}_{aw} = (A_p x_{aw} + B_p v_1) - B_p \phi_{(u_0)}(y_c + v_1) \\ y_{aw} = C_p x_{aw} \\ v_1 = F_{aw} x_{aw} \\ v_e = E_{aw} \phi_{(u_0)}(y_c + v_1) \end{cases} \tag{3.5.3}$$

where $x_{aw} \in \Re^{n_{aw}}$ is the anti-windup compensator state with $n_{aw} = n_p$, $y_{aw} \in \Re^q$ and $v_1 \in \Re^m$ are the outputs generated by MRAW stage and $v_e \in \Re^{n_c}$ is the output issued by the static DLAW stage (gain E_{aw}) .

Notice E_{aw} is an static DLAW as it feedbacks the dead-zone function $\phi_{(u_0)}$ directly into the controller dynamics x_c through the signal v_e.

The EMRAW presents an anti-windup loop stabilized with v_1. Like in the MRAW approach the chanllenge is to find a control law to compute a feedback v_1 stabilizing the anti-windup compensator (3.5.3). If the anti-windup loop is stable with a feedback v_1 the output y_{aw} converges to zero. Consequently, the output of the system y_p converges towards the reference y_{ref}.

The choice of the stabilizing feedback v_1 is not trivial for non-stable exponentially plants. In this work only local stability is sought. Therefore we have set v_1 like a static feedback

$$v_1 = F_{aw} x_{aw} \tag{3.5.4}$$

Given this choice of v_1 the EMRAW approach is, indeed, a MRAW with v_1 as a static feedback plus a static DLAW. Considering v_1 in (3.5.4), the anti-windup loop (3.5.3) reads:

$$\begin{aligned} \dot{x}_{aw} &= (A_p + B_p F_{aw}) x_{aw} - B_p \phi_{(u_0)}(y_c + F_{aw} x_{aw}) \\ y_{aw} &= C_p x_{aw} \end{aligned} \tag{3.5.5}$$

where F_{aw} is a static gain ensuring the asymptotic stability of matrix $A_p + B_p F_{aw}$, that is the existence of a matrix $P_p = P_p' > 0$ such that $(A_p + B_p F_{aw})' P_p + P_p (A_p + B_p F_{aw}) < 0$.

From [TK97a] it is known that, if the anti-windup loop (3.5.3) is locally stable with $v_1 = F_{aw} x_{aw}$, then the system (3.5.1)-(3.5.3) is also locally stable. The goal is then to optimize the stability domain in order to assure the reliability of the mission. Thus, the F_{aw} computation has to be done maximizing the stability region.

The stability is then guaranteed by v_1 (3.5.4) and the stability domain is maximized with F_{aw} computation. Therefore, the extra degrees of freedom of the EMRAW approach, with respect to a MRAW, introduced by the static gain E_{aw} can be used to improve the performance of system.

3.5.1 Introducing a performance criterion

Previously in Section 3.3.1, the closed-loop system (3.3.2) has been extended with the linear system (3.3.6). The goal of this technique was to steer the solution of the anti-windup problem providing a non-linear behavior as close as possible to the linear one. In the EMRAW approach, one may use this strategy but with a slightly different goal.

In the EMRAW structure, assuming an anti-windup loop stable, the system output y_p converges to y_{ref}. A system denoted *ideal* is set in parallel to the closed-loop system (3.5.1)-(3.5.3). The ideal system output y_{id} describes the desired behavior for y_p. That is, we would like y_p to behave like y_{id}. y_p converges to the reference y_{ref} instead. Then, if y_{ref} is as close as possible to y_{id}, the saturated output y_p will converge to a better response. Therefore, the difference between y_{ref} and y_{id} has to be minimized to improve the performance of the system.

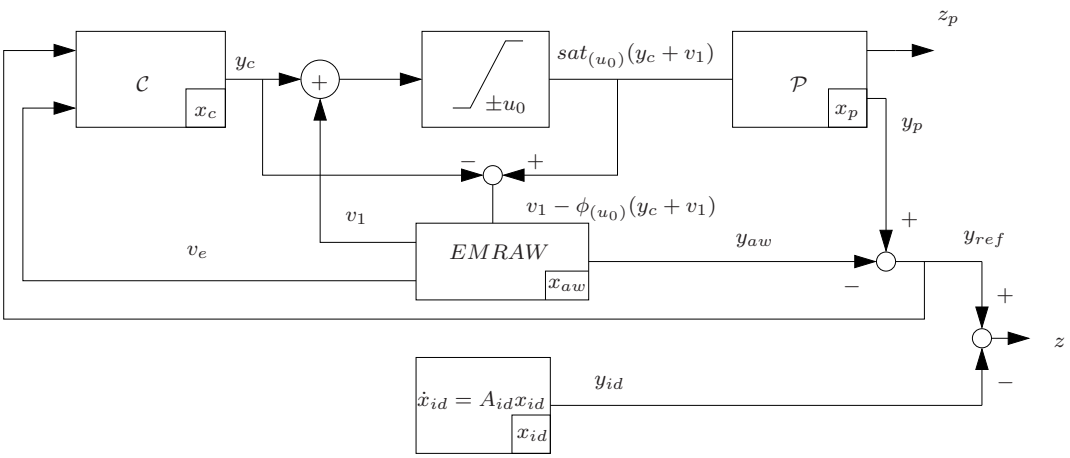

Figure 3.6: Performance optimization strategy for the EMRAW.

The optimization criterion in the EMRAW context is to minimize the $\mathcal{L}_2\{z\}$ where $z = y_{ref} - y_{id}$. Figure 3.6 block diagram describes this performance optimization strategy.

The ideal system dynamics are expressed in the following state space representation:

$$\dot{x}_{id} = A_{id}x_{id}; \qquad y_{id} = C_{id}x_{id} \tag{3.5.6}$$

where $x_{id} \in \Re^{n_{id}}$ and $y_{id} \in \Re^q$, and matrices A_{id} and C_{id} of appropriate dimensions. A_{id} is Hurwitz. Matrices A_{id} and C_{id} are chosen in the synthesis process by the designer. However the choice has to be done regarding to the system dynamics. This choice is illustrated in further Section 3.7.4.

Defining the extended state vector $\xi = [x_p' \quad x_c' \quad x_{aw}' \quad x_{id}']'$, the closed-loop system (3.5.1), (3.5.2), (3.5.3) and (3.5.6) reads:

$$\begin{aligned} \dot{\xi} &= (\mathbb{A} - \mathbb{B}_\phi F_{aw}\mathbb{C}_s)\xi + (\mathbb{B}_\phi + \mathbb{B}_v E_{aw})\,\phi_{(u_0)}((\mathbb{K} + F_{aw}\mathbb{C}_s)\xi) \\ z &= y_{ref} - y_{id} = y_p - y_{aw} - y_{id} = \mathbb{C}\xi \end{aligned} \tag{3.5.7}$$

where $z \in \Re^p$ and

$$\mathbb{A} = \begin{bmatrix} A_p + B_p D_c C_p & B_p C_c & B_p D_c C_p & 0 \\ B_c C_p & A_c & B_c C_p & 0 \\ 0 & 0 & A_p & 0 \\ 0 & 0 & 0 & A_{id} \end{bmatrix}; \mathbb{B}_\phi = \begin{bmatrix} -B_p \\ 0 \\ -B_p \\ 0 \end{bmatrix}; \mathbb{B}_v = \begin{bmatrix} 0 \\ I_{n_c} \\ 0 \\ 0 \end{bmatrix};$$

$$\mathbb{C}_s = [0 \;\; 0 \;\; I_{n_{aw}} \;\; 0]; \mathbb{C} = [C_p \;\; 0 \;\; -C_p \;\; -C_{id}]; \mathbb{K} = [D_c C_p \;\; C_c \;\; -D_c C_p \;\; 0].$$

Remark 3.11. *Roughly speaking, the two stages of the EMRAW carry out different missions. The first stage, i.e. the MRAW one, ensures the convergence of y_p towards y_{ref}, while the second stage, i.e. the static DLAW, modifies the y_{ref} to be as close as possible to y_{id}.*

The EMRAW strategy given by Figure 3.5 can be presented in a generic anti-windup structure as shown in Figure 3.7. Signals v_x and v_y considered in (3.2.2) can be reconstructed easily from the EMRAW outputs:

$$\begin{aligned} v_x &= v_e - B_c y_{aw} \\ v_y &= -D_c y_{aw} + v_1 \end{aligned} \tag{3.5.8}$$

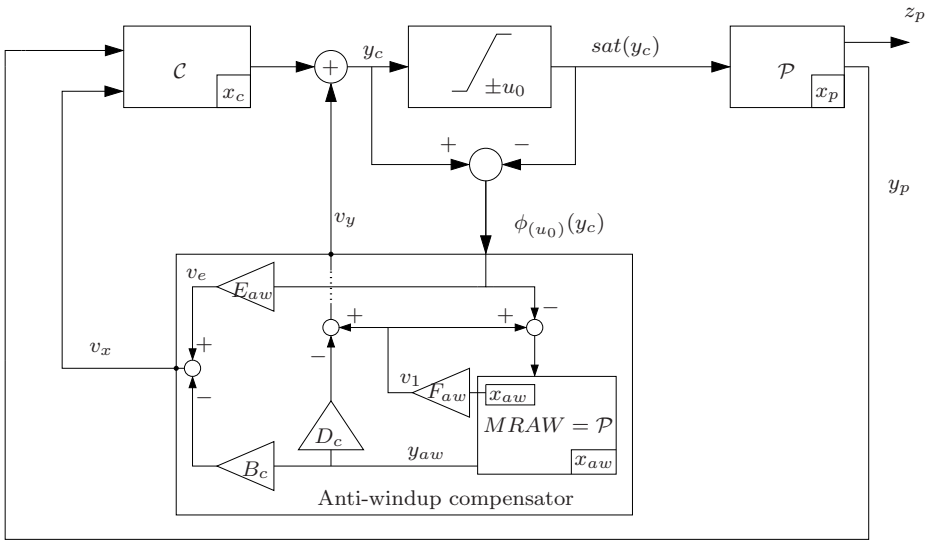

Figure 3.7: Extended MRAW on a generic Anti-windup structure.

3.5.2 EMRAW design procedure

Given the system (3.5.7) and defining $n = n_p + n_c + n_{aw} + n_{id}$ and $He(A) = A + A'$, the following theorem can be stated:

Theorem 3.2. *[BPT+ 10b] Given $v \in \Re^n$, k_γ and k_ρ positive values, if there exist positive scalars γ and ρ, a symmetric positive-definite matrix $W \in \Re^{n\times n}$, a matrix $Y \in \Re^{m\times n}$, a matrix $Z \in \Re^{n_c\times m}$, a diagonal positive-definite matrix $S \in \Re^{m\times m}$ and a matrix $F_{aw} \in \Re^{m\times n_p}$ satisfying min $(k_\gamma\gamma + k_\rho\rho)$ s.t.*

$$\begin{bmatrix} He\left[\mathbb{A}W - \mathbb{B}_\phi F_{aw}\mathbb{C}_s W\right] & \mathbb{J}_1 & W\mathbb{C}' \\ * & -2S & 0 \\ * & * & -\gamma I_p \end{bmatrix} < 0 \tag{3.5.9}$$

$$\begin{bmatrix} W & W\mathbb{K}'_{(i)} - Y'_{(i)} \\ * & u^2_{0(i)} \end{bmatrix} \geq 0;\ i = 1, ..., m. \tag{3.5.10}$$

$$\begin{bmatrix} W & v \\ * & \rho \end{bmatrix} \geq 0 \tag{3.5.11}$$

where $\mathbb{J}_1 = \mathbb{B}_\phi S + \mathbb{B}_v Z + Y' + W\mathbb{C}'_s F'_{aw}$, then $\mathcal{E}(P) = \left\{\xi \in \Re^n; \xi' P\xi < 1\right\}$ with $P = W^{-1}$ is a domain of stability for the system (3.5.7) with $E_{aw} = ZS^{-1}$ and F_{aw}. Furthermore, $\mathcal{E}(P)$ is maximized in the direction v, with the weight k_ρ, and the performance $1/\gamma$ is maximized with the weight k_γ.

Remark 3.12. *If $v = x_p(0)$ in (3.5.11) then the stability domain is maximized towards the selected states of the saturated plant.*

Proof of Theorem 3.2: Let us consider a quadratic Lyapunov function such as $V(\xi) = \xi' P\xi$, $P = P' > 0$. Then a sufficient condition for the stability of the system (3.5.7) in the ellipsoid domain $\mathcal{E}(P)$ with the constraint $\|z\|_2^2 = \int_0^\infty z'zdt \leq \gamma$ is given by $\dot{V}(\xi) + \gamma^{-1}z'z < 0$, for any $\xi \in \mathcal{E}(P)$ [BT09].

The expression of the time-derivative $\dot{V}(\xi)$ along the trajectories of system (3.5.7) gives:

$$\begin{aligned} \dot{V}(\xi) &= \dot{\xi}' P\xi + \xi' P\dot{\xi} \\ &= \xi' \left(He[P(\mathbb{A} - \mathbb{B}_\phi F_{aw}\mathbb{C}_s)]\right)\xi \\ &\quad + 2\xi' P \left(\mathbb{B}_\phi + \mathbb{B}_v E_{aw}\right)\phi_{(u_0)}((\mathbb{K} + F_{aw}\mathbb{C}_s)\xi) \end{aligned}$$

Lemma 1.1 applies by considering $u = (\mathbb{K} + F_{aw}\mathbb{C})\xi$ and $\omega = (-G - F_{aw}\mathbb{C}_s)\xi$, and the set:

$$S(u_0) = \left\{\xi \in \Re^n; \left|(\mathbb{K}_{(i)} - G_{(i)})\xi\right| \leq u_{0_{(i)}}, i = 1, ..., m\right\}$$

Hence by setting $W = P^{-1}$ and $Y = GW$, the satisfaction of relation (3.5.10) guarantees that $\mathcal{E}(P) \subseteq S(u_0)$.

Thus, for any $\xi \in \mathcal{E}(P) \subseteq S(u_0)$ one gets:

$$\begin{aligned}\dot{V}(\xi)+\gamma^{-1}\xi'\mathbb{C}'\mathbb{C}\xi \leq & \xi'\left(He[P(\mathbb{A}-\mathbb{B}_\phi F_{aw}\mathbb{C}_s)]\right)\xi \\ & +2\xi' P\left(\mathbb{B}_\phi+\mathbb{B}_v E_{aw}\right)\phi_{(u_0)}((\mathbb{K}+F_{aw}\mathbb{C}_s)\xi) \\ & -2\phi'_{(u_0)}S^{-1}\left(\phi_{(u_0)}-G\xi-F_{aw}\mathbb{C}_s\xi\right)+\gamma^{-1}\xi'\mathbb{C}'\mathbb{C}\xi\end{aligned} \tag{3.5.12}$$

Then the right-hand side writes: $\mathcal{L}=\mathbb{X}'\mathbb{M}\mathbb{X}$ with $\mathbb{X}'=\left[\xi' W^{-1}\ \phi'_{(u_0)}S^{-1}\right]$ and

$$\mathbb{M}=\begin{bmatrix} He\left[\mathbb{A}W-\mathbb{B}_\phi F_{aw}\mathbb{C}_s W\right]+\gamma^{-1}W\mathbb{C}'\mathbb{C}W & \mathbb{J}_1 \\ \star & -2S \end{bmatrix}$$

with $\mathbb{J}_1=\mathbb{B}_\phi S+\mathbb{B}_v Z+Y'+W\mathbb{C}'_s F'_{aw}$ and $Z=E_{aw}S$. Finally, using Schur complement on $\gamma^{-1}W\mathbb{C}'\mathbb{C}W$, one gets relation (3.5.9). Therefore, the satisfaction of relation (3.5.9) ensures that $\mathcal{L}<0$ or equivalently, $\dot{V}(\xi)+\gamma^{-1}z'z\leq\mathcal{L}<0$ for any $\xi\in\mathcal{E}(P)$. In other words, as in the proof of Theorem 3.1, one can conclude that $\mathcal{E}(P)$ is a region of asymptotic stability for system (3.5.7) with $\|z\|_2^2\leq\gamma$.

Relation (3.5.11) allows the maximization of the stability domain towards v by adding the optimization criterion *min* ρ. Moreover k_γ and k_ρ are the optimization weights which perform the trade-off between performance (γ^{-1}) and stability (ρ).

End of Proof.

Nevertheless, one can infer from previous equations that F_{aw} and W cannot be computed in one shot as inequalities are not linear in these decision variables (see the product $F_{aw}\mathbb{C}_s W$ in (3.5.9)). Therefore a method is proposed hereafter to solve the anti-windup problem.

3.5.3 EMRAW computation

3.5.3.a Coordinate-descending Algoritm

The bilinear matrix inequality (BMI) (3.5.9) can be expressed differently allowing the adaptation of a coordinate-descending algorithm [PA01].

Proposition 3.4. *Given k_γ and k_ρ positive values, there exist anti-windup gains F_{aw} and E_{aw} such as conditions in Theorem 3.2 are satisfied if there exist positive scalars γ and ρ, a symmetric positive-definite matrix $W\in\Re^{n\times n}$, a matrix $Y\in\Re^{m\times n}$, a matrix $Z\in\Re^{n_c\times m}$, a diagonal positive-definite matrix $S\in\Re^{m\times m}$, matrices $K_s\in\Re^{n\times n_p}$, $\mathbb{F}\in\Re^{n_p\times n_p}$ and $\mathbb{R}\in\Re^{m\times n_p}$ satisfying $min(k_\gamma\gamma+k_\rho\rho)$ s.t. (3.5.10), (3.5.11) and*

$$\begin{bmatrix} He\left[\mathbb{A}W\right] & W\mathbb{C}_s' & \mathbb{B}_\phi S+\mathbb{B}_v Z+Y' & W\mathbb{C}' \\ * & 0 & 0 & 0 \\ * & * & -2S & 0 \\ * & * & * & -\gamma I_p \end{bmatrix}$$
$$+He\left[\begin{bmatrix} K_s \\ I_{n_{aw}} \\ 0 \\ 0 \end{bmatrix}\begin{bmatrix} \mathbb{R}'\mathbb{B}_\phi' & \mathbb{F} & -\mathbb{R}' & 0 \end{bmatrix}\right]<0 \tag{3.5.13}$$

Furthermore $\mathcal{E}(W^{-1})=\left\{\xi\in\Re^n;\xi' W^{-1}\xi<1\right\}$ *is a domain of stability for the system* (3.5.7) *with* $E_{aw}=ZS^{-1}$ *and* $F_{aw}=\mathbb{R}(\mathbb{F}')^{-1}$.

Proof of Proposition 3.4: First, let us rewrite relation (3.5.9) of theorem 3.2 as a product of matrices:

$$\Phi\begin{bmatrix} He\left[\mathbb{A}W\right] & W\mathbb{C}_s' & \mathbb{B}_\phi S+\mathbb{B}_v Z+Y' & W\mathbb{C}' \\ * & 0 & 0 & 0 \\ * & * & -2S & 0 \\ * & * & * & -\gamma I_p \end{bmatrix}\Phi' \tag{3.5.14}$$

where $\Phi=\begin{bmatrix} I_n & -\mathbb{B}_\phi F_{aw} & 0 & 0 \\ 0 & F_{aw} & I_m & 0 \\ 0 & 0 & 0 & I_p \end{bmatrix}$. Then by applying the elimination lemma [OS01] backwards one obtains:

$$\begin{bmatrix} He\left[\mathbb{A}W\right] & W\mathbb{C}_s' & \mathbb{B}_\phi S+\mathbb{B}_v Z+Y' & W\mathbb{C}' \\ * & 0 & 0 & 0 \\ * & * & -2S & 0 \\ * & * & * & -\gamma I_p \end{bmatrix}$$
$$+He\left[\begin{bmatrix} F_1 \\ \mathbb{F} \\ 0 \\ 0 \end{bmatrix}\begin{bmatrix} F_{aw}'\mathbb{B}_\phi' & I_{n_{aw}} & -F_{aw}' & 0 \end{bmatrix}\right]<0 \tag{3.5.15}$$

where F_1 and $\mathbb{F}$ are Lagrange multipliers. Let us remark that there are not more multipliers because are set to zero. Finally $\mathbb{F}$ multiplies and divides the second term as follows:

$$\begin{bmatrix} He\left[\mathbb{A}W\right] & W\mathbb{C}_s' & \mathbb{B}_\phi S+\mathbb{B}_v Z+Y' & W\mathbb{C}' \\ * & 0 & 0 & 0 \\ * & * & -2S & 0 \\ * & * & * & -\gamma I_p \end{bmatrix}$$
$$+He\left[\begin{bmatrix} F_1\mathbb{F}^{-1} \\ I_{n_{aw}} \\ 0 \\ 0 \end{bmatrix}\begin{bmatrix} \mathbb{F}F_{aw}'\mathbb{B}_\phi' & \mathbb{F} & -\mathbb{F}F_{aw}' & 0 \end{bmatrix}\right]<0 \tag{3.5.16}$$

Then by setting $F_1\mathbb{F}^{-1} = K_s$ and $\mathbb{F}F_{aw}' = \mathbb{R}'$ one obtains expression (3.5.13).

End of Proof.

Given the new formulation of Proposition 3.4 one can adapt the algorithm presented in [PA01]. It does not prevent from using a relaxation scheme, but allows to search for the matrix related to the Lyapunov function at each step. This algorithm is decomposed in four operations as follows:

Algorithm 3.2. *(***Coodinate-descending***)*

1. *(Initializing step - k=1) choose an initializing gain* K_s.
2. *(Step k - first part) for this choice of* K_s*, solve the following LMI minimization problem:*
$$min(k_\gamma\gamma + k_\rho\rho) \quad s.t. \quad (3.5.10),\ (3.5.11) \text{ and } (3.5.13)$$
Keep the values of $\mathbb{R}$ *and* $\mathbb{F}$ *obtained.*
3. *(Step k - second part), for this choice of* $\mathbb{R}$ *and* $\mathbb{F}$*, solve the following LMI minimization problem:*
$$Crit_k = min(k_\gamma\gamma + k_\rho\rho) \quad s.t. \quad (3.5.10),\ (3.5.11) \text{ and } (3.5.13)$$
Keep the value of K_s *obtained.*
4. *(Termination step) if* $|Crit_{k+1} - Crit_k| < \epsilon$*, then stop,* $F_{aw} = \mathbb{R}(\mathbb{F}')^{-1}$*, otherwise* $k \leftarrow k+1$ *and go to step* 2.

The delicate point of Algorithm 3.2 is the initialization step where K_s has to be chosen. However, this choice can be easier if some properties of K_s related to the stability of the closed-loop system (3.5.7) are provided.

Lemma 3.1. *The variable* K_s *of inequality* (3.5.13) *is a stabilizing feedback such that the Lyapunov function* $V(\xi) = \xi' W^{-1}\xi$ *proves simultaneously the stability of both systems* (3.5.7) *and* $\dot{\xi} = (\mathbb{A} + K_s\mathbb{C}_s)\xi$.

Proof of Lemma 3.1: Multiplying inequality (3.5.13) on the left by $\begin{bmatrix} I_n & K_s & 0 & 0 \\ 0 & 0 & I_m & I_p \end{bmatrix}$ and on the right by its transpose, on the left up corner of the resulting matrix one gets:

$$He[(\mathbb{A} + K_s\mathbb{C}_s)W] < 0 \tag{3.5.17}$$

Hence, the existence of a symmetric positive matrix W satisfying (3.5.13) and (3.5.17), ensures the stability of the matrix $(\mathbb{A} + K_s\mathbb{C}_s)$ and the stability of the saturated system (3.5.7).

End of Proof.

Remark 3.13. *Knowing the necessary condition expressed in Lemma 3.1 one has a useful guide to initialize Algorithm 3.2.*

3.5.3.b Objective-based Algorithm

An alternative algorithm is proposed. It is based on the knowledge of the objective of each gain in the EMRAW approach. That means, that in one hand F_{aw} computation is sought knowing that the gain stabilizes the anti-windup loop dynamics, and in the other hand the E_{aw} computation is performed considering the convergence of y_{ref} towards y_{id}. This algorithm is divided in two independent parts which yield the third last part.

Algorithm 3.3. *[BPT+10b](***Objective-based***)*

- *(Analysis part - 1) Tune F_{aw} which guarantees $(A_p+B_pF_{aw})'P_p+P_p(A_p+B_pF_{aw}) < 0$ with $P_p = P_p' > 0$ providing the best possible dynamics (fast time of respose and low oscillation). Simulate the system with $E_{aw} = 0$ and analyze the reference.*

  Keep the value of F_{aw} obtained.

- *(LMI part - 2) Choose a big ratio k_γ/k_ρ. Then tune F_{aw}^* verifying $(A_p+B_pF_{aw}^*)'P_p+P_p(A_p+B_pF_{aw}^*) < 0$ and providing a fast dynamics[3]. Since F_{aw}^* is fixed, relations (3.5.9)-(3.5.11) become LMIs in the other decision variables. Solve Theorem 3.2 with k_γ/k_ρ and F_{aw}^* to compute E_{aw}.*

  Keep the value of E_{aw} obtained.

- *(Verification Part) Solve relations (3.5.9)-(3.5.11) with F_{aw} (from Analysis part - step 1) and $Z = E_{aw}S$ (E_{aw} from LMI part - step 2).*

  Evaluate the stability parameter ρ: if $\rho < \rho_{desired}$ stop, otherwise go back to LMI part (step 2) with a smaller k_γ/k_ρ and/or slower $(A_p + B_pF_{aw}^*)$ speed dynamics.

In contrast to Algorithm 3.2, there is no proof of convergence for Algorithm 3.3. However in certain applications the knowledge of the system can be used in the first part of Algorithm 3.3, leading to better results in terms of time of response can be obtained.

[3] Analysis part (step 1) gives directions about the way to choose the poles of $(A_p + B_pF_{aw}^*)$ (generally ten times faster than poles of $(A_p + B_pF_{aw})$).

3.6 Anti-windup with asymmetric saturations

The objective of this thesis is to adapt and develop the anti-windup to the control with high precision for the angular and the linear axis of a satellite. In this control problem the thrusters are used as actuators. The saturation describing the thrusters limitation presents asymmetric bounds.

In Chapter 2 several techniques to symmetrize the saturation have been presented. At the beginning of this chapter the saturations of the considered system have been supposed symmetric. Regarding the system considered in this manuscript this assumption demands the application of the symmetrizing techniques.

In previous sections, three approaches for the anti-windup computation have been presented. In the three cases, the anti-windup problem can be represented under a generic formulation presented in Figure 1.6 (See also Figures 3.1, 3.4 and 3.7). Therefore, considering the block diagram in Figure 3.8, the anti-windup problem can be expressed under the following formulation:

$$\begin{cases} \dot{\xi} = \mathcal{A}\xi + \mathcal{B}_\phi M \phi_{(0,\bar{u})}(\nu + N\zeta) \\ \nu = \mathcal{C}\xi + \mathcal{D}_\phi M \phi_{(0,\bar{u})}(\nu + N\zeta) \end{cases} \tag{3.6.1}$$

where the state vector is $\xi = [x_p^{'}\ x_c^{'}\ x_{aw}^{'}]^{'}$.

Notice that the influence matrix, a symmetrizing vector $N\zeta$ and the asymmetric saturation have been introduced in order to characterize the considered problem in Figure 3.8.

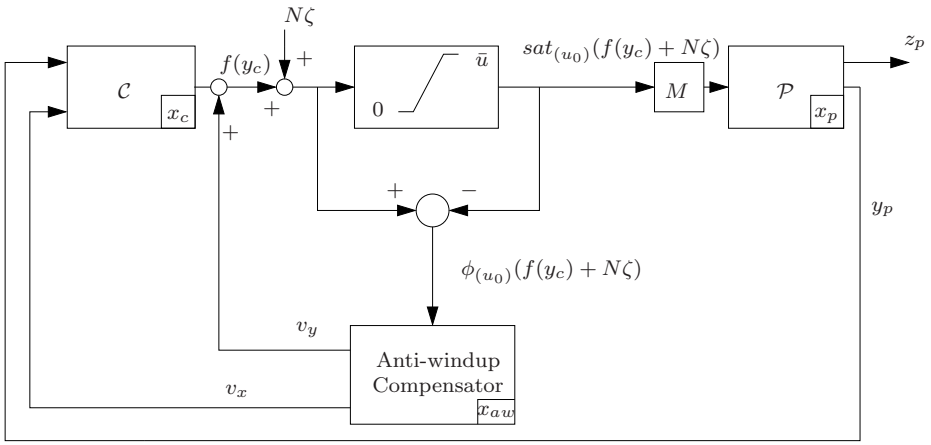

Figure 3.8: General anti-windup structure

Figure 3.8 shows the block diagram of the generic problem to deal with. In the figure, $N\zeta$ can be a symmetrizing vector verifying from Definition 2.3 or a function satisfying the VKF definition (Definition 2.5.3).

In this section, conditions on the validity of the anti-windup results when the system saturation is symmetrized are given. First the system kernel symmetrization technique is applied. Then, the variable kernel function is used to symmetrize the saturation.

3.6.1 Anti-windup design with Kernel symmetrization

The following proposition can be stated:

Proposition 3.5. *[BPT+09] If there exists $N\zeta_{sym}$ verifying the conditions of Definition 2.2 then the anti-windup synthesis applies on system (3.6.1) regardless of the symmetrizing process.*

Proof of Proposition 3.5: Initially the symmetrizing vector $N\zeta_{sym}$ (2.5.6) verifying Definition 2.2 is considered. $N\zeta_{sym}$ modifies the bounds of the dead-zone function. Then the system (3.6.1) reads:

$$\begin{cases} \dot{\xi} = \mathcal{A}\xi + \mathcal{B}_\phi M\phi_{(-N\zeta_{sym},\bar{u}-N\zeta_{sym})}(\nu) + \mathcal{B}_\phi MN\zeta_{sym} \\ \nu = \mathcal{C}\xi + \mathcal{D}_\phi M\phi_{(-N\zeta_{sym},\bar{u}-N\zeta_{sym})}(\nu) + \mathcal{D}_\phi MN\zeta_{sym} \end{cases} \tag{3.6.2}$$

From Definition 2.2 $N\zeta_{sym} \in Ker(M)$ then it holds:

$$\begin{cases} \dot{\xi} = \mathcal{A}\xi + \mathcal{B}_\phi M\phi_{(-N\zeta_{sym},\bar{u}-N\zeta_{sym})}(\nu) \\ \nu = \mathcal{C}\xi + \mathcal{D}_\phi M\phi_{(-N\zeta_{sym},\bar{u}-N\zeta_{sym})}(\nu) \end{cases} \tag{3.6.3}$$

Given $N\zeta_{sym} = \frac{\bar{u}}{2}$, the dead-zone bounds are symmetrized with $u_0 = \frac{\bar{u}}{2}$ as symmetric bound (see Lemma 2.3). Then the system (3.6.1) is equivalent to the following one:

$$\begin{cases} \dot{\xi} = \mathcal{A}\xi + \mathcal{B}_\phi M\phi_{(-u_0,u_0)}(\nu) \\ \nu = \mathcal{C}\xi + \mathcal{D}_\phi M\phi_{(-u_0,u_0)}(\nu) \end{cases} \tag{3.6.4}$$

Therefore, the anti-windup compensator and the guaranteed domain stability of stability computed for the *symmetric*[4] system (3.6.4) are valid for the *asymmetric* system (3.6.1).

End of Proof.

Remark 3.14. *Proposition 3.5 implies that the anti-windup techniques presented in Chapter 3 apply to system (3.6.4) regardless of if it was symmetrized or it was already symmetric.*

[4] A system with symmetric saturation bounds is denoted *symmetric* system.

3.6.2 Anti-windup design with Variable Kernel Function (VKF)

The following result can be stated:

Proposition 3.6. *[BPT+09] If there exists $N\zeta_{var}$ verifying the conditions of Definition 2.4 (VKF definition) then the anti-windup and the stability domain $\mathcal{E}(P)$ for the system (3.6.1) with $N\zeta_{sym}$ verifying Definition 2.2, are also valid for the system (3.6.1) using a variable kernel function $N\zeta_{var}$.*

Proof of Proposition 3.6: Let us consider system (3.6.1). It has been proven by Proposition 3.5 that one can find an anti-windup and a guaranteed stability domain for the system (3.6.1) with $N\zeta_{sym}$.

In the saturation region, as $N\zeta_{var(i)} = N\zeta_{sym(i)}$, the system is unchanged and it is stable in $\mathcal{E}(P)$. The computation of anti-windup compensator is unchanged as well. In the linear zone, $N\zeta_{var(i)}$ verifies $0 \leq \left(f_{(i)}(y_c) + N\zeta_{var(i)}\right) \leq \bar{u}_{(i)}$, then system (3.6.1) is described by:

$$\begin{cases} \dot{\xi} = \mathcal{A}\xi + \mathcal{B}_\phi M \underbrace{\phi_{(0,\bar{u})}(\nu + N\zeta_{var})}_{=0} \\ \nu = \mathcal{C}\xi + \mathcal{D}_\phi M \underbrace{\phi_{(0,\bar{u})}(\nu + N\zeta_{var})}_{=0} \end{cases} \tag{3.6.5}$$

In the linear domain, the symmetrizing term does not appear in the linear closed-loop system because the saturation is not active. Therefore the system (3.6.1) behavior with a symmetrizing vector $N\zeta_{sym}$ is the same as the behavior with a VKF $N\zeta_{var}$.

Finally we need to assure the equivalence between the system (3.6.1) with $N\zeta_{sym}$ and the system (3.6.1) with VKF in the transition from the linear domain to the saturation region. From Definition 2.4 $N\zeta_{var(i)} = N\zeta_{sym(i)}$ in the commutation surface. Therefore the equivalence is verified.

In conclusion, the system (3.6.1) is equivalent with both symmetrizing techniques in the whole state space. Therefore, the computation of the anti-windup compensator and the stability domain for the system (3.6.1) with $N\zeta_{sym}$ are also valid for the system (3.6.1) using $N\zeta_{var}$.

End of Proof.

Remark 3.15. *The symmetrizing vector $N\zeta_{sym}$ does not affect the anti-windup computation as proven in Proposition 3.5. The system can be considered with symmetric bounds. On the other hand, Proposition 3.6 means that for anti-windup purposes, $N\zeta_{var}$ is equivalent to $N\zeta_{sym}$ as they are equal when the saturation is active. In the linear domain the*

dead-zone is null, then the anti-windup compensator input is null even if $N\zeta$ in (3.6.1) is a constant symmetrizing ($N\zeta_{sym}$) or a VKF($N\zeta_{var}$) is used.

3.6.3 Conclusion on the anti-windup with asymmetric saturations

In this section the validity of the anti-windup techniques in asymmetric saturations is tackled. First Proposition 3.5 shows that an anti-windup compensator valid for a system with symmetric saturation bounds is also valid for a system which bounds have been symmetrized previously.

Proposition 3.6 proves that, for anti-windup computation purposes, the use of a symmetrizing vector $N\zeta_{sym}$ or a VKF $N\zeta_{var}$is equivalent. Then the anti-windup compensator computed on a system symmetrized with symmetrizing vector is also valid for the system with a VKF function.

Therefore, the anti-windup compensator techniques presented in this chapter can be applied regardless of the symmetrizing techniques defined in Chapter 2.

3.7 Educational example

The educational example is used to illustrate the anti-windup techniques presented in this chapter. The pseudo-inverse matrix allocation function given by (2.4.1) is used in the system (8).

In the educational example, the saturation function considered is asymmetric. Results on anti-windup synthesis consider symmetric saturations. Thus, before computing an anti-windup compensator the saturation has to be symmetrized. Therefore the symmetrizing techniques from Chapter 2 are used. From Section 3.6 it is deduced that the symmetrizing techniques do not effect the anti-windup compensator synthesis.

The symmetrizing vector $N\zeta_{sym}$ (2.5.6) is applied to system (8) to symmetrize its saturation. Then, the formulation of the educational example considered for anti-windup purposes reads:

$$\begin{cases} \dot{x}_p = A_p x_p + B_p M sat_{(u_0)}(M^* y_c) \\ \dot{x}_c = A_c x_c + B_c C_p x_p \\ y_c = C_c x_c + D_c C_p x_p \\ z_p = C_z x_p \end{cases} \tag{3.7.1}$$

where $u_0 = \frac{1}{2}150 \cdot 10^{-6}$.

3.7.1 Educational example on static DLAW

Let us consider first the static DLAW. Introducing this anti-windup compensator in the system (3.7.1) the system reads

$$\begin{cases} \dot{x}_p = A_p x_p + B_p M sat_{(u_0)}(M^* y_c) \\ \dot{x}_c = A_c x_c + B_c C_p x_p + D_{aw} \phi_{(u_0)}(M^* y_c) \\ y_c = C_c x_c + D_c C_p x_p \\ z_p = C_z x_p \end{cases} \tag{3.7.2}$$

With some mathematical development, the system (3.7.2) meets formulation (3.3.7).

Remark 3.16. *The disturbance is not considered in the educational example. However that does not imply any difference in the previous results as the system remains essentially the same.*

For this example, the stability domain is maximized in the first state variable direction, that is, in the θ direction. That means that we maximize the allowed initial condition $\theta_{max}(0)$ where the system remains stable. Then Theorem 3.1 is applied with $v = [1 \quad 0 \quad 0_{1\times 4} \quad 0_{1\times 6}]'$ and $[k_\gamma, k_\rho] = [10^{10}, 1]$ as optimization weights. The resulting anti-windup gain is:

$$D_{aw} = \begin{bmatrix} 0.0448 & -0.0448 \\ 0.008 & -0.008 \\ 0.5856 & -0.5856 \\ -0.8572 & 0.8572 \end{bmatrix} \tag{3.7.3}$$

Figure 3.9 presents the attitude response of the education example. The simulations are performed setting an initial condition for the plant $x_p(0) = [-7 \cdot 10^{-4} \quad 0]'$ and leaving the system naturally evolve towards the origin. The solid line stands for the system (3.7.1) without anti-windup and the dash-dotted line corresponds to the response with static DLAW. The positive effect of the static DLAW is shown as the oscillations are reduced.

In Figure 3.10 the estimations of the stability domain in the $(\theta, \dot{\theta})$ plan are presented. The domains for the system (3.7.1) without anti-windup (solid line ellipsoid) and with anti-windup (dashed-line ellipsoid) are presented. The trajectories related to the simulations of Figure 3.10 are also plotted. The solid line depicts the trajectory without static DLAW and the dashed-line the trajectory with static DLAW. Finally, the parallel dotted lines limit the linear region.

The anti-windup compensator increases the stability domain. However notice that the initial condition $x_p(0) = [-7 \cdot 10^{-4} \quad 0]'$ simulated is not included in the stability domain.

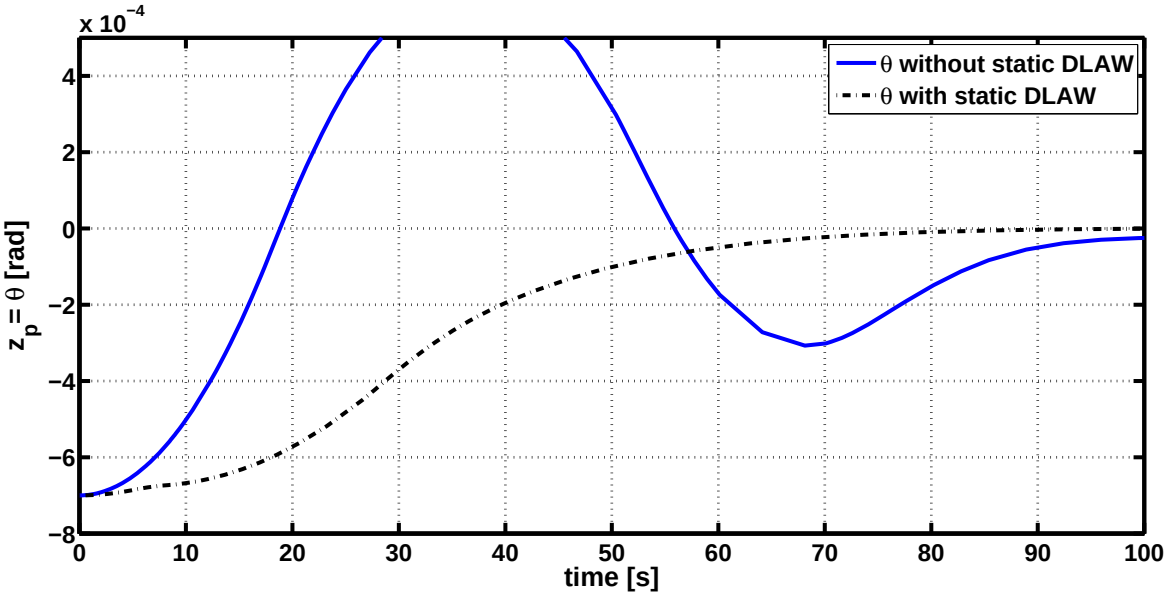

Figure 3.9: Educational example attitude response for $x_p(0) = [-7 \cdot 10^{-4} \quad 0]'$.

By simulation, it has been shown that the system (with and without anti-windup) is stable for this initial condition. Therefore the estimated stability domains are conservative. This conservatism has been introduced in different steps of the anti-windup design such as the Lyapunov function considered, the sector condition modelling and the application of the $\mathcal{S}$-procedure.

However, the following strategy can be used to improve the estimation: once the anti-windup is computed, a stability analysis of the system is performed. Applying Theorem 3.1 with $Z = D_{aw}S$ and $[k_\gamma, k_\rho] = [0, 1]$ a less conservative estimation of the stability domain is obtained. Actually in Figure 3.10 the dash-dotted line is the estimation issued by this analysis (post-analysis estimation). The dashed ellipsoid shows the estimation obtained from the gain D_{aw} synthesis (pre-analysis estimation).

Optimization weights $[k_\rho, k_\gamma]$ permit to tune the stability-performance trade-off. Figure 3.11 shows the θ response for an increasing k_γ ($k_\rho = 1$). The figure demonstrates the enhancement on the performance when k_γ increases. However, the improvement in the performance comes with a reduction of the stability domain estimation. Tested values of k_γ go from 0 to 10^{10}. In Figure 3.12 the estimation of the stability domain is shown for different k_γ. Notice that the estimation of the stability domain decreases when k_γ grows. In any case, as it is an estimation no conclusion can be obtained about the influence of k_γ on the actual stability domain.

Theorem 3.1 gives us, a stability criterion ρ. This criterion is related to the stability domain estimation by the following expression:

$$v' \xi_{max}(0) = \frac{1}{\sqrt{\rho}} \tag{3.7.4}$$

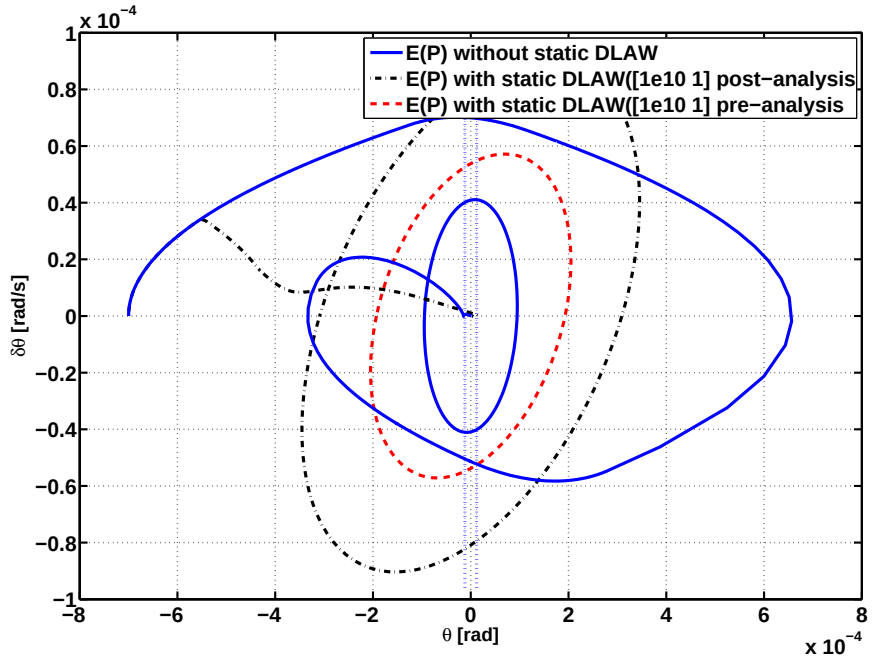

Figure 3.10: Stability domain estimations for different static anti-windup cases.

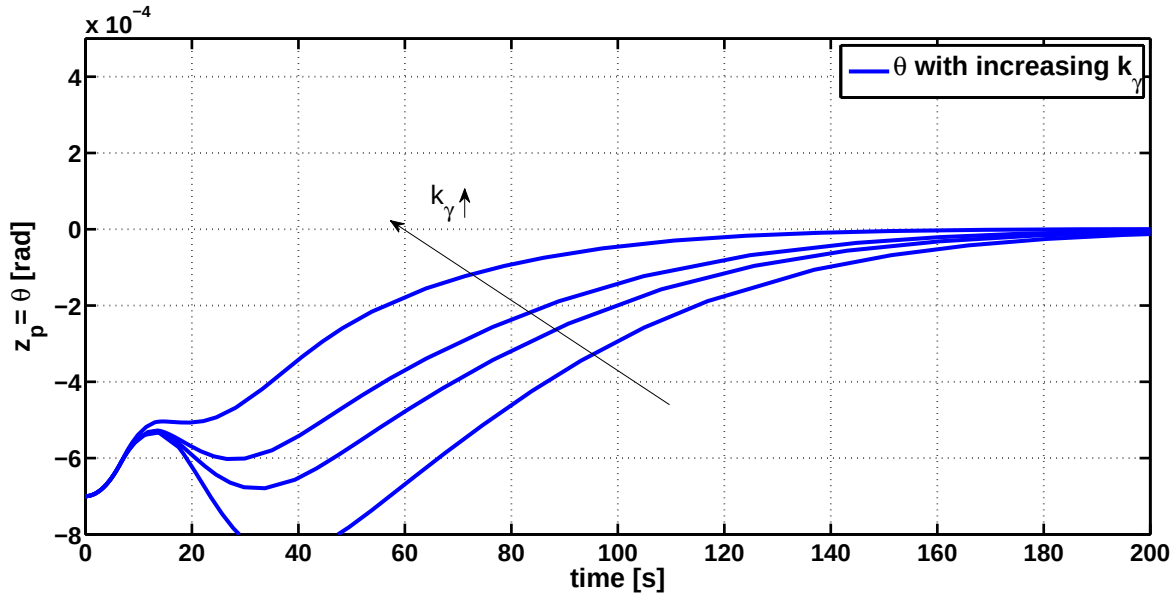

Figure 3.11: Attitude response for different performance weights k_γ ($k_\rho = 1$).

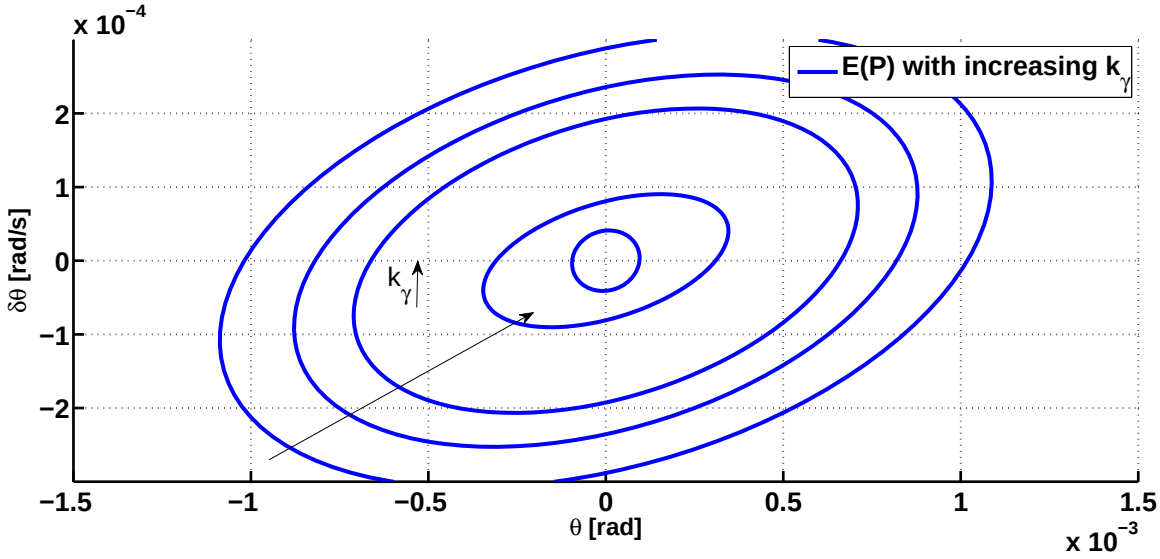

Figure 3.12: Stability domain for different performance weights k_γ ($k_\rho = 1$).

where $\xi_{max}(0)$ is the maximal admissible initial condition for the state vector.

Fixing ρ in Theorem 3.1, the computed anti-windup compensator ensures a given stability $\frac{1}{\sqrt{\rho}}$. However, because of the estimation conservatism one may run a risk of not finding a solution to the LMI problem. The stability criterion obtained for the system (3.7.2) is:

$$\rho_s(synthesis) = 2.68 \cdot 10^7; \rho_a(analysis) = 1.047 \cdot 10^7; \tag{3.7.5}$$

In this study case $v^{'}\xi_{max}(0) = x_{p(1)}(0) = \theta_{max}(0)$. Therefore, the maximal admissible initial attitude $\theta_{max}(0)$ can be obtained from the parameter ρ_a: $\theta_{max}(0) = \frac{1}{\sqrt{\rho_a}} = 3.091 \cdot 10^{-4}$. This is exactly the point where the dot-dashed ellipsoid in the Figure 3.10 cuts the $\dot{\theta}$-axis (i.e. $x_{p(2)}(0) = 0$-axis).

In Figure 3.13 the thrust of the system (3.7.1) with the static DLAW (3.7.3) is presented. Two thrust responses are depicted: first, the system (3.7.1) symmetrized with $N\zeta_{sym}$ (dashed-line) and second, the system (3.7.1) symmetrized with VKF (2.5.14) (dot-dashed line). A constant thrust is provided at the equilibrium for the system (3.7.1) with $N\zeta_{sym}$. On the contrary, the thrust at the equilibrium is null when a VKF is used. This implies a significant saving of fuel. The integral of the thrusters response has been computed as a measurement of the Consumption

$$Consumption \text{ with } N\zeta_{sym} \quad : \quad \sum_{i=1}^{n} \int_0^t T(n)dt = 8 \cdot 10^{-2} \tag{3.7.6}$$

$$Consumption \text{ with } VKF \quad : \quad \sum_{i=1}^{n} \int_0^t T(n)dt = 2.7 \cdot 10^{-3} \tag{3.7.7}$$

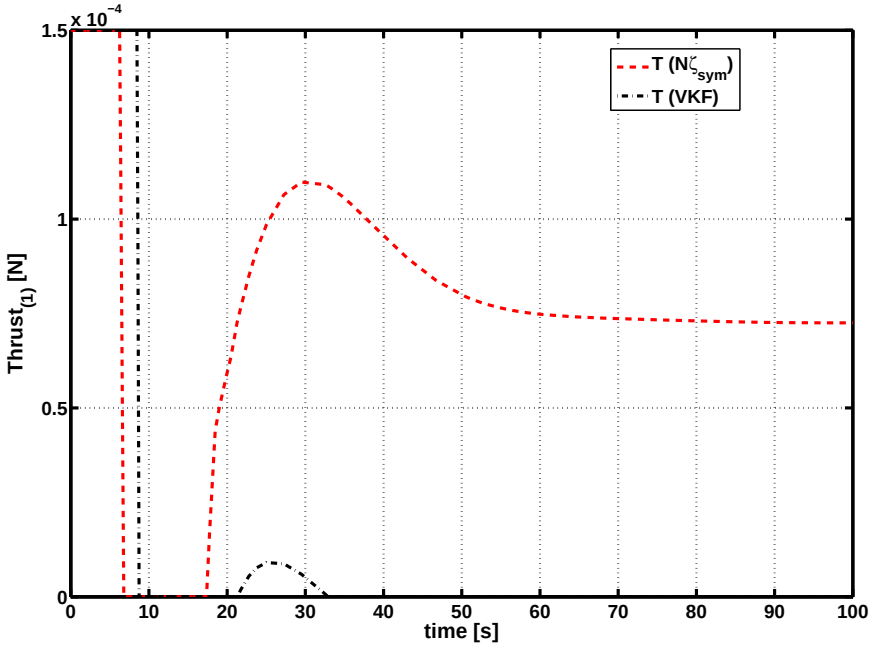

Figure 3.13: First thruster response for different symmetrizing approaches.

Remark 3.17. *The benefits of the VKF in comparison to $N\zeta_{sym}$ are independent on the anti-windup approach considered. Results on Section 3.6 considers a generic formulation of the anti-windup synthesis problem. Therefore, the previous analysis on the symmetrizing techniques are not repeated hereafter.*

3.7.2 Educational example on dynamic DLAW

The results on the dynamic DLAW computation are applied to the education example (3.7.1). With some mathematical development, the system (3.7.1) meets formulation (3.3.8).

The idea is first to apply Proposition 3.2 and from the eigenvalues of the full order anti-windup compensator, choose the representative ones and then apply Algorithm 3.1.

First, Proposition 3.2 is applied with optimization weights $[k_\gamma, k_\rho] = [10^{10}, 1]$. The stability domain is maximized in the θ direction. The anti-windup compensator matrices are reconstructed and the obtained eigenvalues of A_{aw} are presented in Table 3.1.

From all the poles of the computed full order compensator, just the poles of A_{aw} sharing the same magnitude order as those of A_l are conserved. Table 3.1 shows the full order anti-windup eigenvalues and the selected ones are marked with $*$. With this choice the fixed order anti-windup synthesis via Algorithm 3.1 can be implemented.

Table 3.1: Full order DLAW eigenvalues in the educational example

$\text{eig}(A_{aw})(* \equiv selected)$	$\text{eig}(A_l)$
$(-1.27 \pm j5.88) \cdot 10^5$	-6.84
$(-3.43 \pm j50.76) \cdot 10^4$	-4.63
$-1.28 \cdot 10^3$	$(-1.04 + j1.24) \cdot 10^{-1}$
-9.55	$(-3.05 + j1.07) \cdot 10^{-2}$
$-4.29(*)$	
$(-1.23 \pm j1.18) \cdot 10^{-1}(*)$	
$(-3.28 \pm j0.69) \cdot 10^{-3}$	
$-1.46 \cdot 10^{-2}$	

Remark 3.18. *Some of the poles of full order DLAW have an extremely fast dynamics. Pole* $p = (-1.27 \pm j5.88) \cdot 10^5$ *is too fast to be considered in real industrial applications. Therefore, the selection is mandatory to obtain a realistic anti-windup compensator. In addition we have decided to choose the poles sharing the same magnitude order as those of the linear closed-loop. This selection criterion is established to obtain a better conditioning number of the closed-loop matrices and, consequently, reduced the numerical problems in the LMI problem resolution [BcPS07].*

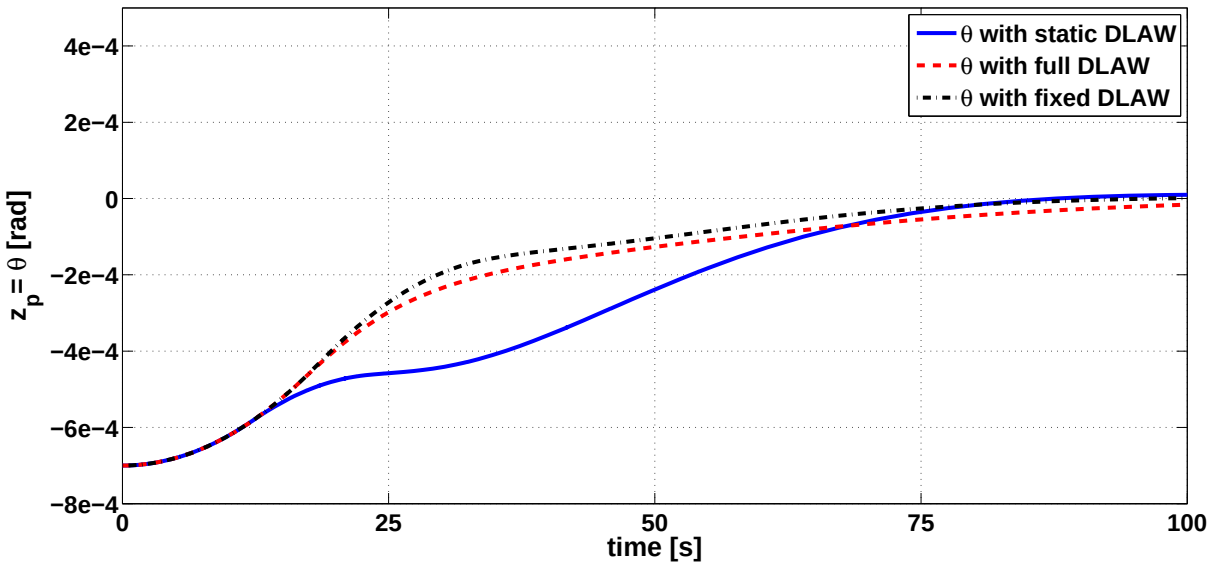

Figure 3.14: Attitude responses for a static, a full order and fixed order DLAW.

Figure 3.14 shows the responses of the system (3.7.1) with an initial condition $x_p(0) = [-7 \cdot 10^{-4} \quad 0]'$ for the three different DLAW. The responses present a similar time of response slightly improved in the dynamic anti-windup case, particularly in the fixed order one. Notice that the dynamic DLAW presents a smoother trajectory than the static DLAW. The dynamic behavior of the anti-windup allows the compensator to be active even if the actuator does not saturate, providing this smoother response.

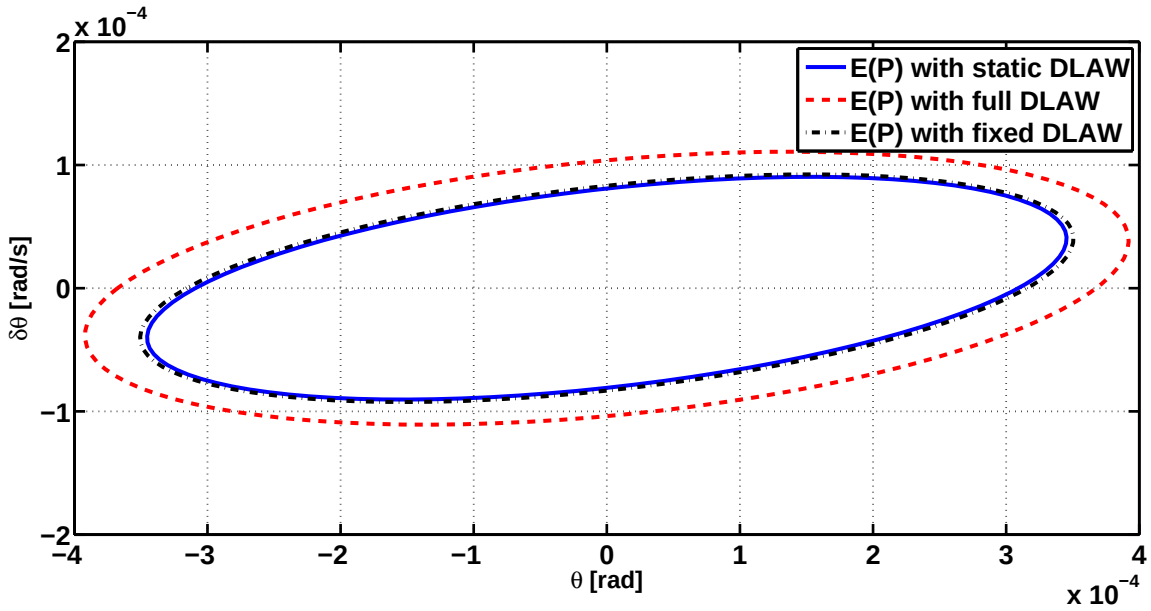

Figure 3.15: Stability Domain for a static, a full order and fixed order DLAW.

The stability domains are depicted in Figure 3.15. The dynamic anti-windup compensator provides a larger stability domain estimation. This phenomenon could be expected as the dynamic DLAW provides more degrees of freedom than the static DLAW to the LMI computation

Conclusions on the stability-performance trade-off are omitted because they are equivalent to those obtained for the static DLAW. Parameters $[k_\gamma, k_\rho]$ can be modified to improve either the performance or the stability domain estimation.

3.7.3 Educational example on MRAW

Results for the MRAW approach are illustrated with system (3.7.1). The anti-windup matrices in the MRAW are characterized by the model of the plant. Hence, A_p, B_pM, C_p and D_p are the matrices[5] of system (3.7.1) defining the MRAW dynamics.

In the educational example (3.7.1) the plant is modelled by a double integrator. Then, the stabilizing feedback v_1 (3.4.7) can be used.

The considered non-linear law is limited to a family of systems. Hence the analysis is not focused on the tuning of the v_1 (3.4.7), but on the characteristics of the MRAW approach.

The tuning of the non-linear law is done by trial and error. Three tunings are presented

[5] $D_p = 0$.

on simulations. The parameters characterizing these tunings are the followings:

- $[k = 0.01, \xi = 1]$ denoted MRAW 1 (solid line);
- $[k = 0.005, \xi = 1]$ denoted MRAW 2 (dot-dashed line);
- $[k = 0.01\ \xi = 0.5]$ denoted MRAW 3 (dashed-line).

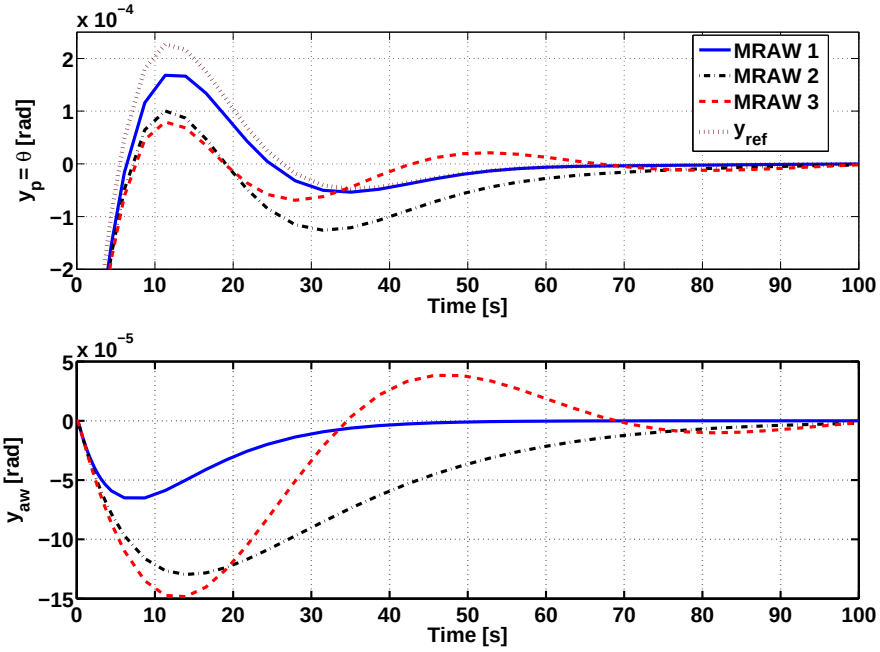

Figure 3.16: Attitude responses with several MRAW.

System (3.7.1) is simulated with an initial condition $x_p(0) = [-7 \cdot 10^{-4}\ \ 0]'$. Figure 3.16 shows $y_p = \theta$ and y_{aw} responses for the three tunings. The reference signal y_{ref} (dotted-line) is plotted together with the different y_p responses. The MRAW 1 approach presents the fastest y_p response. An explanation to this behavior is found in the MRAW design. In the MRAW approach only v_1 has to be tuned as the matrices are fixed by the plant. v_1 stabilizes the anti-windup loop (i.e. the convergence of y_{aw} to the origin). According to the relation $y_{ref} = y_p - y_{aw}$, it can be deduced that the faster y_{aw} convergence, the faster y_{ref} response is attained by y_p. The y_p signal will then converge to the origin following y_{ref}. The time of response of y_p is then either given by:

- y_{ref} time of response if y_{aw} converges to zero before y_{ref} has attained the origin;
- y_{aw} time of response, if y_{aw} converges to zero after y_{ref} has attained the origin.

In Figure 3.16, y_{aw} with MRAW 1 converges sooner to the origin than y_{ref}. On the other hand, y_{aw} with MRAW 2 and 3 converges later to the origin than y_{ref}. Therefore,

the attitude response (y_p) of system (3.7.1) is faster with the MRAW 1 than MRAW 2 and 3.

3.7.4 Educational example on EMRAW

The educational example is used to present practical considerations on the EMRAW. The EMRAW follows the MRAW paradigm. Thus, the anti-windup matrices are characterized by the plant of the system (3.7.1). Finally, two gains, F_{aw} and E_{aw}, have to be computed to complete the EMRAW.

In Section 3.5.3 two algorithms allowing the computation of the EMRAW gains are presented. Practical issues of these algorithms are presented in the following sections. First the coordinate-descending algorithm is applied. Then the objective-based algorithm is described.

3.7.4.a Coordinate-descending algorithm

The main difficulty to apply coordinate-descending algorithm (Algorithm 3.2) lies on the initialization of the gain K_s. A necessary condition to initialize the gain K_s are given in Lemma 3.1. The choice of K_s is difficult even if some necessary conditions are available. Generally there is no insurance of finding a solution to the conditions in Proposition 3.4 for a K_s satisfying (3.5.17). However if we analyze in detail the condition in (3.5.17) some helps can be extracted in order to hit a good K_s candidate. The goal of K_s is to stabilize the matrix $\mathbb{A} + K_s\mathbb{C}_s$ studied in Lemma 3.1. Moreover, recall that matrix $\mathbb{A}$ in system (3.5.7) is issued from a concatenation of the linear closed-loop matrix[6] A_l, the plant state matrix A_p and the ideal dynamics state matrix A_{id}. Among these three matrices only A_p presents unstable eigenvalues. Therefore, K_s can be seen as a feedback stabilizing the anti-windup dynamics.

Given these considerations, we have decided to constraint the placement of $(\mathbb{A}+K_s\mathbb{C}_s)$ poles to steer the initialization of K_s. Then the following conjecture can be stated:

Conjecture 3.1. *Constraining the eigenvalues of* $(\mathbb{A} + K_s\mathbb{C}_s)$ *to be in the same region of the* A_l *eigenvalues (see Figure 3.17), a* K_s *candidate is obtained. This candidate has more chances to start Algorithm 3.2, that is to find a solution to Proposition 3.4* .

Conjecture 3.1 is based on several trial and error tests and it is just proposed here as a possible manner to initialize K_s based on the experience. However, if the poles of $(\mathbb{A} + K_s\mathbb{C}_s)$ are forced to be in the same zone as those of A_l, since A_l is part of $\mathbb{A}$,

[6] with $A_l = \begin{bmatrix} A_p + B_pD_cC_p & B_pC_c \\ B_cC_p & A_c \end{bmatrix}$.

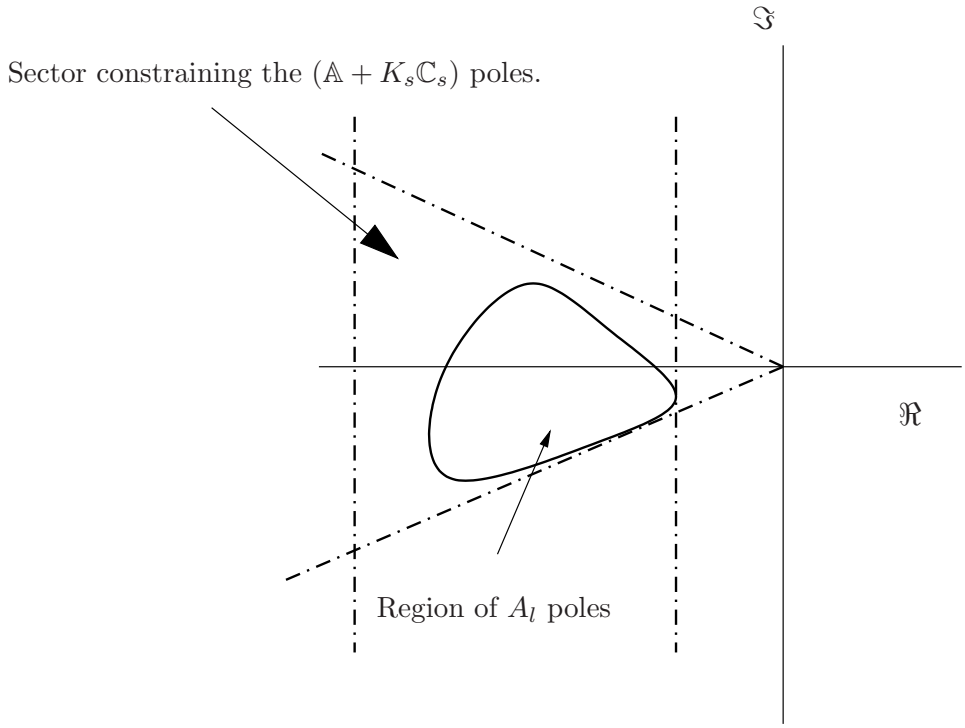

Figure 3.17: Sector definition including closed-loop poles

the conditioning number of the resulting matrix will be better than leaving the poles placement free.

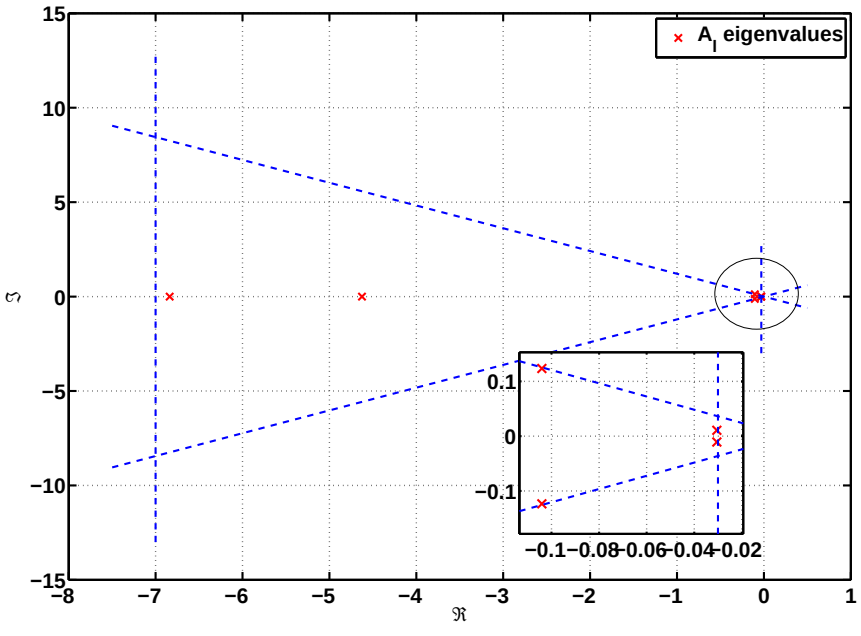

Figure 3.18: Region of the complex plane defined by the eigenvalues of A_l.

Therefore, in addition to the necessary condition (3.5.17), constraints delimiting the complex plane have to be introduced in the computation of K_s to find the "best suitable K_s". The expression of the LMIs defining a region on the complex plane can be found in [SW05, CG56].

The educational example has been used to test the previous considerations. In Table 3.1 the poles of A_l are given for the system (3.7.1). Then, the initialization of K_s is done by constraining the poles of $(\mathbb{A} + K_s\mathbb{C}_s)$ to the region presented in the Figure 3.18

A K_s verifying Lemma 3.1 and the constrained region is computed. For this K_s the Proposition 3.4 finds a solution, and thus the Algorithm 3.2 may be implemented. Then two gains F_{aw} and E_{aw} are found. They are used in a EMRAW structure. The simulation of the system (3.7.1) with this EMRAW is presented later in Figure 3.22.

3.7.4.b Objective-based algorithm

The objective-based (Algorithm 3.3) proposes an alternative method to find the EMRAW gains F_{aw} and E_{aw}. The educational example is used to steer the analysis on Algorithm 3.3. System (3.7.1) is simulated with $x_p = [-10^{-2} \quad 0]'$.

First, we compute F_{aw} to assure anti-windup loop stability. F_{aw} can be easily found through a pole placement. We select a second order behavior with damping ζ and natural frequency ω_n. After system analysis the best choice is $\zeta = 1$ and $\omega_n = 0.1$ which corresponds to a pair of poles $p_{1,2} = -0.1 \pm 0j$. Figure 3.19 shows system reference y_{ref} (solid line) and the saturated one for three different ω_n, $\zeta = 1$ and $E_{aw} = 0$. As $E_{aw} = 0$, we have[7] $y_{ref} = y_l$. When $\omega_n = 10$ (line with dots) system response is fast but the oscillations are induced. Otherwise, with $\omega_n = 0.01$ (dashed line), there is no presence of oscillations but the response is too slow. When $\omega_n = 0.1$ (dot-dashed line) no oscillations are induced and system response is fast even if an overshoot appears. Therefore we choose $F_{aw}(\omega_n = 0.1, \zeta = 1)$ as stabilizing gain of the anti-windup loop.

This choice presents an overshoot for the saturated system response. Thus, in order to improve this response, the reference should be modified. From the analysis (Analysis part of Algorithm 3.3) one infers that the ideal reference should not present overshoot. The ideal response with the dynamics (3.5.6) is presented in Figure 3.20 (solid line). The ideal dynamics matrices are:

$$A_{id} = \begin{bmatrix} 0 & 1 \\ -0.1 & -0.6 \end{bmatrix}; C_{id} = [1 \quad 0]. \tag{3.7.8}$$

Then, in the second part, we tune the ratio k_γ/k_ρ and F_{aw}^* to compute a E_{aw} which provides a reference as close as possible to the ideal one. First, the ratio has to be chosen

[7] With $E_{aw} = 0$ the EMRAW is indeed a MRAW, then the relation $y_{ref} = y_l$ holds.

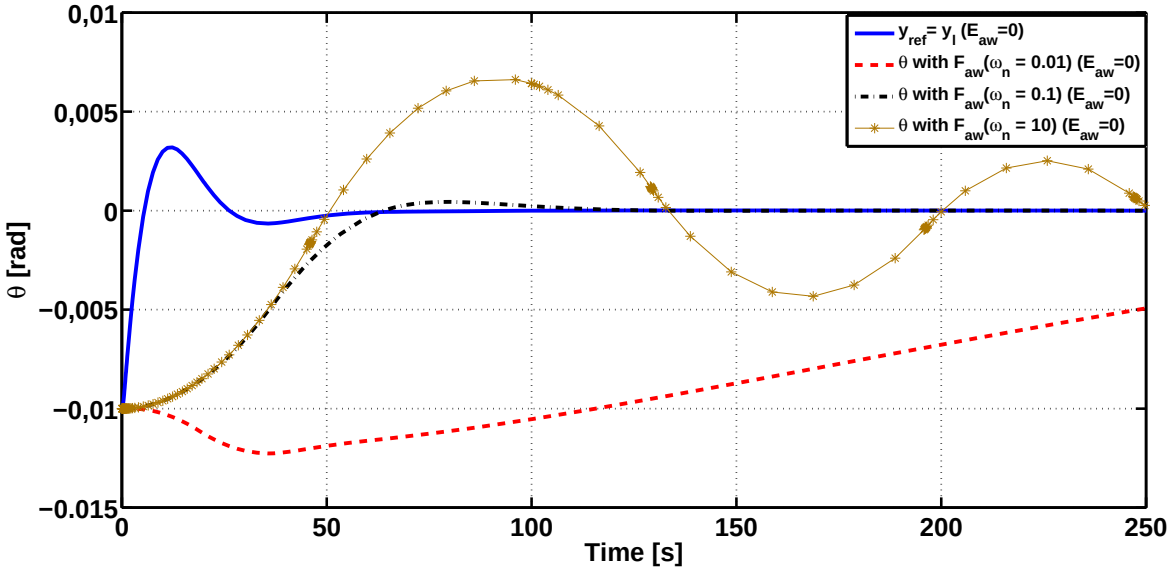

Figure 3.19: Analysis of the EMRAW filter with $E_{aw} = 0$.

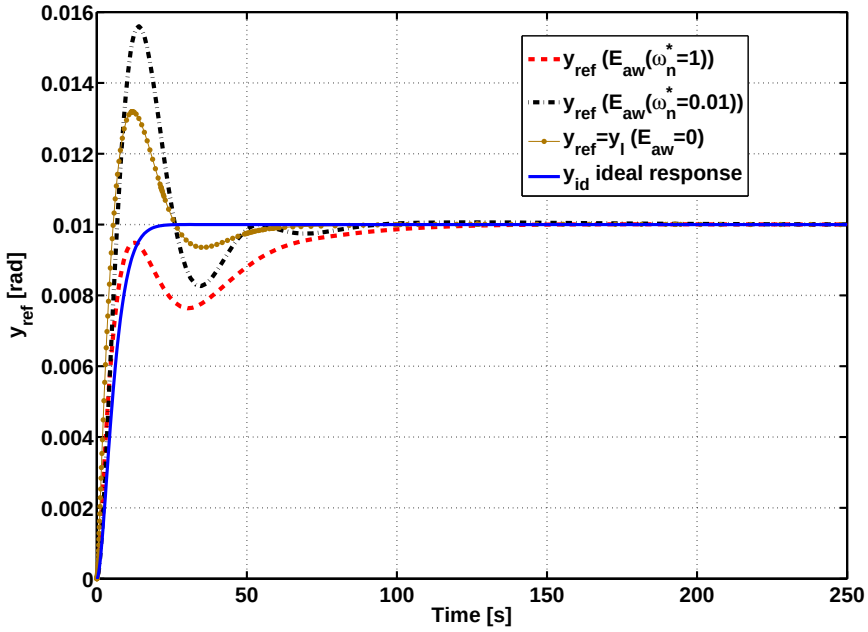

Figure 3.20: References evolution with E_{aw}.

as large as possible to obtain a reference close to the ideal one. Then we perform a pole placement of $A_p + B_p F^*_{aw}$ selecting a pair ζ and ω^*_n defining a second order dynamics. For simplicity we fix $\zeta = 1$ and only ω^*_n is tuned. Once k_γ/k_ρ and F^*_{aw} are set, we apply Theorem 3.2 to compute E_{aw} (step 3.3).

Figure 3.20 presents the reference output for different E_{aw}. The ratio is fixed to $k_\gamma/k_\rho = 10^9$ and F_{aw}^* is computed through a pole placement for different ω_n^*. In the legend $E_{aw}(\omega_n^*)$ means that the gain E_{aw} has been obtained for a F_{aw}^* set with $\zeta = 1$ and ω_n^*. Solid line stands for the ideal reference while dot-solid line shows the unconstrained behavior. Dot-dashed line is the reference obtained for $\omega_n^* = 0.01$, in that case the overshoot has been increased. Differently, when $\omega_n^* = 1$ the overshoot is clearly reduced. The best choice is $E_{aw}(\omega_n^* = 1)$.

Finally, combining first and second parts, we verify that the stability criterion is inside the limits. The combination of $F_{aw}(\omega_n = 0.1, \zeta = 1)$ and $E_{aw}(\omega_n^* = 1)$ provides an admissible attitude error of $\theta_{max}(0) = \frac{1}{\rho^2} = 2.8 \cdot 10^{-4}$. The process have been stopped because this guaranteed stability is close enough to the stability obtained for the static DLAW. We have tried to obtain a similar guaranteed stability domain for all the anti-windup compensators to compare their performances. Therefore, the EMRAW compensator is composed by $F_{aw}(\omega_n = 0.1, \zeta = 1)$ and $E_{aw}(\omega_n^* = 1)$.

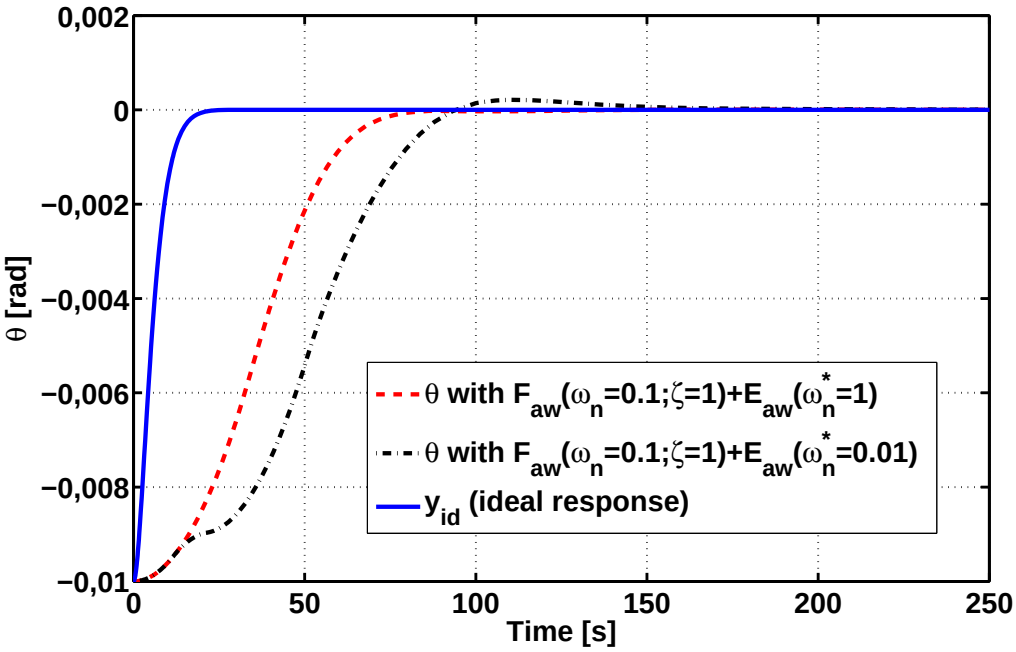

Figure 3.21: Attitude for different EMRAW compensators.

Figure 3.21 shows the ideal reference (solid line) and the system response for $F_{aw}(\omega_n = 0.1, \zeta = 1)$ with $E_{aw}(\omega_n^* = 1)$ (dashed line) and the response for $F_{aw}(\omega_n = 0.1, \zeta = 1)$ and $E_{aw}(\omega_n^* = 0.01)$ (dash-dotted line). In other words, the figure depicts the system response for the two modified references presented in Figure 3.20. One can see that the dash-dotted line presents an overshoot while the dashed line does not. At the same time, the response for the chosen gains converges faster than the other. Hence the choice of reference is justified.

Let us summarize the main ideas that can be extracted from the educational example.

The first Analysis part provides an idea about how the reference y_{ref} (with $E_{aw} = 0$) has to be modified. Thus the choice of the ideal reference will be much easier. Then, if we want E_{aw} to provide a reference close to the ideal one, k_γ/k_ρ has to be large. Moreover, F^*_{aw} has to be chosen providing a fast dynamics. If the dynamics are fast then computed E_{aw} will have more influence on the reference modification.

A large ratio k_γ/k_ρ will provide a E_{aw} which pushes y_{ref} towards y_{id}. Because of the nature of the system the ideal reference is not achievable. Then if the ratio is too big the reference could be destabilized because of this physical limitation.

The choice of F^*_{aw} is less efficient that the one of the optimization ratio. However, one can note that, if the anti-windup loop converges faster, the input on E_{aw} will decrease sooner. Then the computed E_{aw} will have more influence to palliate the early lack of $F^*_{aw}x_{aw}$ on its input. However, if the anti-windup loop dynamics for F^*_{aw} is too fast the system could diverge.

Remark 3.19. *Tuning the anti-windup gains through the analysis is not easy and this chapter only shows how it has been done for the educational example. However, if there is a certain knowledge of the system behavior, this can be a better method to find an anti-windup compensator instead of using the descending algorithm.*

3.7.5 Conclusion on the educational example

The educational example has been used to illustrate the different anti-windup techniques. Finally all the anti-windup compensators are briefly compared.

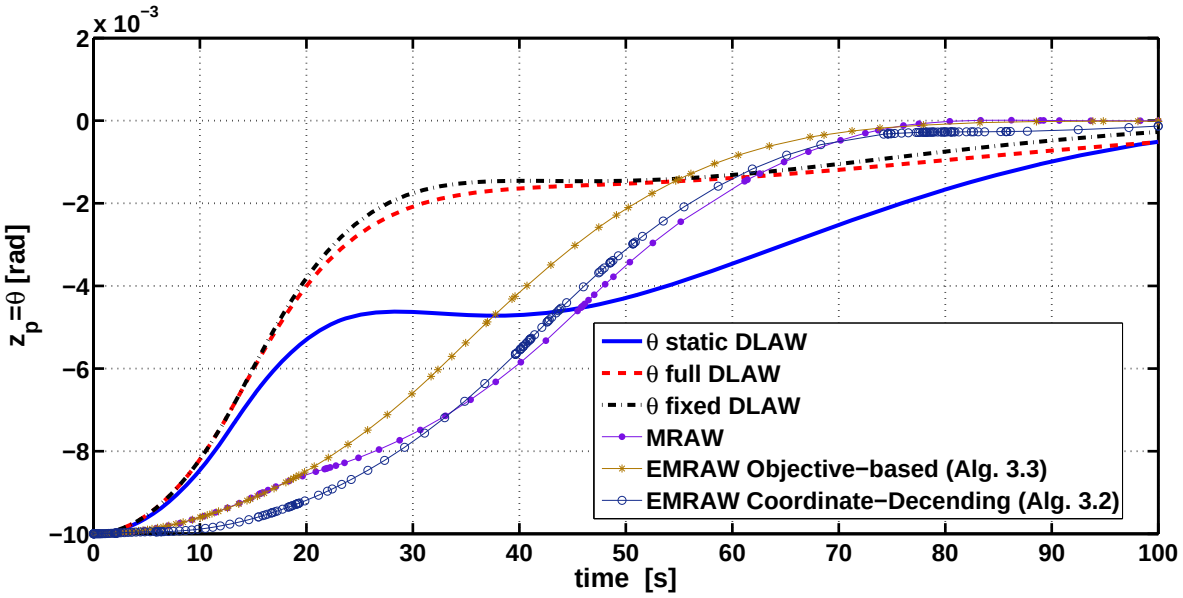

Figure 3.22: Attitude responses comparison between several anti-windup compensators.

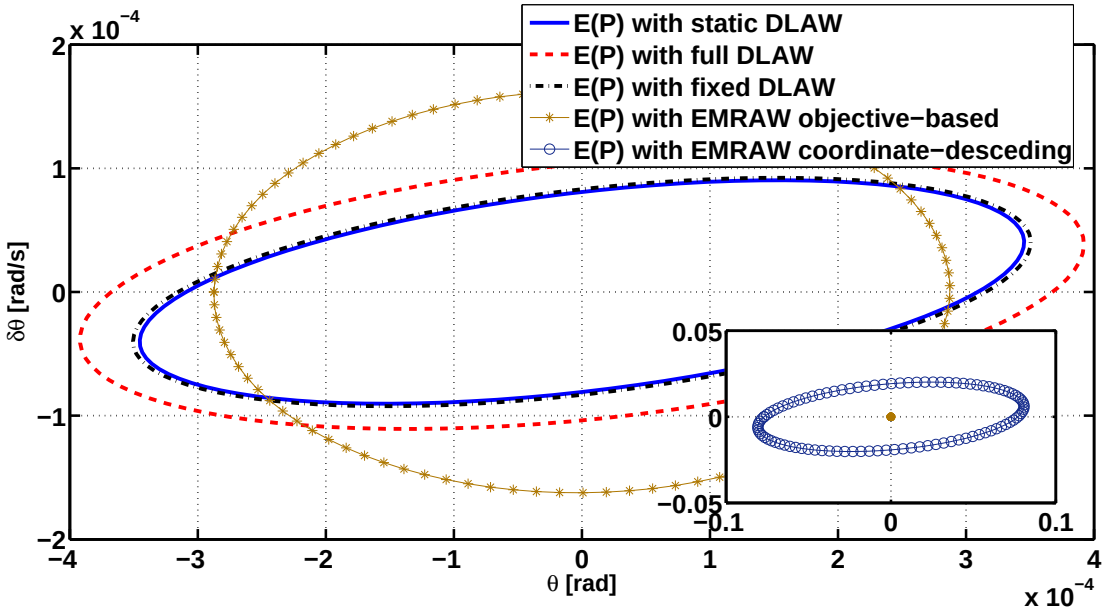

Figure 3.23: Stability domain comparison between several anti-windup compensators.

Figure 3.22 presents the response of the system (8) with several anti-windup compensator approaches for an initial condition of $x_p = [-1 \cdot 10^{-2} \quad 0]'$. The anti-windup computation approaches presented in Figure 3.22 are the following:

- A static DLAW compensator (solid line);
- A full order dynamic DLAW compensator (dashed line);
- A fixed order dynamic DLAW compensator (dot-dashed line);
- A MRAW compensator with v_1 (3.4.7) (line with dots);
- A EMRAW compensator computed with Algorithm 3.3 (line with stars);
- A EMRAW compensator computed with Algorithm 3.2 (line with circles).

The EMRAW computed with either the coordinate-descending algorithm (Algorithm 3.2) or the objective-based (Algorithm 3.3) permits to reach performances close to those obtained with a non-linear law v_1 (3.4.7).

Figure 3.23 shows the stability domains estimations obtained for the different anti-windup compensators. Algorithm 3.2 provides a clearly larger estimation than in any other case (see zoom out in Figure 3.23). This can be related to the nature of the algorithm, which optimizes at each step the Lyapunov related matrix P. Thus, Algorithm 3.2 optimizes at each step the size of the stability domain.

3.8 Conclusion

This chapter has presented a possible strategy to handle the saturation introducing an extra layer to the original controller, called anti-windup compensator.

The anti-windup compensator design has been addressed from three ways: The Direct Linear Anti-Windup (DLAW), the Model Recovery Anti-Windup (MRAW) and the Extended Model Recovery Anti-Windup (EMRAW).

The DLAW approach is based on the introduction of modifications in the control state and in the control output. Two possible structures for DLAW have been presented. First the case where DLAW is reduced to a simple static gain. Then the dynamic DLAW is tackled. Matrix inequations conditions are given in both cases for the computation of the DLAW, however, only in the static case these conditions are LMI. Two cases providing LMI conditions in the dynamics case have been given: when the anti-windup compensator order is the same of the closed-loop system and when the anti-windup dynamics are set *a priori*.

The MRAW has been presented as an alternative to the DLAW. The anti-windup synthesis between both methods differs on the definition of the anti-windup matrices. MRAW recovers the dynamics of the plant for the anti-windup compensator design. An overall vision on the MRAW has been given and some references containing interesting algorithms to compute a part of the anti-windup compensator have been provided. A particular attention has been given to the case where the plant is described as double integrator.

The last anti-windup compensator considered has been the EMRAW. It represents the main contribution of this manuscript. The EMRAW takes the idea from the MRAW as it recovers the plant dynamics for the anti-windup matrices design. In addition, a static DLAW has been added to the initial MRAW. The combination of both approaches has been called EMRAW. BMI conditions for the synthesis of the EMRAW have been provided. Consequently, some relaxations have been given to obtain LMI conditions which can be solved with the current solvers. Two algorithms have been presented as constructive strategies for the EMRAW approach.

The anti-windup techniques have been presented for systems presenting symmetric saturations. The validity of anti-windup techniques on system with asymmetric saturations have been analyzed. The results obtained show that the anti-windup synthesis techniques presented in this chapter can be applied regardless of the saturation symmetrization.

Finally, the educational example has been recalled to illustrate the different anti-windup compensators presented.

Chapter 4

Formation flying control

Outline of the chapter

4.1 Introduction

Formation flying control problem has been an important field of research since the 1990's. Several possible applications in the space exploration domain make this field very interesting [Gau07, PCU+05, Abs04]. In these kinds of missions one seeks to control the formation with a fine precision in both attitude and relative position. Consequently, the actuator is based on a precise propulsive system. However, these kind of actuators have a limited capacity which can be exceeded. Therefore, the interest of the anti-windup compensator arises.

For anti-windup study purposes, the flying formation problem can be described by a block diagram as presented in Figure 4.1. If y_p appears as attitude and/or relative position, the control loop would be illustrative of a flight formation configuration.

Remark 4.1. $y_r = 0$ *for consistency reasons without loss of generality.*

In this chapter three different formation flying control problems are modelled. These ones are the relative position, the attitude and relative position and a 16-state formation

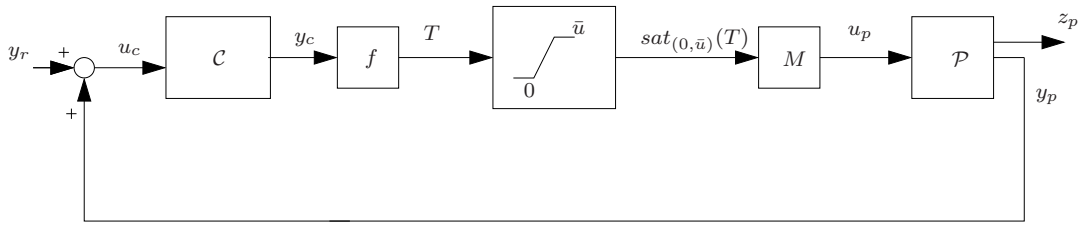

Figure 4.1: Control loop block diagram.

control. The models are simplified in order to enable the application of the anti-windup methods and study their effect. With more complex modelling numerical problems have appeared blocking the anti-windup computation.

Initially, Section 4.2 presents the model of the relative position between two satellites. Only the control of an axis is considered. Then, in Section 4.3 the anti-windup techniques presented in Chapter 3 are applied to the relative position control.

The attitude and relative position control problem is presented in Section 4.4. In Section 4.5 the anti-windup compensator is introduced in the attitude and relative position control loop. Simulations illustrate the benefits provided by the anti-windup compensator.

Finally, Section 4.6 presents a 8-DOF-two satellites formation model. A brief illustration of the formation with anti-windup compensator is given in Section 4.7.

4.2 Relative position control

4.2.1 Relative position plant model

The first relative dynamics to be described is the relative position between two satellites along the z-axis. Let us consider two satellites and two frames fixed to each satellite. $\mathcal{F}_{sat1}$ is the first satellite associated frame and $\mathcal{F}_{sat2}$ the second satellite associated frame. From the third theorem of the rigid body dynamics, the acceleration of a rigid body is proportional to the sum of external forces:

$$\ddot{z}_i = m_i^{-1} \sum (F_i) \tag{4.2.1}$$

where z_i is the displacement on the $z-$axis of satellite i. Hence, $\ddot{z}_i$ denotes the acceleration on this axis. m_i denotes the mass of satellite i and $\sum(F_i)$ stands for the sum of external forces on satellite i.

The control objective is to cancel the lateral position error on the z coordinate between the satellites, (see Figure 4.2). Therefore, the relative dynamics can be described applying

(4.2.1) to the difference of the z_i coordinate with $i = 1, 2$, that is $\Delta z = z_1 - z_2$. The control objective is then $\Delta z = 0$. Denoting $\sum(F_i)$ by F_i for consistency reasons, it yields

$$\Delta\ddot{z} = -m_2^{-1}F_2 + m_1^{-1}F_1 \tag{4.2.2}$$

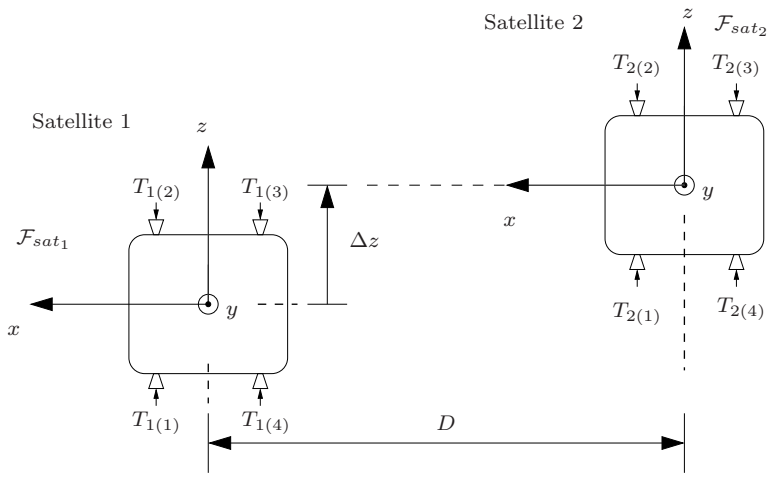

Figure 4.2: Relative position control configuration.

The state space representation associated to (4.2.2) reads:

$$\begin{cases} \dot{x}_p = A_p x_p + B_p u_p = \begin{bmatrix} 0 & 1 \\ 0 & 0 \end{bmatrix} \begin{bmatrix} \Delta z \\ \Delta\dot{z} \end{bmatrix} + \begin{bmatrix} 0 & 0 \\ m_1^{-1} & -m_2^{-1} \end{bmatrix} u_p \\ \\ y_p = C_p x_p = [1 \quad 0] x_p = \Delta z \\ z_p = C_z x_p = [1 \quad 0] x_p = \Delta z \end{cases} \tag{4.2.3}$$

where the state variables included in the state vector x_p are the relative position (Δz) and the relative velocity ($\Delta\dot{z}$), $u_p = [F_1 \quad F_2]'$ the control input, $y_p = \Delta z$ the measured output and $z_p = \Delta z$ the regulated output.

4.2.2 Relative position controller

The controller computes the control output y_c. A centralized controller is used. This means that a unique controller takes the measurements from all satellites in the formation and computes a vector y_c which contains the control output of each satellite.

The controller can be described through a state space representation:

$$\begin{cases} \dot{x}_c = A_c x_c + B_c u_c \\ y_c = C_c x_c + D_c u_c \end{cases} \tag{4.2.4}$$

In the relative position problem, the controller is an 1-input 2-outputs SIMO (Single Input Multiple Output) linear system with a 5 dimension state vector. The controller

input is $u_c = y_p = \Delta z$ and its outputs are $y_c = [y_{c1} \quad y_{c2}] = [F_{c1} \quad F_{c2}]'$. F_{c1} (resp. F_{c2}) stands for the controller output for the first (resp. second) satellite.

4.2.3 Relative position actuator model

The satellite formation is actuated by a propulsive system composed of 4 proportional thrusters on each of the two satellites. To apply the required control forces (F_1 and F_2) using this propulsive system, thruster management functions have to be introduced in the control loop. These functions are composed by an allocation function that transforms the required control efforts ($F_{c1} \quad F_{c2}$) into thrusters forces, and an influence matrix that transform the thruster outputs into forces applied on the system. Moreover, the actual forces delivered by each thruster are saturated. The general expression for the actuator is given as follows:

$$u_p = M sat_{(0,\bar{u})}(f(y_c)) \tag{4.2.5}$$

4.2.3.a The influence matrix

The influence matrix describes the geometric distribution of the thrusters. The physical distribution of the thrusters is presented in Figure 4.2.

The influence matrices are described as follows:

$$M_1 = [1 \quad -1 \quad -1 \quad 1]; M_2 = [1 \quad -1 \quad -1 \quad 1] \tag{4.2.6}$$

Influence matrices M_1 and M_2 are associated to satellite 1 and Satellite 2 respectively.

4.2.3.b Thruster saturation

The saturation function is modelled by (2.2.3). The saturation bounds for the relative position control problem are $\underline{u} = 0$ and $\bar{u} = 1mN$.

4.2.3.c Allocation function

In Section 2.4, we have insisted on the non-linear character of allocation function (AF). The given non-linear AF is based in a switching structure. This non-linear allocation function lies on the fact that the control output y_c is treated component-wise. The AF computes a set of thrust T for each component of the control output. These are denoted by $y_{c(k)}$ and the set of thrusts associated is denoted by T^k. Finally, the thrust vector

applied is the sum of all T^k with $k = 1, ..., m_c$. The switching structure can be described by the following expression:

$$f(y_c) = \begin{cases} T^k_{(i)} = \begin{cases} 0 & \text{if} \quad sign(M_{(k,i)}) \neq sign(y_{c(k)}) \\ \frac{y_{c(k)}}{\tau_{(k)} M_{(k,i)}} & \text{if} \quad sign(M_{(k,i)}) = sign(y_{c(k)}) \end{cases} \quad k = 1, ..m_c. \\ T_{(i)} = \sum_{k=1}^{m_c} T^k_{(i)}, i = 1, .., m. \\ T = [T_{(1)} \quad ... \quad T_{(m)}]' \end{cases} \tag{4.2.7}$$

where $sign(\cdot)$ stands for the function sign and $\tau_{(k)}$ stands for the number of thrusters generating an effort of the same sign as $y_{c(k)}$. $\tau_{(k)}$ is described as follows:

$$\tau_{(k)} = \sum_{i=1}^{m} \{sign(M_{(k,i)}) = sign(y_{c(k)})\} \tag{4.2.8}$$

where $\{sign(M_{(k,i)}) = sign(y_{c(k)}))\}$ is a boolean function that returns 1 if both elements are equal or 0 if they are not.

The relative position control problem presents $m = 4$ thrusters and $k = 1$ control output. Then the switching AF (4.2.7) has the following form for both satellites:

$$f(y_c) = \begin{cases} T_{(1)} = T_{(4)} = \begin{cases} 0 & \text{if} \quad y_c < 0 \\ \frac{y_c}{2} & \text{if} \quad y_c \geq 0 \end{cases} \\ T_{(2)} = T_{(3)} = \begin{cases} 0 & \text{if} \quad y_c \geq 0 \\ \frac{y_c}{2} & \text{if} \quad y_c < 0 \end{cases} \end{cases} \tag{4.2.9}$$

Remark 4.2. *AF (4.2.7) inspired the multi-sat AF (2.4.3) presented in Section 2.4.2.*

Other AF have been introduced in Section 2.4. In the relative position control the pseudo-inverse matrix based AF given by (2.4.1) is also considered.

To sum up, the actuator is modelled as follows:

$$u_p = M sat_{(0,\bar{u})}(f(y_c)) = \begin{bmatrix} M_1 & 0 \\ 0 & M_2 \end{bmatrix} sat_{(0,\bar{u})} \left(\begin{bmatrix} f(y_{c1}) \\ f(y_{c2}) \end{bmatrix} \right) \tag{4.2.10}$$

Two possibilities are considered for $f(y_c)$: AF (4.2.9) and AF (2.4.1). In this last case the control input u_p reads:

$$u_p = \begin{bmatrix} M_1 & 0 \\ 0 & M_2 \end{bmatrix} sat_{(0,\bar{u})} \left(\begin{bmatrix} M_1^* y_{c1} \\ M_2^* y_{c2} \end{bmatrix} \right) \tag{4.2.11}$$

4.2.4 Relative position closed-loop model

With the previously presented plant (4.2.3), controller (4.2.4) and actuator (4.2.10) the closed-loop system describing the relative position control reads:

$$\begin{cases} \dot{x}_p = A_p x_p + B_p u_p = \begin{bmatrix} 0 & 1 \\ 0 & 0 \end{bmatrix} \begin{bmatrix} \Delta z \\ \Delta \dot{z} \end{bmatrix} + \begin{bmatrix} 0 & 0 \\ m_1^{-1} & -m_2^{-1} \end{bmatrix} u_p \\ \dot{x}_c = A_c x_c + B_c C_p x_p \\ y_p = C_p x_p = [1 \;\; 0] x_p = \Delta z \\ z_p = C_z x_p = [1 \;\; 0] x_p = \Delta z \\ u_p = M sat_{(0,\bar{u})}(f(y_c)) = \begin{bmatrix} M_1 sat_{(0,\bar{u})}(f(y_{c1})) \\ M_2 sat_{(0,\bar{u})}(f(y_{c2})) \end{bmatrix} \\ y_c = C_c x_c + D_c C_p x_p \end{cases} \tag{4.2.12}$$

with $f(y_c)$ defined by (4.2.9).

System (4.2.12) provides a benchmark for further simulations. However the non-linearity introduced by the AF (4.2.9) does not allow the computation of the anti-windup compensator for this system. For this reason another formulation is defined. The closed-loop system with the actuator (4.2.11) reads:

$$\begin{cases} \dot{x}_p = A_p x_p + B_p u_p = \begin{bmatrix} 0 & 1 \\ 0 & 0 \end{bmatrix} \begin{bmatrix} \Delta z \\ \Delta \dot{z} \end{bmatrix} + \begin{bmatrix} 0 & 0 \\ m_1^{-1} & -m_2^{-1} \end{bmatrix} u_p \\ \dot{x}_c = A_c x_c + B_c C_p x_p \\ y_p = C_p x_p = [1 \;\; 0] x_p = \Delta z \\ z_p = C_z x_p = [1 \;\; 0] x_p = \Delta z \\ u_p = M sat_{(0,\bar{u})}(M^* y_c) = \begin{bmatrix} M_1 sat_{(0,\bar{u})}(M_1^* y_{c1}) \\ M_2 sat_{(0,\bar{u})}(M_2^* y_{c2}) \end{bmatrix} \\ y_c = C_c x_c + D_c C_p x_p \end{cases} \tag{4.2.13}$$

This alternative formulation allows the computation of the anti-windup compensator presented in Chapter 3. System (4.2.13) is then simulated with the anti-windup compensator. The responses obtained for the system (4.2.13) with anti-windup are compared to the responses of the system (4.2.12) without anti-windup.

4.3 Anti-windup on the relative position control

The relative position control problem has been modelled. The results from Chapter 3 are applied to synthesize an anti-windup compensator. For anti-windup computation purposes the closed-loop system (4.2.13) is considered.

The saturation function in (4.2.13) is asymmetric. Results on anti-windup synthesis consider symmetric saturations. Thus, before computing the anti-windup compensator the saturation has to be symmetrized. Therefore results from Section 2.5 results are used.

Influence matrix (4.2.6) satisfies the Lemma 2.4 conditions. Therefore the symmetrizing vector $N\zeta_{sym} = \bar{u}/2$ can be applied. Additionally, the VKF (2.5.14) is also considered to symmetrize the saturation while solving the problems of extra consumption exposed in Section 2.5.3.

With the saturation symmetrized, the closed-loop system (4.2.13) reads:

$$\begin{cases} \dot{x}_p = A_p x_p + B_p u_p = \begin{bmatrix} 0 & 1 \\ 0 & 0 \end{bmatrix} \begin{bmatrix} \Delta z \\ \Delta \dot{z} \end{bmatrix} + \begin{bmatrix} 0 & 0 \\ M_1^{-1} & -M_2^{-1} \end{bmatrix} u_p \\ \dot{x}_c = A_c x_c + B_c y_p \\ y_p = C_p x_p = [1 \;\; 0] x_p = \Delta z \\ z_p = C_z x_p = [1 \;\; 0] x_p = \Delta z \\ u_p = M sat_{(u_0)}(M^* y_c) = \begin{bmatrix} M_1 sat_{(u_0)}(M_1^* y_{c1}) \\ M_2 sat_{(u_0)}(M_1^* y_{c2}) \end{bmatrix} \\ y_c = C_c x_c + D_c C_p x_p \end{cases} \tag{4.3.1}$$

with symmetric bounds $u_0 = \frac{1}{2} 1mN$

In Chapter 3 anti-windup compensator design has been decomposed in three techniques: the Direct Linear Anti-Windup, the Model Recovery Anti-windup and the Extended Model Recovery Anti-windup. These techniques are applied hereafter. Let us notice that the relative position problem is essentially the same as the educational example. Hence the analysis about the computation of each technique has been omitted to avoid redundant comments.

4.3.1 Anti-windup compensator synthesis

First let us first consider the DLAW case. In Section 3.3 the system considered was described as follows:

$$\begin{cases} \dot{\xi} = \mathbb{A}\xi + \mathbb{B}_\phi \phi_{(u_0)}(\nu) + \mathbb{B}_v v_x \\ \nu = \mathbb{K}\xi \\ z = \mathbb{C}\xi + \mathbb{D}_\phi \phi_{(u_0)}(\nu) \end{cases} \tag{4.3.2}$$

System (4.3.1) can be recognized on (4.3.2) with some mathematical development. Both the static and dynamic DLAW are tackled

4.3.1.a Static DLAW synthesis

In the static case the anti-windup compensator is limited to a static feedback gain. Thus, the anti-windup output is given by $v_x = D_{aw}\phi_{(u_0)}(\nu)$.

The DLAW static gain D_{aw} can be easily computed by applying Theorem 3.1. In this particular case the stability domain optimization is done in the Δz direction. In that manner, the term v in LMI (3.3.12) becomes $v = [1 \quad 0 \quad 0_{1\times5} \quad 0_{1\times7}]'$. The performance-stability weights are $[k_\gamma \quad k_\rho] = [10, 1]$. The D_{aw} obtained reads:

$$D_{aw} = \begin{bmatrix} -0.32 & -0.32 & 0.32 & 0.32 & -1.65 & -1.65 & 1.65 & 1.65 \\ 0.28 & 0.28 & -0.28 & -0.28 & 3.5 & 3.5 & -3.5 & -3.5 \\ 2.95 & 2.95 & -2.95 & -2.95 & -6.39 & -6.39 & 6.39 & 6.39 \\ 0.88 & 0.88 & -0.88 & -0.88 & -1.81 & -1.81 & 1.81 & 1.81 \\ 376.78 & 376.78 & -376.78 & -376.78 & -665.5 & -665.5 & 665.5 & 665.5 \end{bmatrix} \tag{4.3.3}$$

Let us give a brief comment on the structure of the static DLAW (4.3.3). First, observe the difference between the first four columns and the last four. That is due to the relation of the first four columns with the first satellite thrusters, and the relation of the last four with the second satellite thrusters. Finally, notice that in each group of four columns there are two positive values and two negative. This sign is related to the positive or negative effort that each thruster performs.

In addition, it is important to remark that there is a row (the fifth one) whose values outstand in comparison with the others. Actually this line affects the state of the controller related to the integration. The anti-windup mission is to attenuate the integral state of the controller which is the more sensible state to the saturation effects. Therefore it is normal to find a more important effect on this controller state than on the others.

4.3.1.b Dynamic DLAW synthesis

Consider a dynamic DLAW like in (3.3.3). The anti-windup compensator is then described by:

$$\mathcal{AW} \begin{cases} \dot{x}_{aw} &= A_{aw}x_{aw} + B_{aw}\phi_{(u_0)}(y_c) \\ v_x &= C_{aw}x_{aw} + D_{aw}\phi_{(u_0)}(y_c) \end{cases} \tag{4.3.4}$$

Then the results presented in Section 3.3 are applied to system (4.3.1) to compute a dynamic DLAW.

Proposition 3.2 is used to compute a full order anti-windup compensator, that is $n_{aw} = n_M$. Moreover, this computation provides a guide on the choice of the poles for the fixed order anti-windup synthesis. The computation is decomposed in two steps. The

first consist in computing the full order DLAW. From all the poles of the computed full order compensator, just the poles of A_{aw} sharing the same magnitude order as those of A_l are conserved. The fix order Algorithm 3.1 is then applied.

The proposition 3.2 is called with the optimization weight $[k_\gamma \quad k_\rho] = [10, \quad 1]$. The stability domain is maximized in the relative position direction Δz. Table 4.1 shows the poles of the full order dynamic DLAW and the poles of the linear closed-loop system A_l. The selected poles for the fixed oder DLAW synthesis are marked with $*$.

Table 4.1: Full order DLAW eigenvalues in relative position control

$\text{eig}(A_{aw})(* \equiv selected)$	$\text{eig}(A_l)$
$-8.28 \cdot 10^6$	$(-2.61 \pm j2.88) \cdot 10^{-1}$
$-6.21 \cdot 10^6$	$(-1.62 \pm j2.02) \cdot 10^{-1}$
$-4.74 \cdot 10^4$	$(-8.23 \pm j8.23) \cdot 10^{-3}$
$-1.93 \cdot 10^2$	$-2.73 \cdot 10^{-3}$
-1.61	
$(-9.11 \pm j27.5) \cdot 10^{-2}$	
-0.13	
$-4.38 \cdot 10^{-2}(*)$	
$(-8.97 \pm j5.17) \cdot 10^{-3}(*)$	
$-8.61 \cdot 10^{-3}(*)$	
$-7.46 \cdot 10^{-3}(*)$	
$-4.11 \cdot 10^{-3}$	

With the proposed choice of poles the Algorithm 3.1 is applied.

4.3.1.c MRAW synthesis

The MRAW approach is characterized by the model of the plant. Hence the plant (4.2.3) matrices define the anti-windup compensator.

The main difficulty in the MRAW approach is the definition of the stabilizing law v_1. However, the plant (4.2.3) is defined by a double integrator. Therefore, in this particular case, one may use the non-linear law (3.4.7) as stabilizing feedback v_1.

The tuning of the non-linear law (3.4.7) is done by trial and error and finally the parameters are set to: $k = 0.01$; $\xi = 1$.

4.3.1.d EMRAW synthesis

The EMRAW structure is finally considered. First the coordinate-descending algorithm (Algorithm 3.2) is applied to system (4.3.1) to compute the EMRAW gains. The weights performance-stability have been set to $[k_\gamma \quad k_\rho] = [2.5, 1]$. The stability domain is maximized in the relative position direction Δz. As commented before in Conjecture 3.1 the initialization of K_s is done by constraining the poles of $(\mathbb{A} + K_s\mathbb{C}_s)$ to be in the region of A_l. The ideal dynamics are given by: $A_{id} = -0.01$ and $C_{id} = 1$.

The computed F_{aw} and E_{aw} read:

$$E_{aw} = \begin{bmatrix} -1.5 & -1.5 & 1.5 & 1.5 & -1.96 & -1.96 & 1.96 & 1.96 \\ 3.12 & 3.12 & -3.12 & -3.12 & -4 & -4 & 4 & 4 \\ -1.22 & -1.22 & 1.22 & 1.22 & 1.59 & 1.59 & -1.59 & -1.59 \\ 0.05 & 0.05 & -0.05 & -0.05 & -0.012 & -0.012 & 0.012 & 0.012 \\ 6.28 & 6.28 & -6.28 & -6.28 & -3.87 & -3.87 & 3.87 & 3.87 \end{bmatrix} \tag{4.3.5}$$

$$F_{aw} = \begin{bmatrix} -0.0051 & -0.67 \\ -0.0051 & -0.67 \\ 0.0051 & 0.67 \\ 0.0051 & 0.67 \\ 0.0043 & 0.57 \\ 0.0043 & 0.57 \\ -0.0043 & -0.57 \\ -0.0043 & -0.57 \end{bmatrix} \tag{4.3.6}$$

Then the EMRAW gains are tuned following the objective-based algorithm (Algorithm 3.3). The first part of the objective-based algorithm consists in tuning F_{aw}. After some trial and error iterations, F_{aw} has been set such that the $(A_p + B_pF_{aw})$ dynamics respond as a second order system with natural frequency $w_n = 0.1rad/s$ and damping $\zeta = 1$. The second part of the algorithm accounts for the computation of E_{aw}. After several iterations, the process was stopped with $[k_\gamma \quad k_\rho] = [10^9, 1]$ and with F^*_{aw} that yields a second order dynamics in $(A_p + B_pF^*_{aw})$ with natural frequency $w_n = 10rad/s$ and damping $\zeta = 1$. The ideal reference taken is the same as used in the coordinate-descending algorithm.

The computed F_{aw} and E_{aw} read:

$$E_{aw} = \begin{bmatrix} -1.08 & -1.08 & 1.08 & 1.08 & 2.21 & 2.21 & -2.21 & -2.21 \\ 2.52 & 2.52 & -2.52 & -2.52 & -4.48 & -4.48 & 4.48 & 4.48 \\ -1.11 & -1.11 & 1.11 & 1.11 & 2.11 & 2.11 & -2.11 & -2.11 \\ 0.073 & 0.073 & -0.073 & -0.073 & -0.16 & -0.16 & 0.16 & 0.16 \\ 1.76 & 1.76 & -1.76 & -1.76 & -19.27 & -19.27 & 19.27 & 19.27 \end{bmatrix} \tag{4.3.7}$$

$$F_{aw} = \begin{bmatrix} -0.0053 & -0.75 \\ -0.0053 & -0.75 \\ 0.0053 & 0.75 \\ 0.0053 & 0.75 \\ 0.0065 & 0.93 \\ 0.0065 & 0.93 \\ -0.0065 & -0.93 \\ -0.0065 & -0.93 \end{bmatrix} \tag{4.3.8}$$

4.3.2 Simulations on relative position control

All the strategies on the anti-windup compensation presented in the Chapter 3 have been applied. System (4.3.1) is simulated with the different anti-windup compensators.

However the closed-loop system (4.2.12) is first simulated without anti-windup. System (4.2.12) is simulated from an initial condition of $x_p(0) = [\Delta z \quad \Delta\dot{z}]' = [-1 \quad 0]'$ and[1] $x_c = 0_{1\times 5}$. Let us remind that (4.2.12) describes the relative position closed-loop system with the switching AF (4.2.9).

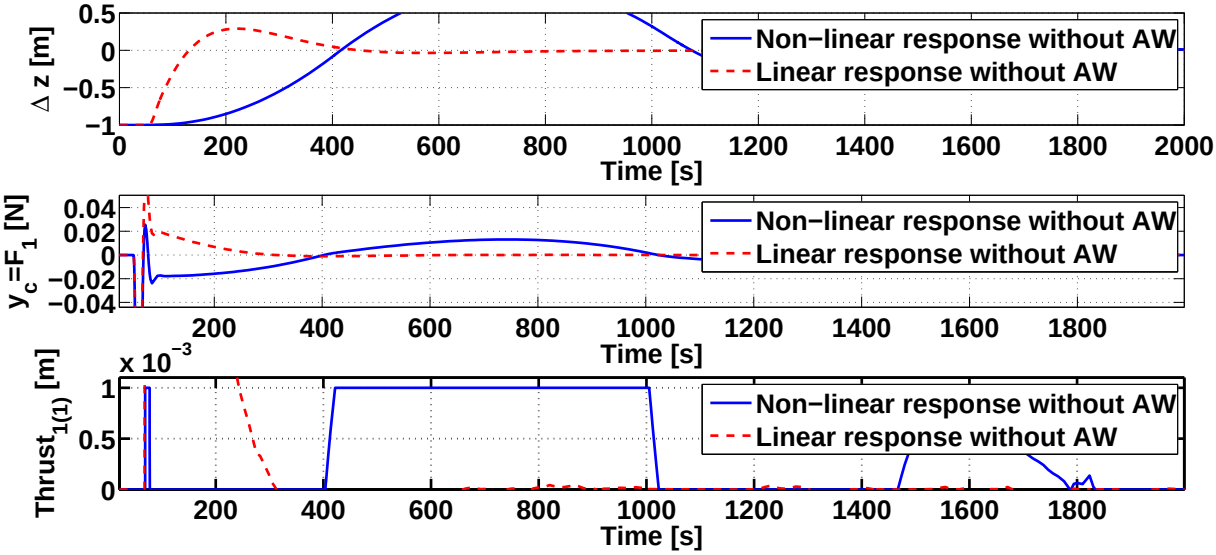

Figure 4.3: Responses of the relative position without Anti-windup compensator.

In the Figure 4.3, the solid line presents the Δz response of the system (4.2.12) (i.e. non-linear response). The dot-dashed line shows the response of the system without saturation (i.e. linear response). One can realize the effects of the saturation as oscillations are induced in the non-linear response of Δz. The control output and the performed thrust are also shown in the Figure 4.3. The thrust response is saturated and the control output

[1] Let us remind that the controller state is considered to be always initialized at the origin.

oscillates. The remarkable effects of the saturation on the system (4.2.12) justify the introduction of the anti-windup compensator.

Remark 4.3. *From an industrial point of view the response presented in Figure 4.3 is unacceptable. Thus, the linear controller used in system (4.2.12) would not be applied. In practice, a non-linear controller is used.*

The closed-loop system (4.3.1) is simulated with the following anti-windup compensators:

- static DLAW compensator (solid line);
- full order dynamic DLAW compensator (dashed line);
- fixed order dynamic DLAW compensator (dot-dashed line);
- MRAW compensator with v_1 (3.4.7) (line with dots);
- EMRAW compensator computed with Algorithm[2] 3.3 (line with stars);
- EMRAW compensator computed with Algorithm[3] 3.2 (line with circles).

Figure 4.4 shows the response of the relative position with the different anti-windup compensators in the control loop. The Δz responses have been split in two small figures for clarity purposes.

From a general overview of the Figure 4.4 one can conclude that the oscillation observed in Figure 4.3 has disappeared with the introduction of the anti-windup compensator.

Let us start analyzing the response with DLAW. In Figure 4.4 the response with a dynamic DLAW is smoother than in the static DLAW case which presents a drop on its slope. The anti-windup action, in the static case, ends as soon as there is no saturation. Therefore the drop appears. On the contrary, the dynamic DLAW keeps modifying the controller action even without actuator saturation. In Figure 4.5 the thrust response suddenly falls with the static DLAW case while it decreases progressively with the dynamic one. The advantage of a dynamic DLAW is then proven.

Also in Figure 4.5, the thrust response with a full order DLAW is noisy. The fast dynamics in the full order case induces the high frequency oscillation. The presence of fast and slow modes in the full order DLAW generates numerical problems for both LMI computation step (bad conditioning effects) and simulation step (numerical precision effects). On the contrary, the fixed order DLAW does not present this oscillation because

[2]Objective-based algorithm.
[3]Coordinate-descending algorithm.

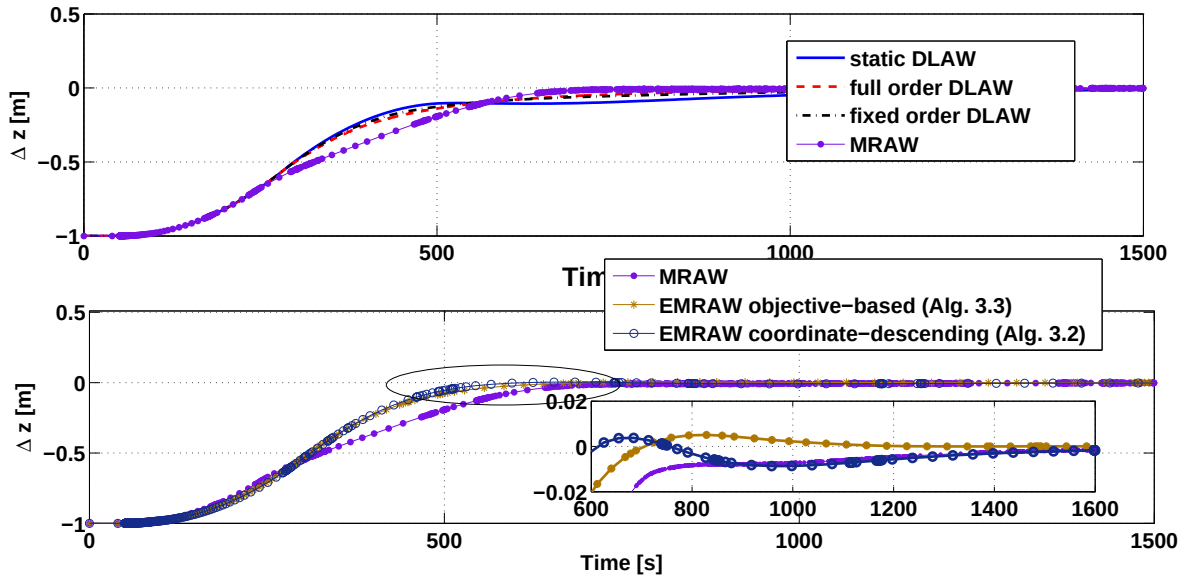

Figure 4.4: Response of the relative position with several Anti-windup compensators.

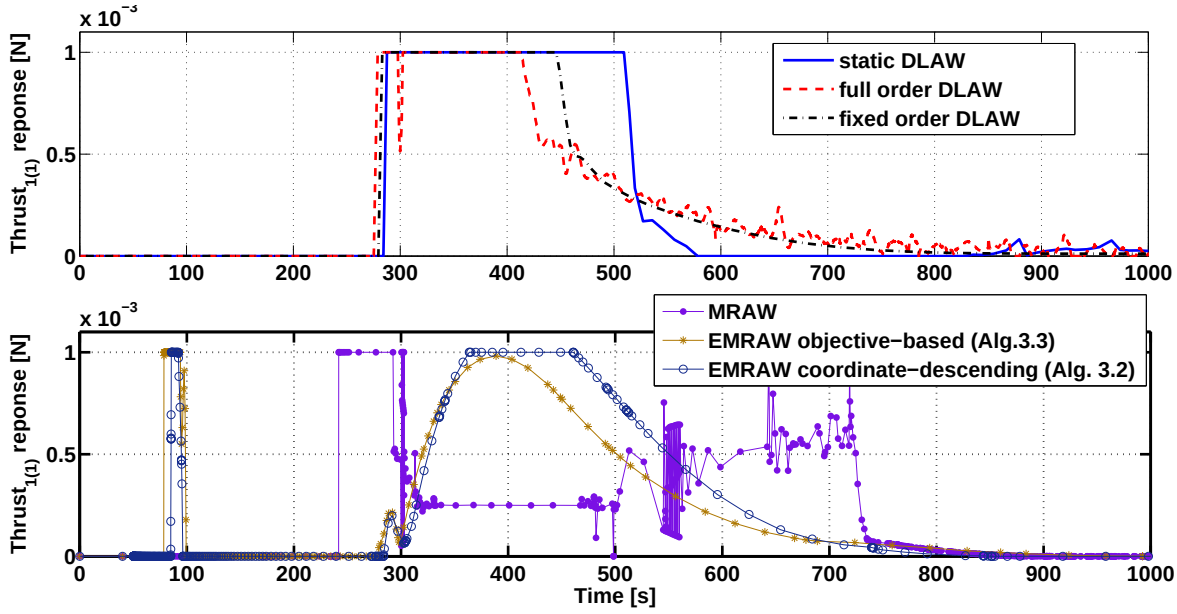

Figure 4.5: Response of the first Thruster with several Anti-windup compensators.

the fast dynamics were not chosen in the synthesis process. Therefore, the fixed order provides a smooth response without high frequency oscillations.

Let us go back again to Figure 4.4 to analyze the Δz response with a MRAW/EMRAW. The responses show that fast responses are attained with the MRAW/EMRAW. Moreover the response Δz of the system (4.3.1) is faster with the EMRAW. An explanation to this behavior is find in Figures 4.6 and 4.7 where the anti-windup output y_{aw} and the reference signal y_{ref} are compared. The MRAW anti-windup output y_{aw} converges faster due to

the stabilizing law v_1 (3.4.7) which is more performant than the static feedback (3.5.4). Thus, the system response with the MRAW attain the reference, that is, $y_p = y_{ref}$, before the response with the EMRAW. However the reference y_{ref} for the MRAW is slower than the one for the EMRAW. Therefore, the actual response $y_p = \Delta z$ of the system (4.3.1) is faster with the EMRAW.

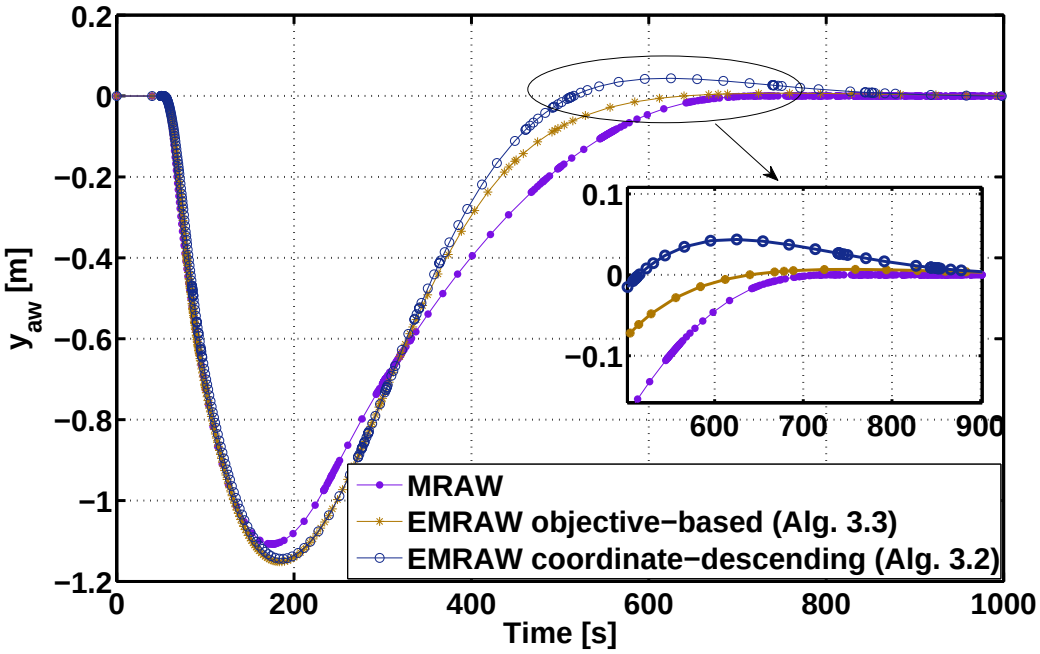

Figure 4.6: Anti-windup output response for MRAW/EMRAW approaches.

Remark 4.4. *Let us remind that the mission of v_1 is to stabilize the anti-windup loop (i.e. $y_{aw} \to 0$). The optimality of this process does not ensure a fast response for the system output y_p, but a fast convergence of y_p towards y_{ref}. If the reference y_{ref} is slow, one will obtain a slow response for the output y_p even if the convergence of y_{aw} is fast. The extra degree of freedom introduced in the EMRAW approach (gain E_{aw}) allows us to get faster references with a small modification of the control dynamics. Therefore, the EMRAW may provide faster Δz responses even with a non-optimal v_1.*

Another comment on the MRAW approach can be done by the analysis of the thrust response. In Figure 4.5 a strong oscillations on the MRAW approach can be noticed. The used v_1 is based on a bang-bang law which works efficiently far from the origin. However the closer it gets to the origin the higher the bang-bang frequency and hence the stronger the noise induced into the thrust action.

Finally, Figure 4.8 presents the stability domain estimation for the different anti-windup compensators. The MRAW case has been omitted. LMI conditions cannot be provided with the non-linear v_1. However for this specific v_1, global asymptotic stability can be obtained [FGZ10, TK97a].

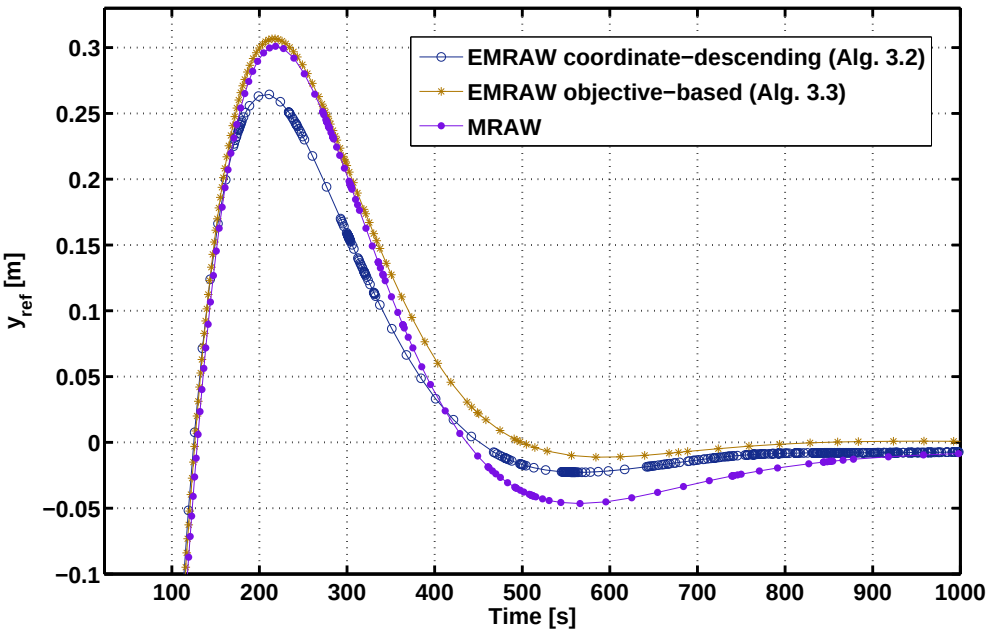

Figure 4.7: Reference response for MRAW/EMRAW approaches.

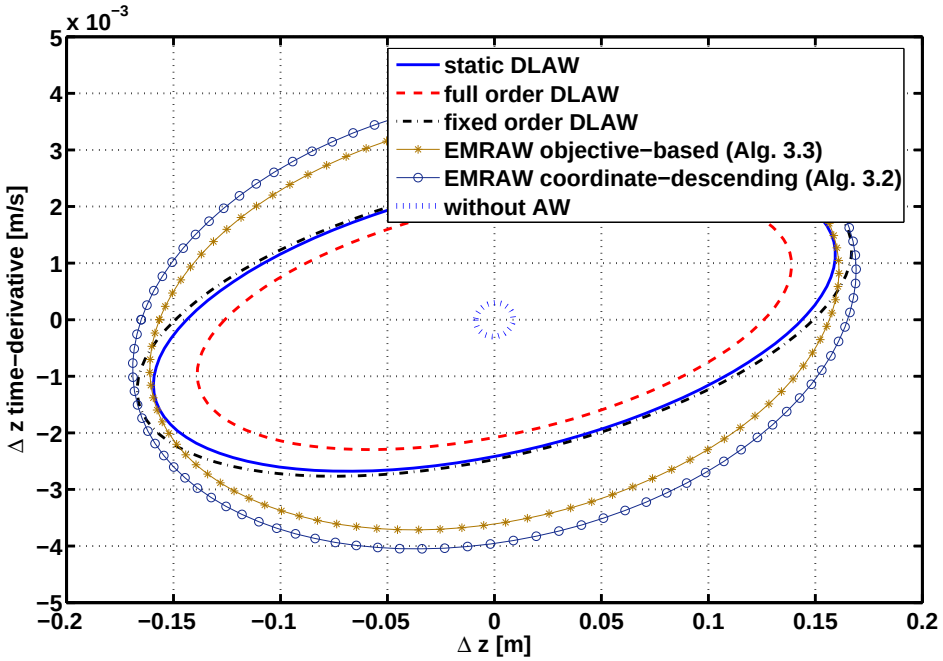

Figure 4.8: Stability domain with several Anti-windup compensators.

The EMRAW computed with the Algorithm 3.2 provides a larger estimation[4]. Despite slight differences, all the compensators ensure (more or less) the same estimated maximal

[4]Let us recall that the stability domain is optimized at each step of Algorithm 3.2.

admissible $\Delta z_{max}(0)$ (cutting point with $\Delta\dot{z} = 0$ axis). However, the estimation obtained with the full order DLAW is smaller than the one obtained with the other compensators. This is due to some numerical problems. The difference between the maximum and the minimum eigenvalue of A_{aw} results on a bad conditioning of the LMIs conditions. As a consequence, the stability domain analysis for the full order DLAW is unfeasible.

Two final remarks on the stability domain estimation. First notice that the size of the stability domain without anti-windup (dots line) is clearly smaller. The second point is the conservatism of the estimation. Simulations show that the system is stable (even without anti-windup) for an initial condition $x_p(0) = [-1 \quad 0]'$. However, considering the estimated domain the maximal admissible initial condition is around $x_p(0) = [-0.15 \quad 0]'$.

Table 4.2: Summary values on the relative position control

	Static DLAW	full order DLAW	fixed order DLAW
γ	5.127	5.122	5.125
$\Delta z_{max}(0) = \frac{1}{\sqrt{\rho}}$ $[m]$	0.14	0.130.15	
Time of response $[s]$	1570	1160	1390
Consumption $[Ns]$	2.017	1.829	1.82
AW Order	0	14	5
	MRAW	EMRAW Alg. 3.2	EMRAW Alg. 3.3
γ	?	0.622	0.624
$\Delta z_{max}(0) = \frac{1}{\sqrt{\rho}}$ $[m]$	?	0.17	0.16
Time of response $[s]$	750	580	630
Consumption $[Ns]$	1.679	1.894	1.8192
AW Order	2	2	2

Table 4.2 summarizes the main values characterizing the anti-windup compensators. These values are:

- the performance criterium γ;
- the maximal admissible initial condition for the relative position $\Delta z_{max}(0)$;
- the *time of response* for Δz in seconds;
- the integral of the thrust response (value related to the *consumption*);
- the *order* of the anti-windup (AW) compensator.

The time of response appears as a remarkable value for the comparison. It has been defined as the time when the Δz response has reached the 99% of the gap between its initial condition and the origin. In these simulations the initial relative position is $\Delta z = -1m$. Thus, the time of response is read when $\Delta z = \pm 0.01m$.

Note the important gap between the time of response of the system with a DLAW or with a MRAW/EMRAW. With these last approaches the responses are certainly faster. In addition, this improvement does not come with an undesirable increase of the consumption.

Let us remind that the value representing the consumption is just the integral of the thrusters response with relation to the time, and not the actual consumption. These values are however proportional. Finally, it is important to understand that the performance criterium γ has not the same meaning in the DLAW case as in the EMRAW case. Hence the comparison is not relevant.

Remark 4.5. *Because of its simplicity, its efficiency in terms of time of response and its guaranteed stability domain the EMRAW structure arises as an interesting architecture for the anti-windup computation. However the initialization process for the associated algorithms is not trivial. In addition, the anti-windup compensator order is restricted to the order of the plant.*

Remark 4.6. *The full order DLAW presents fast and slow modes. These modes generate numerical problems for both LMI computation step (bad conditioning effects) and simulation step (numerical precision effects). Therefore, the fixed order DLAW is an interesting alternative to the full order one. Although some strategies are proposed in the literature, the choice of the A_{aw} poles is not strictly formalized.*

Remark 4.7. *Let us say a word on the static DLAW. Even if in Table 4.2 the static DLAW presents the worst values of all compensators, these values are not too much far from those obtained with other approaches. On the other hand, the static DLAW is easy to compute because of the associated LMIs simplicity. It is also easy to implement because it is simply a static gain. Therefore, a systematic procedure can be designed for the static DLAW computation.*

4.4 Attitude and relative position control

4.4.1 Attitude and relative position plant

The next relative control study case consists in a two satellites framework where the relative position in the z-axis is controlled like in Section 4.2, together with the attitude of one of the satellites (Satellite 2 in this model). The other satellite (Satellite 1) only presents a displacement in the linear z-axis and remains steady in its angular behavior.

The attitude dynamics, under the assumption of small angles, are described by the classical double integrator modelling [CNE05, Hug04]:

$$\ddot{\theta} = J_{Gi}^{-1} C_i \tag{4.4.1}$$

where J_{Gi} denotes the inertia matrix of satellite i at the center of mass and C_i the sum of the external torques applied on satellite i.

Relative position dynamics were described as a double integrator in Section 4.2.1. However, when the attitude is considered, the modelling (4.2.2) is modified. Because of the particular characterization of relative position sensors, the angular dynamics of Satellite 2 are coupled with the relative position dynamics [Gau07, PCU+05, WPK05].

The sensor providing the relative position is on-board of Satellite 2. This sensor measures the lateral distance with respect to Satellite 1 in Satellite 2 frame. This is the distance between the x_2-axis of Satellite 2 and its parallel intersecting the center of mass of Satellite 1 . This measurement is affected by the attitude[5] θ_y. Figure 4.9 illustrates the error on the relative measured position. Thus, the measured relative position error can be modelled by:

$$\Delta z_m = \Delta z + D \sin \theta_y \tag{4.4.2}$$

where the constant D is the intersatellite distance in the x-axis. $D = 250m$ in further simulations.

Remark 4.8. *The control of the relative position in the x-axis is performed by another control loop which is supposed to be perfect.*

Then, under the assumption of small angles, relation (4.4.2) becomes:

$$\Delta z_m = \Delta z + D\theta_y \tag{4.4.3}$$

Derivating twice (4.4.3) and using relationships (4.4.1) and (4.2.2), the measured relative position dynamics are described as follows:

$$\Delta \ddot{z}_m = \Delta \ddot{z} + D\ddot{\theta}_y = -m_2^{-1} F_2 + m_1^{-1} F_1 + D J_{G_2}^{-1} C_2 \tag{4.4.4}$$

Finally, (4.4.1) and (4.4.4) have to be concatenated to describe the angular and relative position dynamics:

$$\begin{cases} \dot{x}_p = A_p x_p + B_p u_p = \begin{bmatrix} 0 & 1 & 0 & 0 \\ 0 & 0 & 0 & 0 \\ 0 & 0 & 0 & 1 \\ 0 & 0 & 0 & 0 \end{bmatrix} \begin{bmatrix} \theta_y \\ \dot{\theta}_y \\ \Delta z \\ \Delta \dot{z} \end{bmatrix} + \begin{bmatrix} 0 & 0 & 0 \\ 0 & 0 & J_{G_2}^{-1} \\ 0 & 0 & 0 \\ m_1^{-1} & -m_2^{-1} & 0 \end{bmatrix} u_p \\ y_p = C_p x_p = \begin{bmatrix} 1 & 0 & 0 & 0 \\ D & 0 & 1 & 0 \end{bmatrix} x_p = \begin{bmatrix} \theta_y \\ \Delta z_m \end{bmatrix} \\ z_p = C_z x_p = C_p x_p = y_p \end{cases} \tag{4.4.5}$$

[5]No satellite marker subindex is inserted on the attitude as only Satellite 2 is controlled in attitude. However, rigorously, the correct notation should be θ_{y_2}.

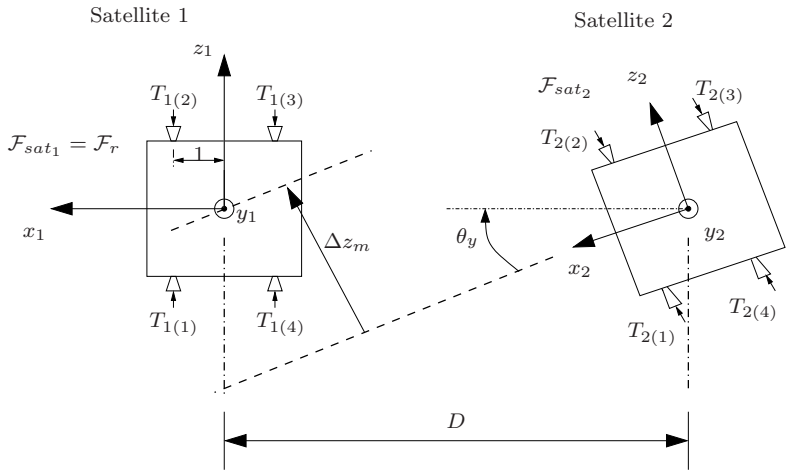

Figure 4.9: Relative position error generated by an attitude error.

where x_p is composed by the attitude θ_y, the angular velocity $\dot{\theta}_y$, the relative position Δz and the relative velocity $\Delta \dot{z}$. The control input is $u_p = [F_1 \;\; C_2 \;\; F_2]'$. The measured output y_p is composed by the attitude θ_y and the measured relative position Δz_m of Satellite 2. The regulated output z_p is indeed the measured output y_p.

4.4.2 Attitude and relative position controller

The controller computes the control output y_c. A centralized controller is used. A unique controller takes the measurements from all satellites in the formation and computes a vector y_c which contains the control output of each satellite.

The controller can be described through the state space representation given in (4.2.4).

In the relative position problem, the controller is a 2-input 3-outputs MIMO (Multiple Input Multiple Output) linear system whose state vector dimension is 6. The controller input is $u_c = y_p = [\theta_y \;\; \Delta z_m]'$ and the computed outputs are $y_c = [y_{c1} \;\; y'_{c2}]' = [F_{c1} \;\; [C_{c2} \;\; F_{c2}]]'$. $y_{c1} = F_{c1}$ (respectively $y_{c2} = [C_{c2} \;\; F_{c2}]'$) stands for the control output for Satellite 1 (respectively 2).

4.4.3 Attitude and relative position actuator model

The satellite formation is actuated by a propulsive system composed of 4 proportional thrusters on each of the two satellites. To apply the required control forces (F_1, C_2 and F_2) using this propulsive system, thrusters management functions have to be introduced in the control loop. These functions are composed by an allocation function that transforms the required control efforts $y_c = [F_{c1} \;\; [C_{c2} \;\; F_{c2}]]'$ into thrusters forces, and an influence

matrix that transform the thrusters outputs into forces applied on the system. Moreover, the actual forces delivered by each thruster are saturated. The general expression for the actuator is given by (4.2.5).

4.4.3.a The influence matrix

The influence matrix describes the geometric distribution of the thrusters. The physical distribution of the thrusters is presented in Figure 4.9. $M_1 \in \Re^{1\times 4}$ and $M_2 \in \Re^{2\times 4}$ are the influence matrices associated to Satellite 1 and Satellite 2 respectively. They are stated as follows:

$$M_1 = [1 \quad -1 \quad -1 \quad 1]; M_2 = \begin{bmatrix} 1 & -1 & -1 & 1 \\ -1 & 1 & -1 & 1 \end{bmatrix} \tag{4.4.6}$$

4.4.3.b Thruster saturation

The saturation function is modelled by (2.2.3). Saturation bounds for the attitude and relative position control problem are $\underline{u} = 0$ and $\bar{u} = 5mN$.

4.4.3.c Allocation function

Satellite 1 only controls its displacement. Thus, Satellite 1 control y_{c1} is single dimensional. The switching AF (4.2.7) takes the particular formulation given by (4.2.9) for Satellite 1.

On the other hand, Satellite 2 is able to control its displacement in the z-axis as well as its attitude in the y-axis. Then two control outputs are needed. In the switching AF (4.2.7) strategy the two components of the control output ($y_{c2(1)}$ and $y_{c2(2)}$) are treated piece-wise to compute two thrust vectors (T^1 and T^2). The final applied thrust is computed as the sum of these two. Therefore, the switching AF (4.2.7) takes the following formulation for Satellite 2:

$$f(y_c) = \begin{cases} T^k_{2(1)} = T^k_{2(4)} = \begin{cases} 0 & \text{if} \quad y_c < 0 \\ \frac{y_c}{2} & \text{if} \quad y_c \geq 0 \end{cases} \\ T^k_{2(2)} = T^k_{2(3)} = \begin{cases} 0 & \text{if} \quad y_c \geq 0 \\ \frac{y_c}{2} & \text{if} \quad y_c < 0 \end{cases} \\ T_{2(i)} = \sum_{k=1}^{2} T^k_{2(i)} \quad \forall i = 1, ..., 4. \end{cases} \tag{4.4.7}$$

Let us recall the notation used for $T^k_{j(i)}$ where i stands for the component index in the thrust vector, k for the considered control output component and j for the associated satellite.

Therefore, the actuator in the relative position control is modelled as follows:

$$u_p = Msat_{(0,\bar{u})}(f(y_c)) = \begin{bmatrix} M_1 & 0 \\ 0 & M_2 \end{bmatrix} sat_{(0,\bar{u})} \left(\begin{bmatrix} f_1(y_{c1}) \\ f_2(y_{c2}) \end{bmatrix} \right) \tag{4.4.8}$$

where $f_1(\cdot)$ (resp. $f_2(\cdot)$) is the allocation function of Satellite 1 (resp. 2).

Some other AF from those introduced in Section 2.4 are considered in the attitude and relative position problem. Satellite 1 presents a 1-dimension control output, thus only pseudo-inverse matrix based AF, given by (2.4.1), is considered. However, Satellite 2 presents a 2-dimension control output. Then AF (2.4.1) and AF (2.4.3) are not equivalent. Hence, these two additional AF are considered for Satellite 2.

Two possible alternative combinations are then considered for the pair $f_1(y_{c1})$-$f_2(y_{c2})$:

1. Both $f_1(y_{c1})$ and $f_2(y_{c2})$ are described by AF (2.4.1);
2. $f_1(y_{c1})$ is described by pseudo-inverse matrix AF (2.4.1) and $f_2(y_{c2})$ by the multi-sat AF (2.4.3).

In the first case the control input u_p takes the following expression:

$$u_p = \begin{bmatrix} M_1 & 0 \\ 0 & M_2 \end{bmatrix} sat_{(0,\bar{u})} \left(\begin{bmatrix} M_1^* y_{c1} \\ M_2^* y_{c1} \end{bmatrix} \right) \tag{4.4.9}$$

With the second combination the control input u_p reads:

$$u_p = \begin{bmatrix} M_1 sat_{(u_0)}(M_1^* y_{c1}) \\ M_2 sat_{(u_0)} \left(sat_{(u_0)}(M^*_{2(:,1)} y_{c2(1)}) + sat_{(u_0)}(M^*_{2(:,2)} y_{c2(2)}) \right) \end{bmatrix} \tag{4.4.10}$$

4.4.4 Attitude and relative position closed-loop model

With the plant (4.4.5), controller (4.2.4) and actuator (4.4.8) the closed-loop system describing the attitude and relative position control reads:

$$\begin{cases} \dot{x}_p = A_p x_p + B_p u_p = \begin{bmatrix} 0 & 1 & 0 & 0 \\ 0 & 0 & 0 & 0 \\ 0 & 0 & 0 & 1 \\ 0 & 0 & 0 & 0 \end{bmatrix} \begin{bmatrix} \theta_y \\ \dot{\theta}_y \\ \Delta z \\ \Delta \dot{z} \end{bmatrix} + \begin{bmatrix} 0 & 0 & 0 \\ 0 & 0 & J_{G_2}^{-1} \\ 0 & 0 & 0 \\ m_1^{-1} & -m_2^{-1} & 0 \end{bmatrix} u_p \\ y_p = C_p x_p = \begin{bmatrix} 1 & 0 & 0 & 0 \\ D & 0 & 1 & 0 \end{bmatrix} x_p = \begin{bmatrix} \theta_y \\ \Delta z_m \end{bmatrix} \\ \dot{x}_c = A_c x_c + B_c C_p x_p z_p = C_z x_p = C_p x_p = y_p \\ u_p = M sat_{(0,\bar{u})}(f(y_c)) = \begin{bmatrix} M_1 sat_{(0,\bar{u})}(f_1(y_{c1})) \\ M_2 sat_{(0,\bar{u})}(f_2(y_{c2})) \end{bmatrix} \\ y_c = C_c x_c + D_c C_p x_p \end{cases} \tag{4.4.11}$$

with $f_1(y_c)$ given by (4.2.9) and $f_2(y_c)$ by (4.4.7).

System (4.4.11) provides a benchmark for further simulations. However the non-linearities introduced by the AF (4.2.9) and (4.4.7) do not allow the computation of the anti-windup compensator for this system. This is why it is necessary to define another formulation for the system (4.4.11).

Two alternatives are proposed: taking u_p like in (4.4.9) and taking u_p like in (4.4.10). With u_p in (4.4.9) the attitude and relative position control loop reads:

$$\begin{cases} \dot{x}_p = A_p x_p + B_p u_p \dot{x}_c = A_c x_c + B_c C_p x_p \\ y_p = C_p x_p \\ z_p = C_z x_p \\ u_p = M sat_{(0,\bar{u})}(M^* y_c) = \begin{bmatrix} M_1 sat_{(0,\bar{u})}(M_1^* y_{c1}) \\ M_2 sat_{(0,\bar{u})}(M_2^* y_{c2}) \end{bmatrix} \\ y_c = C_c x_c + D_c C_p x_p \end{cases} \tag{4.4.12}$$

With u_p in (4.4.9) the closed-loop system reads:

$$\begin{cases} \dot{x}_p = A_p x_p + B_p u_p \dot{x}_c = A_c x_c + B_c C_p x_p \\ y_p = C_p x_p \\ z_p = C_z x_p \\ u_p = \begin{bmatrix} M_1 sat_{(u_0)}(M_1^* y_{c1}) \\ M_2 sat_{(u_0)}\left(sat_{(u_0)}(M_{2(:,1)}^* y_{c2(1)}) + sat_{(u_0)}(M_{2(:,2)}^* y_{c2(2)}) \right) \end{bmatrix} \\ y_c = C_c x_c + D_c C_p x_p \end{cases} \tag{4.4.13}$$

These alternative formulations allow the computation of the anti-windup compensator. All the anti-windups presented in Chapter 3 are computed for the system (4.4.12).

The presence of the multi-sat AF (2.4.3) in system (4.4.13) introduces nested saturations that change the stability conditions. An extension of Theorem 3.1 for the static DLAW computation adapted to the AF (2.4.3) is introduced in Appendix 3.1. Only the static DLAW is tested on system (4.4.13).

The responses obtained for the system (4.4.12) and system (4.4.13), together with their related anti-windup compensators, are compared to the response of the system (4.4.11) without anti-windup.

4.5 Anti-windup on the attitude and relative position control

The attitude and relative position control problem has been modelled. Then, the results from Chapter 3 are applied to synthesize an anti-windup compensator. For anti-windup computation purposes the closed-loop system (4.4.12) is considered. System (4.4.13) applies only to the static DLAW case.

Like in Section 4.3 the saturation function is asymmetric and influence matrix (4.2.6) satisfies the Lemma 2.4 conditions. Then the symmetrizing vector $N\zeta_{sym} = \bar{u}/2$ and the VKF (2.5.14) are considered to symmetrize the saturation.

Influence matrix (4.4.6) satisfies the Lemma 2.4 conditions. Like in the relative position case the symmetrizing vector $N\zeta_{sym} = \bar{u}/2$ is a suitable option for our study case. The VKF (2.5.14) is also considered to symmetrize the saturation while solving the problem of extra consumption (exposed in Section 2.5.3). Moreover, the function (2.5.15), for the influence matrix (4.4.6), verifies the VKF Definition 2.4 (proven in Section 2.5.5). Hence, function (2.5.15) is used in the simulations presented hereafter.

Being the saturation symmetrized, the closed-loop system (4.4.12) reads:

$$\begin{cases} \dot{x}_p = A_p x_p + B_p u_p \dot{x}_c = A_c x_c + B_c C_p x_p \\ y_p = C_p x_p \\ z_p = C_z x_p \\ u_p = M sat_{(u_0)}(M^* y_c) = \begin{bmatrix} M_1 sat_{(0,\bar{u})}(M_1^* y_{c1}) \\ M_2 sat_{(u_0)}(M_2^* y_{c2}) \end{bmatrix} \\ y_c = C_c x_c + D_c C_p x_p \end{cases} \tag{4.5.1}$$

with $u_0 = \frac{1}{2}5mN$.

Applying the symmetrizing techniques on the system (4.4.13) we obtain:

$$\begin{cases} \dot{x}_p = A_p x_p + B_p u_p \dot{x}_c = A_c x_c + B_c C_p x_p \\ y_p = C_p x_p \\ z_p = C_z x_p \\ u_p = \begin{bmatrix} M_1 sat_{(u_0)}(M_1^* y_{c1}) \\ M_2 sat_{(u_0)}\left(sat_{(u_0)}(M^*_{2(:,1)} y_{c2(1)}) + sat_{(u_0)}(M^*_{2(:,2)} y_{c2(2)})\right) \end{bmatrix} \\ y_c = C_c x_c + D_c C_p x_p \end{cases} \tag{4.5.2}$$

4.5.1 Anti-windup compensator synthesis

4.5.1.a Static DLAW synthesis

Given the expressions (4.5.1) and (4.5.2) Theorem 3.1, and its extension[6] to compute the static DLAW in both cases, may be applied. The theorem uses the optimization weights $[k_\gamma \;\; k_\rho] = [3 \;\; 1]$. The stability domain is maximized in the attitude direction θ_y, that is, $v = [1 \;\; 0 \;\; 0 \;\; 0 \;\; 0_{1\times 6} \;\; 0_{1\times 10}]'$. The D_{aw} obtained for the system (4.5.1) is given by:

$$D_{aw} = \begin{bmatrix} -50.76 & -50.76 & 50.76 & 50.76 & 0.96 & 0.69 & -0.96 & -0.69 \\ 6.2 & 6.2 & -6.2 & -6.2 & -0.29 & 0.1 & 0.29 & 0.1 \\ -71.87 & -71.87 & 71.87 & 71.87 & -0.19 & 2.56 & 0.19 & -2.56 \\ 0.62 & 0.62 & -0.62 & -0.62 & -89.39 & -105.12 & 89.39 & 105.12 \\ 222.68 & 222.68 & -222.68 & -222.68 & 7.01 & -16.37 & 7.01 & 16.37 \\ a & a & -a & -a & -b & -c & b & c \end{bmatrix} \tag{4.5.3}$$

where $a = 8.14 \cdot 10^4; b = 1.48 \cdot 10^3; c = 1.07 \cdot 10^3$. The D_{aw} obtained for the system (4.5.2) is given in Appendix A.4.1.

Note the difference between the first four columns and the last four columns in D_{aw} (4.5.3). The first four are related to Satellite 1 thrusters and the second set of columns are related to Satellite 2 thrusters. Observe that the first four values of each row are the same, while the last four are different. This is due to the fact that the second satellite thrusters have to generate two control outputs.

Remark 4.9. *Only the static DLAW has been considered when the multi-sat allocation function is used (system (4.5.2)) because the LMI complexity is increased by the introduction of extra saturation. The associated numerical problems only allow the consideration of this allocation function for the static case. Therefore no extensions for the dynamic DLAW have been given.*

[6] An extension of Theorem 3.1 for the static DLAW computation adapted for the multi-sat AF (2.4.3) is introduced in Appendix A.3.2.

4.5.1.b Dynamic DLAW synthesis

The next step is to increase the complexity of the anti-windup compensator by considering a dynamic system. The anti-windup compensator is then described by (3.3.3). Applying the results presented in Section 3.3 the dynamic DLAW is computed for the system (4.5.1).

Proposition 3.2 is used to compute a full order anti-windup compensator, that is $n_{aw} = n_M$. The computation is decomposed in two steps. The first consist in computing the full order DLAW. Using some of the poles calculated in this step the fix order Algorithm 3.1 is then applied.

The proposition 3.2 is applied with the optimization weight $[k_\gamma \quad k_\rho] = [3,\ 1]$. The stability domain is maximized in the attitude direction θ_y. Table 4.3 shows the poles of the full order dynamic DLAW, the poles of the linear closed-loop system A_l. The final selected poles for the fixed DLAW are marked with $*$. With the proposed choice of poles

Table 4.3: Full order DLAW eigenvalues in attitude and relative position control

$\text{eig}(A_{aw})(* \equiv selected)$	$\text{eig}(A_l)$
$-3.8 \cdot 10^2$	$(-3.54 \pm j4.85) \cdot 10^{-1}$
-77.4	$(-2.63 \pm j4.26) \cdot 10^{-1}$
-22.4	$(-1.06 \pm j9.86) \cdot 10^{-2}$
$-6.59 \pm j4.54$	$(-2.14 \pm j2.14) \cdot 10^{-2}$
$1.08 \pm j4.32$	$-1.48 \cdot 10^{-2}$
-1.63	$-3.71 \cdot 10^{-3}$
-0.99	
$-0.16 \pm j0.45$	
$(-8.82 \pm j11.8) \cdot 10^{-2}(*)$	
$-1.90 \pm j2.52 \cdot 10^{-2}(*)$	
$-2.88 \cdot 10^{-2}(*)$	
$-2.02 \cdot 10^{-2}(*)$	
$-1.03 \cdot 10^{-2}$	
$-4.55 \cdot 10^{-3}$	
$-2.92 \cdot 10^{-4}$	

Algorithm 3.1 is implemented. This time, the constraint forcing A_{aw} chosen eigenvalues to share the same order of magnitude of A_l eigenvalues is not applied. This is because a large order on the fixed order DLAW is not desired. Choosing too many poles can lead to numerical problems. Therefore 6 poles of A_{aw}, all centered in the range of A_l dynamics, were chosen.

4.5.1.c MRAW synthesis

The MRAW approach is characterized by the model of the plant. Hence the plant (4.4.5) matrices define the anti-windup compensator. On the other hand, the main difficulty in the MRAW synthesis is the definition of the stabilizing law v_1. The v_1 law (3.4.7) cannot be applied because the system is not modelled as a double integrator. A simple alternative consists in taking v_1 as a static feedback. However, this approach does not ensure global asymptotic stability but a local one. Nevertheless, it presents the advantages of not restricting the v_1 to a particular type of system. With these considerations v_1 is stated as follows:

$$v_1 = F_{aw} x_{aw} \tag{4.5.4}$$

The same notation as the EMRAW approach has been used because, indeed, the EMRAW approach is a MRAW with v_1 as a static feedback plus a static DLAW. Then the proposed MRAW is just the first part of the EMRAW.

The F_{aw} gain is tuned by trial and error like in the first part of Algorithm 3.3 (objective-based algorithm) in the EMRAW computation. After some iterations the best F_{aw} is attained. F_{aw} places the poles of $(A_p + B_p F_{aw})$ to $p_i = -0.04 \; \forall i = 1, .., 4$. This corresponds to a second order dynamics with natural frequency $w_n = 0.04 rad/s$ and damping $\zeta = 1$. Finally, the obtained gain F_{aw} is:

$$F_{aw} = \begin{bmatrix} 13.2 & 661 & -0.05 & -2.64 \\ 13.2 & 661 & -0.05 & -2.64 \\ -13.2 & -661 & 0.05 & 2.64 \\ -13.2 & -661 & 0.05 & 2.64 \\ -10.7 & -536 & 0.04 & 2.16 \\ -10.8 & -541 & 0.04 & 2.16 \\ 10.7 & 536 & -0.04 & -2.16 \\ 10.8 & 541 & -0.04 & -2.16 \end{bmatrix} \tag{4.5.5}$$

Given F_{aw} (4.5.5) and setting $E_{aw} = 0$ the Theorem 3.2 is applied to compute an estimation of the stability domain.

4.5.1.d EMRAW synthesis

Finally, the EMRAW is the last anti-windup compensator to be considered. The coordinate-descending algorithm (Algorithm 3.2) is initially applied to system (4.5.1) to compute the EMRAW gains. The performance-stability weights are set to $[k_\gamma \;\; k_\rho] = [3, 1]$. The stability domain is maximized in the attitude direction θ_y. The initialization of K_s is done by constraining the poles of $(\mathbb{A} + K_s \mathbb{C}_s)$ to be in the region of A_l. The ideal dynamics are given by: $A_{id} = diag(-0.05, -0.05)$ and $C_{id} = I_2$.

The computed gain E_{aw} and F_{aw} reads:

$$E_{aw} = \begin{bmatrix} -0.58 & -2.16 & 2.16 & 2.16 & 31.93 & 644.98 & -31.93 & -644.98 \\ 0.04 & 0.26 & -0.26 & -0.26 & -4.75 & -74.2 & 4.75 & 74.2 \\ 0.5 & 2.38 & -2.38 & -2.38 & -86.9 & -425.4 & 86.9 & 425.4 \\ 89.23 & 376.7 & -376.7 & -376.7 & -6890 & -10^5 & 6890 & 10^5 \\ -13.22 & -57.3 & 5.73 & 5.73 & 1390 & 1370 & -1390 & -1370 \\ a & b & -b & -b & -c & -d & c & d \end{bmatrix} \tag{4.5.6}$$

where $a = 1.75 \cdot 10^3; b = 7.68 \cdot 10^3; c = 1.52 \cdot 10^5; d = 1.99 \cdot 10^6$

$$F_{aw} = \begin{bmatrix} 8.5 & 3.46 \cdot 10^3 & -0.75 & -17.3 \\ 17.2 & -373.9 & -0.05 & 1.56 \\ -17.2 & 373.9 & 0.05 & -1.56 \\ -17.2 & 373.9 & 0.05 & -1.56 \\ -18.5 & -240 & 0.17 & 1.04 \\ -17.6 & -202.5 & 0.05 & 0.66 \\ 18.5 & 536 & -0.17 & -1.04 \\ 17.6 & 541 & -0.05 & -0.66 \end{bmatrix} \tag{4.5.7}$$

Then the EMRAW gains are tuned following the objective-based algorithm (Algorithm 3.3). The first part of Algorithm 3.3 consists in tuning F_{aw}. The best F_{aw} (4.5.5) has already been found in the MRAW approach. On the other hand, the second part of Algorithm 3.3) accounts for the computation of E_{aw}. After several iterations, the process is stopped with $[k_\gamma \;\; k_\rho] = [10^9, 1]$ and with a F^*_{aw} that yields a second order dynamics in to $A_p + B_p F^*_{aw}$ natural frequency $w_n = 4 rad/s$ and damping $\zeta = 1$. The ideal reference taken is the same as used in the coordinate-descending algorithm. The computed F_{aw} is given by (4.5.5) and E_{aw} is presented in Appendix A.4.2.

Remark 4.10. *When the Algorithm 3.2 is applied to compute the EMRAW the order of magnitude of the obtained gain E_{aw} is significantly high. Let us remind that the EMRAW structure is composed by a MRAW and a static DLAW. With this value of E_{aw} the DLAW part becomes dominant. For that reason the EMRAW computed with Algorithm 3.2 is essentially a static DLAW. These results are due to the difficulty in the algorithm initialization. With Conjecture 3.1 an initial K_s can be obtained which helps to find a feasible solution for the LMI problem. However we have observed an important sensitivity of the final result towards the initialization [PA01]. Further research is still needed to improve the initializing process.*

4.5.2 Simulations on the attitude and relative position control

The attitude and relative position control can now be simulated with the computed anti-windup compensators. However, as done previously for relative position control, a first simulation for the system (4.4.11) without anti-windup compensator is done.

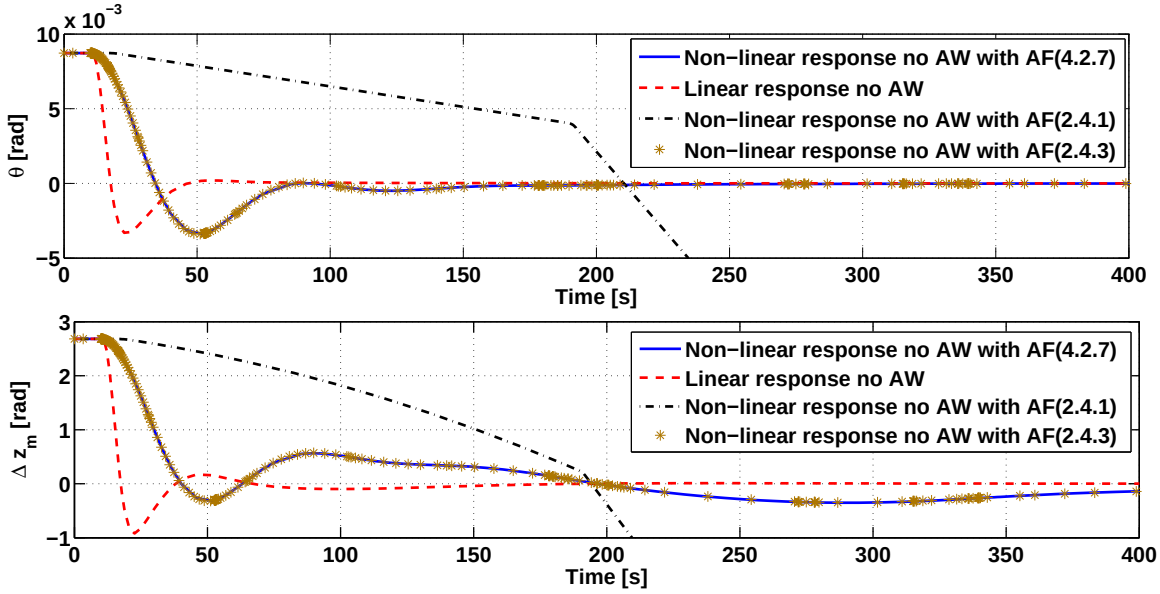

Figure 4.10: Temporal responses without anti-windup and different allocation functions.

Figure 4.10 presents the simulations of the attitude θ_y and the relative position Δz for an initial condition $x_p(0) = [\theta_y \quad \dot{\theta}_y \quad \Delta z \quad \Delta\dot{z}]' = [8.72 \cdot 10^{-3} \quad 0 \quad 0.5 \quad 0]'$ and $x_c = 0_{1\times 6}$. Given this intial conditions the initial mesured relative position is $\Delta z_m = 0.5 + 250 * 8.72 \cdot 10^{-3} = 2.68m$. Four responses are presented in Figure 4.10: the solid line describes the behavior of the system[7] (4.4.11), the dashed line presents system (4.4.11) response without saturation (i.e. the linear behavior), the dot-dashed line depicts the response of the system[8] (4.5.1) and finally the line of dots shows the system[9] (4.5.2) response.

Figure 4.10 illustrates the degradation of the system (4.4.11) response induced by the saturation. Observe that system (4.5.1) (with pseudo-inverse matrix AF (2.4.1)) is unstable. In Section 2.4.2, some simulations showed that the use of the AF (2.4.1) can destabilize a multi-variable system. On the other hand, system (4.5.2) (with multi-sat AF (2.4.3)) manages to recover the response obtained for the system (4.4.11) (with switching AF (4.4.7)).

Remark 4.11. *If one analyzes the matrix C_p in (4.4.5), one realizes that the θ_y dynamics influence the Δz measurement. As explained in Section 4.4.1, this is due to the sensor measurement characteristics. Consequently, the relative position is coupled with the attitude. On the contrary, the attitude is not influenced by Δz dynamics. Hence, the control strategy used in the synthesis of the linear controller consists in stabilizing first the attitude and then, once its influence is eliminated, in stabilizing the relative position as a decoupled variable.*

[7] Attitude and position control model considering the switching AF (4.4.7).
[8] Attitude and position control model considering the pseudo-inverse matrix AF (2.4.1).
[9] Attitude and position control model considering the multi-sat AF (2.4.3).

This control strategy can be observed in Figure 4.10. As in the non-linear response, the attitude converges before (around 200 seconds) the relative position (around 1000 seconds).

We recall that even if both systems do not have anti-windup compensators, their behaviors are strictly different. System (4.5.1), which uses a simple AF (the pseudo-inverse matrix AF), is unstable. On the other hand, system (4.5.2), which uses a complex but more efficient AF (the multi-sat AF), is stable. Therefore, one of the interests of this subsection is to analyze how these two systems react in the presence of an anti-windup compensator. Results depicting the different performances are given in Figure 4.11 and Figure 4.12.

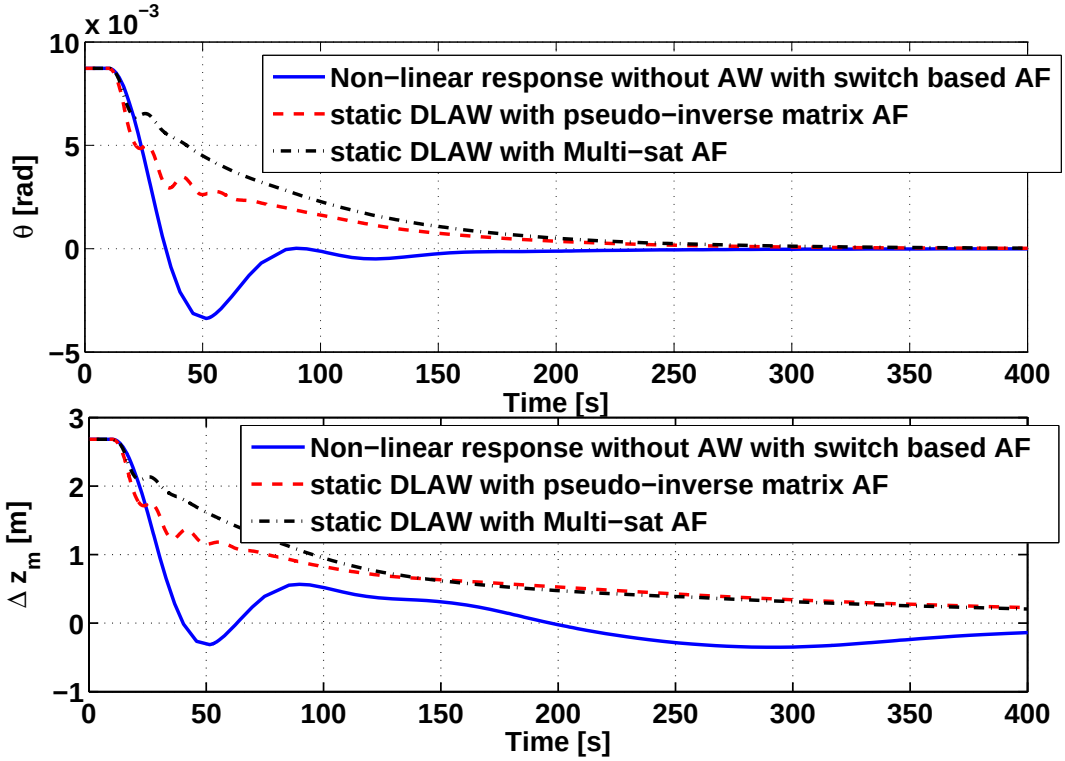

Figure 4.11: Temporal responses with DLAW and different allocation functions.

Figure 4.11 presents the attitude and the relative position for an initial condition $x_p(0) = [8.72 \cdot 10^{-3} \quad 0 \quad 0.5 \quad 0]'$. Both (4.5.1) and (4.5.2) systems have equivalent behaviors. The introduction of an anti-windup compensator in the control loop has *compensated* the limitation of the AF. On the other hand, stability domain results are given in Figure 4.12. Observe that system (4.5.1) has the largest stability domain. The non-linearities introduced by use of the multi-sat AF in system (4.5.2) add extra conservatism affecting the stability domain estimation.

Remark 4.12. • *Considering the aforementioned results the analysis of system (4.5.2) will be set aside. At the beginning of our researches the use of the multi-sat AF*

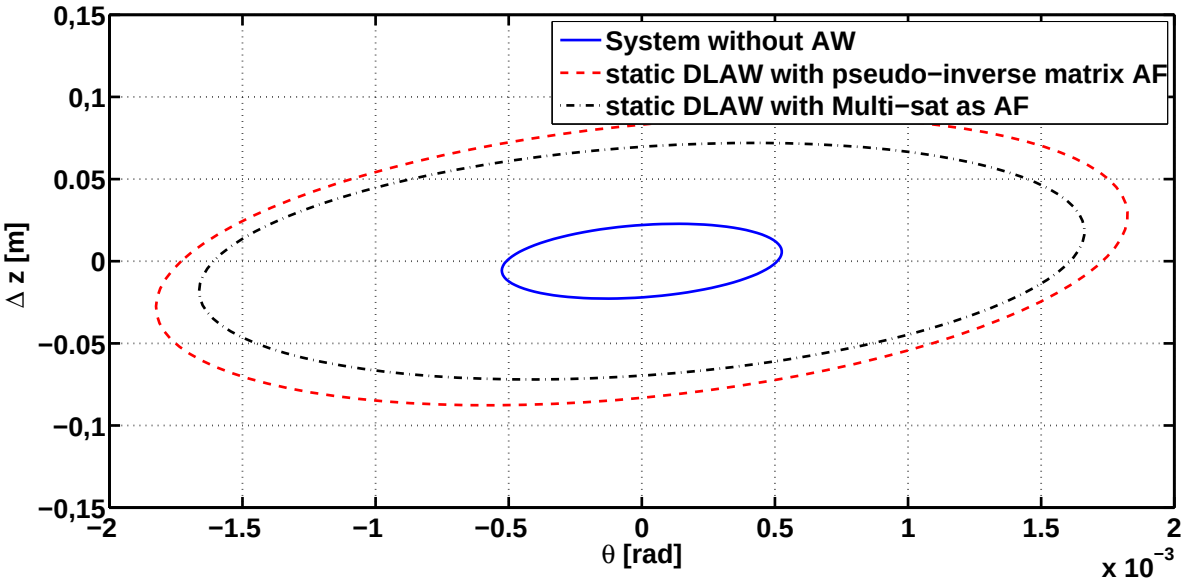

Figure 4.12: Stability domain with static DLAW and different allocation functions.

(2.4.3) *in the attitude and relative position control problem appeared to have a potential interest. However simulations show that with the anti-windup compensator in the loop no remarkable enhancements were obtained. Moreover, the LMI problem complexity is increased as well as the conservatism induced on the stability domain estimation.*

- *Then the question of the necessity of a complex and non-linear allocation function arises. It can suggest that in the presence of the anti-windup the difficult task of designing the allocation function may be avoided. Therefore, two options appear: to design an optimal allocation function that ensures the constrains for all the operational domain or to use a simple allocation function along with an anti-windup compensator. The optimal allocation functions have the disadvantage of presenting convergence problems in iterative approaches [NW99, Dur94a]. On the other hand, the anti-windup computation can be complicated for high order systems because of LMI solvers limitations [BcPS07].*

From now on only the closed-loop system[10] (4.5.1) is considered. For this system all the anti-windup compensators presented in Chapter 3 are simulated and compared. Figures given hereafter present simulations of system (4.5.1) with the following different anti-windup:

- static DLAW compensator (solid line);
- full order dynamic DLAW compensator (dashed line);

[10]System (4.5.1) is the closed-loop using the pseudo-inverse matrix AF (2.4.1).

- fixed order dynamic DLAW compensator (dot-dashed line);
- MRAW compensator with v_1 (4.5.4) (line with dots);
- EMRAW compensator computed with Algorithm[11] 3.3 (line with stars);
- EMRAW compensator computed with Algorithm[12] 3.2 (line with circles).

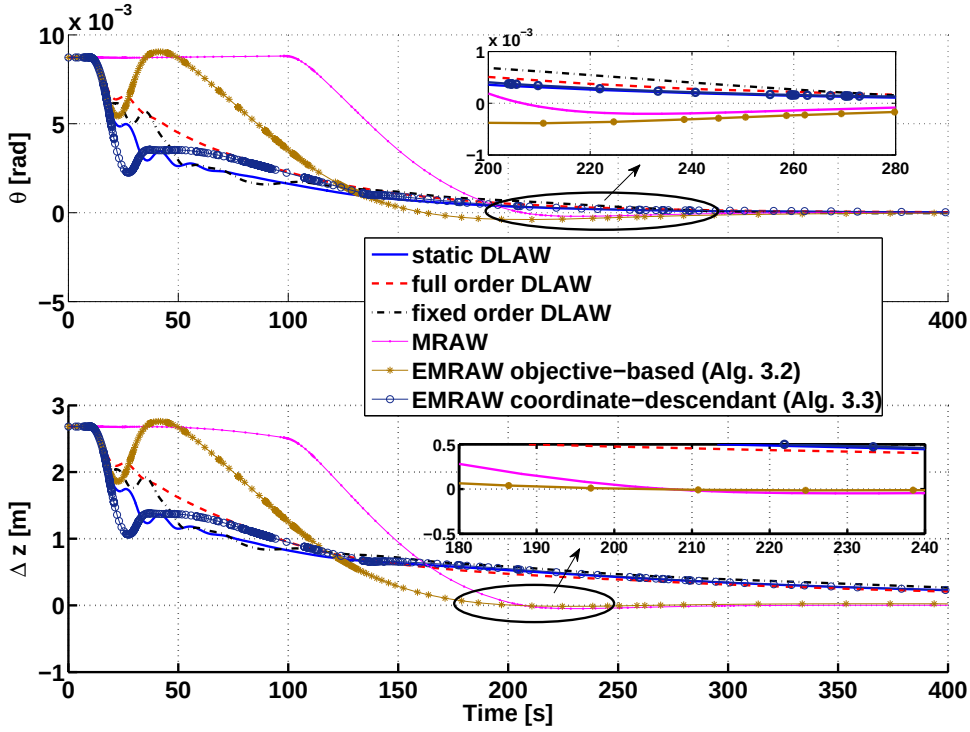

Figure 4.13: Attitude and relative position with several Anti-windup compensators.

Figure 4.13 presents the attitude and the relative position responses. An important characteristic stands out: The nature of the response in DLAW approach is completely different from the MRAW/EMRAW one.

In the DLAW case the attitude is the first state to converge followed by the relative position. This is the control strategy commented in Remark 4.11. Also notice that, as it has already advanced in the E_{aw} (4.5.6) gain analysis, as the EMRAW approach (computed with Algorithm 3.2) behaves like a DLAW.

Nevertheless, when the MRAW and the EMRAW (computed with Algorithm 3.3) are applied, the control stategy is changed: attitude and relative position converge simultaneously. This phenomenon sensitively reduces the time of response of the system as the relative position does not have to wait for the attitude to be controlled.

[11]Objective based algorithm.
[12]Coordinate-descending algorithm.

To undestand why the control strategy is changed with a MRAW/EMRAW several considerations have to be taken into account:

- the same thruster generates the torque and the force to control both θ_y and Δz;
- the stabilizing feedback v_1 introduces modifications in the thrusters;
- from MRAW/EMRAW state matrix definition, the signal v_1 is related to θ_y and Δz dynamics.

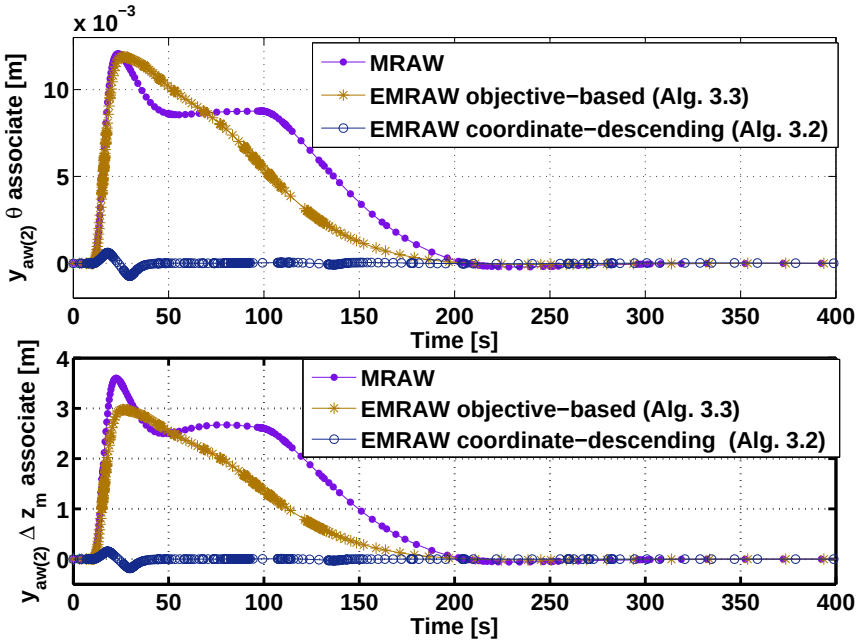

(a) y_{aw} response for MRAW/EMRAW approaches

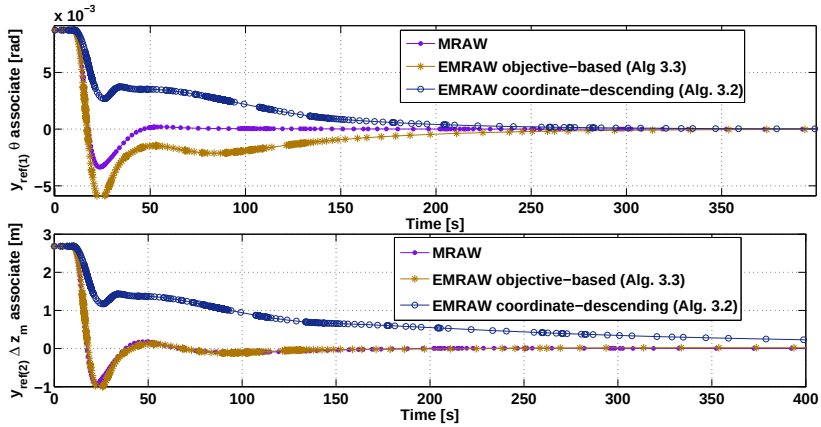

(b) y_{ref} response for MRAW/EMRAW approaches

Figure 4.14: y_{aw} and y_{ref} responses for MRAW/EMRAW approaches

A signal v_1 depending on θ_y and Δz is added to the thrusters . Additionally, thrusters control simultaneously both θ_y and Δz. Then, a coupling attitude over relative position

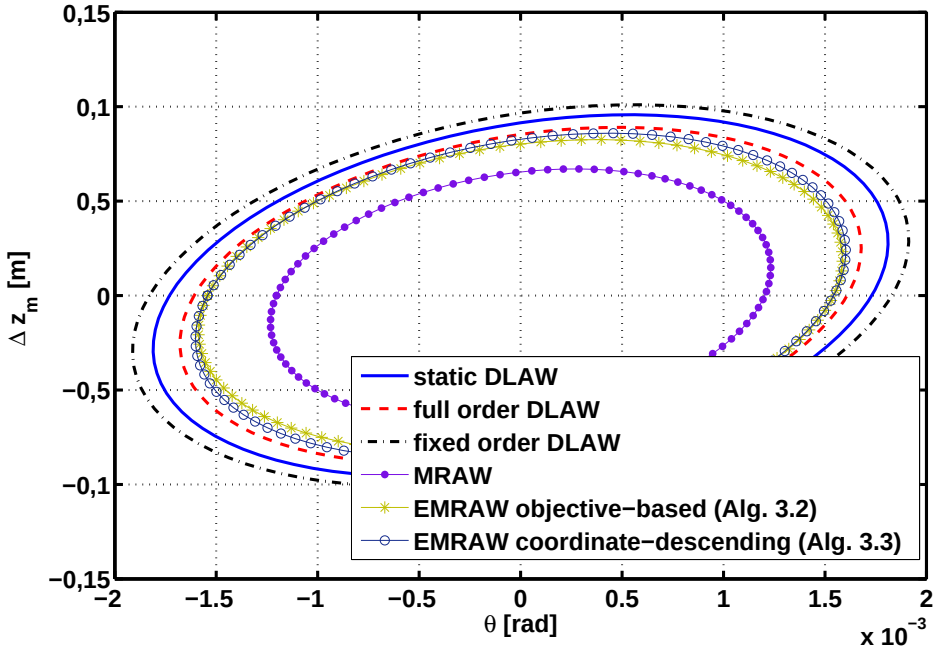

Figure 4.15: Stability domain with several anti-windup compensators.

is introduced and viceversa. Finally, v_1 exploits thrusters control capacity to steer θ_y and Δz simultaneouly.

Remark 4.13. *In conclusion, the feedback v_1 generates a coupling relative position over the attitude in addition to the existent coupling attitude over relative position. This induced coupling allows us to exploit the thrusters capacity to simultaneously control the plant states. Therefore, the system response is significantly improved.*

In Figure 4.13 the response obtained with the MRAW is slightly faster than the one obtained with EMRAW (EMRAW from Algorithm 3.3). An explanation to this behavior is found in Figure 4.14 where the anti-windup output y_{aw} and the reference signal y_{ref} are compared for the different anti-windup compensators. Before drawing any conclusion it is important to understand that even if the system performance is a trade-off between the convergence time and reference quality, the contribution of the last variable will have a stronger importance in the final system performance. With this in mind MRAW appears as a best solution in Figure 4.13 because it has a slightly slower convergence time of y_{aw}, but faster reference signal y_{ref}.

The EMRAW has extra degrees of freedom thanks to the E_{aw} gain which may improve y_{ref} response. However, this time the reference presented for the MRAW was the best reference we can obtain. Therefore, there is not actual necessity of the E_{aw} gain. The only advantage of the EMRAW with respect the MRAW is the enhancement of the stability domain estimation presented in Figure 4.15.

Table 4.4: Summary values on the attitude and relative position control

	Static DLAW	full order DLAW	fixed order DLAW
$\theta_{y_{max}}(0)$ $[rad]$	$1.73 \cdot 10{-}3$	$1.85 \cdot 10{-}3$	$1.62 \cdot 10{-}3$
$\Delta z_{max}(0)$ $[m]$	0.93	0.98	0.84
θ_y Time of response $[s]$	300	330	290
Δ Time of response $[s]$	980	970	990
Consumption with (2.5.14)$[Ns]$	3.93	3.11	3.22
Consumption with (2.5.15)$[Ns]$	3.80	3.08	3.21
AW Order	0	20	6
	MRAW	EMRAW Alg. 3.2	EMRAW Alg. 3.3
$\theta_{y_{max}}(0)$ $[rad]$	$1.21 \cdot 10{-}3$	$1.55 \cdot 10{-}3$	$1.55 \cdot 10{-}3$
$\Delta z_{max}(0)$ $[m]$	0.63	0.82	0.81
θ_y Time of response $[s]$	290	330	320
Δ Time of response $[s]$	290	980	300
Consumption with (2.5.14)$[Ns]$	3.51	3.96	3.43
Consumption with (2.5.15)$[Ns]$	3.50	3.94	3.41
AW Order	4	4	4

Table 4.4 summarizes the main values characterizing the previously tested anti-windup compensators. The presented values are listed as follows:

- the maximal admissible initial condition for the attitude $\theta_{y_{max}}(0)$;
- the maximal admissible initial condition for the relative position $\Delta z_{max}(0)$;
- the *time of response* for θ_y in seconds;
- the *time of response* for Δz in seconds;
- the integral of the thrust response as related value to the *consumption* with (2.5.14) as VKF;
- the integral of the thrust response as related value to the *consumption* with (2.5.15) as VKF;
- the *order* of the anti-windup (AW) compensator.

The time of response is an interesting value for comparison purposes. It has been defined as the time when the response reaches the 99% of the gap between the initial condition and the origin. In these simulation $\theta_y = \pm 8.72 \cdot 10^{-5} rad$ and $\Delta z = \pm 0.027 m$.

There is an important difference between the time of response of the system with a DLAW and the one with a MRAW/EMRAW. With these last approaches the response of the relative position is certainly faster. Moreover this improvement does not come with

an increase on the consumption. Let us notice that the difference on the consumption when (2.5.14) or (2.5.15) are applied it is not as important as we expected (related to comparison done in Section 2.5.5).

Remark 4.14. *Both MRAW and EMRAW approaches present the interesting capacity to converge the states of the plant at the same time. Their structure exploits the capacity for the thrusters as unique control of both attitude and relative position. Consequently, these methods arise as an interesting anti-windup structure to control MIMO systems under thrusters saturation.*

4.6 16 state formation control

4.6.1 16 state formation plant

The final plant model consists in a 8-DOF two satellites formation. Two satellites are controlled in three possible rotations plus two relative positions.

The full plant is a sixteen state model with a state vector x_p composed by as follows:

- Three inertial attitudes θ_{x_1}, θ_{y_1}, θ_{z_1} and their derivatives for Satellite 1.
- Three inertial attitudes θ_{x_2}, θ_{y_2}, θ_{z_2} and their derivatives for Satellite 2.
- Two relative positions, the first one in the z-axis Δz and the second one in the y-axis Δy, and their derivatives.

Remark 4.15. *The control of the relative position in the x-axis Δx is performed by another control loop which is supposed to be perfect.*

Showing the 3-D figure representing all the states would be more confusing than helpful. Refer to Figures 4.2 and 4.9 for a geometric representation of the states variables.

All these states are controlled with eight control inputs u_p. Those are:

- Two lateral forces F_{y_1} and F_{z_1} on the y-axis (resp. z-axis) performed by Satellite 1.
- Three torques, C_{x_1}, C_{y_1} and C_{z_1} performed by Satellite 1.
- Three torques, C_{x_2}, C_{y_2} and C_{z_2} performed by Satellite 2.

Finally the measured output y_p, which is in feedback with the controller, consists of eight signals which are:

- The two relative positions, Δy and Δz;
- The three inertial attitudes, θ_{x_1}, θ_{y_1} and θ_{z_1}, of Satellite 1;
- The three relative attitudes of Satellite 2 with respect to Satellite 1, that is, $\theta_{x_{12}}$, $\theta_{y_{12}}$ and $\theta_{z_{12}}$.

The 16-state plant representation can be described by the following equations:

$$\begin{cases} \dot{x}_p &= A_p x_p + B_p u_p \\ y_p &= C_p x_p \end{cases}$$

where matrices A_p, B_p and C_p are given in Appendix A.5.1.

4.6.2 16-state formation controller

In the 16-state formation control the state space representation (4.2.4) holds. The controller is a 8-input 8-output MIMO linear system whose state vector dimension is 32.

4.6.3 16-state formation actuator

The forces controlling the satellite formation are performed by an actuator that is based on a propulsive system. The general expression for the actuator is given by (4.2.5).

4.6.3.a The influence matrix

The 16-state formation is controlled with an 8-thruster configuration for each satellite. However, the influence matrices for each satellite do not have the same dimension. Satellite 1 controls its rotations and its longitudinal motion while Satellite 2 only controls its rotations. Influence matrices $M_1 \in \Re^{5\times 8}$ and $M_2 \in \Re^{3\times 8}$ are associated to Satellite 1 and Satellite 2 respectively. The physical distribution of the thrusters on a satellite is presented in Figure 4.9. Their numerical values are given in Appendix A.5.2

4.6.3.b Thruster saturation

The saturation function is modelled by (2.2.3). The saturation bounds for the relative position control problem are $\underline{u} = 0$ and $\bar{u} = 150\mu N$.

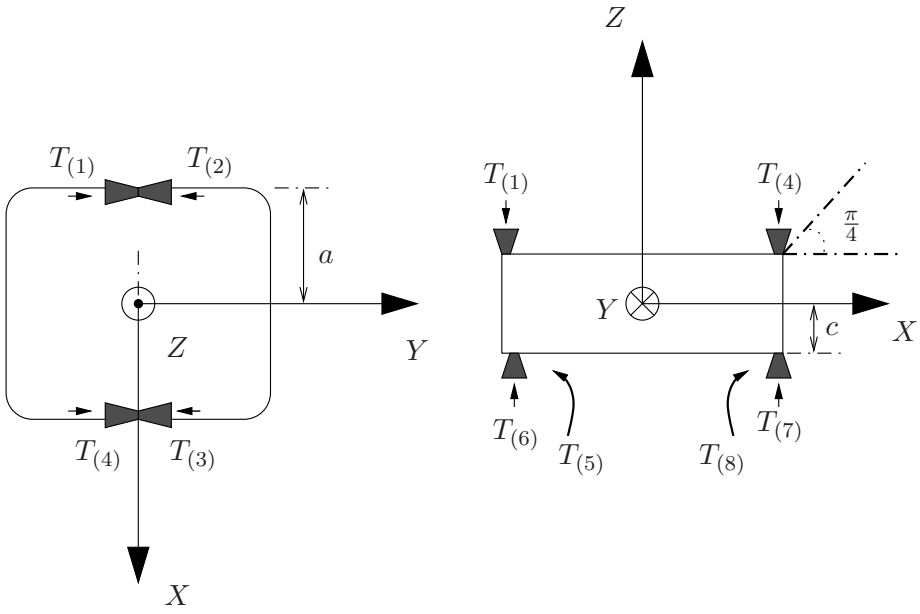

Figure 4.16: Geometric distribution of the thrusters for a 8-DOF control configuration.

4.6.3.c Allocation function

The 16-state formation presents two satellites whose AF is given by (4.2.7). The implemented AF is similar to the one used in example (4.4.7). Only the index values of $T^k_{j(i)}$ are given for both satellites. The values are $j = 2$ (two satellites), $i = 8$ (8 thrusters by satellite) and $k = 5$ for Satellite 1 and $k = 3$ for Satellite 2.

In the 16-state formation control the pseudo-inverse matrix based AF given by (2.4.1) is also considered as allocation function for both satellites.

4.6.4 16-state formation closed-loop

The 16-state closed-loop system can be described with a generic state space formulation:

$$\begin{cases} \dot{x}_p = A_p x_p + B_p u_p \\ \dot{x}_c = A_c x_c + B_c C_p x_p \\ y_p = C_p x_p \\ u_p = Msat_{(0,\bar{u})}(f(y_c)) \\ y_c = C_c x_c + D_c C_p x_p \end{cases} \tag{4.6.1}$$

Two formulations of system (4.6.1) will be simulated. The first one considers the switching based AF given in (4.2.7). This system formulation is tested without anti-windup compensator. The second one considers the pseudo-inverse matrix based AF given in (2.4.1). This system formulation is tested with anti-windup compensator.

4.7 Anti-windup on a 16 states formation control

In this section, the computation of the anti-windup compensator for the system (4.6.1) have been pretended. However, because of the dimension of the problem no solution for the LMI problem has been obtained. Therefore, both DLAW and EMRAW have not been computed. According to the messages[13] obtained from the LMI solver we suppose that the LMI could be solved using a different LMI solver or a more powerful computer, at least the static DLAW.

Despite the numerical problems the MRAW approach could be tested. As previously done for the attitude and relative position problem v_1 has been set as a static feedback:

$$v_1 = F_{aw} x_{aw} \tag{4.7.1}$$

The gain has been tuned in order to place the 16 poles of $(A_p + B_p F_{aw})$ at $p_i = -0.04$ $\forall i = 1, .., 16$. This implies that the modes of the anti-windup loop have been set at a natural frequency $\omega_n = -0.04$ and damping $\zeta = 1$. This tuning can be obviously improved but we just want to show the potential of the technique through a quick and simple tuning.

4.7.1 Simulations on the 16 state formation

Two formulations of system (4.6.1) are tested. First, the switching AF (4.2.7) is considered without anti-windup compensator. Second, the pseudo-inverse matrix AF (2.4.1) is taken with anti-windup compensator. The plant (4.6.1) (with AF (2.4.1)) has been simulated with the MRAW.

Figure 4.17 shows the time of response of the relative positions (Δz, Δy), Satellite 1 attitudes (θ_{x_1}, θ_{y_1}, θ_{z_1}) and the relative attitudes ($\theta_{x_{1_2}} = \theta_{x_1} - \theta_{x_2}$, $\theta_{y_{12}} = \theta_{y_1} - \theta_{y_2}$, $\theta_{z_{12}} = \theta_{z_1} - \theta_{z_2}$) for the following initial condition:

$$\begin{array}{l} \Delta y = \Delta z = 0.01m \\ \theta_{x_1} = \theta_{y_1} = \theta_{z_1} = 4.85 \cdot 10^{-5} rad = 10'' \\ \theta_{x_{12}} = \theta_{y_{12}} = \theta_{z_{12}} = 4.85 \cdot 10^{-5} rad = 10'' \end{array} \tag{4.7.2}$$

Remark 4.16. *All the initial time-derivative are set to zero.*

Three kinds of behaviors are shown in Figure 4.17: the linear one in solid line (i.e. system (4.6.1) without saturation), the non-linear one without anti-windup compensator and the non-linear one with the MRAW.

In Figure 4.17a the relative position responses are presented. The relative position responses with the MRAW are faster than the responses obtained without anti-windup.

[13] Matlab run out of memory.

However Figures 4.17b and 4.17c depicts a loss of performance on the attitude when the MRAW is used with respect the non-linear response without anti-windup. The MRAW introduces a coupling between the different state variables like in the attitude and relative position control case. With the MRAW all the states converge to the origin simultaneously. Previously a loss of performance on the attitude responses when the MRAW is applied has been commented. With a more judicious tuning of F_{aw} this problem could be avoided.

The 16 state plant system has been simulated again but this time the initial conditions given in (4.7.2) is three times larger, that is: Figure 4.18 shows how the system remains stable for the initial conditions (4.7.3) when the MRAW is in the control loop while it diverges without it. Therefore, the MRAW guarantees the stability for larger initial conditions than the system without anti-windup.

$$\begin{aligned} &\Delta y = \Delta z = 0.03m \\ &\theta_{x1} = \theta_{y1} = \theta_{z1} = 14.54 \cdot 10^{-5} rad = 30'' \\ &\theta_{x_{12}} = \theta_{y_{12}} = \theta_{z_{12}} = 14.54 \cdot 10^{-5} rad = 30'' \end{aligned} \tag{4.7.3}$$

In conclusion, despite of the numerical problems that prevented us from computing the majority of the anti-windup compensators, the MRAW has allowed us to show, in a high order problem, the advantage of the anti-windup compensator. Moreover, the MRAW has appeared again as an interesting approach to control MIMO systems under thruster saturation.

4.8 Conclusion

Anti-windup compensator design represents the core of this manuscript. In this chapter the different anti-windup compensators have been tested into several study cases.

Initially the relative position control system has been taken as a study case. The closed-loop system modelling this control problem is initially provided. The simplicity of the system has allowed the characterization of the main features of the anti-windup compensators. The simulation have arisen the interest of the EMRAW approach.

Then the attitude and relative position control system has been tackled as a study case. Again, first the modelling of the control loop has been given. This application presents the particularity of being a multi-variable system with a coupling of the attitude over the relative position. First one has realized that the presence of an anti-windup compensator may save the allocation function definition phase. Then, the MRAW and the EMRAW approaches have been appeared as a performing approaches to control both attitude and relative position as the states converges simultaneously.

Finally, a high order system controlling relative position and attitudes (absolute and

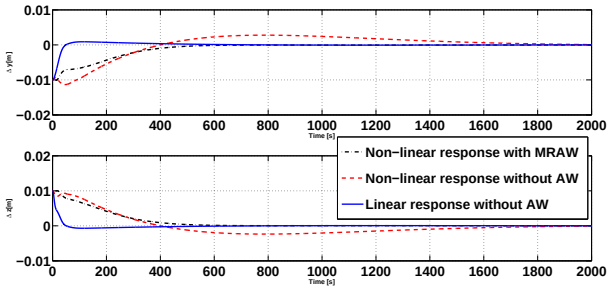

(a) Relative position responses

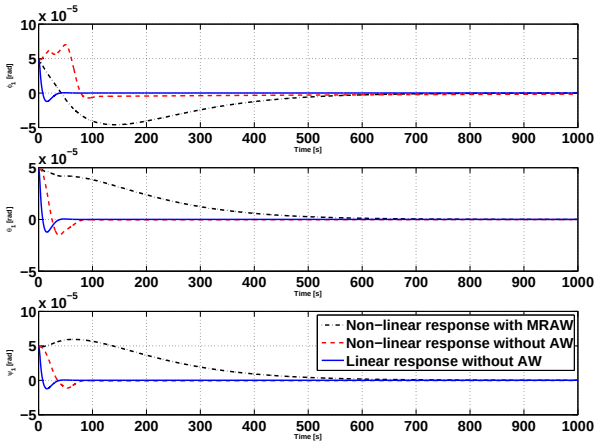

(b) Satellite 1 attitudes responses

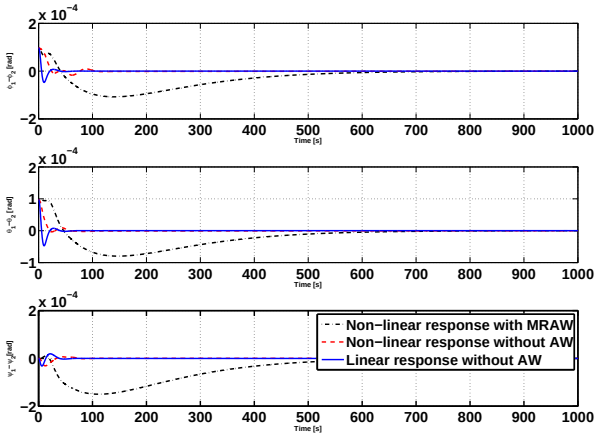

(c) Relative attitude response

Figure 4.17: 16-state formation outputs responses

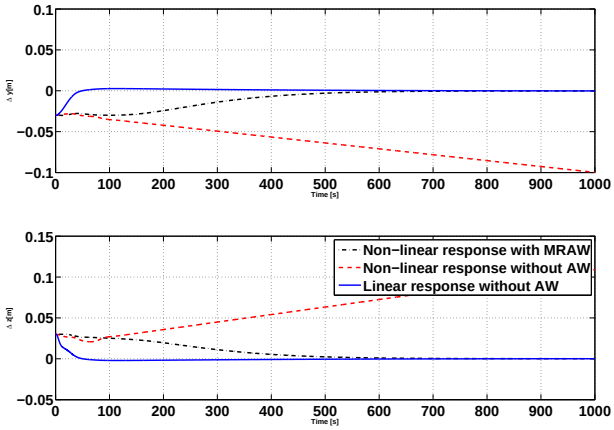

(a) Relative position responses

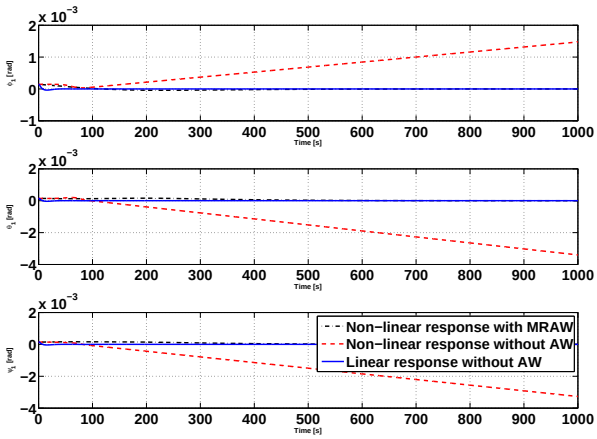

(b) Satellite 1 attitudes responses

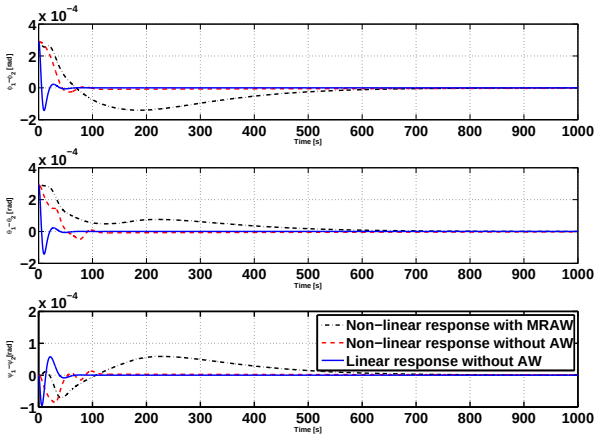

(c) Relative attitude responses

Figure 4.18: 16-state formation outputs with an unstable initial condition.

relative) of two satellites have been considered. Unfortunately, the LMI complexity has not allow us to compute the DLAW and EMRAW compensators. However, the MRAW has been tested and interesting results, even with a poor tuning, have been shown.

Chapter 5

Drag-free control

Outline of the chapter

5.1 Introduction

A particular case of continuous short range thrusters use is in drag-free control[PHS06], where one controls directly the acceleration and the attitude instead of the relative position plus the attitude. Drag-free missions may be composed of a satellite formation [PHS06] or by a unique satellite [PPT+05]. This chapter is focused on a one-satellite linear acceleration control (the attitude control is similar to the formation flying issue

tackled in Chapter 4). The benchmark of the chapter is the CNES [1] mission Microscope [PPT+05].

First in Section 5.2 a modelling of the linear acceleration control problem is given. A particular attention has to be paid to the modelled plant. Only the control of the acceleration is considered. Then the plant presents a characteristic model that may be exploited for anti-windup purposes.

In the second part of this chapter, constructive methods for the anti-windup computation are given. In Section 5.3, LMI conditions are given on the static DLAW case. These results are similar to those presented in Chapter 3. The main contribution on the drag-free control is the definition of the *trivial* anti-windup compensator presented. The formulation of this anti-windup providing global asymptotic stability is presented in Section 5.3.2.

Finally, in Section 5.4, the control of one-axis one-satellite acceleration is simulated with the trivial anti-windup compensator. Results are compared to the system without anti-windup.

5.2 Drag-free modelling

Drag-free control consists of controlling both attitude and acceleration. In this simplified case only the acceleration control is considered. For this particular control problem some particular characteristics can be exploited for anti-windup synthesis purposes.

The control objective is to reject the external disturbances in order to keep a null acceleration. Although the mission consists of a satellite formation or of a simple satellite, the common point is that this type of missions have to perform an action on the longitudinal axis. Hence a propulsive system is used as actuator. Therefore, the actuator modelled by the asymmetric saturation, the influence matrix and the allocation function presented in Chapter 2 applies.

Similarly to the other problems considered in this thesis, a linear controller is given satisfying the stability of the linear closed-loop system.

5.2.1 Drag-free plant model

Let us consider a satellite and a frame fixed to it. $\mathcal{F}_{sat}$ is the satellite associated frame. From the third theorem of the rigid body dynamics, the acceleration of a rigid body is

[1] Centre National d'Etudes Spatiales.

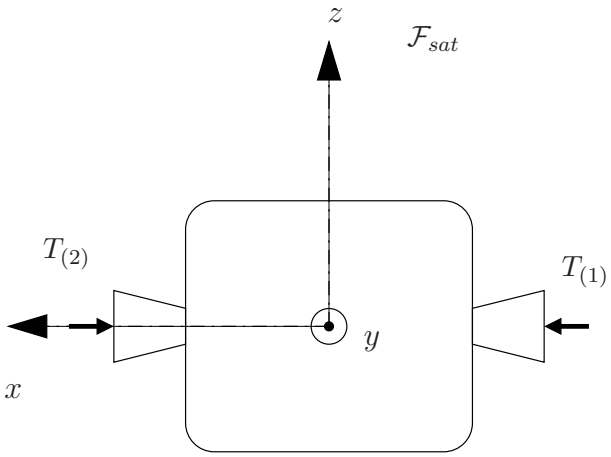

Figure 5.1: Drag-free control configuration.

proportional to the sum of external forces:

$$\ddot{x} = m^{-1} \sum_{G} (F) \tag{5.2.1}$$

where $\ddot{x}$ is the acceleration in the x-axis, m is the mass of the satellite and $\sum_G(F)$ is the sum of the external forces at the center of mass.

The interesting point of this system is that the variable to regulate $z_p = \ddot{x}$ is proportional to the control input $u_p = \sum_G(F)$. Then the plant is simply a direct transmission between the control input and the regulated output. The system can be described by space state representation where the state vector x_p is empty, $A_p = []$, $B_p = []$ and $C_p = []$ are empty matrices:

$$y_p = D_p u_p = m^{-1} F \tag{5.2.2}$$

where $F = \sum_G(F)$ and $m = 191.1kg$ (data taken from [PPT+05]).

Therefore the plant (5.2.2) is exponentially stable, even more, no dynamics are associated as it is simply a static gain. This situation can be exploited in terms of anti-windup design as it will be described later.

5.2.2 Drag-free controller

The drag-free problem controller is described as a 4-dimension SISO linear system. Then the generic state space representation applies:

$$\begin{cases} \dot{x}_c = A_c x_c + B_c u_c \\ y_c = C_c x_c + D_c u_c \end{cases} \tag{5.2.3}$$

The matrices numerical values are omitted but given in [PPT+05]. The controller input is $u_c = y_p$ and computes the force to control the acceleration $y_c = F_c$.

5.2.3 Drag-free actuator model

The actuator is composed by a two thrusters propulsive system. The physical distribution of the thrusters is presented in Figure 5.2.2. This information is contained in the influence matrix $M = [1 \quad -1]$.

The thrusters limitation is modelled by the saturation function (2.2.3). The saturation bounds for the drag-free control problem are $\underline{u} = 0$ and $\bar{u} = 150\mu N$.

The allocation function given by (2.4.1), based on the pseudo-inverse matrix is considered for the drag-free problem.

Summing up, the actuator in the relative position control is modelled as follows:

$$u_p = Msat_{(0,\bar{u})}(M^* y_c) \tag{5.2.4}$$

5.2.4 Drag-free closed-loop

The closed-loop system representing the drag-free control problem is easily written with the plant model (5.2.2), the controller (5.2.3) and the actuator (5.2.4):

$$\begin{cases} y_p = D_p u_p \\ \dot{x}_c = A_c x_c + B_c y_p \\ y_c = C_c x_c + D_c y_p \\ u_p = Msat_{(0,\bar{u})}(M^* y_c) \end{cases} \tag{5.2.5}$$

Replacing the saturation function by the dead-zone function (1.3.4), the closed-loop system (5.2.5), with some mathematical work, can be expressed as follows:

$$\begin{cases} \dot{\xi} = \mathbb{A}\xi + \mathbb{B}\phi_{(0,\bar{u})}(\nu) \\ \nu = \mathbb{C}\xi + \mathbb{D}\phi_{(0,\bar{u})}(\nu) \end{cases} \tag{5.2.6}$$

where $\xi = x_c$, $\mathbb{A} = A_c + B_c D_p \Delta^{-1} C_c$, $\mathbb{B} = -B_c D_p \Delta^{-1} M$, $\mathbb{C} = M^* \Delta^{-1} C_c$, $\mathbb{D} = -M^* \Delta^{-1} D_c D_p M$ and $\Delta = (I - D_c D_p)$.

Remark 5.1. *The plant is a direct transmission and, as consequence, there are nested saturations.*

Remark 5.2. *Notice that the only element of the control-loop which participates in the closed-loop dynamics is the controller. Indeed, if one changes the roles of the elements in the closed-loop, then the system can be seen as a dynamic system (the controller) which is controlled with a static feedback (the plant) with a sensor (the actuator) saturation.*

In any case this problem cannot be considered as a general sensor saturation problem [TT06] because the measure (the controller output) is known.

5.3 Anti-windup Computation for a drag-free problem

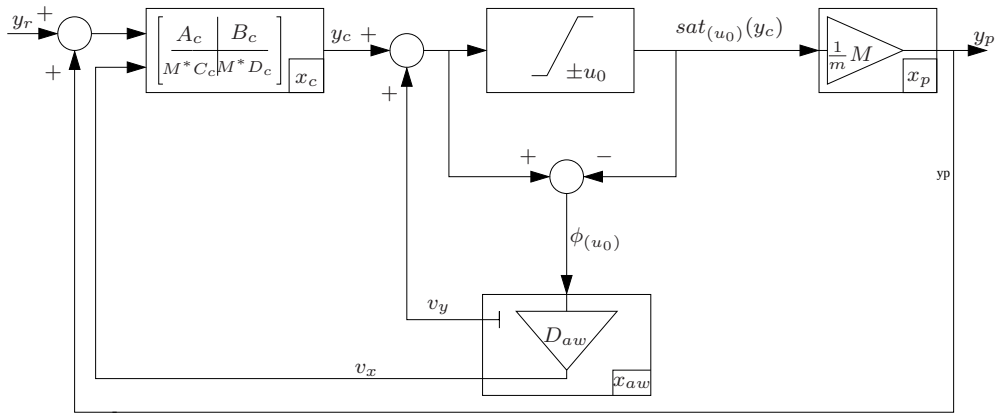

Figure 5.2: Anti-windup structure for a drag-free configuration

The next section deals with the anti-windup problem on a drag-free configuration. The block diagram describing the problem tackled is presented in Figure 5.2.

Remark 5.3. *The control objective is set up with* $y_r = 0$ *in Figure 5.2.*

Only the static Direct Linear Anti-Windup (DLAW) is considered. The static DLAW is enough to show the particularities of the anti-windup compensator on this application case.

First, LMI conditions are recalled for the computation of the static DLAW. Then, the existence of a *trivial* anti-windup compensator is shown.

5.3.1 Anti-windup synthesis

A static Direct Linear Anti-Windup (DLAW) is introduced in the system (5.2.6). However, the anti-windup computation process applies on symmetric saturation, therefore, we first

apply the techniques on Chapter 2. u_0 denotes the symmetric saturation bound obtained from the symmetrizing process. In the drag-free problem case $u_0 = \bar{u}/2 = 75\mu N$. Finally, the resultant closed-loop system with the anti-windup compensator reads:

$$\begin{cases} \dot{\xi} = \mathbb{A}\xi + \mathbb{B}\phi_{(u_0)}(\nu) + v_x \\ \nu = \mathbb{C}\xi + \mathbb{D}\phi_{(u_0)}(\nu) \\ v_x = \mathbb{B}_v D_{aw}\phi_{(u_0)}(\nu) \end{cases} \tag{5.3.1}$$

where $\mathbb{B}_v = I_{n_c}$.

Let us recall the notation $n = n_p + n_c + n_{aw}$ where $n_p = 0$, $n_c = 4$ and $n_{aw} = 0$ are the order of the plant, the controller and the anti-windup compensator respectively. The number of thruster is denoted $m = 2$.

Finally, a proposition with respect to the system (5.3.1) can be stated:

Proposition 5.1. *If there exists a symmetric positive-definite matrix $W \in \Re^{n\times n}$, a diagonal positive-definite matrix $S \in \Re^{m\times m}$, a matrix $Y \in \Re^{m\times n}$ and a matrix $Z \in \Re^{n_c\times m}$ satisfying min ρ s.t.*

$$\begin{bmatrix} W\mathbb{A}' + \mathbb{A}W & \mathbb{B}S + \mathbb{B}_v Z + Y' \\ * & -2S + \mathbb{D}S + S\mathbb{D}' \end{bmatrix} < 0 \tag{5.3.2}$$

$$\begin{bmatrix} W & W\mathbb{C}'_{(i)} - Y'_{(i)} \\ \star & u^2_{0(i)} \end{bmatrix} \geq 0, \quad \forall i = 1, ..., m \tag{5.3.3}$$

$$\begin{bmatrix} W & I_n \\ * & \rho I_n \end{bmatrix} \geq 0 \tag{5.3.4}$$

then the static DLAW $D_{aw} = ZS^{-1}$ stabilizes the system (5.3.1) for any initial condition in the ellipsoid

$$\mathcal{E}(P) = \left\{ \xi \in \Re^n ; \xi' P \xi \leq 1 \right\}$$

with $P = W^{-1}$

Proof of Proposition 5.1: The proof follows the same process of Theorem 3.1 proof presented in Appendix A.3.1. The only difference lies on the application of Lemma 1.1. Lemma 1.1 for the drag-free system (5.3.1) applies with $\omega = -G\xi - \mathbb{D}\phi_{u_0}(\nu)$ due to the presence of nested saturations.

End of Proof.

Remark 5.4. *Relation 5.3.4 allows the maximization of the stability domain $\mathcal{E}(P)$. Unlike the formation flying problem, no direction is favored in the stability domain optimization. The reason lies on the fact that there is no plant state towards which one can optimize the stability domain. Thus, instead of choosing a random state of the controller we have decided to apply the maximization of the whole stability domain.*

5.3.1.a Global stability

The plant on the drag-free control problem is exponentially stable. Then one may be interested on finding an anti-windup controller which ensures the global stability for the system (5.3.1).

Finally, the following proposition can be stated:

Proposition 5.2. *The satisfaction of relations* (5.3.2) *and* (5.3.4) *ensures the global asymptotic stability of system* (5.3.1) *with the static DLAW* $D_{aw} = ZS^{-1}$

Proof of Proposition 5.2: The global stability conditions are obtained by applying on Proposition 5.1 the Lemma 1.1 with $\omega = -\mathbb{C}\xi - \mathbb{D}\phi_{u_0}(\nu)$. Then relation (5.3.3) reads:

$$\begin{bmatrix} W & 0 \\ 0 & u_{0(i)}^2 \end{bmatrix} \geq 0, \quad \forall i = 1, ..., m \tag{5.3.5}$$

Relation (5.3.5) is equivalent to $W \geq 0$ and $u_0 \geq 0$. Then, as W is positive definite and u_0 is positive, the condition (5.3.5) can be removed from Theorem 5.1 leading to Proposition 5.2.

End of Proof.

5.3.2 The *trivial* static anti-windup

The Proposition 5.1 gives constructive conditions to find a static DLAW ensuring a certain domain of stability $\mathcal{E}(P)$. However in the drag-free control problem there exists a *trivial* static DLAW satisfying global asymptotic stability.

Proposition 5.3. *The system* (5.3.1) *is globally asymptotically stable with a static DLAW defined by:*

$$D_{awT} = -\mathbb{B} \tag{5.3.6}$$

Proof of Proposition 5.3: Let us consider system (5.3.1) dynamics.

$$\dot{\xi} = \mathbb{A}\xi + \mathbb{B}\phi_{(u_0)}(\nu) + \mathbb{B}_v D_{aw}\phi_{(u_0)}(\nu) \tag{5.3.7}$$

Considering the matrix $\mathbb{B}_v = I_{n_c}$, the relation (5.3.7) becomes:

$$\dot{\xi} = \mathbb{A}\xi + (\mathbb{B} + D_{aw})\phi_{(u_0)}(\nu) \tag{5.3.8}$$

Then imposing $D_{aw} = -\mathbb{B}$, the dead-zone function multiplier on relation (5.3.8) is cancelled and hence, the system (5.3.1) is simplified to a linear system:

$$\dot{\xi} = \mathbb{A}\xi \tag{5.3.9}$$

where $\mathbb{A}$ is Hurwitz.

Therefore, with $D_{aw} = -\mathbb{B}$, the system (5.3.1) becomes a globally asymptotically stable linear system.

End of Proof.

Remark 5.5. *$\mathbb{A}$ is Hurwitz from anti-windup preliminary assumptions. In any anti-windup problem the linear closed-loop is assumed to be asymptotically stable.*

Remark 5.6. *The existence of the* trivial *static DLAW is due to the lack of plant dynamics. Thus, only the controller dynamics are affected by the saturation non-linearity. On the other hand we can modify the controller dynamics with the anti-windup compensator. A logical choice is to use the anti-windup compensator to delete the non-linearity from the system dynamics. Therefore, the controller state (i.e. the system state for the drag-free control problem) evolves like it was a linear system.*

The *trivial* anti-windup can be easily related to the IMC approach [MZ89] as the IMC anti-windup compensator is exactly the same as the *trivial* anti-windup when $D_c = 0$. With $D_c \neq 0$ the relationship is not exactly the same as the IMC approach modifies the controller output. This could be reproduced by a static anti-windup with two outputs, a feedback and a feedforward.

5.4 Anti-windup application on a drag-free problem

The *trivial* static DLAW is computed for system (5.3.1). Then the system (5.3.1) is simulated with the *trivial* anti-windup compensator and the results are compared with the linear system and with the non-linear system without anti-windup (5.2.6)

5.4.1 Anti-windup design results

The *trivial* static DLAW for system (5.3.1) has the following numerical expression:

$$D_{awT} = \begin{bmatrix} -6.1 \cdot 10^{-7} & 6.1 \cdot 10^{-7} \\ -8.95 \cdot 10^{-8} & 8.95 \cdot 10^{-8} \\ 9.05 \cdot 10^{-8} & -9.05 \cdot 10^{-8} \\ -1.15 \cdot 10^{-2} & 1.15 \cdot 10^{-2} \end{bmatrix} \tag{5.4.1}$$

On the other hand, applying Proposition 5.2 for synthesis purposes the following static DLAW is obtained:

$$D_{aw} = \begin{bmatrix} 1.32 \cdot 10^{-4} & 1.32 \cdot 10^{-4} \\ 5.94 \cdot 10^{-4} & 5.94 \cdot 10^{-4} \\ 1.46 \cdot 10^{-3} & -1.14 \cdot 10^{-3} \\ 1.94 \cdot 10^{-3} & -1.94 \cdot 10^{-3} \end{bmatrix} \tag{5.4.2}$$

Trivial anti-windup (5.4.1) is not equal to the anti-windup gain (5.4.2) issued from the LMI computation. The LMI solvers do not guarantee unity of solution [BcPS07]. Then it is possible to find different anti-windups satisfying global asymptotic stability conditions.

5.4.2 Simulations on drag-free control

Finally the system (5.2.6) is simulated without anti-windup and with the *trivial* anti-windup (5.4.1) (i.e. system. (5.3.1)). Figure 5.3 shows the response of the drag-free system (the acceleration dynamics). A decreasing step has been introduced in the system through the signal y_r. This step has an initial amplitude of $10^{-2} m/s^2$ and lasts 10 seconds. No initial condition can be imposed to the acceleration, only the controller initial condition can be predefined. However, the controller initial condition has always been considered as null. Then, a decreasing step has been chosen as suitable manner to excite the system and observe the system behavior.

The linear response (solid line), the non-linear response without anti-windup (dashed line) and the non-linear response with the trivial anti-windup (dot-dashed line) are plotted in Figure 5.3. Actually the figure is a zoom of the actual simulation. The whole simulation is plotted in a superposed window. Regarding this window, one can realize that the non-linear response without anti-windup has entered a limit cycle, switching from the maximum acceleration to the minimum acceleration. On the contrary, with the trivial anti-windup, the acceleration converges to the origin following the linear response.

Finally, a simulation of the thrust of the system (5.3.1) is presented in Figure 5.4. Previously we have remarked that the saturation had to be symmetrized to apply anti-windup synthesis techniques. Two approaches has been considered for the symmetrization: the symmetrizing vector (2.5.6) ($N\zeta_{sym} = \frac{\bar{u}}{2}$ in solid line) and the VKF (2.5.14)[2] (dashed line).

[2]Given M in Section 5.2.3 Proposition 2.1 holds and function (2.5.14) is a VKF.

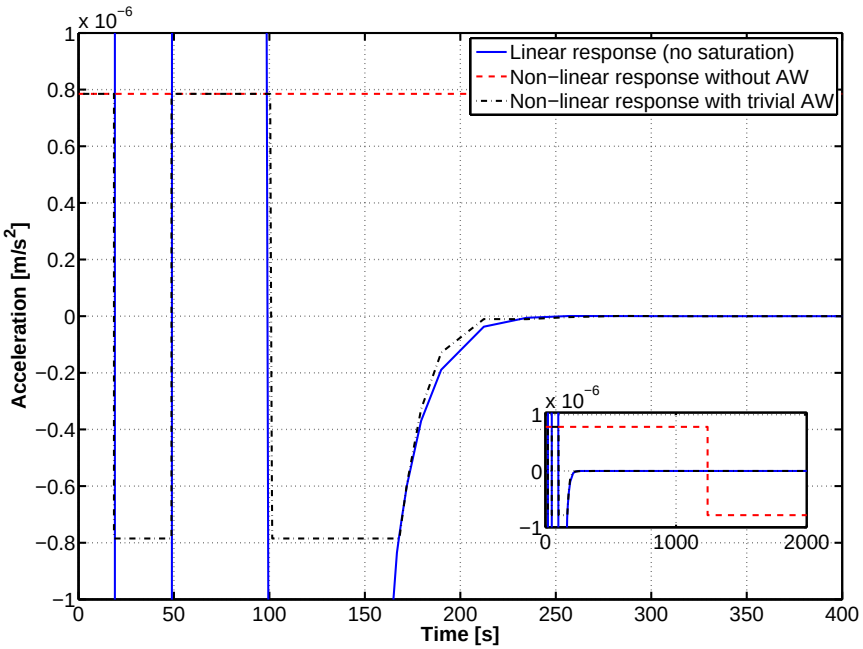

Figure 5.3: Acceleration response with and without anti-windup.

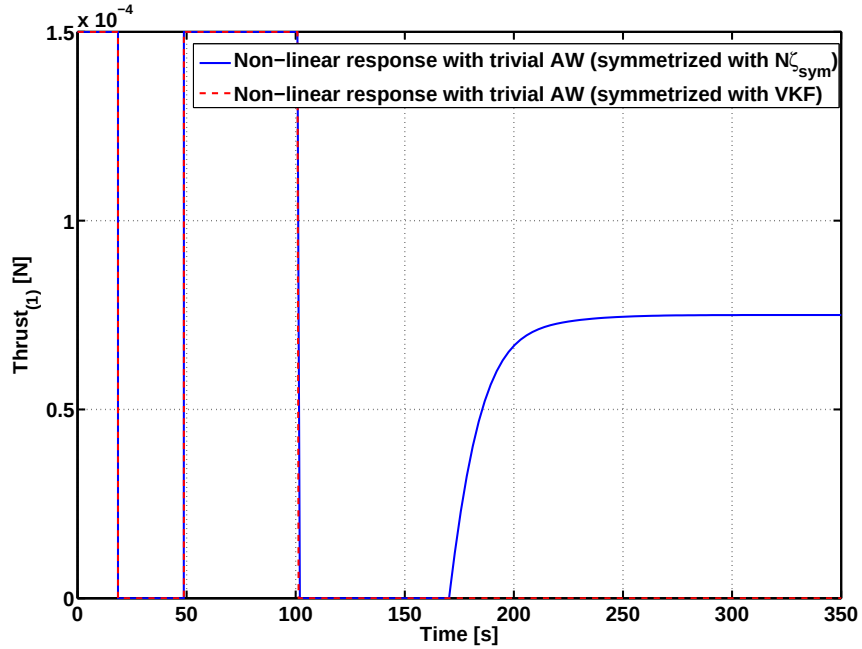

Figure 5.4: Thrust response with $N\zeta_{sym}$ (2.5.6) and VKF (2.5.14).

Figure 5.4 illustrates again the advantage of applying a VKF instead of a symmetrizing vector as the extra-consumption problem is avoided. Let us recall that the response of the system (5.3.1) in Figure 5.3 is unchanged by the symmetrizing technique.

5.5 Conclusion

Initially a modelling of the drag-free control problem has been given. Only the control of the linear acceleration has been considered, then the plant has been modelled as a static gain. Therefore, the plant is exponentially stable and this characteristic has been exploited for anti-windup purposes.

Constructive methods for the anti-windup computation have been given. In Section 5.3 LMI conditions have been stated on the static DLAW case. However the main contribution on the drag-free control has been the definition of the *trivial* anti-windup compensator. We have shown that there exists a particular expression for the static DLAW which deletes the influence of the saturation on the controller and, by drag-free modelling, on the whole system. Hence, this particular anti-windup provides global asymptotic stability.

The *trivial* static DLAW has been computed for the considered simplified model of the Microscope satellite. The control of one-axis one-satellite acceleration has been simulated with the trivial anti-windup compensator. Results have been compared to the system without anti-windup showing the improvement obtained with this technique.

Conclusion

This manuscript is organized into two parts. The first one is dedicated to the theoretical concepts and the main results of the thesis. On the other hand, the second part is completely focused on the application of the previous results to different satellite configurations.

Chapter 1 has presented the basic definitions for the stability analysis of the systems presenting a saturation non-linearity. Concepts like Lyapunov stability, non-linear sector condition and dead-zone functions have been reminded.

The main issue of the manuscript is the anti-windup compensator design. However, first, in Chapter 2 the problem of the saturation symmetrization has been tackled. The chapters have introduced the context in which the anti-windup problem has been solved. Symmetrizing techniques have been given and tested on the educational example.

Chapter 3 has been dedicated to the anti-windup compensator design. Two main approaches in anti-windup design, the DLAW and the MRAW, has been fully described. Constructive techniques for each approach have been given. In addition a third new approach has been introduced. Finally the validity of the anti-windup results when the system is symmetrized has been proven.

The last two chapters have presented the anti-windup techniques which have been tested. First, Chapter 4 has presented three formation flying scenarios. Simulations have illustrated the advantages of the anti-windup compensator as well as the differences between the anti-windup compensators. Second, Chapter 5 has treated the drag-free control problem. A model of drag-free configuration has been tested with an anti-windup compensator in the loop. Simulations have shown the benefits of the anti-windup compensator.

Personal contributions

The first contribution presented in this manuscript consists in some solutions allowing the symmetrization of the saturations. In Chapter 2 the particularity of the systems

presenting thrusters as actuator has been exploited to develop symmetrizing techniques for the saturation function. From a theoretic point of view, we have given necessary and sufficient conditions to find a symmetrizing vector candidate. Then one may apply conservative techniques existing in the literature which obtain a symmetric bound by keeping the smaller of both bounds in absolute value. A particular vector which modifies the saturation such as the upper and the lower bounds have the same absolute value has been introduced. Sufficient conditions where the symmetrizing vector is a symmetrizing one have been provided [BPT+09]. Then, regarding the application behind these methods, a variable kernel function have been defined in order to avoid the problem of over consumption. More precisely, we has presented sufficient conditions for an example of a variable kernel function along with some numerical tests.

The symmetrization has been arisen as a crucial step in order to apply the anti-windup techniques. The current anti-windup compensators that one can find in the literature consider the saturation to be symmetric. Then, in asymmetric cases one have first to apply the symmetrization techniques. The second contribution of this manuscript is presented in Chapter 3 and deals with the relationship between the anti-windup synthesis and the saturation symmetrization. We have proven that the introduction of a symmetrizing vector does not effect the results of the anti-windup synthesis process whether one considers the stability domain estimation or the anti-windup compensator [BPT+09]. Like with the symmetrizing vector, it has been proven that the anti-windup results are not affected by the variable kernel function.

The third contribution of this manuscript consists in proposing a new structure on the dynamic anti-windup compensator. This new approach has been denoted as Extended Model Recovery Anti-Windup (EMRAW) [BPT+10b]. The main idea has been to recover the synthesis procedure of the Model Recovery Anti-Windup (MRAW) and extend the method applying the Direct Linear Anti-Windup (DLAW). The combination of both approaches leads to non-convex conditions. Hence, two algorithms have been presented in order to find a solution to the anti-windup problem. The first one is an iterative algorithm, based on a coordinate-descending process. The second one is an heuristic algorithm, based on the objective of the elements composing the anti-windup compensator. In the context of the first algorithm, conditions on the initialization have been given.

Finally, the last contributions are given in the methodological field. First, some guidelines on how to improve the initialization of the first algorithm have been proposed. Then, the judicious application of the EMRAW synthesis techniques has permitted us to show the advantage of this structure on a coupled formation flying application. Finally, another important result has arisen in the context of the relationship between the allocation function and the anti-windup compensator design. Simulations have shown that the introduction of an anti-windup compensator can *compensate* the limitations of a simple allocation function and provide the same performance as a system with a more complex and efficient allocation function. Therefore we have opened the discussion regarding the necessity of an optimal complex non-linear allocation function if one want to obtain similar results with an anti-windup compensator [BPT+10a].

Perspectives

The anti-windup compensator has been shown as a useful tool to handle the actuator saturation. Particularly, the EMRAW has presented good results on the formation flying control problem. In this manuscript we have observed that the anti-windup compensator based on the model recovery approach assumes the perfect knowledge of the plant. However this is not generally the case. The presence of modelling errors like parametric uncertainty, flexible modes simplification or neglected non-linearities makes the perfect knowledge of the plant impossible in practice. Therefore, a first field for future research is the analysis of the validity of the anti-windup compensator applied to uncertain systems. Similarly, the synthesis of the anti-windup compensator for uncertain systems represents a potential research field for the future. Some works have already treated that issue [THP04, MTBP06, FB07] but the conservatism of these approaches is still important [KTP10].

Concerning this subject and related to the missions looking for both linear and angular dynamics, a particular uncertainty arises: the misalignment of the thrusters plus uncertainty in thrust amplitude and direction. This kind of modelling error is described by an uncertain influence matrix. Basically this problem is equivalent to consider an uncertainty on the system input matrix B_p. However, if one considers the physical meaning of the influence matrix some simplifications to the general problem might be done reducing, eventually, the conservatism.

Another interesting point for further research, regarding the EMRAW, concerns on the anti-windup order reduction. As remarked in this thesis, one main drawback of the EMRAW is that the plant and the anti-windup compensator are forced to have the same order. In large order models, this constraint is unacceptable for future physical implementations. Therefore, it would be interesting to develop constructive methods to reduce the anti-windup order, for example, eliminating secondary dynamics of the considered plant. In this scenario, the results could be related with the anti-windup synthesis on an uncertain system.

Finally, a last direction toward which the next studies may be steered is the definition of a different methodology for the anti-windup synthesis. The anti-windup compensators based on the model recovery approach have the particular property of recovering the linear behavior of the system. Let us remind the relationship $y_l = y_p - y_{aw}$. Then there is a stabilizing feedback v_1 which brings y_{aw} to zero and consequently y_p to y_l. The whole MRAW plus non-linear plant block could be considered as an observer of the linear system. Then the research objective would be to reformulate the anti-windup problem like an observation/estimation problem. Once the problem is rewritten under this alternative form, the idea would consist in applying the existing techniques on observers/estimators design to compute the anti-windup compensator.

Appendix A

Appendix

Outline of the chapter

The goal of this appendix is to provide some definitions, some omitted proofs and several numerical values which can be useful for the comprehension of this manuscript. Some references are given in order to help the reader to complete the explanations of the appendix with demonstrations and examples.

A.1 Linear Matrix Inequalities (LMI)

A.1.1 Historical background

The origins of Lyapunov equation for stable linear systems go back to the end of the nineteenth century, when Lyapunov published his works on the stability of dynamics systems [Lya92]. Particularly, he shows that a system described by the differential equation $\dot{x} = Ax$ is stable if and only if there exist a matrix $P = P^{'} > 0$ such as $A^{'}P + PA < 0$, and this inequality can be solved analytically. In 1940, Lur'e and Postnikov are the first to apply this theory to practical problems of control. They propose a stability criterium presented through a LMI formulation, moreover, this formulation allows the study of the systems with an actuator presenting a non-linearity [LP44]. The obtained inequalities are solved manually which restricts its application to small order problems. However, their works have shown that the Lyapunov theory had a great potential [Lur57]. Remarkable improvements are performed in the 1960's, particularly with the works done by Yakubovich:

- Real positive lemma, also called Kalman-Yakubovich-Popov [Kal63, Pop62, Yak62] leads to graphical techniques for the resolution of systems presenting a unique non-linearity (circle criterium, Popov criterium, Tsypkin criterim).
- The LMI problem related to this lemma was solved several years later from symmetric solutions of a Riccati equation [Wil71].

These works have allowed the consideration of larger order problems. However these problems are restricted to a specific family of LMI. The possibility to solve a general expression of LMI problems by convex optimization techniques comes up at the beginning of the 1980's. The development of the efficient technique of the interior-point [NN94] and the improvement of the computational capacity have motivated the formulation of several problems under a LMI formulation, becoming one of the main tools for the automatic control theory [BEGFB01, SW05, BS04].

A.1.2 LMI definition

The following defintions have been extracted from Scherer and Weiland's works [SW05].

Definition A.1. *(Linear Matrix Inequality) A Linear Matrix Inequality is described by any equation described as follows:*

$$F(z) > 0 \tag{A.1.1}$$

where $F : V \to S^N$ stands for an affine function defined on a vectorial space V towards the set $S^N = \left\{M \in \Re^{N \times N} : M = M^{'}\right\}$.

Remark A.1. *Inequality $F(z) > 0$ means that the symmetric matrix $F(z) > 0$ is positive definite, i.e. $u^{'}F(z)u > 0\ \forall u \in \Re^N \backslash \{0\}$. Equivalently, the smaller eigenvalue of $F(z)$ is positive.*

Remark A.2. *A set of LMI can be considered as a unique structured LMI. The two expressions below are equivalent:*

1. $F_i(z) > 0\ \forall i = 1, ..., m$
2. $diag(F_1(z), ..., F_m(z)) > 0$

Remark A.3. *In practice, the decision variables z are generally stacked in a matrix variable. Then, there exist two positive scalars p and q such as $V = \Re^{p \times q}$.*

A.1.3 LMI problems and resolution methods

Being $F, G : V \to S^{N_1}$ and $H : V \to S^{N_2}$ affine functions. Being $f : S \to \Re$ a convex function, where $\mathcal{S} = \{z \in V : F(z) > 0\}$. There exist three generic problems presenting LMI:

- The feasibility problem consist on finding a value of $z \in V$ such as $F(z) > 0$. Actually, one looks for a vector z minimizing the scalar $t \in \Re$ constrained to $-F(z) < tI_{N_1}$. If the minimum value obtained for t is negative, the problem is feasible.
- The eigenvalues problem is designed as computing the value of $z \in V$ which minimizes $f(z)$ constrained to $F(z)$.
- The generalized eigenvalues problem is defined as finding the scalar $\lambda \in \Re$ under the constraints:

$$\begin{cases} \lambda F(z) - G(z) > 0 \\ F(z) > 0 \\ H(z) > 0 \end{cases} \tag{A.1.2}$$

Remark A.4. *Let us denote that in all the previously presented problems the inequalities are strict. However this is not restrictive as numerically any non-strict LMI can be expressed as a strict one [BEGFB01].*

Mostly all the optimization problems present in the control field, the identification field and in the signal analysis field can be expressed with an LMI formulation under the previous presented problems framework. For example, the stability of an linear system $\dot{x} = Ax$ with $A \in \Re^{n \times n}$ can be described as finding a matrix $P \in S^n$ such as $F(P) = diag(P, -A^{'}P - PA) \in S^{2n}$. The stability problem is, indeed, a LMI feasibility problem.

Remark A.5. *The three first problems described previously are convex or almost-convex, thus there exists a global optimum. Nevertheless, they are not differentiable. There are two principal families of methods which allow the resolution of LMI problems:*

- *The cutting plane methods. They were introduced in the convex optimization framework in the 1970's [EM75] and then were applied several years later in the robust control framework [GPB91]*
- *The interior-point methods. They were developed for the LMI resolution [NN94].*

These methods allow the computation of the global optimum in a polynomial time. However, the interior-point methods present the advantage of being faster and being able to handle problems of bigger size composed by thousand of variables. In fact, they have been implemented in the Robust Control Toolbox for Matlab [BcPS07].

A.1.4 Schur's complement

Schur's complement is a practical mathematical tool to express under an LMI formulation certain non-linear matrix inequalities.

Lemma A.1. *Consider symmetric matrices $R \in \Re^{n\times n}$, $S \in \Re^{m\times m}$ and a matrix $M \in \Re^{n\times m}$. The following conditions are equivalent:*

1. $\left[\begin{array}{cc} R & M \\ M' & S \end{array}\right] > 0$
2. $\left\{\begin{array}{l} R > 0 \\ S - M'R^{-1}M > 0 \end{array}\right.$
3. $\left\{\begin{array}{l} S > 0 \\ R - MS^{-1}M' > 0 \end{array}\right.$

A.1.5 Elimination lemma

The elimination lemma was presented in [GA94] and it was also applied under the name of Finsler lemma in [OS01, SIG97]. The lemma may transform BMI in LMI by the elimination of some variables.

Lemma A.2. *Consider a symmetric matrix $\Phi \in \Re^{m\times m}$ and matrices $P \in \Re^{p\times m}$, $Q \in \Re^{q\times m}$. There exists a matrix $\Theta \in \Re^{m\times m}$ such as:*

$$\Phi + P'\Theta'Q + Q'\Theta P < 0 \tag{A.1.3}$$

if and only if:

$$\begin{cases} N_p^{'}\Phi N_p < 0 \\ N_Q^{'}\Phi N_Q < 0 \end{cases} \tag{A.1.4}$$

where N_P and N_Q describe matrices where the columns constitute the basis of the kernels of P and Q.

The idea is to stack all the variables to eliminate in Θ and then apply the elimination lemma. Once the problem (A.1.4) solved one may reconstruct the matrix Θ through the completion lemma presented in [PZPB94].

Lemma A.3. *Consider symmetric Hermitian matrices $X, Y \in \mathbb{C}^{n\times n}$ and a positive integer m. There exist a matrix $X_2 \in \mathbb{C}^{n\times m}$ and a Hermitian matrix $X_3 \in \mathbb{C}^{m\times m}$ such as:*

$$\begin{bmatrix} X & X_2 \\ X_2^* & X_3 \end{bmatrix} > 0 \text{ and } \begin{bmatrix} X & X_2 \\ X_2^* & X_3 \end{bmatrix}^{-1} = \begin{bmatrix} Y & ? \\ ? & ? \end{bmatrix} \tag{A.1.5}$$

where ? denotes undefined elements, if and only if:

$$X - Y^{-1} \geq 0 \text{ and } rank(X - Y^{-1}) \leq m \tag{A.1.6}$$

Remark A.6. *Another possible technique in order to transform BMI to LMI consist in applying the variable change introduced by [SGC97]. This technique becomes interesting as it allows the separation between the Lyapunov related matrices and the state matrices of the sought controller.*

A.1.6 $\mathcal{S}$-Procedure

The $\mathcal{S}$-Procedure which was first denote like that by [AG64] is applied by the control theory to study the stability and the performance of the non-linear systems. The technique allows the transformation of a non-convex condition to a sufficient condition and, hence conservative, but convex. A similar procedure was implicitly used in the 1950's, but the first remarkable results were provided by Yakubovich in the 1970's.

The idea of the $\mathcal{S}$-procedure is based on the next statement. Considering functions $f : V \to \Re$ and $h_i : V \to \Re$, $i = 1, ..., m$, the following equations are contemplated:

$$f(x) > 0 \ \forall x \in V\backslash\{0\} \text{ such as } h_i(x) \geq 0, \ i = 1, ..., m \tag{A.1.7}$$

$$\exists \tau_i \in \Re_+, i = 1, ..., m \text{ such as } f(x) - \sum_{i=1}^{m} \tau_i h_i(x) > 0 \tag{A.1.8}$$

These two conditions are not equivalent in general, however it is evident that (A.1.8) always implies (A.1.7). The reverse is true under certain hypothesis. The $\mathcal{S}$-procedure is then called lossless. Proposition A.1 presents practical results.

Definition A.2. *The constraint $h_i(x) \geq 0$, for a $i = 1, ..., m$ is called regular if exists $x_0 \in V$ such as $h_i(x_0) > 0$, $i = 1, ..., m$.*

Proposition A.1. *Let us suppose the constraints $h_i(x) \geq 0$, for all $i = 1, ..., m$ to be regular.*

- *If functions $f : \Re^n \to \Re$ and $h_i : \Re^n \to \Re$ are linear, the $\mathcal{S}$-procedure is lossless for any m.*
- *If functions $f : \Re^n \to \Re$ and $h_i : \Re^n \to \Re$ are quadratic, the $\mathcal{S}$-procedure is lossless for $m = 1$ [Yak71, Yak73].*
- *If functions $f : \mathcal{C}^n \to \Re$ and $h_i : \mathcal{C}^n \to \Re$ are quadratic, the $\mathcal{S}$-procedure is lossless for any $m \leq 2$ [FY79].*

Remark A.7. *The quadratic function case becomes interesting when it is related with the stability problem with the Lyapunov theory.*

Several extensions have been proposed by [Yak92], and more recently by [IH05] who proposes the following result in the case of complex quadratic functions.

Definition A.3. *Being $\mathcal{Q}$ a set of Hermitian matrices of $n \times n$ dimension is called non-conservative if the following properties are satisfied:*

1. *$\mathcal{Q}$ is convex*
2. *$Q \in \mathcal{Q} \Rightarrow \tau Q \in \mathcal{Q} \quad \forall \tau > 0$*
3. *for all non-null matrix $H \in \mathbb{C}^{n \times n}$ such as $H = H^* \geq 0$ and $trace(QH) \leq 0 \; \forall Q \in \mathcal{Q}$, there exist vectors $x_i \in \mathbb{C}$, $i = 1, ..., r$ such as $H = \sum_{i=1}^{r} x_i x_i^*$ and $x_i^* Q x_i \leq 0$ $\forall Q \in \mathcal{Q}$.*

Proposition A.2. *Consider a Hermitian matrix P and $\mathcal{Q}$ a non-conservative set of Hermitian matrices. The following statements are then equivalent:*

1. *$x^* P x > 0 \quad \forall x \in \mathbb{C}^n \backslash \{0\}$ such as $x^* Q x \geq 0 \quad \forall Q \in \mathcal{Q}$*
2. *$\exists Q \in \mathcal{Q}$ such as $P - Q > 0$*

Therefore, the lossless character of the $\mathcal{S}$-procedure is not longer linked to the number of constraints m which is unlimited as long as matrices Q satisfy definition A.3.

A.2 Bilinear Matrix Inequalities (BMI)

Several optimization problems found in control theory are presented under a BMI formulation, but they can be transformed with some of the techniques presented before into LMI. For instance, two algorithms have been proposed in Section 3.5.3 transforming BMIs from Theorem 3.2 into LMIs. However, because the conservatism derived from the reformulation is too important, or just because the transformation is not possible (and one does not desire to apply iterative methods which do not present any kind of convergence), the possibility of the direct resolution of BMI should be considered. Nevertheless the generalization brings the problem to the loss of convexity with the numerical problems that can be derived.

Nowadays there exist BMI solvers. Unfortunately, the resolution techniques are far from being matures and they do not allow the consideration of problems where an important number of variables are involved. For instance, when the Lyapunov functions optimization are sought, it is not judicious to apply these techniques.

A.3 Complements of Chapter 3

A.3.1 Proof of Theorem 3.1

Let us consider the following candidate quadratic Lyapunov function defined by $V(\xi) = \xi' P \xi$, $P = P' > 0$ for all $\xi \in \Re^n$. Then a sufficient condition of stability in the ellipsoid domain $\mathcal{E}(P)$ with the constraint $\|z\|_2^2 = \int_0^\infty z'z dt \leq \gamma$ is given by $\dot{V}(\xi) + \gamma^{-1} z'z < 0$, for any $\xi \in \mathcal{E}(P)$ [BT09].

The expression of the time-derivative $\dot{V}(\xi)$ along the trajectories of system (3.3.8) reads

$$\begin{aligned} \dot{V}(\xi) &= \dot{\xi}' P \xi + \xi' P \dot{\xi} \\ &= \xi' \left(\mathbb{A}' P + P \mathbb{A} \right) \xi + 2 \xi' P \left(\mathbb{B}_\phi + \mathbb{B}_v D_{aw} \right) \phi_{(u_0)}(\mathbb{K}\xi)) \end{aligned}$$

By using Lemma 1.1, it follows that

$$\text{for any } \xi \in S(u_0) = \left\{ \xi \in \Re^n ; \left| (\mathbb{K}_{(i)} - G_{(i)}) \xi \right| \leq u_{0(i)}, i = 1, ..., m \right\}$$

one gets: $-2\phi'_{(u_0)}(\mathbb{K}\xi) S^{-1} (\phi_{(u_0)}(\mathbb{K}\xi) + G\xi) \geq 0$. Hence by setting $W = P^{-1}$ and $Y = GW$, the satisfaction of relation (3.3.11) guarantees that $\mathcal{E}(P) \subseteq S(u_0)$.

Thus, for any $\xi \in \mathcal{E}(P) \subseteq S(u_0)$ one gets:

$$\begin{aligned}\dot{V}(\xi)+\gamma^{-1}z'z \leq & \dot{V}(\xi)+\gamma^{-1}\xi'\mathbb{C}'\mathbb{C}\xi+2\gamma^{-1}\xi\mathbb{C}'\mathbb{D}_\phi\phi_{(u_0)} \\ & +\gamma^{-1}\phi'_{(u_0)}\mathbb{D}'_\phi\mathbb{D}_\phi\phi_{(u_0)}-2\phi'_{(u_0)}S^{-1}\left(\phi_{(u_0)}-G\xi\right)\end{aligned} \tag{A.3.1}$$

The right-hand term writes:

$$\mathcal{L}=\begin{bmatrix} W^{-1}\xi \\ S^{-1}\phi_{u_0}\end{bmatrix}'\mathbb{M}\begin{bmatrix} W^{-1}\xi \\ S^{-1}\phi_{u_0}\end{bmatrix}$$

with $\mathbb{M}=\begin{bmatrix} W\mathbb{A}'+\mathbb{A}W+\gamma^{-1}W\mathbb{C}'\mathbb{C}W & \mathbb{B}_\phi S+\mathbb{B}_v Z+Y'+\gamma^{-1}W\mathbb{C}'\mathbb{D}_\phi S \\ * & -2S+\gamma^{-1}S\mathbb{D}'_\phi\mathbb{D}_\phi S\end{bmatrix}$ and $Z=D_{aw}S$.

Finally, applying Schur complement one gets inequality (3.3.10). Therefore, the satisfaction of relation (3.3.10) ensures that $\mathcal{L}<0$ or equivalently $\dot{V}(\xi)+\gamma^{-1}z'z\leq\mathcal{L}<0$ for any $\xi\in\mathcal{E}(P)$. In other words, for any $\xi\in\mathcal{E}(P)$ one gets $\dot{V}(\xi)<-\gamma^{-1}z'z<0$ and therefore $\mathcal{E}(P)$ is a region of asymptotic stability for system (3.3.8). Furthermore by integrating the expression $\dot{V}(\xi)+\gamma^{-1}z'z<0$ it follows:

$$V(\infty)-V(\xi(0))+\gamma^{-1}\int_0^\infty z'zdt<0$$

or equivalently since $V(\infty)>0$:

$$\int_0^\infty z'zdt<\gamma V(\xi(0))\leq\gamma$$

for any $\xi(0)\in\mathcal{E}(P)$.

A.3.2 Extension of Theorem 3.1

Let us consider the following closed-loop system :

$$\begin{cases}\dot{\xi} &= \mathbb{A}\xi+\mathbb{B}_\phi M\phi_{(u_0)}(f(y_c))+\mathbb{B}_v D_{aw}\phi_{(u_0)}(f(y_c)) \\ y_c &= K\xi \\ z &= z_p-z_l=\mathbb{C}\xi \\ v_x &= D_{aw}\phi_{(u_0)}(f(y_c))\end{cases} \tag{A.3.2}$$

where $\xi=[x'_p\ x'_c\ x'_d\ x'_l]'\in\Re^{n_M}$ with $n_M=n_p+n_c+n_d+n_l$ is the closed-loop state vector, $y_c\in\Re^{m_c}$ is the control output and $v_x\in\Re^{n_c}$ the anti-windup output. The matrices in (A.3.2) are defined by state matrices presented in Chapter 3 as follows:

$$\mathbb{A}=\begin{bmatrix} A_p+B_pD_cC_p & B_pC_c & B_dC_d & 0 \\ B_cC_p & A_c & 0 & 0 \\ 0 & 0 & A_d & 0 \\ 0 & 0 & 0 & A_{cl}\end{bmatrix}$$

$\mathbb{B}_\phi = [B'_\phi \;\; 0 \;\; 0]'$, $\mathbb{B}_v = [0 \; I_{n_c} \;\; 0 \;\; 0]'$, $K = [D_c C_p \;\; C_c \;\; 0 \;\; 0]$ and $\mathbb{C} = [C_z \;\; 0 \;\; 0 \;\; -C_l]$.

An extension of Theorem 3.1 can be stated for the system (A.3.2) where $f(y_c)$ is the multi-sat AF (2.4.3). The formulation of the multi-sat AF expressed with the dead zone function (1.3.4) reads:

$$f(y_c) = M^* y_c - \sum_{i=1}^{m_c} \phi_{i(u_0)}(M^*_{(:,i)} y_{c(i)}) \tag{A.3.3}$$

Given (A.3.3), system (A.3.2) is rewritten as follows:

$$\begin{cases} \dot{\xi} = \mathbb{A}\xi + \mathbb{B}_\phi M \phi_{(u_0)} \left(\mathbb{K}\xi - \sum_{i=1}^{m_c} \phi_{i(u_0)}(\mathbb{K}_i \xi) \right) + \mathbb{B}_\phi M \sum_{i=1}^{m_c} \phi_{i(u_0)}(\mathbb{K}_i \xi) + \mathbb{B}_v v_x \\ v_x = D_{aw}[\phi' \;\; \phi'_1 \;\; \phi'_2 \;\; \cdots \;\; \phi'_{m_c}]' \end{cases} \tag{A.3.4}$$

where $\mathbb{K} = M^* K$ and $\mathbb{K}_i = M^*_{(:,i)} K_{(i,:)}$. Figure A.1 shows the anti-windup synthesis block diagram for the multi-sat case.

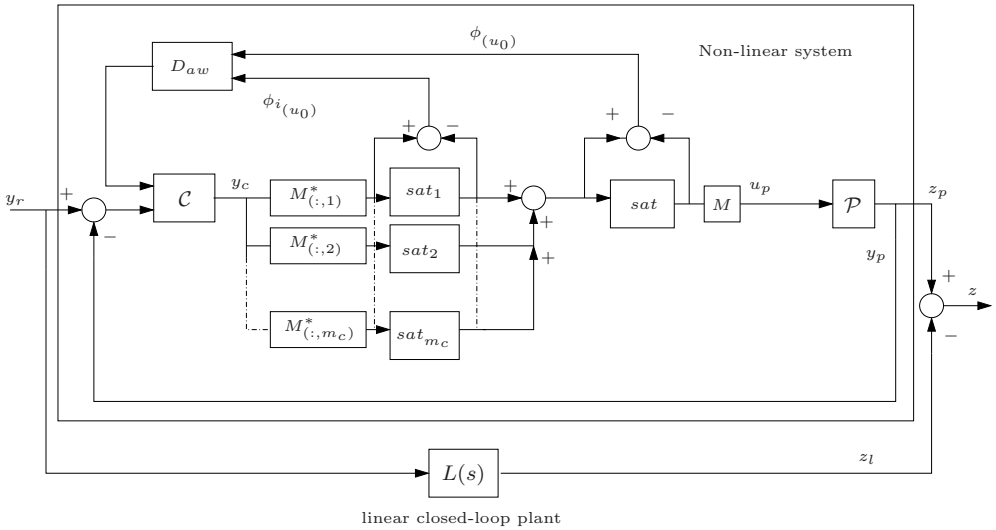

Figure A.1: Control Loop with multi-saturation Anti-windup

Then the following theorem for the system (A.3.4) can be stated:

Theorem A.1. *(Static anti-windup design 2). Given $v \in \Re^n$, k_γ and k_ρ two positive values, if there exist a symmetric positive-definite matrix $W \in \Re^{n \times n}$, a matrix $Y \in \Re^{m \times n}$, m_c matrices $Y_i \in \Re^{m \times n}$, a matrix $Z \in \Re^{n_c \times m}$, m_c matrices $Z_i \in \Re^{n_c \times m}$, a diagonal positive-definite matrix $S \in \Re^{m \times m}$, and m_c diagonal positive-definite matrices $S_i \in \Re^{m \times m}$ satisfying*

$$min \quad k_\gamma \gamma + k_\rho \rho$$

$$\begin{bmatrix} H_e & J & J_1 & J_2 & \cdots & J_{m_c} & W\mathbb{C}' \\ * & -2S & -S_1 & -S_2 & \cdots & -S_{m_c} & 0 \\ * & * & -2S_1 & 0 & \cdots & 0 & 0 \\ * & * & * & -2S_2 & 0 & \cdots & 0 \\ \vdots & \vdots & \ddots & \cdots & \ddots & \vdots & \vdots \\ * & * & \cdots & * & * & -2S_{m_c} & 0 \\ * & * & \cdots & \cdots & * & * & -\gamma I \end{bmatrix} < 0 \tag{A.3.5}$$

$$\begin{bmatrix} W & W\mathbb{K}'_{(j,:)} - Y'_{(j,:)} \\ \star & u^2_{0(j)} \end{bmatrix} \geq 0, \quad \forall j = 1, ..., m \tag{A.3.6}$$

$$\begin{bmatrix} W & W\mathbb{K}'_{i(j,:)} - Y'_{i(j,:)} \\ \star & u^2_{0(j)} \end{bmatrix} \geq 0, j = 1, ..., m; i = 1, ..., m_c \tag{A.3.7}$$

$$\begin{bmatrix} W & \xi'_0 \\ \star & \rho I \end{bmatrix} \geq 0 \tag{A.3.8}$$

with $H_e = W\mathbb{A}' + \mathbb{A}W$, $J = \mathbb{B}MS + \mathbb{B}_v Z + Y'$, $J_i = \mathbb{B}MS_i + \mathbb{B}_v Z_i + Y'_i$,..., $i = 1, ..., m_c$ *then the static anti-windup gain* $D_{aw} = [ZS^{-1} \quad Z_1 S_1^{-1} \quad \cdots \quad Z_{m_c} S_{m_c}^{-1}]$ *is such that* $\int_0^\infty z(t)'z(t)dt \leq \gamma$ *and the system* (A.3.4) *is locally asymptotically stable for any initial condition in the ellipsoid* $\mathcal{E}(P) = \left\{\xi \in \Re^n; \xi' P \xi \leq 1\right\}$, *with* $P = W^{-1}$. *Furthermore,* $\mathcal{E}(P)$ *is maximized in the direction of* v *with the weight* k_ρ, *and the performance* $1/\gamma$ *is maximized with the weight* k_γ.

Proof of Theorem A.1: Consider a quadratic Lyapunov function $V(\xi) = \xi' P \xi$, $P = P' > 0$. A sufficient condition for the stability of the system (A.3.4) in the ellipsoid domain $\mathcal{E}(P)$ with the performance constraint is given by $\dot{V}(\xi) + \gamma^{-1} z'z < 0$.

Writing $D_{aw} = [E_c \quad E_{c_1} \quad E_{c_2} \quad \cdots \quad E_{c_{mc}}]$, one gets $v_x = E_c\phi + \sum_{i=1}^{m_c} E_{ci}\phi_i$. The expression of the time-derivative of $V(\xi)$ along the trajectories of system (A.3.4) gives

$$\dot{V}(\xi) = \xi' \left(\mathbb{A}'P + P\mathbb{A}\right)\xi + 2\xi' P \left(\mathbb{B}M + \mathbb{R}E_c\right)\phi_{(u_0)}(\mathbb{K}\xi - \sum_{i=1}^{m_c}\phi_{i(u_0)}) + 2\xi' P \sum_{i=1}^{m_c}\left(\mathbb{B}M + \mathbb{R}E_{ci}\right)\phi_{i(u_0)}(\mathbb{K}_i\xi)$$

Let us emphasize that the non-linearities present different sector conditions as ϕ_i is nested in ϕ. Thus, using Lemma 1.1 in [GdSJT05], we can verify that

$$-2\phi'_{(u_0)} S^{-1}(\phi_{(u_0)} - \mathbb{G}\xi + \sum_{i=1}^{m_c}\phi_{i(u_0)}) \geq 0$$

with S a diagonal positive-definite matrix, provided that

$$\xi \in S(u_0) = \left\{\xi \in \Re^n; \left|(\mathbb{K}_{(j)} - G_{(j)})\xi\right| \leq u_{0_{(j)}}, j = 1, ..., m\right\}$$

By the same way, Lemma 1.1 can be used m_c times to verify that

$$-2\sum_{i=1}^{m_c}\phi'_{i(u_0)}S_i^{-1}(\phi_{i(u_0)}-G_i\xi)\geq 0$$

with S_i a positive diagonal matrix, provided that

$$\xi\in S_i(u_0)=\left\{\xi\in\Re^n;\left|(\mathbb{K}_{i(j,:)}-G_{i(j,:)})\xi\right|\leq u_{0_{(j)}},j=1,...,m\right\}\forall\quad i=1,...,m_c$$

Hence by setting $W=P^{-1}$, $Y=GW$ and $Y_i=G_iW$ the satisfaction of relations (A.3.6), (A.3.7) guarantees that $\mathcal{E}(P)\subseteq(S(u_0)\cap(\bigcap_{i=1}^{m_c}S_i(u_0)))$.

Thus, for any $\xi\in\mathcal{E}(P)$, one gets:

$$\dot{V}(\xi)+\gamma^{-1}z'z\leq\dot{V}(\xi)-2\phi'_{(u_0)}S^{-1}\left(\phi_{(u_0)}-\mathbb{G}\xi-\sum_{i=1}^{m_c}\phi_{i(u_0)}\right)$$
$$-2\sum_{i=1}^{m_c}\phi'_{i(u_0)}S_i^{-1}\left(\phi_{i(u_0)}-G_i\xi\right)+\gamma^{-1}\xi'\mathbb{C}'\mathbb{C}\xi$$

Then the right hand term writes: $\mathcal{L}=\mathbb{X}'\mathbb{M}\mathbb{X}$ with

$$\mathbb{X}'=\left[\xi'W^{-1}\ \phi'_{(u_0)}S^{-1}\ \phi'_{1(u_0)}S_1^{-1}\quad\phi'_{2(u_0)}S_2^{-1}\cdots\phi'_{m_c(u_0)}S_{m_c}^{-1}\right]$$

and

$$\mathbb{M}=\begin{bmatrix}H_e+\frac{W\mathbb{C}'\mathbb{C}W}{\gamma} & J & J_1 & J_2 & \cdots & J_{m_c}\\ \star & -2S & -S_1 & -S_2 & \cdots & -S_{m_c}\\ \star & \star & -2S_1 & 0 & \cdots & 0\\ \star & \star & \star & -2S_2 & 0 & \cdots\\ \vdots & \vdots & \ddots & \cdots & \ddots & \vdots\\ \star & \star & \cdots & \star & \star & -2S_{m_c}\end{bmatrix}$$

with $H_e=W\mathbb{A}'+\mathbb{A}W$, $J=\mathbb{B}MS+\mathbb{R}Z+Y'$, $Z=E_cS$, $J_i=\mathbb{B}MS_i+\mathbb{R}Z_i+Y_i'$, and $Z_i=E_{ci}S_i\quad i=1,...,m_c$. Finally, using Schur complement on $\gamma^{-1}W\mathbb{C}'\mathbb{C}W$, one gets LMI (A.3.5). Therefore, the satisfaction of relation (A.3.5) ensures that $\mathcal{L}<0$ or equivalently, $\dot{V}(\xi)+\gamma^{-1}z'z\leq\mathcal{L}<0$ for any $\xi\in\mathcal{E}(P)$. In other words, $\mathcal{E}(P)$ is a region of asymptotic stability for system (A.3.4) with $\|z\|_2^2\leq\gamma$.

End of Proof

A.3.3 Proof of Proposition 3.2

First, matrices W and $P = W^{-1}$ introduced in Proposition 3.1 have to be decomposed as follows[1]:

$$W = \begin{bmatrix} Y & N' \\ N & F \end{bmatrix}; P = \begin{bmatrix} X^{-1} & M' \\ M & E \end{bmatrix} \tag{A.3.10}$$

with $X, Y \in \Re^{n_M \times n_M}$. If anti-windup matrices are stocked in matrix $\Omega_{aw} = \begin{bmatrix} A_{aw} & B_{aw} \\ C_{aw} & D_{aw} \end{bmatrix}$, then Z is decomposed in $Z = [V \quad \tilde{U}]$, with $V, \tilde{U} \in \Re^{m \times n_M}$, inequality (3.3.14) can be written like:

$$\Theta + \mathcal{U}'\Omega_{aw}\mathcal{V} + \mathcal{V}'\Omega\mathcal{U} < 0 \tag{A.3.11}$$

where:

$$\Theta = \begin{bmatrix} \mathbb{A}'Y + Y\mathbb{A} & * & * & * \\ N\mathbb{A}'Y & 2\lambda F & * & * \\ S\mathbb{B}'_\phi + V & \tilde{U} & -2S & * \\ \mathbb{C}Y & \mathbb{C}N' & \mathbb{D}_\phi S & -\gamma I_p \end{bmatrix} \tag{A.3.12}$$

$$\mathcal{U} = \begin{bmatrix} 0 & I_{n_M} & 0 & 0 \\ \mathbb{B}'_v & 0 & 0 & 0 \end{bmatrix} \tag{A.3.13}$$

$$\mathcal{V} = \begin{bmatrix} 0 & I_{n_M} & 0 & 0 \\ 0 & I_{n_M} & 0 & 0 \end{bmatrix} diag(W, S, I) \tag{A.3.14}$$

Then by applying the elimination lemma [OS01, GA94, SIG97], inequality (A.3.11) has a solution Ω_{aw} if and only if:

$$N'_{\mathcal{U}}\Theta N_{\mathcal{U}} < 0 \tag{A.3.15}$$

$$N'_{\mathcal{V}}\Theta N_{\mathcal{V}} < 0 \tag{A.3.16}$$

where $N_{\mathcal{U}}$ and $N_{\mathcal{V}}$ stands for the matrices of the basis of the kernels $Ker(\mathcal{U})$ and $Ker(\mathcal{V})$, respectively. That is:

$$N_{\mathcal{U}} = \begin{bmatrix} N_v & 0 & 0 \\ 0 & 0 & 0 \\ 0 & I_m & 0 \\ 0 & 0 & I_p \end{bmatrix} \text{ where } N_v = Ker(\mathbb{B}'_v) \tag{A.3.17}$$

[1] Inequality (3.3.21) implies $\begin{bmatrix} X^{-1} & I_{n_M} \\ I_{n_M} & Y \end{bmatrix} > 0$, i.e. $X^{-1} > 0$, $Y > 0$ and $X^{-1}Y > I_{n_M}$, which means that condition of the lemma of matrix completion [PZPB94] is satisfied. Therefore decomposition (A.3.10) is valid and one may reconstruct W matrix from X and Y by the relationship

$$W = \begin{bmatrix} Y & I_{n_M} \\ N & 0 \end{bmatrix} \begin{bmatrix} I_{n_M} & X^{-1} \\ 0 & M \end{bmatrix}^{-1} \tag{A.3.9}$$

where non-singular matrices $M, N \in \Re^{n_M \times n_M}$ satisfy $M'N = I_{n_M} - X^{-1}Y < 0$.

$$N_{\mathcal{V}} = diag(W^{-1}, S^{-1}, I_p) \begin{bmatrix} I_{n_M} & 0 \\ 0 & 0 \\ 0 & 0 \\ 0 & I_p \end{bmatrix} \tag{A.3.18}$$

For this choice of $N_{\mathcal{U}}$, one shows that inequality (A.3.15) is equivalent to (3.3.19). On the other hand, inequality (A.3.16) reads:

$$\begin{bmatrix} X^{-1}A + A'X^{-1} + 2\lambda M'FM & \mathbb{C}' \\ \mathbb{C} & -\gamma I \end{bmatrix} < 0 \tag{A.3.19}$$

From decomposition (A.3.10), one gets $M'FM = -X^{-1} + X^{-1}YX^{-1}$. Then, the inequality (A.3.19) by applying the Schur complement and pre- and post-multiplying by diag(X,Y) one gets:

$$\begin{bmatrix} \mathbb{A}X + X\mathbb{A}' - 2\lambda X & 2\lambda Y & X\mathbb{C}' \\ * & -2\lambda Y & 0 \\ * & * & -\gamma I \end{bmatrix} \tag{A.3.20}$$

which coincides with (3.3.20).

Let us define the matrix $\Psi = \begin{bmatrix} I & I \\ MX & 0 \end{bmatrix}$. Pre- and post-multiplying (3.3.15) by $diag(\Psi', I)$ and $diag(\Psi, I)$ one gets:

$$\begin{bmatrix} X & X & X\mathbb{C}'_{\phi(i)} - XM'\tilde{U}_{(i)}{}' - V'_{(i)} \\ * & Y & Y\mathbb{C}'_{\phi(i)} - V'_{(i)} \\ * & * & u^2_{0(i)} \end{bmatrix} \geq 0 \tag{A.3.21}$$

By the change of variables $U = (\mathbb{C}_\phi - \tilde{U}M)X - V$ one recovers equation (3.3.21) showing that it is equivalent to (3.3.15).

Finally condition (3.3.22) is obtained by pre- and post-multiplying by $diag(\Psi', 1)$ and $diag(\Psi, 1)$ the relation (3.3.16).

A.3.4 Proof of Proposition 3.3

Let S a positive definite matrix, and consequently non-singular, one has only to impose the variables change $\tilde{B}_{aw} = B_{aw}S$ and $\tilde{D}_{aw} = D_{aw}S$. With this change of variables the relation (3.3.14) becomes LMI and the Proposition 3.1 can be checked by the standard LMI solvers.

A.4 Results of the anti-windup synthesis

In Chapter 4 some matrices issued from the anti-windup synthesis have been omitted. Thus, they are given in the sequel.

A.4.1 Static DLAW gain for system (4.5.2)

The following static DLAW has been computed in the context of the attitude and relative position control:

$$D_{aw} = \left[\begin{array}{cccccc} -0.93 & -0.93 & -0.07 & -0.07 & 6.44 & 8.76 \\ 0.11 & 0.11 & 0.01 & 0.01 & -0.96 & -0.77 \\ 0.07 & 0.07 & 0.003 & 0.003 & -6.03 & 4.79 \\ 126.7 & 126.7 & 106.02 & 106.02 & -956.25 & -1109 \\ -10.7 & -10.7 & -10.2 & -10.2 & 128.6 & 51.2 \\ 2.38 \cdot 10^3 & 2.38 \cdot 10^3 & 189.9 & 189.9 & -1.94 \cdot 10^4 & -1.93 \cdot 10^4 \end{array}\right.$$
$$\begin{array}{cccccc} -6.44 & -8.76 & -0.05 & -0.002 & -0.05 & -0.002 \\ -0.96 & -0.77 & -0.16 & 0.15 & 0.16 & -0.15 \\ 6.03 & -4.79 & -2.14 & 1.77 & 2.14 & -1.77 \\ 956.25 & 1109 & 7.1 & -2.1 & -7.1 & 2.1 \\ -128.6 & -51.2 & 18.4 & -17.1 & -18.5 & 17.1 \\ 1.94 \cdot 10^4 & 1.93 \cdot 10^4 & -285 & 188 & 285 & -188 \end{array}$$
$$\left.\begin{array}{cccc} 5.2 & 4.84 & -5.2 & -4.84 \\ -0.7 & -0.4 & 0.7 & 0.4 \\ -1.38 & 0.15 & 1.38 & -0.15 \\ -654 & -723 & 654 & 723 \\ 65.4 & 56.8 & -65.4 & -56.8 \\ -1.24 \cdot 10^4 & -1.35 \cdot 10^4 & 1.24 \cdot 10^4 & 1.35 \cdot 10^4 \end{array}\right] \quad \text{(A.4.1)}$$

A.4.2 EMRAW gain for system (4.5.1)

An EMRAW has been computed in Section 4.5.1 has been computed using the objective-based algorithm. The gain E_{aw} obtained reads:

$$E_{aw} = \left[\begin{array}{cccccccc} -0.03 & -0.03 & 0.03 & 0.03 & 1.38 & 1.87 & -1.38 & -1.87 \\ -0.001 & -0.001 & 0.001 & 0.001 & 0.03 & 0.07 & -0.03 & -0.07 \\ -0.21 & -0.21 & 0.21 & 0.21 & 8.98 & 10.7 & -8.98 & -10.7 \\ 19.05 & 19.05 & -19.05 & -19.05 & -85.1 & -91.7 & 85.1 & 91.7 \\ 0.82 & 0.82 & -0.82 & -0.82 & -36.1 & -42.3 & 36.1 & 42.3 \\ -39.6 & -39.6 & 39.6 & 39.6 & 156 & 210 & -156 & -210 \end{array}\right] \quad \text{(A.4.2)}$$

A.5 16-state formation numerical values

A.5.1 16-states formation state matrices

The 16-state plant representation can be described by the following equations:

$$\begin{aligned} \dot{x}_p &= A_p x_p + B_p u_p \\ y_p &= C_p x_p \end{aligned} \tag{A.5.1}$$

where:

$$x_p = \left[\theta_{x_1}\ \theta_{y_1}\ \theta_{z_1}\ \dot{\theta}_{x_1}\ \dot{\theta}_{y_1}\ \dot{\theta}_{z_1}\ \theta_{x_2}\ \theta_{y_2}\ \theta_{z_2}\ \dot{\theta}_{x_2}\ \dot{\theta}_{y_2}\ \dot{\theta}_{z_2}\ \Delta y\ \Delta z\ \Delta\dot{y}\ \Delta\dot{z}\right]'$$

$$y_p = \left[\theta_{x_1} \quad \theta_{y_1} \quad \theta_{z_1} \quad (\theta_{x_2} - \theta_{x_1}) \quad (\theta_{y_2} - \theta_{y_1}) \quad (\theta_{z_2} - \theta_{z_1}) \quad \Delta y \quad \Delta z\right]'$$

$$u_p = \left[F_{y_1}\ F_{z_1}\ C_{x_1}\ C_{y_1}\ C_{z_1}\ C_{x_2}\ C_{y_2}\ C_{z_2}\right]'$$

$$A_p = \begin{bmatrix} 0_{(3\times3)} & I_3 & & & & \\ 0_{(3\times3)} & 0_{(3\times3)} & & & & \\ & & 0_{(3\times3)} & I_3 & & \\ & & 0_{(3\times3)} & 0_{(3\times3)} & & \\ & & & & 0_{(2\times2)} & I_2 \\ & & & & 0_{(2\times2)} & 0_{(2\times2)} \end{bmatrix}$$

$$B_p = \begin{bmatrix} 0_{(3\times2)} & \cdots & 0_{(3\times3)} \\ 0_{(3\times2)} & J_{G_1}^{-1} & 0_{(3\times3)} \\ 0_{(3\times2)} & \cdots & 0_{(3\times3)} \\ 0_{(3\times2)} & 0_{(3\times3)} & J_{G_2}^{-1} \\ 0_{(2\times2)} & 0_{(2\times3)} & 0_{(2\times3)} \\ M_1^{-1}\ 0 & 0_{(1\times3)} & \Delta x J_{G_2(3,:)}^{-1} \\ 0\ M_1^{-1} & 0_{(1\times3)} & \Delta x J_{G_2(2,:)}^{-1} \end{bmatrix}$$

$$C_p = \begin{bmatrix} I_3 & 0_{(3\times3)} & 0_{(3\times3)} & \cdots & \cdots & 0_{(3\times2)} \\ -I_3 & 0_{(3\times3)} & I_3 & 0_{(3\times3)} & \cdots & 0_{(3\times2)} \\ 0_{(2\times3)} & \cdots & \cdots & 0_{(2\times3)} & I_2 & 0_{(2\times2)} \end{bmatrix}$$

with J_{G_i} is the inertia matrix of the satellite $i = 1, 2$ at the center of mass and $J_{G_i(j,:)}^{-1}$ stands for the j^{th} line of the inverse of the inertia matrix.

A.5.2 16-states formation influence matrices

The influence matrices for the two satellites in the 16-state formation are described as follows:

$$M_1 = \begin{bmatrix} [1 & -1 & -1 & 1 & -1 & 1 & 1 & -1]\cos\alpha \\ [-1 & -1 & -1 & -1 & 1 & 1 & 1 & 1]\cos\alpha \\ [-c & c & c & -c & -c & c & c & -c]\cos\alpha \\ [-a & -a & a & a & a & a & -a & -a]\cos\alpha \\ [-a & a & -a & a & a & -a & a & -a]\cos\alpha \end{bmatrix} \tag{A.5.2}$$

$$M_2 = \begin{bmatrix} [-c & c & c & -c & -c & c & c & -c]\cos\alpha \\ [-a & -a & a & a & a & a & -a & -a]\cos\alpha \\ [-a & a & -a & a & a & -a & a & -a]\cos\alpha \end{bmatrix} \tag{A.5.3}$$

where a and c are dimensions associated to the distance of the thrusters to the satellite frame axes. $\alpha = \frac{\pi}{4}$ stands for the angle of the thrusters with respect to the satellite frame axes. Figure A.2 shows physical distribution of the thrusters for both satellites, as well as, the geometrical meaning of a, c and α.

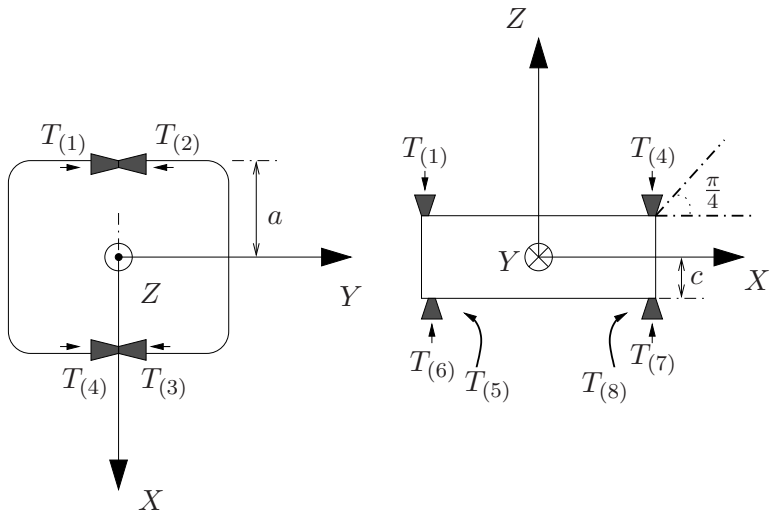

Figure A.2: Geometric distribution of the thrusters for a 8-DOF control configuration.

Bibliography

[Abs04] O. Absil. Science with pegase. *In Proceedings of* 2^{nd} *TPF/Darwin International Conference*, San Diego, CA, USA, July, 2004.

[ACL05] T. Alamo, A. Cepeda, and D. Limon. Improved computation of ellipsoidal invariant sets for saturated control systems. *In Proceedings of Conference on Decision and Control and European Control Conferenceas*, Seville, Spain, December, 2005.

[AG64] M.A. Azeirman and F.R. Gantmacher. Absolute stability of control systems. *Holden-Day, San Francisco*, 1964.

[AR89] K.J. Aström and L. Rundqwist. Integrator windup and how to avoid it. *In Proceedings of the American Control Conference*, Pittsburgh, PA, USA, 1989.

[BcPS07] G. Balas, R. chiang, A. Packard, and M. Safonov. Robust Control Toolbox user's guide. *The MathWorks Inc.*, 2007.

[BD95] K.A. Bordignon and W.C. Durham. Closed-form solutions to constrained control allocation problems. *AIAA Journal of Guidance, Control and Dynamics*, 18:1000-1007, 1995.

[BEGFB01] S. Boyd, L. El Ghaoui, E. Feron, and V. Balakrishnan. Linear matrix inequalities in systems and control theory. *Studies in Applied Mathematics 15, SIAM*, 2001.

[BHSB96] J.M. Berg, K.D. Hammet, C.A. Schwartz, and S.S. Banda. Analysis of the destabilizing effect of daisy chained rate-limited actuators. *IEEE Transactions on Control Systems Technology*, 4:171-176, 1996.

[BL02] A. Bateman and Z. Lin. An analysis and design methods for linear systems under nested saturations. *IEEE Transactions on Automatic Control*, 47(8):1305-1310, 2002.

[BPT+09] J. Boada, C. Prieur, S. Tarbouriech, C. Pittet, and C. Charbonnel. Anti-windup design for satellite control with microthrusteurs. *In Proceedings of AIAA GN&C conference*, Chicago, IL, USA, August, 2009.

[BPT+10a] J. Boada, C. Prieur, S. Tarbouriech, C. Pittet, and C. Charbonnel. Multi-saturation anti-windup structure for satellite control. *In Proceedings of the American Control Conference*, Baltimore, MD, USA, July, 2010.

[BPT+10b] J. Boada, C. Prieur, S. Tarbouriech, C. Pittet, and C. Charbonnel. Extended model recovery anti-windup for satellite control. *In Proceedings of the* 16^{th} *IFAC Symposium on Automatic Control in AeroSpace*, Nara, Japan, September, 2010.

[BRT07] J.M. Biannic, C. Roos, and S. Tarbouriech. A practical method for fixed-order anti-windup design. *In Proceedings of* 7^{th} *IFAC Symposium on Nonlinear Control Systems (NOLCOS)*, Pretoria, South Africa, August, 2007.

[BRTZ00] C. Barbu, R. Reginatto, A.R. Teel, and L. Zaccarian. Anti-windup for exponentially unstable linear systems with inputs limited in magnitude and rate. *In Proceedings of the American Control Conference*, Chicago, Il, USA, 2000.

[BS04] S. Boyd and L. S.P.Vandenberghe. Convex optimization. *Cambridge Univesity Press*, 2004.

[BT96] C. Burgat and S. Tarbouriech. Stability and control of saturated linear systems. *In A.J. Fossard and D. Normand-Cyrot (editors),* Non-Linear Systems*, vol.2. Chapman & Hall*, 1996.

[BT09] J.M. Biannic and S. Tarbouriech. Optimization and implementation of dynamics anti-windup compensators with multiple saturations in flight control systems. *Control Engineering Practice*, 17:703-713, 2009.

[BTF06] J.M. Biannic, S. Tarbouriech, and D. Farret. A practical approach to performance analysis of saturated systems with application to fighter aircraft controllers. *In Proceedings of the* 5^{th} *IFAC Symposium on Robust Control Design*, Toulouse, France, July, 2006.

[CG56] M. Chilali and P. Gahinet. H_∞ Design with pole placement contraints: an LMI approach. *IEEE Transactions on Automatic Control*, 41(3):358-367, 1956.

[Che84] C.T. Chen. Linear system theory and design. *Holtm Rinehart and Winston, Inc., New York*, 1984.

[CLW02] Y.Y. Cao, Z. Lin, and D. Ward. An anti-windup approach to enlarging domain of attraction for linear systems subject to actuator saturation. *IEEE Transactions on Automatic Control*, 47(1):140-145, 2002.

[CM90] P.J. Campo and M. Morari. Robust control of processes subject to saturation nonlinearities. *Computers and Chemical Engineering*, 14:343-358, 1990.

[CNE05] CNES. Spacecraft techniques and technology. *Volume 3. Cépaduès Editions*, 2005.

[CTQ08] E.B. Castelan, S. Tarbouriech, and I. Queinnec. Control design for a class of nonlinear continuous-time systems. *Automatica*, 44(8): 2034-2039, 2008.

[DS91] R.M. Dolphus and W.E. Schmitendorf. Stability analysis for a class of linear controllers under control constraints. *In Proceeding of* 30^{th} *IEEE Conference of Decision and Control*, Brighton, UK, December, 1991.

[Dur93] D.C. Durham. Constrained control allocation. *AIAA Journal of Guidance, Control and Dynamics*, 16:717-725, 1993.

[Dur94a] D.C. Durham. Attainable moments for the constrained control allocation problem. *AIAA Journal of Guidance, Control and Dynamics*, 17(6):1371-1373, 1994.

[Dur94b] D.C. Durham. Constrained control allocation: Three moment problem. *AIAA Journal of Guidance, Control and Dynamics*, 17(2):330-336, 1994.

[EM75] J. Elzinga and T.G. Moore. A central cutting plane algorithm for the convex programming problem. *Mathematical Programming*, 8(2):134-145, 1975.

[FB07] G. Ferreres and J.M. Biannic. Convex design of a robust anti-windup controller for an LFT model. *IEEE Tansactions on Automatic Control*, 52(11):2173-2177, 2007.

[FGZ10] F. Forni, S. Galeani, and L. Zaccarian. A family of global stabilizers for quasi-optimal control of planar linear saturated systems. *IEEE Transactions on Automatic Control*, 55(5):1175-1180, 2010.

[Fos02] T.I. Fossen. Marine control systems: Guidance, navigation and control of ships, rigs and underwater vehicles. *Trondheim: Marine Cybernetics*, 2002.

[FR67] H.A. Fertik and C.W. Ross. Direct digital control algorithm with anti-windup feature. *ISA Transactions*, 6:317-328, 1967.

[FY79] A.L. Fradkov and V.A. Yakubovich. The $\mathcal{S}$-procedure and a duality relations in nonconvex problems of quadratic programming. *Vestnik Leningrad University*, 6:101-109, 1979.

[GA94] P. Gahinet and P. Apkarian. A linear matrix inequality approach to H_∞ control. *International Journal Robust and Nonlinear Control*, 4(4):421-448, 1994.

[Gau07] S. Gaulocher. *Commande boucle fermée multivariable pour le vol en formation de vaisseaux spatiaux*. PhD thesis, Université de Toulouse, Toulouse, France, 2007.

[GdSJ97] J.M. Gomes da Silva Jr. *Sur la stabilité locale de systèmes linéaires avec saturation des commandes*. PhD thesis, Université Paul Sabatier, Toulouse, France, 1997.

[GdSJT99] J.M. Gomes da Silva Jr. and S. Tarbouriech. Polyhedral regions of local stability for linear discrete-time systems with saturating controls. *IEEE Transactions on Automatic Control*, 44(11): 2081-2085, 1999.

[GdSJT05] J.M. Gomes da Silva Jr. and S. Tarbouriech. Anti-windup design with guaranteed regions of stability: An LMI-based approach. *IEEE Transactions on Automatic Control*, 50(1):106-111, 2005.

[GdSJT06] J.M. Gomes da Silva Jr. and S. Tarbouriech. Anti-windup design with guaranteed regions of stability for discrete-time linear systems. *Systems and Control Letters*, 55(3):184-192, 2006.

[GdSJTR05] J.M. Gomes da Silva Jr., S. Tarbouriech, and R. Reginatto. Application of hybrid and polytopic modelling to the stability analysis of linear systems with saturation inputs. *Revista Controle & Automação*, 50(1):106-111, 2005.

[GH85] P.O. Gutman and P. Hagander. A new design of constrained controllers for linear systems. *IEEE Transactions on Automatic Control*, 30(1):22-33, 1985.

[GHP+03] G. Grimm, J. Hatfield, I. Postlethwaite, A.R. Teel, M.C. Turner, and L. Zaccarian. Anti-windup for stable linear systems with input saturation: an LMI-based synthesis. *IEEE Transactions on Automatic Control*, 48(9):1509-1525, 2003.

[GOTZ07] S. Galeani, A.R. Onori, A.R. Teel, and L. Zaccarian. Regional, semiglobal, global nonlinear anti-windup via switching design. *In Proceedings European Control Conference*, Kos, Greece, July, 2007.

[GPB91] J.C. Geromel, P.L.D. Peres, and J. Bernussou. On a convex parameter space method for linear control design of uncertain systems. *SIAM Journal of Control and Optimization*, 29(2):381-402, 1991.

[GT91] G. Gilbert and K.T. Tan. Linear systems with state and control constraints: The theory and application of maximal output admissible sets. *IEEE Transactions on Automatic Control*, 36(9):570-571, 1991.

[GTTZ09] S. Galeani, S. Tarbouriech, M.C. Turner, and L. Zaccarian. *A tutorial on modern anti-windup design*, volume 15(3-4):418-440. European Journal of Control, 2009.

[GTZ07] A.R. Galeani, A.R. Teel, and L. Zaccarian. Constructive nonlinear anti-windup design for exponentially unstable linear plants. *Systems and Control Letters*, 56(5):357-365, 2007.

[HL01] T. Hu and Z. Lin. Control systems with actuator saturation. Analysis and design. *Birkhauser*, 2001.

[HLC02] T. Hu, Z. Lin, and B.M. Chen. An analysis and design method for linear systems subject to actuator saturation and disturbance. *Automatica*, 38(2):351-359, 2002.

[HT99] D. Henrion and S. Tarbouriech. Output feedback robust stabilization of uncertain linear systems with saturating controls: an LMI approach. *IEEE Transactions on Automatic Control*, 44(11):2230-2237, 1999.

[HTP04] G. Herrman, M.C. Turner, and I. Postlethwaite. Some new results on anti-windup-conditioning using the weston-postlethwaite approach. *In Proceedings of IEEE Conference on Decision and Control*, Bahamas, 2004.

[HTZ05] T. Hu, A.R. Teel, and L. Zaccarian. Performance analysis of saturated systems via two forms of differential inclusions. *In Proceedings of IEEE Conference on Decision and Control*, Sevilla, Spain, December, 2005.

[Hug04] P.C. Hughes. Spacecraft attitude dynamics. *Dover books on engineering*, 2004.

[IH05] T. Iwasaki and S. Hara. Generalized KYP lemma: unified frequency domain inequalities with design applications. *IEEE Transactions on Automatic Control*, 50(1):41-59, 2005.

[Isi89] A. Isidori. Nonlinear control systems. *Springer-Verlag*, 1989.

[JFT05] T.A. Johansen, T.I. Fossen, and P. Tondel. Efficient optimal constrained control allocation via multi-parametric programming. *AIAA Journal of Guidance, Control and Dynamics*, 28:506-515, 2005.

[JR98] M. Johansson and A. Rantzer. Computation of piecewise quadratic Lyapunov functions for hybrid systems. *IEEE Transactions on Automatic Control*, 43(4): 555-559, 1998.

[KA01] P. Kokotovic and M. Arcak. Constructive nonlinear control: a historical perspective. *Automatica*, 37(5):637-662, 2001.

[Kal63] R.E. Kalman. Lyapunov functions for the problem of Lure in automatic control. *In Proceedings of the National Academy of Science of the USA*, 49(2):201-205, 1963.

[KCMN94] M.V. Kothare, P.J. Campo, M. Morari, and C.N. Nett. A unified framework for the study of anti-windup designs. *Automatica*, 30(12):1869-1883, 1994.

[KGE02] V. Kapila and K. Grigoriadis (Eds.). Actuator saturation control. *Marcel Dekker, Inc.*, 2002.

[Kha92] H.K. Khalil. Nonlinear systems. *MacMillan*, 1992.

[KM97] M.V. Kothare and M. Morari. Multivariable antiwindup controller synthesis using multi-objective optimization. *In Proceedings of the American Control Conference*, Albuquerque, NM, USA, 1997.

[KTP08] M.L. Kerr, M.C. Turner, and I. Postlethwaite. Practical approaches to low-order anti-windup compensator design: A flight control comparison. *In Proceedings of the World IFAC Congress*, Seoul, Korea, 2008.

[KTP10] M.L. Kerr, M.C. Turner, and I. Postlethwaite. Robust anti-windup control of SISO systems. *In Proceedings of the American Control Conference*, Baltimore, MD, USA, July, 2010.

[Lan03] P. Langouët. *Sur la stabilité locale de systèmes linéaires soumis à des actionneurs limités en amplitude et en dynamique*. PhD thesis, Université Paul Sabatier, Toulouse, France, 2003.

[Lev95] W.S. Levinde. The control handbook. *CRC - IEEE Press*, 1995.

[Loz56] J.C. Lozier. A steady-state approach to the theory of saturable servo systems. *IRE Transactions on Automatic Control*, 1:19-39, 1956.

[LP44] I.A. Lur'e and N.V. Postnikov. On the theory of stability of control systems. *Applied Mathematics and Mechanics*, 8(3):283-286, 1944.

[Lur57] I.A. Lur'e. Some nonlinear problems in the theory of automatic control. *H.M: Stationary Office, London*, 1957.

[Lya92] A.M. Lyapunov. The general problem of stability of motion. *International Journal of Robust and Nonlinear Control*, 55(3):531-773, 1992.

[MP96] V.R. Marcopoli and S.M. Phillips. Analysis and synthesis tools for a class of actuator-limited multivariable control systems: a linear matrix inequality approach. *International Journal of Robust and Nonlinear Control*, 6(9-10):1045-1063, 1996.

[MTBP06] A. Marcos, M.C. Turner, D.G. Bates, and I. Postlethwaithe. Robustification of static and low order anti-windup designs. *In Proceedings of the* 5^{th} *IFAC symposium on Robust Control Design*, Toulouse, France, July, 2006.

[MZ89] F. Morabito and E. Zafiriou. Robust process control. *Prentice Hall, Englewood Cliffs, NJ*, 1989.

[NN94] Y.E. Nesterov and A.S. Nemirovskii. Interior-point polynomial methods in convex programming: theory and applications. *Studies in Applied Mathematics 13, SIAM*, 1994.

[NW99] J. Nocedal and S.J. Wright. Numerical optimization. *New York: Springer-Verlag*, 1999.

[OS01] M.C. de Oliveira and R. Skelton. Stability test for constrained linear systems. *ch.15. LNCIS, 268. Springer*, 2001.

[PA01] D. Peaucelle and D. Arzelier. An efficient numerical solution for H_2 static output feedback synthesis. *In Proceedings of European Control Conference*, Porto, Portugal, 2001.

[PCU+05] L. Pirson, C. Charbonnel, B. Udrea, M. Rennie, P. McGuinness, and P. Palomo. Darwin precursor demonstration mission: The ICC2 study, from GNC design to real-time test bench validation. *In Proceedings of* 6^{th} *GNC ESA*, Loutraki, Greece, 2005.

[PDTP08] C. Pittet, N. Despré, S. Tarbouriech, and C. Prieur. Nonlinear controller design for satellite reaction wheels unloading using anti-windup techniques. *In Proceedings of AIAA GN&C conference*, Honolulu, HW, USA, August, 2008.

[PHS06] S. Ploen, F.Y. Hadaegh, and D.P. Scharf. Dynamics of drag-free formations for earth imaging applications. *In Proceedings of AIAA/AAS Astrodynamics Specialist Conference and Exhibit*, Keystone, CO, USA, August, 2006.

[Pop62] V.M. Popov. Absolute stability of nonlinear systems of automatic control. *Automation and Remote Control*, 22:857-875, 1962.

[PPT+05] C. Pittet, P. Prieur, A. Torres, A. Peus, and C. Fallet. MICROSCOPE: Myriade AOCS adaptation for a drag-free mission. *In Proceedings of* 6^{th} *GNC ESA*, Loutraki, Greece, 2005.

[PTH07] I. Postlethwaite, M.C. Turner, and G. Herrmann. Robust control applications. *An. Reviews Control*, 31(1):27-39, 2007.

[PZCG07] L. Pagnotta, L. Zaccarian, A. Constantinescu, and S. Galeani. Anti-windup applied to adaptive rejection of unknown narrow band disturbances. *In Proceedings of European Control Conference*, Kos, Greece, July, 2007.

[PZPB94] A. Packard, K. Zhou, P. Pandey, and G. Becker. A collection of robust control problems leading to LMI's. *In Proceedings of the* 30^{th} *IEEE Conference on Decision and Control*, Brighton, UK, December, 1994.

[QTG06] I. Queinnec, S. Tarbouriech, and G. Garcia. Anti-windup design for aircraft control. *In Proceedings IEEE Conference Control Applications (CCA)*, Munich, Germany, 2006.

[RB08] C. Roos and J.M. Biannic. A convex characterization of dynamically-constrained anti-windup controllers. *Automatica*, 44(8):2449-2452, 2008.

[RBTP07] C. Roos, J.M. Biannic, S. Tarbouriech, and C. Prieur. On-ground aircraft control law synthesis using an LPV anti-windup approach. *chapter 6. LNCIS, vol.365. Springer*, 2007.

[Roo97] C. Roos. *Contribution à la commande des systèmes saturés en présence d'incertitudes et de variations paramétriques. Application au pilotage de l'avion au sol.* PhD thesis, Université de Toulouse, Toulouse, France, 1997.

[SGC97] C. Scherer, P. Gahinet, and M. Chilali. Multiobjective output-feedback control via LMI optimization. *IEEE Transactions on Automatic Control*, 42(7):896-911, 1997.

[SIG97] R.E. Skelton, T. Iwasaki, and K. Grigoriadis. A unified algebraic approach to linear control design. *Taylor and Francis, London*, 1997.

[SJ09] J. Spjotvold and T.A. Johansen. Fault tolerant control allocation for a thruster-controlled floating platform using parametric programming. *In Proceedings of 28th Conference on Decision and Control*, Shanghai, China, December, 2009.

[SL91] J.J.E. Slotine and W. Li. Applied nonlinear control. *Prentice Hall*, 1991.

[Sor97] O.J. Sordalen. Optimal thrust allocation for marine vessels. *Control Engineering Practice*, 5:1223-1231, 1997.

[SS99] A.A. Stoorvogel and A. Saberi. Special issue: Control problems with constraints. *International Journal Robust Nonlinear Control*, 9(10):583-584, 1999.

[SSY94] H.J. Sussmann, E.D. Sontag, and Y. Yang. A general result on the stabilization of linear systems using bounded controls. *IEEE Transactions on Automatic Control*, 39(12):2411-2425, 1994.

[Sta09] O. Staffans. Well-posed linear systems. *Cambridge University Press*, 2009.

[Ste89] G. Stein. Bode lecture: respect the unstable. *In Proceedings of Conference on Decision and Control*, Tampa, USA, December, 1989.

[SW05] C. Scherer and S. Weiland. Linear Matrix Inequalities in control. *http://www.dcsc.tudelft.nl/%7Ecscherer/2416/lmi.html*, 2005.

[SWHK05] E. Schuster, M.L. Walker, D.A. Humphreys, and M. Krstic. Plasma vertical stabilization with actuation constraints in the DIII-D tokamak. *Automatica*, 41(7):1173-1179, 2005.

[Tee95] A.R. Teel. Semi-global stabilization of linear null controllable systems with input nonlinearities. *IEEE Transactions on Automatic Control*, 40(1):96-100, 1995.

[Tee99] A.R. Teel. Anti-windup for exponentially unstable linear systems. *International Journal Robust and Nonlinear Control*, 9(10):701-716, 1999.

[TGdSJB06] S. Tarbouriech, J.M. Gomes da Silva Jr., and F.A. Bender. Dynamic anti-windup synthesis for discrete-time linear systems subject to input saturations and $\mathcal{L}_2$ disturbances. *In Proceedings of the* 5^{th} *IFAC Symposium on Robust Control Design*, Toulouse, France, July, 2006.

[TGGE07] S. Tarbouriech, G. Garcia, and A.H. Glattfelder (Eds.). Advanced strategies in control systems with input and output constraints. *LNCIS, vol.346, Springer Verlag*, 2007.

[THP04] M.C. Turner, G. Herrmann, and I. Postlethwaite. Accounting for uncertainty in anti-windup synthesis. *In Proceedings of the American Control Conference*, Boston, USA, June, 2004.

[TK97a] A.R. Teel and N. Kapoor. The $\mathcal{L}_2$ antiwindup problem: its definition and solution. *In Proceedings of the* 4^{th} *European Control Conference*, Brussels, Belgium, July, 1997.

[TK97b] A.R. Teel and N. Kapoor. Uniting local and global controllers. *In Proceedings of the* 4^{th} *European Control Conference*, Brussels, Belgium, July, 1997.

[TP04] M.C. Turner and I. Postlethwaite. A new perspective on static and low order anti-windup synthesis. *International Journal of Control*, 77(1):27-44, 2004.

[TPGdSJ06] S. Tarbouriech, C. Prieur, and J.M. Gomes da Silva Jr. Stability analysis and stabilization of systems presenting nested saturations. *IEEE Transactions on Automatic Control*, 51(8):1364-1371, 2006.

[TT06] M.C. Turner and S. Tarbouriech. Anti-windup for linear systems with sensor saturation: sufficient conditions for global stability and $\mathcal{L}_2$ gain. *In Proceedings 45th IEEE Conference on Decision and Control*, San Diego, CA, USA,2006.

[TT09] S. Tarbouriech and M.C. Turner. Anti-windup synthesis: an overview of some recent advances and open problems. *IET Control Theory and Application*, 3(1):1-19, 2009.

[TZM06] A.R. Teel, L. Zaccarian, and J.J. Marcinkowski. An anti-windup strategy for active vibration isolation systems. *Control Engineering Practice*, 14(1):17-27, 2006.

[Val10] G. Valmorbida. *Analyse en stabilité et synthèse de lois de commande pour des systémes polynomiaux saturants*. PhD thesis, Université de Toulouse, Toulouse, France, 2010.

[VBW98] L. Vandenberghe, S. Boyd, and S.P. Wu. Determinant maximisation with linear matrix inequality constraints. *SIAM Journal on Matrix Analysis and Applications*, 29(2):449-533, 1998.

[Vid92] M. Vidyasagar. Nonlinear systems analysis. *Prentice Hall, Englewook Cliffs, second edition*, 1992.

[VMJ06] E. Villota, K. Murray, and S. Jayasuriya. A study of configurations for anti-windup control of uncertain systems. *In Proceedings of IEEE Conference on Decision and Control*, San Diego, CA, USA, 2006.

[Wil71] J.C. Willems. Least squares stationary optimal control and the algebraic Riccati equation. *IEEE Transactions on Automatic Control*, 16(6):621-634, 1971.

[WL03] W. Wu and B. Lu. Anti-windup control design for exponentially unstable LTI systems with actuator saturation. *Systems and Control Letters*, 52:305-322, 2003.

[WP98] P. F. Weston and I. Postlethwaite. Analysis and design of linear conditioning schemes for systems containing saturation actuators. *In Proceedings IFAC Nonlinear Control System Design Symposium*, Enschede, The Netherlands, July, 1998.

[WP00] P. Weston and I. Postlethwaite. Linear conditiong for systems containing saturating actuators. *Automatica*, 36(9):1347-1354, 2000.

[WPK05] H. Wong, H. Pan, and V. Kapila. Output feedback control for spacecraft formation flying with coupled translation and attitude dynamics. *In Proceedings of the American Control Conference*, Portland, OR, USA, June, 2005.

[Yak62] V.A. Yakubovich. The solution of certain matrix inequalities in automatic control theory. *Soviet Mathematics Dokladym*, 3:620-623, 1962.

[Yak71] V.A. Yakubovich. $\mathcal{S}$-procedure in nonlinear control theory. *Vestnik Leningrad University*, 1:62-77, 1971.

[Yak73] V.A. Yakubovich. Minimization of quadratic functionals under quadratic constraints and the necessity of a frequency condition in the quadratic criterion for absolute stability of nonlinear control systems. *Soviet Mathematics Dokladym*, 14(2):593-597, 1973.

[Yak92] V.A. Yakubovich. Nonconvex optimization problem: the infinite-horizon linear-quadratic control problem with quadratic constraints. *System and Control Letters*, 19(1):13-22, 1992.

[ZT02] L. Zaccarian and A.R. Teel. A common framework for anti-windup, bumpless transfer and reliable designs. *Automatica*, 38(10):1735-1744, 2002.

[ZWT07] L. Zaccarian, E. Weyer, and A.R. Teel. Anti-windup for marginaly stable plants and its application to open water chanel control systems. *Control Engineering Practice*, 15(2):261-272, 2007.

List of Publications

1. J. Boada, C. Prieur, S. Tarbouriech, C. Pittet and C. Charbonnel "Anti-windup design for Satellite Control with Microthrusteurs", *In Proceedings of AIAA GN&C conference*, Chicago, IL, USA, 8 - 12 August 2009.

2. J. Boada, C. Prieur, S. Tarbouriech, C. Pittet and C. Charbonnel , "Multi-saturation Anti-windup Structure for Satellite Control", *In Proceedings of IEEE American Control Conference*, Baltimore, MD, USA, 30 - 2 July 2010.

3. J. Boada, C. Prieur, S. Tarbouriech, C. Pittet and C. Charbonnel , "Extended Model Recovery Anti-Windup for Satellite Control", *In Proceedings of the* 16^{th} *IFAC Symposium on Automatic Control in AeroSpace*, Nara, Japan, 6 - 10 September 2010.

Résumé de la thèse:

Sur la commande de satellites à entrées saturantes

(Satellite control with saturating inputs)

Josep Boada Bauxell

Sous l'encadrement de :

Dr. Sophie Tarbouriech Directrice de thèse
Dr. Christophe Prieur Co-directeur de thèse

Travail financé par le CNES et Thales Alenia Space.
Preparé au LAAS-CNRS
7, Avenue Colonel Roche − 31077 Toulouse Cedex 4, France.

Résumé étendu

I.1 Introduction générale

La théorie de la commande a evolué de façon significative dans le domaine de l'automatique non-linéaire. Dernièrement, des méthodes d'analyse et de synthèse sont apparues en proposant des outils de résolution pour des problèmes de commande non-linéaire [TGGE07, KGE02, KA01, Val10]. Cependant, les méthodes utilisées actuellement dans l'industrie aérospatiale sont le plus souvent basée sur des techniques de commande linéaire. Les spécifications, toujours plus exigeantes en termes de fiabilité et performance, demandent l'utilisation de techniques de plus en plus complexes [PCU+05, PDTP08, KTP08]. Ainsi, l'industrie cherche des solutions dans les nouvelles techniques de la théorie de la commande non-linéaire dont le potentiel est encore inexploré lors de son application sur des systèmes réelles. Ces méthodes améliorent la synthèse des lois de commande et la modélisation des phénomènes non-linéaires auparavant négligés. Enfin, la mis en oeuvre des outils d'analyse non-linéaire peut se traduire par une réduction du temps de validation due au fait que la distance entre le modèle considéré et le vrai système serait réduite. Ces améliorations pourraient aussi se traduire par une réduction du coût total des ressources utilisées pour la validation des lois de pilotage. Par conséquent, il y a un vrai besoin d'application de d'adaptation des outils de commande non-linéaire aux problèmes de l'industrie.

En particulier, la limitation de la commande due aux contraintes de capacité des actionneurs répresente un phénomène non-linéaire commun dans la plupart des systèmes physiques. Une solution classique dans l'industrie consiste à imposer des marges importantes afin d'empêcher que les actionneurs ne dépassent leur limite, c'est-à-dire, qu'ils saturent. De cette manière, on essaye d'assurer la linéarité du système sur tout son domaine de fonctionnement. Toutefois, la validation *a posteriori* peut apparaître comme insuffissante car, des perturbations non-nominales, des transitions entre différents modes de mission et la présence de pannes peuvent amener les actionneurs à la limite de leurs capacités. Des actionneurs saturés peuvent engendrer la dégradation des performance, l'apparition de cycles limites ou d'états d'équilibre non désirés et même l'instabilité du système bouclé [AR89, HL01, KGE02, Ste89].

Les techniques de commande non-linéaire concernant la saturation peuvent être classées

selon deux lignes de recherche. La première vise la synthèse d'un unique correcteur qui tient compte de la saturation [GdSJ97, GT91, GH85]. La seconde, ajoute une boucle additionnelle à la boucle de commande linéaire déjà existante. Cette deuxième boucle de commande est dédiée à la gestion de la saturation. Dans un contexte où l'accent est mis sur le coté applicatif, on retiendra la deuxième stratégie. Cette approche, nommée commande anti-windup, permet à l'automaticien de garder les méthodes de commande linéaire qui ont déjà été validées puisqu'il s'agit seulement d'ajouter un contrôleur additionnel, actif seulement lorsque la saturation apparaît. De cette manière, le processus de synthèse du contrôleur n'est pas complètement changé comme cela aurait été le cas avec la première approche. Par conséquent, le développement de méthodes constructives pour la synthèse de l'anti-windup pour les non-linéarités dues aux saturations est complètement justifié. Pour une vision plus complète, les articles [GTTZ09, TT09] et leurs références pourront être consultées.

Le but de la thèse est d'adapter et de développer les techniques de synthèse anti-windup à la commande de haute précision des axes angulaires et linéaires de satellites. Dans le domaine spatial, cet objectif se retrouve dans les missions de commande en accélération et aussi dans celle de vol en formation. Ces missions utilisent des propulseurs de haute précision comme actionneur. Cependant, leur capacité maximale est très baisse. Ces actionneurs ont aussi pour fonction d'assurer la transition entre les modes de la mission, la robustesse face aux perturbations externes et, dans certains cas, la survie de la mission. L'introduction de l'anti-windup est donc une technique d'intérêt afin d'assurer les besoins de la mission et sa fiabilité.

Les missions qui utilisent des systèmes propulsifs comme actionneur présentent une modélisation particulière. En effet, les variables de contrôle ne correspondent pas à la véritable action des propulseurs. Une fonction de répartition est incluse dans la modélisation des actionneurs afin de répartir les commandes du contrôleur parmi les propulseurs [Dur93, NW99, BHSB96]. Dans l'approche linéaire classique cette fonction peut être négligée. Cependant, lorsqu'il y a saturation des propulseurs, son comportement doit être pris en compte pour la synthèse [BHSB96]. Des fonctions de répartition adaptées à la synthèse anti-windup ont été étudiées. De plus, la présence de propulseurs introduit une modélisation particulière de la saturation. La saturation présente des bornes asymétriques dont la valeur minimum est égale à zéro. Tenant compte de l'état de l'art de la synthèse anti-windup, il y a un vrai besoin d'utiliser des techniques de symétrisation pour la saturation.

La procédure de symétrisation ainsi que la définition de la fonction de répartition sont introduites lors de la synthèse de l'anti-windup afin de pouvoir utiliser ce contrôleur dans le cadre d'une mission de vol en formation. Le contrôle simultané de l'attitude et de la position relative constitue un cadre intéressant pour tester les techniques proposées. Le caractère multi-objectifs des missions de vol en formation introduit des couplages parmi les dynamiques angulaires et linéaires. En outre, la transition depuis un mode de basse précision vers un autre de haute précision peut amener à la saturation des actionneurs. Pour ces situations où la commande linéaire n'est pas suffisante, l'utilisation d'un correcteur

anti-windup constitue une voie d'amélioration poténtielle.

Le manuscrit de cette thèse s'organisse de la manière suivante :

- Le chapitre 1 rappelle les outils de base nécessaires à l'analyse de la stabilité pour les systèmes soumis à des non-linéarités de type saturation. Ces outils sont la base des résultats présentés dans le chapitre 3.
- Le problème de la symétrisation de la saturation, abordée dans le chapitre 2, est un préalable à la compréhension du sujet principal de la thèse : la commande anti-windup. Ce chapitre présente la famille des systèmes auxquels ce travail s'intéresse. Des techniques de symétrisation sont proposées avec des exemples pratiques [BPT+09]. Elles permettent d'écrire le problème dans un contexte général où les techniques anti-windup peuvent s'appliquer.
- Le chapitre 3 est dédié au dévéloppement de méthodes anti-windup. Une vision générale du problème est proposée à travers l'analyse de l'état de l'art. En particulier, la description des deux principales approches dans la synthèse anti-windup est donnée. Des outils pour chacune d'elles sont apportés. En plus, une troisième approche est proposée comme alternative aux deux précédentes [BPT+10b]. Le chapitre se conclut par l'analyse de la validité des résultats précédents sur des systèmes présentant des saturations asymétriques. Une illustration de ces approches permet au lecteur d'avoir une vision des avantages et inconvénients de chaque technique.
- Les deux derniers chapitres sont dédiés à la présentation des exemples d'application sur lesquels l'anti-windup est testé. D'abord, le chapitre 4 présente trois configurations de missions en vol en formation. La modélisation de ces cas d'études est présentée. Ensuite, les simulations illustrent les avantages de l'anti-windup [BPT+10a]. Finalement, le chapitre 5 est dédié à l'étude d'une mission en contrôle d'accélération. Le modèle du cas d'étude est présenté ainsi que des simulations. Les résultats mettent en évidence le potentiel du correcteur anti-windup.

Nous présentons ici un résumé des travaux de cette thèse. Chaque chapitre est résumé pour mettre en évidence les différents problèmes abordés. Nous prenons aussi le temps de présenter les théoremes ou propositions qui représentent la contribution de cette thèse. En même temps une application numérique est proposée comme illustration de ces résultats.

I.2 Concepts généraux sur la stabilité de systèmes saturés

Ce chapitre est dédié à la présentation des outils de base pour l'analyse des systèmes non-linéaires soumis à des saturations. La présentation des définitions et résutats n'est

pas exhaustive, mais elle rappelle quelques points clés pour la compréhension des résultats développés dans ce manuscrit. Les résultats sont classiques dans la littérature et peuvent se retrouver, par exemple, dans les travaux de Khalil [Kha92], Slotine et Li [SL91] et Vidyasagar [Vid92].

D'abord, une définition génerale de la stabilité des systèmes autonomes est donnée. Cette définition est concrétisée par la théorie de Lyapunov et la seconde méthode de Lyapunov est détaillée.

I.2.1 Stabilité au sens de Lyapunov

La stabilité au sens de Lyapunov est mise en pratique par ce qu'on appelle la seconde méthode de Lyapunov. Cette méthode vise à caractériser la stabilité du système autour d'un point d'équilibre sans connaître explicitement les trajectoires autour de ce point. La seconde méthode de Lyapunov est définie de la façon suivante :

Définition I.1. *Une fonction de Lyapunov candidate est une fonction* $V : \mathcal{X} \subseteq \Re^n \rightarrow \Re^+$ *telle que* V *est continue, de même que ses dérivés partielles, et* V *est définie positive (i.e* $V > 0\ \forall x \neq 0$ *et* $V(0) = 0$*).*

Le théorème suivant donne des conditions suffisantes pour la stabilité des systèmes autonomes.

Théorème I.1. *Etant donné un ensemble* $\mathcal{X} \subset \Re^n$ *qui contient l'origine et* $V : \mathcal{X} \rightarrow \Re^+$ *une fonction Lyapunov candidate.*

1. *Si* $\dot{V}(x) \leq 0\ \forall x \in \mathcal{X}$*, alors l'origine est* **localement stable**.
2. *Si* $\dot{V}(x) < 0\ \forall x \in \mathcal{X}$*,* $x \neq 0$ *, alors l'origine est* **localement asymptotiquement stable**.

où $\dot{V}$ *est la dérivée temporelle de* V

I.2.2 Fonctions de saturation et zones mortes

La saturation est le type de non-linéarité considérée dans ce manuscrit. Une modélisation pour la fonction de saturation est proposée par la suite. Considerons $u \in \Re^m$ le vecteur de commande, la fonction de saturation se défini comme :

$$\Psi_{(\underline{u},\bar{u})} : \begin{cases} \Re^m & \rightarrow & \Re^m \\ u & \rightarrow & \Psi_{(\underline{u},\bar{u})}(u) = sat_{(\underline{u},\bar{u})}(u) \end{cases} \tag{I.2.1}$$

où $\underline{u}_{(i)} < 0$ et $\bar{u}_{(i)} > 0$, $\forall i = 1, ..., m$, sont les bornes inférieures et supérieures de la saturation. En général, seule la fonction de saturation décentralisée est considérée pour chaque composante $i = 1, ..., m$:

$$sat_{(\underline{u},\bar{u})}(u(t))_{(i)} = sat_{(\underline{u},\bar{u})}(u_{(i)}(t)) = \begin{cases} \bar{u}_{(i)} & \text{if } u_{(i)}(t) > \bar{u}_{(i)} \\ u_{(i)}(t) & \text{if } \underline{u}_{(i)} \leq u_{(i)}(t) \leq \bar{u}_{(i)} \\ \underline{u}_{(i)} & \text{if } u_{(i)}(t) < \underline{u}_{(i)} \end{cases} \tag{I.2.2}$$

Normalement, afin de simplifier le problème, la saturation est considérée symétrique de telle sorte que $\bar{u} = -\underline{u}$. Quand les deux bornes sont égales en valeur absolue la notation est simplifiée. Les bornes sont remplacées par $u_0 = |\bar{u}| = |\underline{u}|$. Les saturations symétriques sont designées avec la notation suivante : $sat_{(u_0)}(u)$.

Une autre répresentation possible de la limitation des actionneurs est donnée par la fonction zone morte qui est définie par :

$$\begin{aligned} \phi_{(u_0)}(u) &= u - sat_{(u_0)}(u) \\ \phi_{(u_0)}(u_{(i)}) &= \begin{cases} u - u_{0(i)} & \text{if } u_{(i)} > u_{0(i)} \\ 0 & \text{if } -u_{0(i)} \leq u_{(i)} \leq u_{0(i)} \\ u + u_{0(i)} & \text{if } u_{(i)} < -u_{0(i)} \end{cases} \end{aligned} \tag{I.2.3}$$

I.2.3 Condition de secteur

Les conditions de stabilité convexes, pour des systèmes soumis à des saturations, peuvent être obtenues en utilisant des non-linéarités de secteur modélisant les fonctions de saturation et les zones mortes. Une approche a été développée par [GdSJT05, TPGdSJ06] afin d'inclure la saturation dans une non-linéarité de secteur. Considerons la fonction zone morte $\phi_{(u_0)}(\cdot)$, definie par (I.2.3). Considerons l'ensemble polyédral suivant :

$$\mathcal{S}(u_0) = \left\{(u, \omega) \in \Re^m \times \Re^m; \left|u_{(i)} + \omega_{(i)}\right| \leq u_{0_{(i)}}, i = 1, ..., m\right\} \tag{I.2.4}$$

Alors le lemme suivant peut être établi.

Lemme I.1. *[GdSJT06] Considerons la fonction $\phi_{(u_0)}(u)$ définie par (I.2.3). Si u et ω appartiennent à $\mathcal{S}(u_0)$ la relation suivante est satisfaisante :*

$$\phi_{(u_0)}(u)'T[\phi_{(u_0)}(u) + \omega] \leq 0 \tag{I.2.5}$$

pour toute matrice $T \in \Re^{m \times m}$ diagonale et définie positive.

Cette dernière caractérisation constitue une importante avancée car elle permet d'obtenir une formulation convexe du problème de synthèse anti-windup, autant dans le cas de la synthèse d'un correcteur statique [GdSJT05, BT09] que dynamique [BRT07].

De plus ce résultat comporte des corollaires pour l'estimation du domaine de stabilité des systèmes soumis à des saturations. Il s'agit d'un résultat classique mis sous forme des LMIs [Kha92, SL91, Vid92, SW05].

I.3 La fonction saturation asymmétrique

D'habitude, le contrôle de satellites est limité au contrôle d'attitude (sans se préoccuper de la position relative). Il s'agit d'assurer la bonne orientation du satellite afin de satisfaire aux exigences de la mission. Les actionneurs utilisés pour ce type de commande sont des roues à réaction [CNE05]. Le principe est de corriger les couples perturbateurs par une boucle de contrôle impliquant les actionneurs précédents. Cependant, les futures missions spatiales exigeront la commande de l'accélération ou de la position relative. Ces spécifications impliquent l'utilisation d'actionneurs capable de réaliser un effort sur l'axe linéaire. Par conséquent, des systèmes propulsifs doivent être utilisés.

Ce genre de systèmes propulsifs présente souvent une fonction de répartition [Dur93]. Les systèmes dynamiques comme les satellites sont modélisés par les équations classiques de la dynamique. Dans ces équations, les accélérations linéaires et angulaires sont définies comme une fonction dépendant d'un vecteur de forces et de couples externes. Pourtant, l'action qui contrôle le satellite est réalisée par un système propulsif qui génère une impulsion continue unidirectionelle. Une fonction déterminant la façon dont on génère le torseur de commande (forces et couples) avec un ensemble redondant d'actionneurs est donc nécessaire. Les fonctions de distribution sont chargées de ce transfert. Dans le chapitre 2, une introduction générale sur la fonction de repartition est proposée. Normalement ces fonctions sont très non-linéaires ce qui empêche les techniques classiques de l'anti-windup de s'appliquer. C'est pourquoi certaines fonctions permettant la synthèse anti-windup ont été preséntées.

Les propulseurs à haute précision ont une capacité limitée. Il faut donc inclure des fonctions de saturation lors de leur modélisation. De plus, c'est la saturation qui nous oblige à devoir tenir compte de la fonction de distribution. L'autre problème lié aux propulseurs est que leurs limites de fonctionnement sont asymétriques et donc la fonction saturation l'est également. En fait, ce genre d'actionneur génère seulement une propulsion positive. Normalement dans la littérature, aussi bien pour l'analyse de la stabilité des systèmes saturés que pour la synthèse anti-windup, seulles les saturations symétriques sont traitées. Quelques travaux ont symétrisé la saturation avec une approche conservative qui consiste à prendre la borne minimale en valeur absolue comme unique borne de la saturation [Lan03]. Cette technique n'est pas valable pour la saturation des propulseurs.

En revanche, dans le chapitre 2 des techniques de symétrisation ont été présentées.

Le système en boucle fermée considéré dans cette thèse est décrit par le schéma bloc de la figure I.3 et est défini par la représentation dans l'espace d'état suivante:

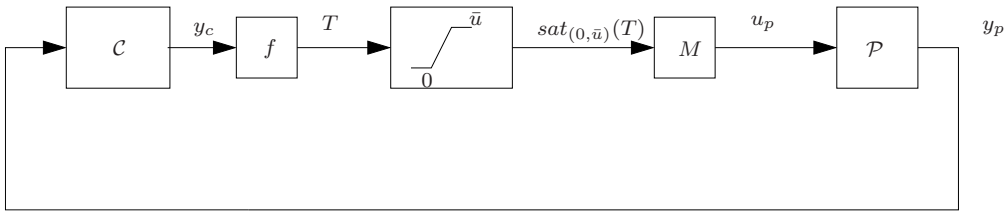

Figure I.3: Système en boucle fermée étudié.

$$\begin{cases} \dot{x}_p = A_p x_p + B_p u_p \\ \dot{x}_c = A_c x_c + B_c C_p x_p \\ u_p = M sat_{(0,\bar{u})}(f(y_c)) \\ y_c = C_c x_c + D_c C_p x_p \end{cases} \tag{I.3.1}$$

où $x_p \in \Re^{n_p}$ est l'état du système, $y_p \in \Re^q$ la sortie mesurée et $u_p \in \Re^{m_c}$ la commande. $x_c \in \Re^{n_c}$ est l'état du contrôleur et $y_c \in \Re^{m_c}$ la sortie de contrôleur.

Le lien entre la sortie du contrôleur y_c et la commande u_p est assuré par le système propulsif. Une fonction de répartition notée f lie y_c au vecteur propulsif $T \in \Re^m$. Ensuite T est lié à u_p à travers la matrice d'influence $M \in \Re^{m_c \times m}$. Entre les deux on retrouve la limitation de capacité décrite par la fonction de saturation décentralisée : $sat_{(0,\bar{u})}(T_{(i)})$

I.3.1 Introduction à la fonction de distribution

Une fonction de répartition (AF) est un algorithme nécessaire pour distribuer la sortie du contrôleur parmi les différents propulseurs. Sans tenir compte de la boucle de contrôle, l'algorithme de répartition calcule la solution optimale pour les propulseurs à partir du torseur de commande issu du contrôleur.

En général, trouver une AF est un problème d'optimisation dynamique non-linéaire étant donné qu'il y a des contraintes à considérer comme la capacité des actionneurs. Le problème peut être résolu en utilisant des techniques d'optimisation non-linéaire [NW99], e.g., programmation quadratique. La communauté aérospatiale a traité ce problème depuis longtemps. Les techniques les plus utilisées sont basées sur les travaux de Durham [Dur93, Dur94b, Dur94a] et des stratégies par chaîne d'actionneurs [BHSB96]. D'autres AF sont établies à partir d'un modèle linéaire qui décrit le rapport entre les propulseurs et le torseur de commande. Celui-ci permet l'application des solutions explicites par moindres carrés. Dans ce dernier cas, l'AF peut être mis en oeuvre à travers de simples opérations matricielles comme l'inverse généralisé [Sor97].

Deux fonctions de répartition sont proposées. Une est linéaire et l'autre est non-linéaire mais avec des non-linéarités traitables avec les techniques présentées dans le chapitre 1. Elles sont présentés ci-dessous :

$$T = f(y_c) = M^* y_c \tag{I.3.2}$$

où M^* est la matrice pseudo-inverese de la matrice d'influence, c'est-à-dire, $M^* = M^{'}(MM^{'})^{-1}$. L'autre fonction de répartition est donnée par :

$$\begin{aligned} T = f(y_c) =& sat_{1(0,\bar{u})}(M^*_{(:,1)} y_{c(1)}) + sat_{2(0,\bar{u})}(M^*_{(:,2)} y_{c(2)}) + \cdots \\ &+ sat_{m_c(0,\bar{u})}(M^*_{(:,m_c)} y_{c(m_c)}) \end{aligned} \tag{I.3.3}$$

I.3.2 Symétrisation de la fonction de saturation

Les saturations considérées étant, elles, asymétriques, on présente des méthodes de symétrisation. Dans [Lan03] il est proposé de garder la valeur de la plus petite de ces deux bornes, supérieure et inférieure, en valeur absolue. Le lemme suivant formalise cette technique:

Lemme I.2. *Soit $sat_{(\underline{u},\bar{u})}(\cdot)$ une saturation asymétrique où $\underline{u} < \bar{u}$. La saturation peut se symétriser comme suit $sat_{(-u_0,u_0)}(\cdot)$ avec u_0*

$$u_0 = min(|\underline{u}|, |\bar{u}|) \tag{I.3.4}$$

Le lemme I.2 néglige une partie de la capacité, ce qui introduit du conservatisme. De plus dans le cas où l'on travaille avec des propulseurs, pour lesquels la borne minimale $\underline{u} = 0$, on ne peut pas utiliser cette technique car la borne symétrique résultant est $u_0 = 0$.

I.3.3 Symétrisation basée sur le noyau

Il est clair que l'introduction d'un vecteur constant dans la saturation modifie ses bornes. Plus précisèment:

Propriété I.1. *Condidérons u et $N\zeta$ appartenant à $\Re^m$, $N\zeta$ un vecteur constant. La propriété suivante est vérifiée:*

$$sat_{(0,\bar{u})}(u + N\zeta) = sat_{(-N\zeta,\bar{u}-N\zeta)}(u) + N\zeta \tag{I.3.5}$$

sous la contrainte que

$$0 < N\zeta_{(i)} < \bar{u}_{(i)}, \quad i = 1, ..., m. \tag{I.3.6}$$

Pourtant, des contraintes supplémentaires doivent être prises en compte si on veut que l'introduction du vecteur $N\zeta$ ne modifie pas la dynamique du système linéaire en boucle fermée :

Lemme I.3. *Soient $N\zeta \in Ker(M)$, c'est-à-dire, $MN\zeta = 0$. Alors:*

1. *pendant la zone linéaire (sans saturation), u_p n'est pas modifié car $u_p = MT = M(f(y_c) + N\zeta) = Mf(y_c) = y_c$.*
2. *pendant la zone non-linéaire (avec saturation), u_p est légèrement modifié car $u_p = Msat_{(0,\bar{u})}(f(y_c) + N\zeta) = Msat_{(-N\zeta,\bar{u}-N\zeta)}(f(y_c))$.*

Avec la Propriété I.1 et le Lemme I.3 on peut définir le vecteur symétrisant candidat.

Définition I.2. *S'il existe $N\zeta$ satisfaisant $0 < N\zeta_{(i)} < \bar{u}_{(i)}$, $i = 1, ..., m$, et $MN\zeta = 0$ (i.e. $N\zeta$ appartient à $Ker(M)$), alors $N\zeta$ est nommé vecteur symétrisant candidat.*

L'existence de $N\zeta$ modifie les bornes de la saturation, mais si on égalise ces dernières, alors on pourrait appliquer la relation (I.3.4) sans introduire de conservatisme. Cela est possible avec un certain $N\zeta$ nommé vecteur symétrisant :

Définition I.3. *Un vecteur symétrisant candidat $N\zeta$ est un vecteur symétrisant $N\zeta_{sym}$ quand les valeurs absolues des deux bornes, supérieure et inférieure, sont égales :*

$$| - N\zeta_{sym(i)}| = |\bar{u}_{(i)} - N\zeta_{sym(i)}|, \quad i = 1, ..., m. \tag{I.3.7}$$

Alors

$$N\zeta_{sym} = \frac{\bar{u}_{(i)}}{2}, i = 1, ..., m. \tag{I.3.8}$$

Si un tel vecteur existe alors la saturation est symétrisée sans conservatisme :

Lemme I.4. *[BPT+09] S'il existe un vecteur symétrisant donné par la Définition I.3, une fonction de saturation asymétrique $sat_{(0,\bar{u})}(\cdot)$, peut se symétriser sous la forme $sat_{(-u_0,u_0)}(\cdot) = sat_{(u_0)}(\cdot)$ où u_0 est défini comme*

$$u_0 = \frac{\bar{u}}{2}. \tag{I.3.9}$$

Selon la Définition I.2, le vecteur symétrisant $N\zeta_{sym} = \frac{\bar{u}}{2}$ doit vérifier l'appartenance au noyau de M, c'est-à-dire, $\frac{\bar{u}}{2} \in Ker(M)$ (i.e. $M\frac{\bar{u}}{2} = 0$). Ceci est vrai si le lemme suivant est vérifié :

Lemme I.5. *$N\zeta_{sym} = \frac{\bar{u}}{2}$ est un vecteur symétrisant candidat si $\sum_{i=1}^{m} M_{(j,i)} = 0$ et $\bar{u}_{(i)} = \bar{u}_{(k)}$ pour $j = 1, ..., m_c$, $i = 1, ..., m$, $k = 1, ..., m$ et $i \neq k$.*

I.3.4 Symétrisation par fonction variable du noyau

Lorsque la fonction de saturation est symétrisée, le terme $N\zeta_{sym}$ est ajouté à f. En l'absence de perturbation, le point d'équilibre est $x_{eq} = 0$ et la sortie du contrôleur est nulle $y_{c_{eq}} = 0$. Cependant la poussée T n'est pas égale à zéro :

$$T_{eq} = f(y_{c_{eq}}) + N\zeta_{sym} = \underbrace{f(0)}_{0} + \frac{\bar{u}}{2} = \frac{\bar{u}}{2} \tag{I.3.10}$$

Cette poussée à l'équilibre est totament inutile et, de surcroît, diminue le temps de vie de la mission de part la consommation de carburant qu'elle implique. La prochaine étape est de proposer une fonction $N\zeta_{var}$ qui évolue avec y_c de telle sorte qu'elle symétrise la saturation quand l'actionneur sature, et qui amène la poussée à zéro à l'équilibre.

Définition I.4. *[BPT+09] Une fonction vecteur $N\zeta_{var}(y_c) : \Re^{m_c} \to \Re^m$ est une fonction variable du noyau (VKF) si :*

1. $N\zeta_{var(i)} = \frac{\bar{u}(i)}{2} = N\zeta_{sym(i)}$ *si*

   $$\left(f_{(i)}(y_c) + N\zeta_{var(i)}\right) < 0 \text{ où } \left(f_{(i)}(y_c) + N\zeta_{var(i)}\right) > \bar{u}_{(i)}$$

   Autrement dit, la fonction variable du noyau est égale au vecteur symétrisant quand le système est saturé : $|f_{(i)}(y_c)| > \frac{\bar{u}_{(i)}}{2}$.

2. *A la surface de commutation,* $|f_{(i)}(y_c)| = \frac{\bar{u}_{(i)}}{2}$, $N\zeta_{var(i)}$ *est continue avec* $N\zeta_{sym(i)}$, *c'est-à-dire,* $N\zeta_{var(i)} = N\zeta_{sym(i)} = \frac{\bar{u}_{(i)}}{2}$.

3. *Dans la zone linéaire,* $|f_{(i)}(y_c)| < \frac{\bar{u}_{(i)}}{2}$, $N\zeta_{var(i)}$ *est tel que*

   $$0 \leq f_{(i)}(y_c) + N\zeta_{var(i)} \leq \bar{u}_{(i)}$$

4. $N\zeta_{var(i)} \in Ker(M)$, *c'est-à-dire,* $MN\zeta_{var} = 0$.

Dans le chapitre 2 deux exemples possibles de fonctions variables du noyau ont été décrits et testés. Une comparaison a été faite entre le vecteur symétrisant et les VKF selon le niveau de la consomation.

Ces techniques permettent de considérer, pour la synthèse du correcteur anti-windup, un système avec saturation asymétrique comme un système avec des saturation symétriques. En se basant sur cela, la synthèse anti-windup a été présentée dans le chapitre 3 pour les systèmes avec saturation symétrique.

I.4 Méthodes de synthèse anti-windup

Le windup est un phénomène qui se manifeste par un important dépassement du signal de commande et un excessif temps de réaction à cause de la saturation des actionneurs. Le phénomène du windup fut detecté à la moitié du 20^{eme} siècle [Loz56]. Il apparaît le plus souvent dans le cas des systèmes qui utilisent des actionneurs de capacité limitée et qui présentent une boucle de contrôle avec un contrôleur composé par des intégrateurs, comme par exemple un PID [FR67, AR89]. Quand la saturation est active, l'erreur continue est intégrée, déformant le signal de commande. Négliger ces limitations peut engendrer des phénomènes indésirables (comme la dégradation de la performance) ou même catastophiques (comme la perte de la stabilité) [BHSB96].

Les saturations étant présentes dans la plupart des applications indutrielles, au vu des conséquences éventuelles présentées dans le paragraphe précédent, le calcul de lois de commande tenant compte de ces saturations constitue un défi de la plus grande importance. Plusieurs travaux ont étudié ce sujet dans la littérature et plusieurs techniques ont été développées vers cette direction.

Dans la littérature, les techniques permettant de faire face aux problèmes de la saturation peuvent globalement être répartie selon deux approches [TT09]. La première sera nommée comme l'approche par *une étape*. Le but est de trouver un unique contrôleur qui prend en compte les besoins en termes de performances ainsi que la présence de saturations. Ce contrôleur, qui peut être non-linéaire, essaie de satisfaire les spécifications nominales, tout en prenant en compte les contraintes de capacité. Cette approche a été étudiée par plusieurs travaux dans la littérature. D'abord quelques recherches ont montré différentes manières de calculer l'ensemble maximal de conditions initiales telles que la saturation est évitée et que le système résultant en boucle fermée suit le comportement linéaire [GT91, DS91]. D'une certaine manière, on pourrait dire que ces travaux essayent de savoir jusqu'à quel point le contrôleur peut traiter linéairement les limitations de l'entrée. Cependant, si la saturation est évitée, la performance et/ou le domaine de stabilité peuvent être moindre par rapport à ce qu'il pourrait être en réalité. Alors, pour ce type d'approche, un pas en avant est fait. Il s'agit de calculer une loi de commande qui maximise le domaine de stabilité tout en permettant la saturation de l'actionneur [GH85, HL01, KGE02, PTH07, TGGE07, SSY94, Tee95]. Même si cette méthode est en principe satisfaisante et qu'une importante portion de la littérature lui est consacrée, elle a été souvent critiquée en raison de son conservatisme, de son manque d'appel à l'intuition, notamment lors de l'étape de réglage, et de sa difficile application à des problèmes pratiques.

De l'autre côté, un deuxième approche consiste à séparer la synthèse du contrôleur en deux étapes. Par conséquent, on l'appellera l'approche à *deux étapes*. D'abord le contrôleur dédiée à la performance nominale est calculé. En fait, le contrôleur est déterminé en considerant un système linéaire. La deuxième partie est dédiée à la gestion de la saturation. Une des principales approches à *deux étapes* est connue comme l'*anti-windup*.

La présence de ce correcteur cherche à faire face à la saturation et à prévenir, autant que possible, l'apparition de ses effets. Une idée classique d'anti-windup est d'introduire des modifications au contrôleur quand la saturation est active. C'est uniquement quand la saturation est active que le correcteur anti-windup commence à agir pour modifier le comportement du système en boucle fermée. Le but est de trouver un correcteur anti-windup qui garantisse la stabilité pour une région de l'espace d'état aussi grande que possible, tout en dégradant le moins possible la performance du système. Il paraît évident qu'un compromis doit se faire entre la taille du domaine de stabilité et la performance assurée. Ce type d'approche est très attractif car la boucle anti-windup peut travailler avec une loi de commande donnée *a priori*. En fait, elle représente une technique intéressante puisque les concepteurs de contrôleurs peuvent utiliser des techniques linéaires qui leur sont familières et intuitives puis simplement ajouter une couche additionnelle afin de tenir compte du comportament non-linéaire. A l'origine, la synthèse anti-windup reposait sur des méthodes ad-hoc pensées pour des contrôleurs PID [FR67, AR89], qui sont les plus courants dans les applications industrielles. L'anti-windup a été proposé pour plusieurs applications dans différents domaines comme l'aéronautique [QTG06, RBTP07], l'aérospatial [PDTP08, BPT+09], la mécanique [TZM06] et même la fusion nucléaire [SWHK05].

Deux architectures principales peuvent être distinguées pour la synthèse de l'anti-windup [GTTZ09]. La première est appelée Anti-Windup Linéarisé Direct (DLAW) et la deuxième nommée Anti-Windup par Récupération de Modèle (MRAW).

Le DLAW appartient à une large famille de correcteurs anti-windup décrite dans une étude récente [KCMN94]. L'idée de base est d'introduire une boucle directe depuis la saturation vers le contrôleur à travers l'anti-windup. Au cours de la dernière décennie, l'anti-windup concernant les systèmes exponentiellement instables a été traité. Un article important dans ce domaine est [KM97, MP96], qui aborde le problème de l'anti-windup statique. [GdSJT05], [CLW02] représentent les premières applications des LMIs à la synthèse d'un anti-windup statique assurant la stabilité locale asymptotique. De plus, [WL03] propose une formulation permettant le calcul d'un anti-windup dynamique. Récemment, [BRT07, GHP+03] ont presenté des conditions LMI pour le calcul d'un anti-windup concernant la performance $\mathcal{L}_2$. Voir [BT09] pour une approche pratique et aussi [WP98, TP04, BRT07, TGdSJB06] dans le contexte de la stabilité globale.

Le MRAW suit un paradigme différent. Il est basé sur la sélection d'un correcteur anti-windup comme un filtre dynamique, qui incorpore un modèle du système. Le but de ce filtre est d'essayer de récupérer la réponse du système linéaire en boucle fermée. Cette approche est basée sur les résultats présentés dans [TK97a] et [TK97b] où le MRAW est nommé comme le problème anti-windup $\mathcal{L}_2$. Des illustrations de cette architecture peuvent être consultées dans [ZT02] pour les systèmes exponentiellement stables, dans [TZM06] pour les systèmes marginallement stables et dans [Tee99] pour les systèmes exponentiellement instables.

Ces architectures sont deux manières différentes d'aborder le problème de synthèse de l'anti-windup. Chacune présente des avantages et des inconvénients. Une troisième

stratégie possible repose sur le mélange des deux approches. Cette nouvelle architecture est appelée Extension de l'Anti-Windup par Récupération de Modèle (EMRAW). L'EMRAW est le résultat principal de ce chapitre. Il utilise la technique de filtrage du MRAW tout en complétant la struture de contrôle par un DLAW statique. Cette extension apporte des résultats intéressants.

I.4.1 Extension de l'anti-windup par récupération de modèle

Cette section présente l'extension de l'approche MRAW en la combinant avec un correcteur DLAW statique afin de calculer un anti-windup dynamique pour des systèmes exponentiellement instables. Cette combinaison est appelée Extension de l'Anti-Windup par Récupération de Modèle (EMRAW). L'EMRAW suit le même schéma que le MRAW. Par conséquence, le correcteur anti-windup est construit avec les matrices du système. Pourtant l'EMRAW élargit l'approche MRAW grâce à l'ajout d'un gain statique. Ce gain peut se concevoir comme un DLAW statique. La Figure I.4 montre la structure de l'approche EMRAW.

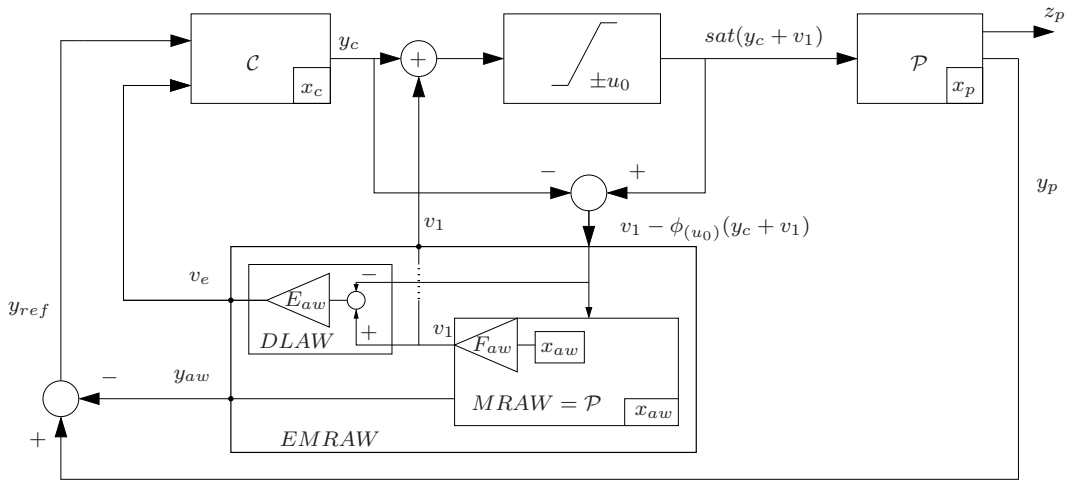

Figure I.4: Schéma bloc de l'EMRAW.

Le modèle du système ($\mathcal{P}$), le contrôleur ($\mathcal{C}$) et le correcteur EMRAW apparaissent dans les équations de la boucle fermée :

$$\mathcal{P} \ : \ \begin{cases} \dot{x}_p = A_p x_p + B_p sat_{(u_0)}(y_c + v_1) \\ y_p = C_p x_p \end{cases} \tag{I.4.1}$$

$$\mathcal{C} \ : \ \begin{cases} \dot{x}_c = A_c x_c + B_c(y_p - y_{aw}) + v_e \\ y_c = C_c x_c + D_c(y_p - y_{aw}) \end{cases} \tag{I.4.2}$$

$$\mathcal{AW} \ : \ \begin{cases} \dot{x}_{aw} = (A_p x_{aw} + B_p v_1) + B_p \phi_{(u_0)}(y_c + v_1) \\ y_{aw} = C_p x_{aw} \\ v_1 = F_{aw} x_{aw} \\ v_e = E_{aw} \phi_{(u_0)}(y_c + v_1) \end{cases} \tag{I.4.3}$$

où $x_p \in \Re^{n_p}$ est l'état du système et $y_p \in \Re^q$ la sortie mesurée. $x_c \in \Re^{n_c}$ est l'état du contrôleur et $y_c \in \Re^{m_c}$ sa sortie. $x_{aw} \in \Re^{n_{aw}}$ est l'état du correcteur anti-windup avec $n_{aw} = n_p$, $y_{aw} \in \Re^q$ et $v_1 \in \Re^m$ sont les sorties générées par la partie MRAW et $v_e \in \Re^{n_c}$ est la sortie issue de la partie DLAW statique (gain E_{aw}) .

Le gain E_{aw} est un DLAW statique car il introduit une boucle directe entre la zone morte $\phi_{(u_0)}$ et l'état du contrôleur x_c via le signal v_e.

Le EMRAW présente aussi un retour stabilisant v_1. Comme dans l'approche MRAW le défi est de trouver une loi de contrôle pour calculer un retour v_1 qui stabilise le correcteur anti-windup (I.4.3). Si la boucle anti-windup est stable avec le retour v_1, alors la sortie y_{aw} converge vers zéro. Par conséquent, la sortie du système y_p converge vers la référence y_{ref}.

Le choix du retour stabilisant v_1 n'est pas trivial pour un système exponentiellement instable. Dans le cadre de ce travail, on cherche uniquement la stabilité locale. Par conséquent, on définit v_1 comme un retour statique

$$v_1 = F_{aw} x_{aw} \tag{I.4.4}$$

Pour ce choix de v_1 le EMRAW est, en fait, un MRAW, pour lequel v_1 serait un retour statique, plus un DLAW statique. Si on considère un v_1 comme (I.4.4), la boucle anti-windup (I.4.3) est reformulée comme suit :

$$\begin{aligned} \dot{x}_{aw} &= (A_p + B_p F_{aw}) x_{aw} - B_p \phi_{u_0}(y_c + F_{aw} x_{aw}) \\ y_{aw} &= C_p x_{aw} \end{aligned} \tag{I.4.5}$$

où F_{aw} est un gain statique garantissant la stabilité asymptotique de la matrice $A_p + B_p F_{aw}$, c'est-à-dire, l'existence d'une matrice $P_p = P_p' > 0$ telle que $(A_p + B_p F_{aw})' P_p + P_p(A_p + B_p F_{aw}) < 0$.

D'après [TK97a], si la boucle anti-windup (I.4.3) est locallement stable avec $v_1 = F_{aw} x_{aw}$, alors le système (I.4.1)-(I.4.3) est aussi locallement stable. Le but consiste alors à optimiser le domaine de stabilité afin de garantir la fiabilité de la mission. Le calcul du gain F_{aw} est tel qu'il maximise le domaine de stabilité.

La stabilité est donc assurée par v_1 (I.4.4) et le domaine est maximisé lors du calcul de F_{aw}. Par conséquence, les degrés de libertés additionnels de l'approche EMRAW, par rapport au simple MRAW, introduits par le gain E_{aw}, peuvent être utilisés pour améliorer la performance du système.

I.4.1.a Introduction d'un critère de performance

Dans l'approche EMRAW, en supposant une boucle anti-windup, la sortie du système y_p converge vers y_{ref}. Un système appelé *idéal* est mis en parallèle du système en boucle fermée (I.4.1)-(I.4.3). La sortie de ce système idéal y_{id} décrit le comportement désiré pour la sortie y_p. Autrement dit, on voudrait que y_p ait le même comportement que y_{id}. Pourtant, y_p converge vers la référence y_{ref}. Si y_{ref} est au plus près possible de y_{id}, alors la sortie du système saturé y_p va converger vers une meilleure réponse. Par conséquence, la différence entre les signaux y_{ref} et y_{id} doit être minimisée afin d'améliorer la performance du système.

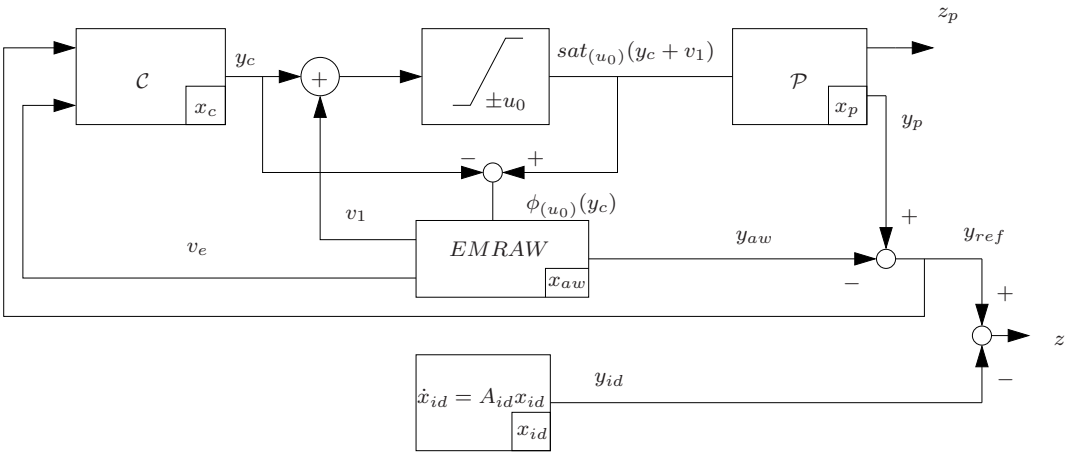

Figure I.5: Strategie d'optimisation de la performance pour le EMRAW.

Dans le contexte du EMRAW, le critère d'optimisation consiste à minimiser la norme $\mathcal{L}_2\{z\}$ où $z = y_{ref} - y_{id}$. La Figure I.5 présente le schéma bloc qui décrit cette stratégie.

La dynamique du système idéal est exprimée avec la représentation d'état suivante :

$$\dot{x}_{id} = A_{id}x_{id}; \qquad y_{id} = C_{id}x_{id} \tag{I.4.6}$$

où $x_{id} \in \Re^{n_{id}}$ et $y_{id} \in \Re^q$. A_{id} est Hurwitz. Les matrices A_{id} et C_{id} sont choisies par le concepteur. Ce choix dépend de la dynamique du système.

Soit le vecteur d'état étendu $\xi = [x_p^{'} \quad x_c^{'} \quad x_{aw}^{'} \quad x_{id}^{'}]^{'}$. Le système en bouclé fermée (I.4.1), (I.4.2), (I.4.3) et (I.4.6) s'exprime comme indiqué ci-dessous :

$$\begin{aligned} \dot{\xi} &= (\mathbb{A} + \mathbb{B}_\phi F_{aw}\mathbb{C}_s)\xi + (\mathbb{B}_\phi + \mathbb{B}_v D_{aw})\,\phi_{(u_0)}((\mathbb{K} + F_{aw}\mathbb{C}_s)\xi) \\ z &= y_{ref} - y_{id} = y_p - y_{aw} - y_{id} = \mathbb{C}\xi \end{aligned} \tag{I.4.7}$$

où $z \in \Re^p$ et

$$\mathbb{A} = \begin{bmatrix} A_p + B_p D_c C_p & B_p C_c & B_p D_c C_p & 0 \\ B_c C_p & A_c & B_c C_p & 0 \\ 0 & 0 & A_p & 0 \\ 0 & 0 & 0 & A_{id} \end{bmatrix}; \mathbb{B}_\phi = \begin{bmatrix} -B_p \\ 0 \\ -B_p \\ 0 \end{bmatrix}; \mathbb{B}_v = \begin{bmatrix} 0 \\ I_{n_c} \\ 0 \\ 0 \end{bmatrix};$$

$$\mathbb{C}_s = [0 \;\; 0 \;\; I_{n_{aw}} \;\; 0]; \mathbb{C} = [C_p \;\; 0 \;\; -C_p \;\; -C_{id}]; \mathbb{K} = [D_c C_p \;\; C_c \;\; -D_c C_p \;\; 0].$$

Remarque I.1. *En schématisant, on peut considérer que les deux parties de l'EMRAW ont différentes fonctions. La première partie, i.e. le MRAW, garantit la convergence de y_p ver y_{ref}, alors que la deuxième, i.e. le DLAW statique, modifie y_{ref} afin qu'il soit le plus près possible de y_{id}.*

I.4.2 Synthèse du correcteur EMRAW

Soit le système (I.4.7). En définisant $n = n_p + n_c + n_{aw} + n_{id}$ et $He(A) = A + A'$, le théorème suivant est établi :

Théorème I.2. *[BPT+10b] Soient $v \in \Re^n$, k_γ et k_ρ à valeurs positives, s'il existe des scalaires positifs γ et ρ, une matrice définie positive $W \in \Re^{n \times n}$, un matrice $Y \in \Re^{m \times n}$, une matrice $Z \in \Re^{n_c \times m}$, une matrice diagonale définie positive $S \in \Re^{m \times m}$ et une matrice $F_{aw} \in \Re^{m \times n_p}$ satisfaisant min $(k_\gamma \gamma + k_\rho \rho)$ sous les contraintes*

$$\begin{bmatrix} He\left[\mathbb{A}W + \mathbb{B}_\phi F_{aw} \mathbb{C}_s W\right] & \mathbb{J}_1 & W\mathbb{C}' \\ * & -2S & 0 \\ * & * & -\gamma I_p \end{bmatrix} < 0 \tag{I.4.8}$$

$$\begin{bmatrix} W & W\mathbb{K}'_{(i)} - Y'_{(i)} \\ * & u^2_{0(i)} \end{bmatrix} \geq 0; \; i = 1, ..., m. \tag{I.4.9}$$

$$\begin{bmatrix} W & v \\ * & \rho \end{bmatrix} \geq 0 \tag{I.4.10}$$

où $\mathbb{J}_1 = \mathbb{B}_\phi S + \mathbb{B}_v Z + Y' + W\mathbb{C}'_s F'_{aw}$, alors $\mathcal{E}(P) = \left\{\xi \in \Re^n; \xi' P \xi < 1\right\}$ avec $P = W^{-1}$ est un domaine de stabilité pour le système (I.4.7) avec $D_{aw} = ZS^{-1}$ et F_{aw}. De plus, $\mathcal{E}(P)$ est maximisé selon la direction v, avec le poids k_ρ, et la performance $1/\gamma$ est maximisée avec le poids k_γ.

Remarque I.2. *Si $v = x_p(0)$ dans (I.4.10) le domaine de stabilité est maximisé selon la direction des états du système saturé.*

Pourtant, on peut déduire des équations précédentes que F_{aw} et W ne peuvent pas être calculées en même temps car les inégalités ne sont pas linéaires en ces variables (voir le produit $F_{aw}\mathbb{C}_s W$ dans (I.4.8)). Une méthode est donc proposée par la suite pour la synthèse du correcteur anti-windup.

I.4.3 Calcul du correcteur EMRAW

I.4.3.a Algorithme Coordonnée-descendant

L'inégalité bilinéaire matricielle (BMI) (I.4.8) peut s'exprimer d'une façon plus adaptée à l'utilisation de l'algorithme coordonnée-descendant présenté par [PA01].

Proposition I.3. *Soient k_γ et k_ρ des valeurs positives, il existe des gains anti-windup F_{aw} et D_{aw} tels que les conditions du Theorème I.2 sont satisfaites s'il existe des scalaires positifs γ et ρ, une matrice symmétrique définie positive $W \in \Re^{n\times n}$, une matrice $Y \in \Re^{m\times n}$, une matrice $Z \in \Re^{n_c\times m}$, une matrice diagonale définie positive $S \in \Re^{m\times m}$, des matrices $K_s \in \Re^{n\times n_p}$, $\mathbb{F} \in \Re^{n_p\times n_p}$ et $\mathbb{R} \in \Re^{m\times n_p}$ satisfaisant $min(k_\gamma\gamma + k_\rho\rho)$ s.t. (I.4.9), (I.4.10) et*

$$\begin{bmatrix} He\left[\mathbb{A}W\right] & W\mathbb{C}_s' & \mathbb{B}_\phi S + \mathbb{B}_v Z + Y' & W\mathbb{C}' \\ * & 0 & 0 & 0 \\ * & * & -2S & 0 \\ * & * & * & -\gamma I_p \end{bmatrix} + He\left[\begin{bmatrix} K_s \\ -I \\ 0 \\ 0 \end{bmatrix} \begin{bmatrix} \mathbb{R}'\mathbb{B}_\phi' & -\mathbb{F} & \mathbb{R}' & 0 \end{bmatrix}\right] < 0 \tag{I.4.11}$$

De plus $\mathcal{E}(W^{-1}) = \left\{\xi \in \Re^n; \xi' W^{-1}\xi < 1\right\}$ est un domaine de stabilité pour le système (I.4.7) avec $D_{aw} = ZS^{-1}$ et $F_{aw} = \mathbb{R}(\mathbb{F}')^{-1}$.

Considérant la nouvelle formulation de la proposition I.3, on peut adapter l'algorithme présenté dans [PA01]. L'algorithme n'évite pas d'introduire des relaxations, mais permet la recherche de la matrice de Lyapunov à chaque itération. Cet algorithme est décomposé en quatre opérations présentées ci-dessous :

Algorithme I.1. *(***Coodonnée-decendant***)*

1. *(Initialisation - k=1) choisir un gain d'initialisation K_s.*
2. *(Pas k - première partie) pour ce choix de K_s, résoudre le problème de minimisation LMI :*
$$min(k_\gamma\gamma + k_\rho\rho) \quad s.t. \quad (I.4.9),\ (I.4.10)\ et\ (I.4.11)$$
Garder les valeurs $\mathbb{R}$ et $\mathbb{F}$ obtenues.
3. *(Pas k - deuxième partie), pour ce choix de $\mathbb{R}$ et $\mathbb{F}$, on résout le problème de minisation LMI :*
$$Crit_k = min(k_\gamma\gamma + k_\rho\rho) \quad s.t. \quad (I.4.9),\ (I.4.10)\ et\ (I.4.11)$$

Garder la valeur de K_s obtenue.

4. *(Finalisation) si $|Crit_{k+1} - Crit_k| < \epsilon$, alors arrêter, $F_{aw} = \mathbb{R}(\mathbb{F}')^{-1}$, sinon $k \leftarrow k+1$ et aller au pas 2.*

Le point délicat de l'algorithme I.1 est l'initialisation de K_s. Pourtant, ce choix peut être facilité par la prise en compte de quelques propriétés sur K_s liées à la stabilité du système en boucle fermée (I.4.7).

Lemme I.6. *La variable K_s de l'inégalité (I.4.11) est un gain de retour tel que la fonction de Lyapunov $V(\xi) = \xi' W^{-1} \xi$ démontre simultanément la stabilité des deux systèmes (I.4.7) et $\dot{\xi} = (\mathbb{A} + K_s \mathbb{C}_s)\xi$.*

I.4.3.b Algorithme basé sur les objectifs

Un algorithme alternatif est ensuite proposé. Il est basé sur la connaissance de l'objectif qu'à chaque gain du EMRAW. Autrement dit, d'un côté on calculera F_{aw} en sachant qu'il stabilise la boucle anti-windup, et de l'autre, on calculera D_{aw} en minimisant la différence entre de y_{ref} et y_{id}. Cet algorithme se divise en deux parties indépendantes conduisant à une troisième partie.

Algorithme I.2. *[BPT+10b](***Basé objectif***)*

- *(Partie analyse - 1) Régler F_{aw} tel que $(A_p + B_p F_{aw})' P_p + P_p (A_p + B_p F_{aw}) < 0$ avec $P_p = P_p' > 0$ avec la meilleure réponse possible. Simuler le système et analyser la réference. Garder F_{aw}.*
- *(Partie LMI - 2) Choisir un rapport k_γ / k_ρ grand. Ensuite, régler un gain F^*_{aw} tel que $(A_p + B_p F^*_{aw})' P_p + P_p (A_p + B_p F^*_{aw}) < 0$ et la dynamique de $(A_p + B_p F^*_{aw})$ soit plus rapide. La partie analyse (pas 1) donne des directions sur la manière dont sont choisis les pôles de $(A_p + B_p F^*_{aw})$ (normalement dix fois plus rapides que ceux de $(A_p + B_p F_{aw})$). Avec F^*_{aw} fixé, les relations (I.4.8)-(I.4.10) deviennent LMIs. Résoudre les LMIS pour calculer D_{aw}.*
- *(Partie vérification) Avec F_{aw} (Partie analyse - pas 1) fixé, et avec D_{aw} de la partie LMI (pas 2), résoudre le problème d'analyse (I.4.8)-(I.4.10). Evaluer la stabilité avec le paramètre ρ. Si $\rho < \rho_{desired}$ arrêter, sinon revenir à la partie LMI (pas 2) avec un rapport k_γ / k_ρ plus petit et/ou une dynamique plus lente pour les pôles de $(A_p + B_p F^*_{aw})$.*

A la différence de l'algorithme I.1, il n'y a pas de preuve de convergence pour l'algorithme I.2. Cependant pour certaines applications, la connaissance du système peut être utilisée dans la première partie de l'algorithme I.2 afin d'obtenir ainsi de meilleurs résultats.

Le chapitre 3 présente aussi deux résultats qui montrent que les différentes techniques de symétrisation du chapitre 2 peuvent être appliquées sans modifier les méthodes de synthèse anti-windup.

Enfin, les résultats du chapitre 3 ont été illustrés avec un système simplifié du contrôle d'attitude de satellite.

I.5 Résultats sur le pilotage des satellites à commande saturante

Dans cette thèse, trois configurations du contrôle du vol en formation de satellites sont présentées et simulées, avec et sans anti-windup. Dans ce résumé on ne présente que les resultats sur le contrôle d'attitude et la position relative d'une formation de deux satellites. C'est dans ce cas que les résultats plus intéressant apparaissent.

I.5.1 Modélisation du problème d'attitude et de position relative

Le problème de vol en formation considéré est composé de deux satellites pour lesquels la position relative selon l'axe z est asservie en même temps que l'attitude du deuxième satellite (satellite 2). Le premier satellite (satellite 1) réalise seulement des déplacements dans l'axe z.

La dynamique de l'attitude, sous l'hypothèse de petits angles, est décrite par la modélisation classique du double intégrateur [CNE05, Hug04]:

$$\ddot{\theta} = J_{Gi}^{-1} C_i \tag{I.5.1}$$

où J_{Gi} est la matrice d'inertie du satellite i par rapport au centre de masse et C_i est la somme des couples externes appliqués au satellite i.

La dynamique de la position relative est également décrite par un double intégrateur:

$$\ddot{z}_i = m_i^{-1} F_i \tag{I.5.2}$$

où z_i est le déplacement selon l'axe z du satellite i et F_i la somme de forces externes de ce même satellite.

Cependant, lorsque l'attitude est considérée, l'équation (I.5.2) est modifiée. A cause de la caratérisation particulière du capteur de position relative, la dynamique angulaire du satellite 2 est couplée avec la position relative [Gau07, PCU+05, WPK05].

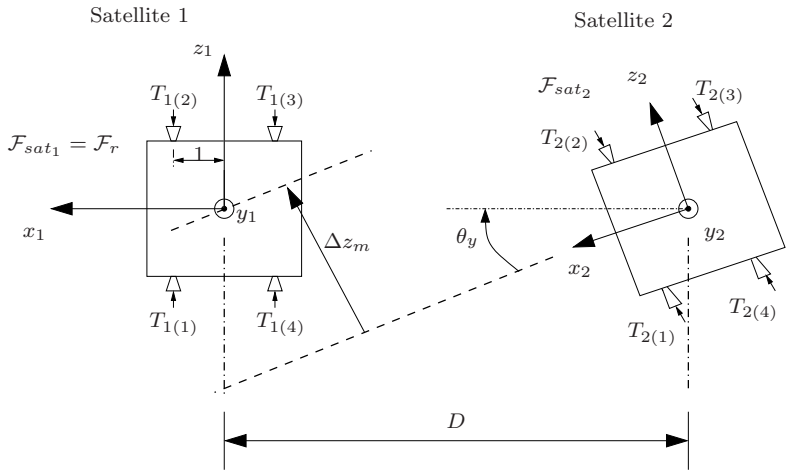

Figure I.6: Erreur de position relative généré par un erreur d'attitude.

La figure I.6 illustre l'erreur de postion relative mesurée. En utilisant les expressions (I.5.1) et (I.5.2), la dynamique de la position relative mesurée est décrite par :

$$\Delta\ddot{z}_m = \Delta\ddot{z} + D\ddot{\theta}_y = -m_2^{-1}F_2 + m_1^{-1}F_1 + DJ_{G_2}^{-1}C_2 \tag{I.5.3}$$

où D est une constante.

Avec cette modélisation, dans le cas où l'actionneur est un système propulsif et où un contrôleur linéaire assure la stabilité de la boucle linéaire, la boucle fermée considérée peut s'écrire de la façon suivante :

$$\begin{cases} \dot{x}_p = A_p x_p + B_p u_p \dot{x}_c = A_c x_c + B_c C_p x_p \\ y_p = C_p x_p \\ z_p = C_z x_p \\ u_p = M sat_{(u_0)}(M^* y_c) = \begin{bmatrix} M_1 sat_{(u_0)}(M_1^* y_{c1}) \\ M_2 sat_{(u_0)}(M_2^* y_{c2}) \end{bmatrix} \\ y_c = C_c x_c + D_c C_p x_p \end{cases} \tag{I.5.4}$$

Remarque I.3. *Les bornes de saturation sont asymétriques avec $\bar{u}$ comme borne supérieure et 0 comme borne inférieure. Or l'expression du système (I.5.4) est donnée avec des bornes symétriques. Une technique de symétrisation par fonction variable de noyau a été utilisée.*

I.5.2 Simulations sur le contrôle d'attitude et de position relative

Le système (I.5.4) est simulé avec les correcteurs anti-windup suivants :

- DLAW statique (ligne pleine);

- DLAW dynamique d'ordre plein (ligne discontinue);
- DLAW dynamique d'ordre fixé (ligne pointillée et discontinue);
- MRAW avec v_1 (I.4.4) (ligne pointillée);
- EMRAW calculé avec l'algorithme[2] I.2 (ligne avec les étoiles);
- EMRAW calculé avec l'algorithme[3] I.1 (ligne avec les cercles).

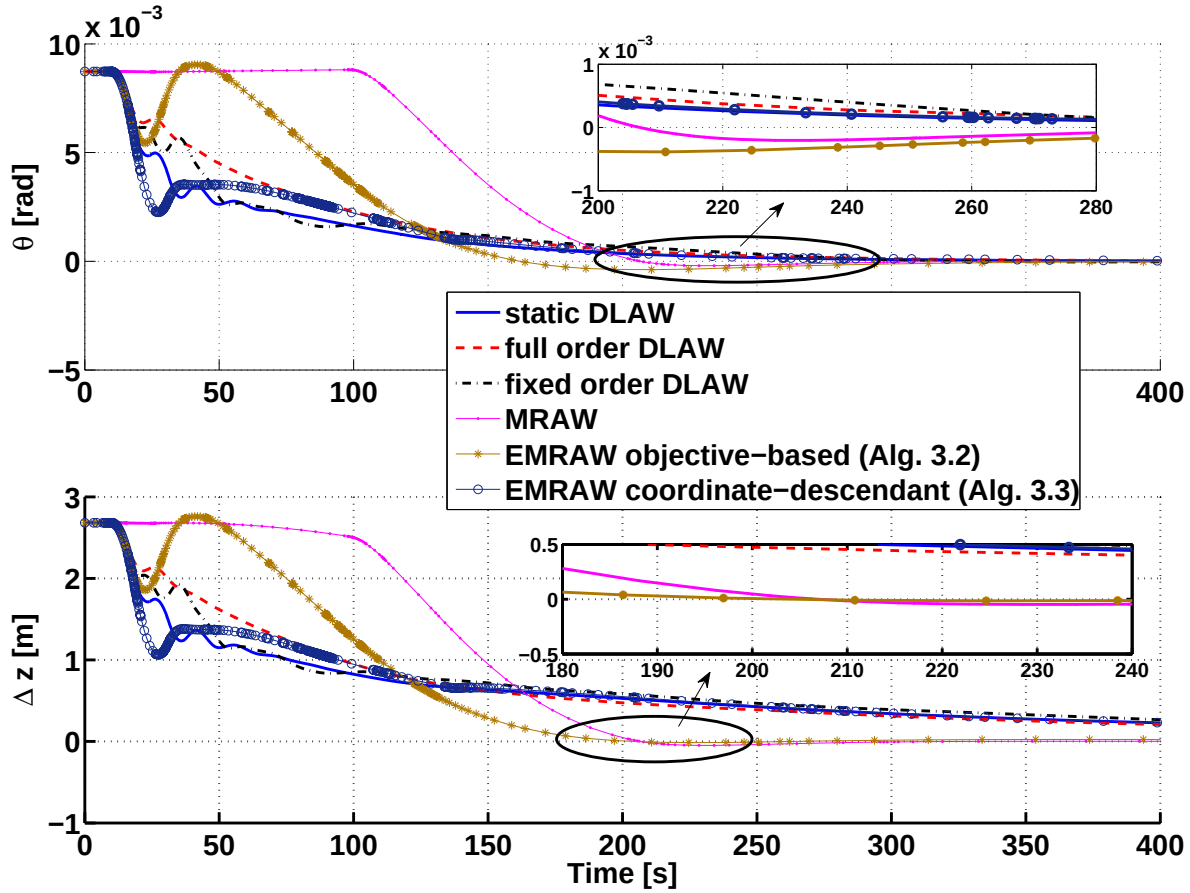

Figure I.7: Attitude et position relative avec plusieurs anti-windup.

La Figure I.7 montre les réponses temporelles de l'attitude et de la position relative. Une caracteristique importante doit être mise en avant : l'allure des réponses avec l'approche DLAW est complètement différente de celle obtenue avec le MRAW/EMRAW. Il faut remarquer aussi que quand l'EMRAW est calculé avec l'algorithme I.1 on obtient un comportement comme s'il était un correcteur de type DLAW. Ceci est dû à des problèmes d'initialisation de l'algorithme I.1.

[2]Algorithme basé objectif.
[3]Algorithme coordonnée-descendant.

Dans le cas du DLAW, l'attitude est la première à converger suivie de la position relative. Comme l'attitude et la position relative sont couplées selon la façon dont la mesure de la position relative est prise, la statégie suivante de contrôle est mise en oeuvre : d'abord l'attitude est stabilisée puis la position relative est contrôlée sans que le problème de couplage n'apparaisse.

Pourtant, lorsque le MRAW et EMRAW (calculé avec l'algorithme I.2) sont utilisés, la stratégie de contrôle change : l'attitude et position relative convergent simultanément. Ce phénomène réduit sensiblement le temps de réponse du système car la position relative n'attend pas que l'attitude soit arrivée à l'équilibre.

Afin de comprendre pourquoi la stratégie de contrôle change avec un correcteur de type MRAW/EMRAW, on doit prendre en compte les considérations suivantes :

- le même propulseur génère le couple et la force pour contrôler les deux états attitude et position relative;
- la retour stabilisant v_1 modifie les propulseurs;
- dans la définition des matrices d'état pour MRAW/EMRAW, le signal v_1 dépend de la dynamique de l'attitude et de la position relative.

De plus, les propulseurs contrôlent simultanément ces deux dynamiques. Ainsi, un couplage de l'attitude vers la position et vice-versa est introduit. En conclusion, v_1 utilise la capacité des propulseurs du contrôleur ainsi que l'attitude et la position relative. v_1 peut introduire un couplage parmi les dynamiques afin de les faire converger simultanément.

Le temps de réponse est un critère de comparaison intéressant. Pour le système (I.5.4) avec un correcteur DLAW, l'attitude converge en $300s$ environ et la position relative en $1000s$ environ en fonction du type de DLAW consideré. Ensuite pour le MRAW l'attitude et la position convergent avec $290s$ ce qui est clairement inférieur (pour la position relative). Ensuite pour l'EMRAW (issu de l'algorithme I.2) l'attitude et la position convergent en $320s$ et $300s$ respectivement. Enfin pour l'EMRAW (issu de l'algorithme I.1), l'attitude et la position convergent en $330s$ et $980s$ respectivement, ce qui montre que le EMRAW se comporte comme un correcteur DLAW.

Remarque I.4. *Les deux approches, MRAW et EMRAW présentent la capacité de faire converger les états du système avec la même rapidité. Leur structure utilise la capacité des propulseurs comme unique actionneur pour les deux, attitude et position relative. Par conséquent ces méthodes sont des approches très intéressantes pour la commande des systèmes MIMO soumis à des saturations de propulseurs.*

Finalement, le chapitre 5 montre l'effet de l'anti-windup dans une configuration type drag-free (contrôle d'accélération). En particulier on démontre l'existence d'un anti-windup trivial qui annule l'influence de la saturation sur le système.

I.6 Conclusion générale

I.6.1 Contributions personnelles

La première contribution des travaux de cette thèse est la mise en place de plusieurs solutions permettant la symétrisation de la saturation. Dans le chapitre 2, la particularité des systèmes utilisant des propulseurs comme actionneurs est mise en avant. Cette structure a été exploitée afin de pouvoir symétriser la saturation. D'un point de vue théorique, des conditions nécessaires et suffissantes pour l'obtention d'un vecteur symétrisant candidat ont été apportées. On peut alors utiliser des approches conservatives existant dans la littérature et permettant d'obtenir une borne symétrique en prenant le minimum entre la valeur absolue de la borne supérieure et inférieure. En particulier, un vecteur modifiant la saturation de telle sorte que la borne supérieure et inférieure sont égales a été présenté. Des conditions suffisantes pour la validité du vecteur symétrisant ont été apportées [BPT+09]. Ensuite, concernant l'application de ces méthodes, une fonction variable du noyau a été définie pour éviter la surconsommation à l'équilibre. Plus précisément, on a présenté des conditions suffisantes pour une fonction variable du noyau particulière.

La symétrisation a été mise en avant comme une étape clé afin de pouvoir utiliser les méthodes de synthèse anti-windup. Les contrôleurs anti-windup actuels existant dans la littérature considèrent seulement des saturations symétriques. Dans les cas où elles sont asymétriques on doit d'abord utiliser des méthodes de symétrisation. La deuxième contribution de la thèse est présentée dans le chapitre 3 et traite du rapport entre la synthèse anti-windup et la symétrisation de la saturation. Nous avons démontré que l'introduction d'un vecteur symétrisant n'affecte pas les résultats du processus de synthèse de l'anti-windup [BPT+09]. De façon similaire au vecteur symétrisant, il a été prouvé que le résultat sur l'anti-windup n'est pas affecté par la fonction variable du noyau.

La troisième contribution de cette thèse consiste à proposer une nouvelle structure pour la synthèse de l'anti-windup dynamique. Cette nouvelle approche a été nommée *Extended Model Recovery Anti-Windup* (EMRAW) [BPT+10b]. L'idée principale consiste à réutiliser la procédure de synthèse du *Model Recovery Anti-Windup* (MRAW) et à l'étendre en ajoutant un *Direct Linear Anti-Windup* (DLAW). La combinaison de ces deux approches amène à des conditions non-convexes. Deux algorithmes ont été présentés afin de pouvoir trouver une solution au problème de synthèse. Le premier est un algorithme itératif, basé sur une procédure coordonnée-descendante. La deuxième est un algorithme heuristique, basé sur l'objectif de chacun des éléments constituant le correcteur anti-windup. Dans le contexte du premier algorithme, des conditions sur son initialisation ont été introduites.

Les principaux résultats du manuscrit ont été évalués et testés dans les chapitres 4 et 5. Ainsi, les dernières contributions apportées sont de type méthodologique. D'abord, un guide sur la façon d'initialiser le premier algorithme a été proposé. Ensuite, l'application

de la synthèse de l'EMRAW nous a permis de montrer l'avantage de cette structure dans une configuration de vol en formation. Finalement, un autre résultat important est apparu dans le contexte du rapport entre la fonction de répartition et l'anti-windup. Des simulations ont montré que l'introduction d'un correcteur anti-windup peut *corriger* la limitation d'une fonction de répartition simple et apporter les mêmes performances que celles retrouvées avec une fonction de distribution plus complexe et efficace.

I.6.2 Perspectives

Le correcteur anti-windup a été montré comme un outil intéressant pour la gestion de la saturation des actionneurs. En particulier, l'EMRAW a présenté de bons résultats sur un problème de vol en formation. Dans la thèse on a observé que l'anti-windup basé sur l'approche par récupération de modèle suppose la parfaite connaissance du modèle du système. Cependant ceci n'est pas vrai en général. La présence d'erreurs de modélisation, comme des incertitudes paramétriques, la simplification de modes flexibles ou des non-linearités négligées rendent impossible, en pratique, la connaissance parfaite du modèle. Par conséquent, un premier domaine de recherche à explorer serait l'analyse de l'anti-windup soumis à des systèmes incertains. De façon similaire, la synthèse de l'anti-windup pour des systèmes incertains représente un domaine de recherche potentiel pour l'avenir. Quelques travaux ont déjà abordé ce sujet [THP04, MTBP06, FB07] mais le conservatisme de ces approches est encore important [KTP10].

Sur ce sujet et sur le cas d'application traité dans ce manuscrit, une type particulier d'incertitudes est mis en avant : les erreurs d'alignement des tuyères et les incertitudes sur la capacité maximale des propulseurs. Ce type d'incertitudes peut être décrit par une matrice d'influence incertaine. Fondamentalement, ce problème est équivalent à celui consistant à considérer une matrice B_p incertaine. Pourtant, en s'appuyant sur le sens physique de la matrice d'influence, il est possible de faire des simplifications qui pourraient réduire le conservatisme.

Un autre point intéressant pour les futures recherches concerne la réduction de l'ordre de l'anti-windup. Comme il a été remarqué dans la thèse, un des principaux inconvénients de l'approche EMRAW est qu'on est forcé d'avoir un correcteur anti-windup du même ordre que le système. Il serait intéressant de développer des méthodes permettant de réduire l'ordre de l'anti-windup en éliminant, par exemple, des dynamiques secondaires du système. Dans ce cadre, les resultats pourraient être liés à la synthèse anti-windup pour des systèmes incertains.

Finalement, une dernière direction vers laquelle pourraient être dirigées les futures études est la définition d'une méthodologie différente pour la synthèse anti-windup. Les correcteurs anti-windup basés sur l'approche par récupération de modèle ont la particularité de reproduire le comportement linéaire du système. Rappelons la relation $y_l = y_p - y_{aw}$. Or, il y a un retour stabilisant v_1 qui amène y_{aw} à zéro et donc y_p vers y_l. L'ensemble

du MRAW et du système non-linéaire peut se voir comme un observateur du système linéaire. Ainsi le but des recherches serait de reformuler le problème anti-windup comme un problème d'estimation/observation. Une fois le problème réécrit sous cette forme alternative, l'idée consisterait à utiliser les techniques de synthèses definies pour les estimateurs/observateurs afin de calculer un correcteur anti-windup.